University of BRISTOL

Development and characterisation of a human *ex vivo* model of aneurysm

Rosaria Bianco

A dissertation submitted to the University of Bristol in accordance with the requirements for award of the degree of Doctor of Philosophy in the Faculty of Health Sciences

School of Clinical Sciences.

October 2019

Word count: 53,435

Abstract

An aneurysm is a localised dilatation of the arterial wall, characterised by thinning of the medial layer and degeneration of the internal elastic lamina. The formation and the rupture of an aneurysm is a significant cause of premature mortality in UK, accounting for 2% of all deaths. Aneurysms are usually asymptomatic until their rupture, and diagnosis is usually incidental in unrelated medical complaints. The sudden rupture of aortic aneurysms commonly results in haemorrhagic shock and death. There are currently no treatments for patients with non-ruptured aneurysms therefore novel treatments to prevent rupture, or biomarkers to identify vulnerability to aneurysm rupture, would represent major scientific breakthroughs. To gain insight into the pathogenesis of aortic aneurysms, several mouse models have been developed which rely upon Angiotensin II (Ang II) or calcium chloride ($CaCl_2$) as inducers of aortic dilatation. However at least 15% of animals suffer aortic dissection and sudden death. The aim of this project is to develop and characterise a reproducible *ex-vivo* human model of aneurysm, to be used alongside or instead of mouse models. To mimic current *in vivo* animal models, a suitable replacement should harbour similar cellular and morphological features such as vessel dilatation, elastin loss and vascular smooth muscle cell (VSMC) apoptosis. In this study, arteries were isolated from human umbilical cords, placed within a bio-reactor and exposed to laminar flow (6.5 dynes/cm^2) for 72 hours with and without Ang II or $CaCl_2$. $CaCl_2$ pre-treatment of umbilical arteries reduced medial thickness, medial elastin content, and medial cell density, despite no change in vessel area. Ang II stimulation significantly increased total vessel area and medial cell density, compared to untreated arteries. Moreover, Ang II significantly decreased medial thickness, and medial elastin content suggesting aneurysm formation. Considering the association of dysregulated MMP-directed elastinolytic activity with aneurysm progression, introduction of exogenous tissue inhibitor of metalloproteinases 3 (TIMP-3), a transforming growth factor beta neutralising antibody (TGFβ NAb) or a matrix metalloproteinase-12 (MMP-12)-specific inhibitor into the *ex vivo* model prevented aneurysm formation, mimicking effects observed in the Ang II-infused mouse model and providing robust validation of the ex vivo aneurysm model. Interestingly, Ang II or $CaCl_2$ treatment of VSMC regulated the expression of a number of metalloproteinases (MMPs) and tissue inhibitors of MMPs (TIMPs), alongside differences in phenotypic markers. In addition, Ang II-induced marked haemodynamic effects on endothelial cells (ECs) which could be reversed by addition of exogenous TIMP-3 or the angiotensin receptor inhibitor Losartan. This study highlights the applicability of the *ex vivo* model for future aneurysm studies, providing a potential replacement for ethically contentious animal models.

Dedication and acknowledgements

First and foremost, I would like to express my sincere gratitude to my supervisor Dr Jason Johnson for the continuous support of my PhD study, for his patience, motivation and for his huge knowledge that guided me through my PhD. Dr Johnson always encouraged me to submit abstracts for conferences which helped me to build up my presentation skills. Additionally, his supervision supported me throughout the time of research and writing of this thesis.

I would also like to extend my gratitude to Professor Sarah George, who gave me the opportunity to start my PhD at Bristol University. I would like to thank her for the endless support, advice and trust in my research.

To both I express my sincere gratitude, I could not have imagined having better supervisors and mentors for my PhD study.

Special thanks to Dr Karina Di Gregoli, who not only trained me in experimental techniques but who was also a friend providing me with advice in all areas of my life. Also, a huge thanks to Dr Bethan Brown to being supportive in the laboratory as well as in my writing.

I would also like to thank the members of Sarah's group, Dr Helen Williams, Dr Alex Ward, Dr Cressida Lyon, Dr Kerry Wadey and Dr Andrew Bond for their precious support.

Importantly, I am truly indebted and thankful to my parents for their patience, huge trust in me and infinite support throughout thesis writing and throughout my life in general.

Thanks to Jordi, who supported me during these long and (sometimes) difficult years.

I would also like to acknowledge my friends from Italy, who have provided me with moral and emotional support.

I warmly thank my brother for simply being the best brother that everybody would love to have, and for this I would love to dedicate this thesis to him.

Thanks to all for your invaluable encouragement.

----------This thesis is dedicated to my brother Vincenzo Bianco----------

Author’s Declaration

I declare that the work in this dissertation was carried out in accordance with the requirements of the University's *Regulations and Code of Practice for Research Degree Programmes* and that it has not been submitted for any other academic award. Except where indicated by specific reference in the text, the work is the candidate's own work. Work done in collaboration with, or with the assistance of, others, is indicated as such. Any views expressed in the dissertation are those of the author.

SIGNED: ..... DATE:.....

Publication List

Published papers

- ANEURYSM SEVERITY IS INCREASED BY COMBINED MMP-7 DELETION AND N-CADHERIN MIMETIC (EC4-FC) OVER-EXPRESSION
  Lyon, C., Williams, H., **Bianco, R.**, Simmonds, S., Brown, B., Wadey, K., Smith, F., Johnson, J. & George, S. 28 Nov 2017. In: Scientific Reports. 7: 17342, DOI:10.1038/s41598-017-17700-8
- MICRORNA-181B CONTROLS ATHEROSCLEROSIS AND ANEURYSMS THROUGH REGULATION OF TIMP-3 AND ELASTIN
  Di Gregoli, K., Mohamad Anuar, N. N., **Bianco, R.**, White, S. J., Newby, A. C., George, S. J. & Johnson, J. L. 6 Jan 2017. In: Circulation Research. 120, 1, p.49-65

Published abstracts

- DEVELOPMENT AND CHARACTERISATION OF A HUMAN *EX-VIVO* MODEL OF ANEURYSM

  Bianco R*, Di Gregoli K, Caputo M, Zakkar M, George SJ, Johnson JL (fcvb 2018) Cardiovascular Research, Volume 114, Issue suppl_1, 1 April 2018, Pages S6–S7, https://doi.org/10.1093/cvr/cvy060.011. Cardiovascular Research Supplements (2018) 114, S6–S8

- DEVELOPMENT AND CHARACTERISATION OF A HUMAN *EX-VIVO* MODEL OF ANEURYSM
  Bianco R*, Di Gregoli K, Caputo M, Zakkar M, George SJ, Johnson JL (EAS 2018) Atherosclerosis, Vol. 275, e144–e145
- VALIDATION OF A NOVEL HUMAN *EX-VIVO* MODEL OF ANEURYSM TO SUPPLANT MOUSE MODELS
  R Bianco*, K Di Gregoli, M Caputo, M Zakkar, SJ George, JL Johnson. Cardiovascular Research, Volume 114, Issue suppl_2, 1 September 2018, Pages S2, https://doi.org/10.1093/cvr/cvy216.005

Meeting abstracts (unpublished)

- EFFECT OF ANEURYSM INDUCERS ON VASCULAR SMOOTH MUSCLE PHENOTYPE AND MATRIX METALLOPROTEINASE EXPRESSION

  R. Bianco*, K. Di Gregoli, M Zakkar, S.J. George, J.L. Johnson (BAS 2016)

- DEVELOPMENT AND CHARACTERIZATION OF A HUMAN EX-VIVO MODEL OF ANEURYSM

  Bianco R*, Di Gregoli K, Caputo M, Zakkar M, George SJ, Johnson JL (BAS 2017)

Awards

- Finalist Young Investigator Award at Frontiers In CardioVascular Biology (Vienna 2018)
- Travel Award European Atherosclerosis Society (Lisbon 2018)
- Travel Award Frontier in Cardiovascular Biology (Vienna 2018)
- Travel Award British Atherosclerosis Society 2018 (from Alumni foundation)
- Oral presentation prize Winner at the Postgraduates Research (University of Bristol, UK, 2018)
- Poster prize winner at the second Annual BHI SRI meeting

TABLE OF CONTENTS

ABSTRACT ..... **II**

DEDICATION AND ACKNOWLEDGEMENTS ..... **III**

AUTHOR'S DECLARATION ..... **IV**

PUBLICATION LIST ..... **V**

AWARDS ..... **VI**

LIST OF FIGURES ..... **XII**

LIST OF TABLES ..... **XV**

ABBREVIATIONS ..... **XVI**

1 GENERAL INTRODUCTION **1**

1.1 CLINICAL IMPACT OF ANEURYSM 1

1.2 DEFINITION OF ANEURYSM 1

1.2.1 Structure of a normal blood vessel *5*

1.2.2 Aetiology of aneurysm and clinical implication *7*

1.2.3 Anatomical sites of aneurysm *10*

1.2.4 Current therapies *12*

1.2.5 Surgical and percutaneous interventions of aneurysms *13*

1.3 PATHOGENESIS AND COMPOSITION 15

1.3.1 Elastin and collagen *16*

1.3.2 MMPs and TIMPs *17*

1.3.3 Vascular smooth muscle cells *19*

1.3.4 Endothelial cells *22*

1.3.5 Inflammation *24*

1.3.6 Calcification *28*

1.3.7 Angiogenesis/neovascularisation *29*

1.3.8 Atherosclerosis *30*

1.3.9 Aortic dissection *32*

1.4 ANIMAL MODELS OF ANEURYSM 34

1.4.1 Mechanism of Angiotensin II induced aneurysm formation *36*

1.4.2 Mechanism of calcium chloride induced aneurysm formation *38*

1.5 MATRIX METALLOPROTEINASES & THEIR ENDOGENOUS TISSUE INHIBITORS (TIMPS) 39

1.5.1 MMP classification, structure and function *39*

1.5.2 MMP domains *43*

1.5.3 Role of MMPs in inflammation *44*
1.5.4 MMP and TIMP expression in human aortic aneurysms *45*
1.5.5 MMP pharmacological intervention in animal models of AAA *47*
1.5.6 MMP inhibitors in clinical trials *48*
1.6 ANIMAL MODELS OF ANEURYSM AND THE 3RS 49
1.7 AIMS 50
1.8 HYPOTHESIS 50
2 MATERIALS AND METHODS 51
2.1 *IN VITRO* STUDIES 51
2.1.1 Cell culture media *51*
2.1.2 Cell culture *55*
2.1.3 Polymerase Chain Reaction (PCR) *59*
2.1.4 Cell Behaviour Studies *66*
2.2 *EX VIVO* STUDIES 72
2.2.1 Development of an ex vivo model of aneurysm *72*
2.2.2 Histological processing *79*
2.3 STATISTICAL ANALYSIS 82
3 DOES ANG II OR $CACL_2$ INDUCE ANEURYSM FORMATION WITHIN AN *EX VIVO* MODEL? 83
3.1 INTRODUCTION 83
3.1.1 Current AAA studies *83*
3.1.2 Ex vivo human model using umbilical cord arteries *84*
3.2 AIM OF THIS CHAPTER 86
3.3 RESULTS 87
3.3.1 Effect of the laminar flow on morphological and compositional parameters in ex vivo bio-reactor cultured human umbilical cord arteries *87*
3.3.2 Effect of $CaCl_2$ pre-treatment on morphological and compositional parameters associated with aneurysm formation in ex vivo bio-reactor cultured human umbilical cord arteries *91*
3.3.3 Effect of Ang II administration on morphological and compositional parameters associated with aneurysm formation in ex vivo bio-reactor cultured human umbilical cord arteries *97*
3.3.4 Effect of Ang II administration on MMP expression in ex vivo bio-reactor cultured human umbilical cord arteries *106*
3.4 CONCLUSION 109
3.5 DISCUSSION 112
3.5.1 The use of $CaCl_2$ application in an ex vivo model of aneurysm *112*
3.5.2 The use of Ang II administration in an ex vivo model of aneurysm *114*
3.5.3 Morphological changes *114*

3.5.4 Medial cell loss *115*
3.5.5 Extracellular matrix proteins and MMPs *116*
3.5.6 Other mouse models of aneurysm formation *120*

4 EFFECTS OF ANEURYSM-INDUCERS ON VASCULAR SMOOTH MUSCLE CELL FUNCTION IN VITRO 121

4.1 INTRODUCTION 121
4.1.1 A comparison of aortic and umbilical cord artery VSMCs *121*
4.1.2 The effect of Ang II or $CaCl_2$ on VSMC *121*
4.1.3 MMP expression in aneurysmal VSMCs *123*
4.1.4 Phenotype markers in aneurysmal VSMCs *123*
4.2 AIM 125
4.3 RESULTS 125
4.3.1 Characterisation of VSMCs isolated from human umbilical cord arteries *125*
4.3.2 VMSC morphology *127*
4.3.3 VSMC senescence *128*
4.3.4 Effect of Ang II or $CaCl_2$ stimulation on human umbilical cord artery VSMC MMP and TIMP mRNA expression *129*
4.3.5 Effect of Ang II or $CaCl_2$ stimulation on human umbilical cord artery VSMC MMP and TIMP protein expression *133*
4.3.6 Effect of Ang II or $CaCl_2$ stimulation on human umbilical cord artery VSMC phenotypic markers 135
4.3.7 Validation of in vitro phenotypic modulation within the ex vivo aneurysm model *136*
4.4 CONCLUSION 139
4.5 DISCUSSION 142
4.5.1 VSMC morphology in response to Ang II or CaCl2 ..... *142*
4.5.2 MMP mRNA and protein expression in response to Ang II or $CaCl_2$ *143*
4.5.3 TIMPs mRNA and protein expression in response to Ang II or $CaCl_2$ *145*
4.5.4 VSMC phenotype marker in response to Ang II or $CaCl_2$ *145*

5 EFFECTS OF ANEURYSM-INDUCERS ON ENDOTHELIAL CELL FUNCTION *IN VITRO* 148

5.7 INTRODUCTION 148
5.7.1 Endothelial cell dysfunction in aneurysms *148*
5.7.2 EC behaviour in an in vitro aneurysm model *150*
5.7.3 TIMP-3 ..... *150*
5.7.4 Losartan *151*
5.8 AIM OF THIS CHAPTER 153
5.9 RESULTS 153

5.9.1 Effect of Ang II on endothelial cell VE-cadherin expression within an ex vivo aneurysm model. 153
5.9.2 Effect of Ang II on endothelial cell VE-cadherin expression within an in vitro aneurysm model 155
5.9.3 Effect of prolonged Ang II-stimulation on endothelial cell behaviour and VE-cadherin expression within an in vitro aneurysm model. 159
5.10 CONCLUSION 170
5.11 DISCUSSION 171
5.11.1 Effects on EC behaviour wihin the ex vivo model of aneurysm *171*
5.11.2 Effects of Ang II and laminar flow on EC behaviour in vitro *172*
5.11.3 Effects of prolonged Ang II-infusion and laminar flow on EC behaviour in vitro *173*
6 VALIDATION OF AN *EX VIVO* MODEL OF ANEURYSM THROUGH MODULATING EITHER MMP OR TGF-B ACTIVITY 175
6.1 INTRODUCTION 175
6.1.1 Therapies for AAA *175*
6.1.2 Effect of MMP or TGF-β modulation on ex vivo aneurysm formation and regression *176*
6.2 AIM OF THIS CHAPTER 179
6.3 RESULTS 180
6.3.1 Validation of an ex vivo model of aneurysm formation *180*
6.3.2 Therapeutic testing in an ex vivo model of established aneurysm formation *192*
6.4 CONCLUSION 197
6.5 DISCUSSION 198
6.5.1 TIMP-3 ..... *198*
6.5.2 Inhibition of TGF-β signalling *200*
6.5.3 MMP-12 inhibitor *202*
7 GENERAL DISCUSSION 204
7.1 DEVELOPMENT AND CHARACTERISATION OF A HUMAN *EX VIVO* MODEL OF ANEURYSM 204
7.1.1 In vitro studies on VSMC *209*
7.1.2 In vitro studies on ECs *211*
7.2 LIMITATIONS 212
7.3 FUTURE WORK 213
7.3.1 Complete the studies on the ex vivo aneurysm model *213*
7.3.2 Effect of long-term ex vivo aneurysm model experiments (7, 14 or 28 days within bio-reactor) 213
7.3.3 Effect of laminar or directional flow to induce fusiform or saccular aneurysm *214*
7.3.4 Ang II administration on MMP expression in ex vivo bio-reactor cultured human umbilical cord arteries 214
7.3.5 In vitro studies on VSMC *214*
7.3.6 In vitro studies on ECs *215*

7.4 FINAL REMARKS 215

8 REFERENCES 219

List of figures

Figure 1.1: Aortic aneurysm and cerebral aneurysm 3
Figure 1.2: Aneurysm formation, progression and rupture. 4
Figure 1.3: Artery and vein structure 6
Figure 1.4: Healthy aorta versus aneurysmal aorta 7
Figure 1.5: Anatomy of thoracic and abdominal aorta and type of aneurysm 1
Figure 1.6: Two main methods of elective intervention for aneurysm repair 14
Figure 1.7: Schematic diagram of aneurysm pathogenesis 15
Figure 1.8: Domain structure of MMPs 18
Figure 1.9: Characteristics of contractile and synthetic VSMC phenotypes 21
Figure 1.10: VE-cadherin signal pathway 23
Figure 1.11: Schematic diagram of the major signalling pathways involved in aneurysm formation. 27
Figure 1.12: Aortic dissection 33
Figure 1.13 : Proposed mechanisms of angiotensin II signalling on abdominal aortic aneurysm formation and progression 37
Figure 1.14 : Classes of MMPs and their structure 42
Figure 2.1: Schematic representative of four-chamber slide experimental set-up 58
Figure 2.2: Feto-placental circulation 73
Figure 2.3: Human umbilical cord dissection and isolation of arteries 74
Figure 2.4: Arterial placement within the bio-reactor system 76
Figure 2.5: Ex vivo aneurysmal model 77
Figure 3.1: Diagram of the ex vivo aneurysm model 86
Figure 3.2: Laminar flow decreases umbilical cord artery medial thickness 88
Figure 3.3: Laminar flow does not affect human umbilical cord artery elastin content 89
Figure 3.4: Laminar flow does not affect human umbilical cord artery total vessel area 90
Figure 3.5: $CaCl_2$ pre-treatment significantly reduced medial thickness 92
Figure 3.6: $CaCl_2$ pre-treatment significantly reduced elastin content 93
Figure 3.7: $CaCl_2$ pre-treatment does not increase total vessel area 94
Figure 3.8: Insertion of umbilical cord arteries within a bio-reactor for 72 hours does not alter cell density 95
Figure 3.9: $CaCl_2$ pre-treatment significantly reduced human umbilical cord artery cell density 96
Figure 3.10: Representative images of ex vivo Ang II-infusion aneurysm model after 72h within a bio-reactor 99

Figure 3.11: Ang II administration significantly reduced human umbilical cord artery medial thickness 100
Figure 3.12: Ang II administration significantly reduced human umbilical cord artery elastin content 101
Figure 3.13: Ang II administration significantly increased human umbilical cord artery total vessel area 102
Figure 3.14: Ang II administration significantly decreased human umbilical cord artery medial cell content 103
Figure 3.15: Insertion of umbilical cord arteries within a bio-reactor for 72 hours does not affect fibrillar collagen content 104
Figure 3.16: Ang II administration significantly reduced human umbilical cord artery fibrillar collagen content 105
Figure 3.17: Effect of umbilical cord artery insertion within a bio-reactor for 72 hours with and without Ang II-infusion, on the expression of MMP-3, MMP-9 and MMP-12 107
Figure 3.18: Effect of umbilical cord artery insertion within a bio-reactor for 72 hours with and without Ang II-infusion, on the expression of MMP-10 and MMP-19 108
Figure 3.19: Comparison between the Ang II mouse model of aneurysm and the novel ex vivo human model of aneurysm 110
Figure 4.1: VSMC phenotype marker expression. 126
Figure 4.2: Human umbilical cord artery VSMC morphology in response to Ang II or CaCl2 127
Figure 4.3: $CaCl_2$ induced senescence of human umbilical cord artery VSMCs 128
Figure 4.4: Effect of Ang II or $CaCl_2$ on mRNA expression of MMPs in human umbilical cord artery VSMCs 130
Figure 4.5: Effect of Ang II or $CaCl_2$ on mRNA expression of TIMPs in human umbilical cord artery VSMCs 131
Figure 4.6: Effect of Ang II on mRNA expression of 36B4 and ELF1 in human umbilical cord artery VSMCs 132
Figure 4.7: Effect of Ang II or $CaCl_2$ on MMP protein expression in human umbilical cord artery VSMCs 134
Figure 4.8: Effect of Ang II or $CaCl_2$ on VSMC phenotypic marker expression in human umbilical cord artery VSMCs 135
Figure 4.9: Effect of ex vivo flow and Ang II-infusion on human umbilical cord artery protein expression of the VSMC phenotypic markers caldesmon and transgelin 137
Figure 4.10: Effect of ex vivo flow and Ang II-infusion on human umbilical cord artery protein expression of the VSMC phenotypic markers αSM-actin and SMMHC11 138
Figure 5.1: In vitro aneurysm model for evaluating EC behaviour 152

Figure 5.2: Effect of Ang II on endothelial cell VE-cadherin expression in ex vivo human umbilical cord artery 154
Figure 5.3: Effect of Ang II on HUVEC cell membrane VE-cadherin expression 156
Figure 5.4: Effect of Ang II on HUVEC intracellular VE-cadherin expression 157
Figure 5.5: Effect of Ang II on HUVEC cell area 158
Figure 5.6: Effect of laminar flow and Ang II on HUVEC proliferation 161
Figure 5.7: Effect of laminar flow and Ang II on HUVEC susceptibility to apoptosis 162
Figure 5.8: Effect of laminar flow and prolonged Ang II stimulation on HUVEC cell membrane VE-cadherin expression 164
Figure 5.9: Effect of laminar flow and prolonged Ang II stimulation on HUVEC F-actin expression 165
Figure 5.10: Effect of laminar flow and prolonged Ang II stimulation on HUVEC co-expression of F-actin and VE-cadherin 166
Figure 5.11 Effect of laminar flow and prolonged Ang II stimulation on HUVEC cell area . 167
Figure 5.12: Effect of laminar flow and prolonged Ang II stimulation on HUVEC intracellular β-catenin accumulation 169
Figure 6.1: TGF-β classical signalling pathway 179
Figure 6.2: Co-administration of TIMP-3 reduced Ang II-induced medial thinning 181
Figure 6.3: Co-administration of TIMP-3 prevented Ang II-induced loss of elastin content 182
Figure 6.4: Co-administration of TIMP-3 suppressed Ang II-induced dilatation 183
Figure 6.5: Co-administration of a TGF-β NAb reduced Ang II-induced medial thinning 185
Figure 6.6: Co-administration of a TGF-β NAb prevented Ang II-induced loss of elastin content 186
Figure 6.7: Co-administration of a TGF-β NAb suppressed Ang II-induced dilatation 187
Figure 6.8: Co-administration of RXP470 reduced Ang II-induced medial thinning 189
Figure 6.9: Co-administration of RXP470 prevented Ang II-induced loss of elastin content190
Figure 6.10: Co-administration of RXP470 suppressed Ang II-induced dilatation 191
Figure 6.11: Effect of rTIMP-3, TGF-β NAb, or RXP470 co-administration on six-day Ang II-induced ex vivo aneurysm medial thickness 193
Figure 6.12: Effect of rTIMP-3, TGF-β NAb, or RXP470 co-administration on six-day Ang II-induced ex vivo aneurysm elastin content 194
Figure 6.13: Effect of rTIMP-3, TGF-β NAb, or RXP470 co-administration on six-day Ang II-induced ex vivo aneurysm dilatation 195
Figure 6.14: Effect of rTIMP-3, TGF-β NAb, or RXP470 co-administration on six-day Ang II-induced ex vivo aneurysm cell density 196
Figure 7.1: Bio-reactor set-up of ex vivo aneurysm model testing 208
Figure 7.2: Main findings from the ex vivo aneurysm model 216

List of tables

Table 2.1: Media composition for Smooth Muscle Cell Growth Medium 2 51
Table 2.2: Media composition for Serum Free DMEM 52
Table 2.3: Media composition for 10% FBS/DMEM 52
Table 2.4: Media composition for Endothelial Cell Medium 53
Table 2.5: Media composition for Endothelial Cell Medium 53
Table 2.6: Media composition for Hepes-buffered RPMI 54
Table 2.7: Programme used for RT-QPCR reaction 61
Table 2.8: List of primers used for QPCR 62
Table 2.9: List of quantitec primers used for QPCR 63
Table 2.10: List of primary antibodies used for western blotting 65
Table 2.11: List of secondary antibodies used for western blotting 65
Table 2.12 : EdU-Click 488 Kit ® reaction cocktails 66
Table 2.13: List of the antibodies (A primary, B secondary) for fluorescent ICC 69
Table 2.14: List of the antibodies (A primary, B secondary) CC3 70
Table 2.15: Staining protocol for EVG 80
Table 2.16: Staining protocol for H&E 81
Table 4.1 Table summarising the QPCR and Western blotting data from human umbilical cord artery VSMCs 140
Table 4.2: Table summarising the QPCR and Western blotting data from human umbilical cord artery VSMCs (in vitro) 141
Table 4.3:Table summarising the Western blotting data from human umbilical cord artery (ex vivo) 141
Table 71: The effect of the bio-reactor system without and with Ang II-infusion on human umbilical cord arteries 217

Abbreviations

18F-NaF: fluorine-18–sodium fluoride

3Rs: Replacement, Reduction, and Refinement

A1AT: alpha-1 antitrypsin

AAA: abdominal aortic aneurysm

AAC: abdominal aortic calcification

ACC/AHA: American College of Cardiology/American Heart Association

ACE-inhibitors: angiotensin-converting enzyme-inhibitors

ADAMTS: ADAM with thrombospondin motifs

Ang II: angiotensin II

Apoe: apolipoprotein E

Apoe−/−: apolipoprotein-E-deficient

ARB: angiotensin II receptor blocker

AT1R: angiotensin II type 1 receptor

AT2R: angiotensin II type 2 receptor

BAV: bicuspid aortic valve

BCA: bicinchoninic Acid

b-FGF: basic fibroblast growth factor

BMP1: bone morphogenetic protein 1

BMPI/ TLL: bone morphogenetic protein 1/tolloid-like MMP

BSA: bovine serum albumin

CAA: calcified AAA

$CaCl_2$: calcium chloride

CCR2: C-C chemokine receptor type 2

CD4+: cluster of differentiation 4+

CD40L: CD40 ligand

CD8+: cluster of differentiation 8+

COX-2: cyclo-oxygenase-2

CRP: c-reactive protein

CT scanning: computed tomography scanning

Ct: cycles to threshold

CTA: calcified TAA

DAPI: 6-diamidino-2-phenylindole

DMEM: dulbecco's modified Eagle's Medium

DMSO: dimethyl sulphoxide

DPBS: Dulbecco's Phosphate Buffered Saline

ECM: extracellular matrix

EC: endothelial cell

EEL: external elastic lamina

ET: endothelin

EVAR: endovascular repair

EVG: elastic van gieson

FBN1: fibrillin 1

FBS: foetal bovine serum

GDP: guanosine diphosphate

GTP: guanosine triphosphate

H&E: haematoxylin and eosin

HCL: hydrochloric acid

Hcy: homocysteine

HPLC: high pressure liquid chromatography water

HRP: horseradish peroxidase

HUVEC: human umbilical vein endothelial cell

ICC: immunohistochemistry

IEL: internal Elastic Lamina

IFN-γ: interferon gamma

IL-10: interlukin-10

IL-13: interlukin-13

IL-4: interleukin 4

IL-5: interlukin-5

ILs: Interleukins

IMS: industrial Methylated Sprits

JNK: c-Jun N-terminal kinases

KO: knock out

LDL: low-density lipoprotein

MASS: multicentre Aneurysm Screening Study

MCP-1: monocyte chemotactic protein-1

MI: myocardial infarction

MIF: macrophage migration inhibitory factor

MMP: matrix metalloproteinase

MPO: myeloperoxidase

MR: magnetic resonance

MRI: magnetic resonance imaging

mRNA: messenger RNA

NC3R: National Centre for the Replacement, Refinement and Reduction of Animals in Research

NF-κB: nuclear factor kappa-light-chain-enhancer of activated B cells

NHS: National Health Service

NK: natural killer cells

NO: nitric oxide

OPG: osteoprotegerin

OPN: osteopontin

OS: open surgery repair

PAF: platelet-activating factor

PCPE: pro-collagen C-terminal proteinase enhancer

PCR: polymerase chain reaction

PDGF-BB: platelet-derived growth factor-BB

PEX: hemopexin-like domain

PGI2: prostacyclin

PKC:protein kinase C

PKD1: polycystic 1

PLA_2: phospholipase A_2

PLC: phospholipase C

PLD: phospholipase D

PPAR-γ: peroxisome proliferator-activated receptor-γ

RANKL: receptor activator of nuclear factor kappa B ligand

RAS: renin-angiotensin system

RECK: reversion-inducing-cysteine-rich protein with Kazal motif

Rho-GEF: Rho guanine exchange factor

RPMI: Roswell Park Memorial Institute

rTIMP-3: recombinantTIMP-3

SEM: standard error of the mean

SFM: serum free Medium

SMC: smooth muscle cell

SMMHC11: smooth muscle myosin heavy chain 11

SMα-actin: smooth muscle α-actin

sPBS: sterile Dulbecco Phosphate Buffer Saline

sPBS: sterile Phosphate Buffer Saline

sPLA2-X: secretory phospholipase A2

sPLA2-X: secretory phospholipase A2

TAA: Thoracic aortic aneurysm

Tc1: type-1 CD8+ T-cytotoxic cell

Tc2: type 2 CD8+ T-cytotoxic cells

TFPI-2: tissue factor pathway inhibitor-2

TGF-β NAb: transforming growth factor beta neutralising antibody

TGF-β: transforming growth factor beta

Th1: CD4+ type 1 T helper cells

Th2: CD4+ type 2 T helper cells

TIMP-3: tissue inhibitor of metalloproteinases 3

TLL1: tolloid-like protein 1

TNF-α: tumour necrosis factor alpha

tPA: tissue plasminogen activator

uPA: urokinase plasminogen activator

VEGF: vascular endothelial growth factor

VSMC: vascular smooth muscle cell

WT: wild type

CHAPTER 1

1 General introduction

1.1 Clinical impact of aneurysm

The formation and subsequent rupture of an aneurysm represents a significant cause of premature mortality in the UK and worldwide. Every year, 4,000 deaths are caused by aortic aneurysms in England and Wales, and more the 175,000 death throughout the world [1]. It is difficult to get an accurate measure of the prevalence of aneurysms however, as aneurysms are asymptomatic before rupture. It is estimated that the prevalence of abdominal aortic aneurysms (AAA) is up to 8% of men over the age of 65, and up to 2.2% of women [2] [3]. The mortality for patients with AAA is 65–85% [1]. Aneurysm repair is achieved with surgical intervention in an attempt to prevent future rupture, however sometimes the surgical intervention is associated with high mortality. As previously mentioned, AAA are clinically silent and therefore difficult to detect, accordingly the National Health Service (NHS) have adopted a screening programme for all men aged 65 or above, who are the most at risk of AAA rupture. Such screening programmes can help to detect aortic dilatation and reduce the associated mortality, as shown in the UK [4]. According to the Multicentre Aneurysm Screening Study (MASS), aortic aneurysms are mainly found in the thoracic and abdominal segments of the aorta (Figure 1.1A)

1.2 Definition of aneurysm

An aneurysm can be described as a localised pathological dilatation of an artery due to structural degenerative changes of the wall. Arteries are blood vessels within the body which have the function of transporting oxygen-rich blood to all tissues, and they harbour thicker walls than veins in order to withstand normal arterial blood pressure [5]. However, the arterial wall can be weakened, or damaged, as excessive force exerted by the blood can push outwards, creating a bulge area called an "aneurysm". Aneurysms can develop in any blood vessel of the human body, but most of them occur either within the aorta, which is the largest artery in the body (Figure 1.1A) or in the cerebral arteries, which are rather small arteries (Figure 1.1B). Aortic aneurysms are principally found Multicentre Aneurysm Screening Study (MASS) within the abdominal and thoracic aorta and are respectively called AAA and TAA. Although the specific cause of AAA is unclear, several risk factors are associated with

aneurysm development, expansion, and rupture; in particular, male gender and increasing age and are the most dominant risk factors. Pathologically, aneurysms are characterised by ongoing chronic inflammation observed as accumulation of lymphocytes and macrophages and thinning of the media through loss of vascular smooth muscle cells (VSMCs) and proteolytic destruction of elastin and collagen. Moreover, there is marked vessel dilatation and neovascularization. Pharmacological therapies are utilised for small aneurysms (less than 5.5 cm in diameter) in an attempt to limit their progression, although these do not directly target the aneurysm but potential contributors to expansion such as elevated blood pressure. However, when the diameter of the aorta has dilated greater than 5.5 cm, elective surgical repair is adopted despite mortality percentages remaining high during and after surgery [6]. Another anatomical district seriously affected by aneurysm formation is the cerebral circulation (Figure 1.1B). Cerebral aneurysms occur in the much smaller cerebral circulation (Figure 1.2) when compared to the aorta, with different rates of anatomical distribution. However, they also have dramatic clinical consequences as they are associated with either stroke due to thrombosis, or rupture leading to stroke or sudden death [7].

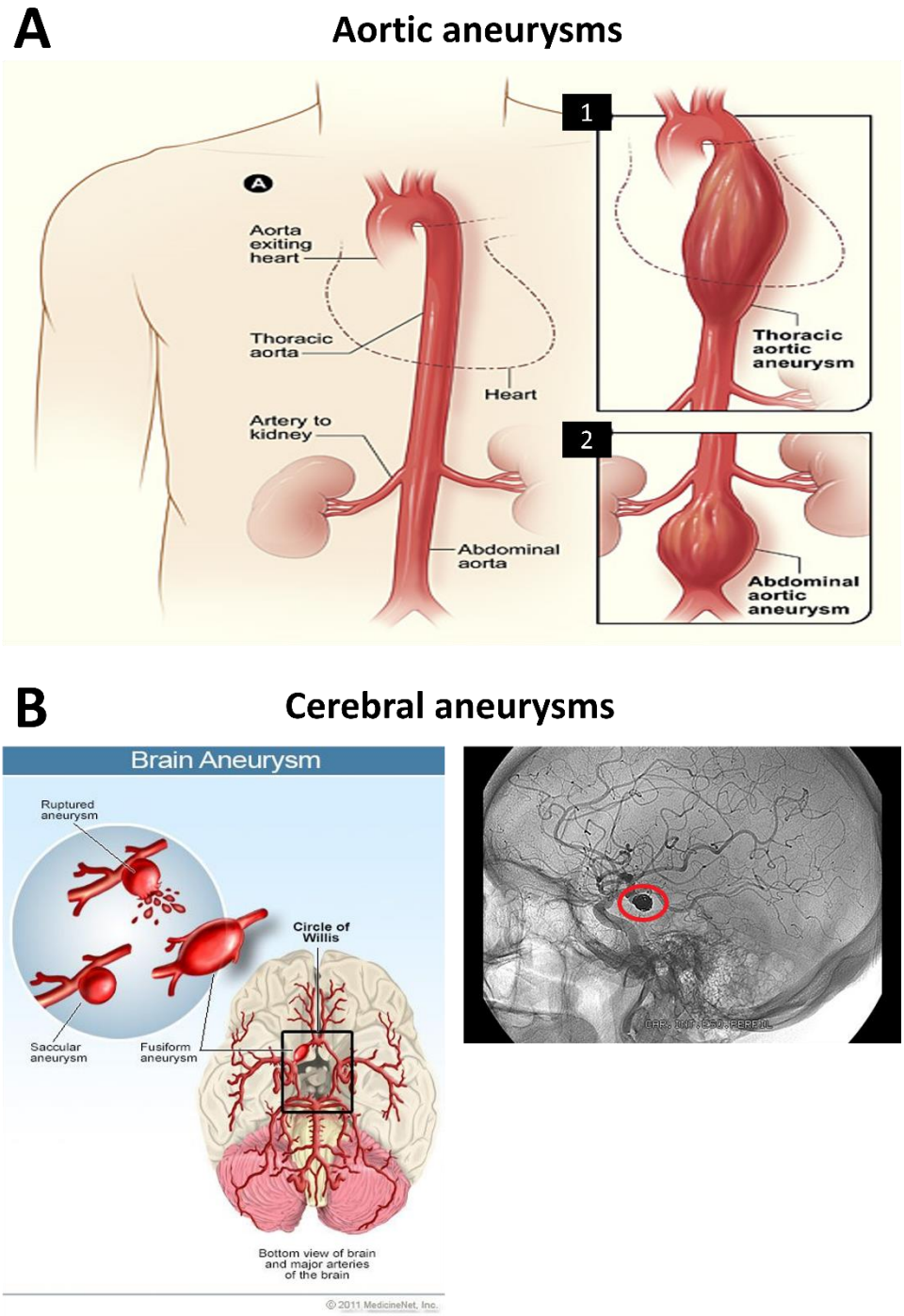

Figure 1.1: Aortic aneurysm and cerebral aneurysm

A The aorta is the largest artery in the body, and aneurysms that develop along the aorta are known as aortic aneurysms. Aortic aneurysms are sub-divided into those located within the abdominal aorta (1), and those within the thoracic aorta (2).
B Four major blood vessels join at the Circle of Willis at the bottom of the brain and from there smaller arteries supply the brain with oxygen and nutrients.
Artery junction points may become weak, causing a ballooning of the blood vessel wall and can potentially form a small saccular or fusiform aneurysm.

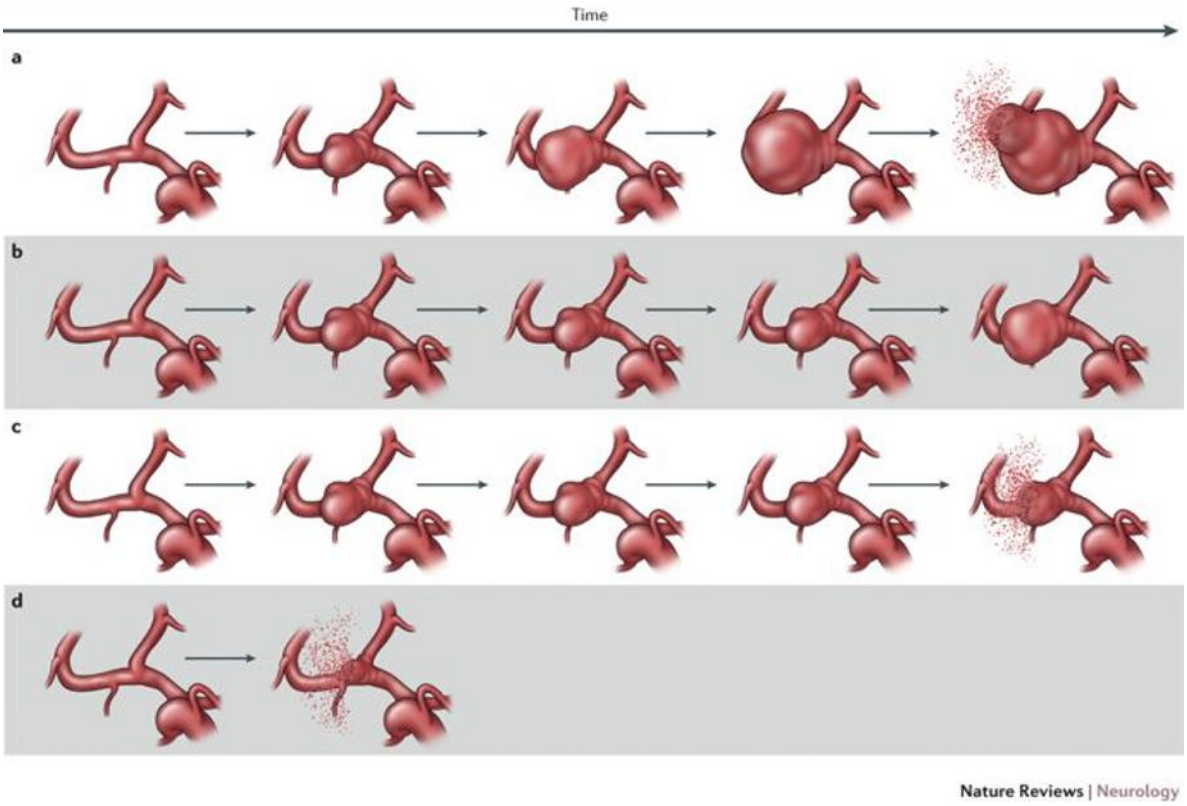

Figure 1.2: Aneurysm formation, progression and rupture.

The cohort studies suggested that intracranial aneurysms can develop and have different outcomes.
a Growth until rupture
b Long-term stability followed by growth without rupture
c Long-term stability followed by rupture without any growth
d Rapid growth and consequently rupture
Figure taken from Nima Etminan et al [7]

1.2.1 Structure of a normal blood vessel

Normal healthy blood vessels consist of three different layers called respectively tunica intima, tunica media and tunica adventitia, which are important for maintaining the structure and function of the arterial wall, as well as other arteries and veins (as illustrated in Figure 1.3). These three layers are vital for the integrity and function of a blood vessel. The tunica intima, nearest the lumen of the vessel, consists of a single layer of endothelial cells (ECs) and a thin layer of sub-endothelial connective tissue. The intima is separated from the media by a thin sheet of elastic tissue called the internal elastic lamina (IEL). Following the IEL, is the media which is the thickest layer and important for structural support, vasoreactivity and elasticity. It is composed of VSMCs, elastic fibres and connective tissue, and this histological composition differs between the major vessels of the circulatory system; in arteries it is much ticker than in veins in order to enable the vessel to transport blood at higher pressure, the VSMCs enable the vessel to expand and contract according to the blood flow. A dense elastic membrane called the external elastic lamina (EEL) separates the media from the adventitia. The adventitia is made up of collagen fibres, few elastic fibres and some VSMCs. Small autonomic nerves and blood vessels (vasa vasorum) are also present within the adventitia [8, 9]. As well as having thinner walls, medium and large veins have venous valves to prevent the back flow of blood.

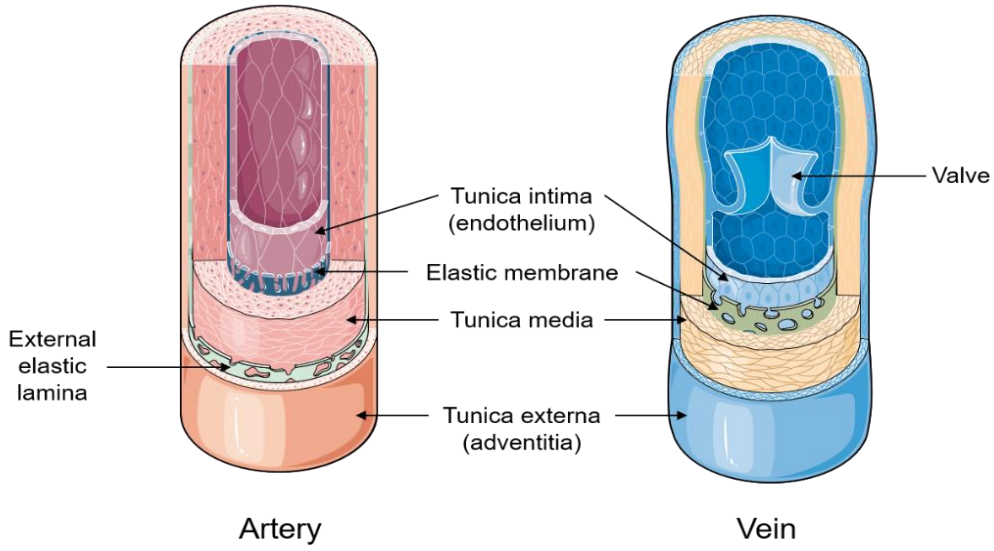

Figure 1.3: Artery and vein structure

Arteries (left side) and veins (right side) are composed of three layers, a tunica intima consisting of endothelial cells, a tunica media composed of vascular smooth muscle cells (thicker in artery), and a tunica adventitia composed of collagenous extracellular matrix and blood vessels. The internal elastic lamina separates the tunica intima and tunica media, the external elastic lamina separates the tunica media and tunica adventitia. Veins also have valves to ensure blood flow in one direction. Figure made using elements from https://smart.servier.com/

1.2.2 Aetiology of aneurysm and clinical implication

All arteries consist of three layers: tunica intima, media and adventitia. Maintaining a healthy aorta is important. Typical risk factors may include smoking, ageing, family history, high blood pressure and atherosclerosis which are thought to contribute to weakening the vessel wall [10]. As illustrated in Figure 1.4 (A and B) when blood flows through a damage vessel (red arrow), the blood pressure causes a small area of dilatation that is identified as an aneurysm. As shown in Figure 1.4 (C and D) in a healthy artery there is a thick medial layer and an intact IEL (blue), whereas in an injured vessel (D) there is a thinning of the medial layer and destruction of the IEL accompanied by dilatation of 50% of its normal diameter [11].

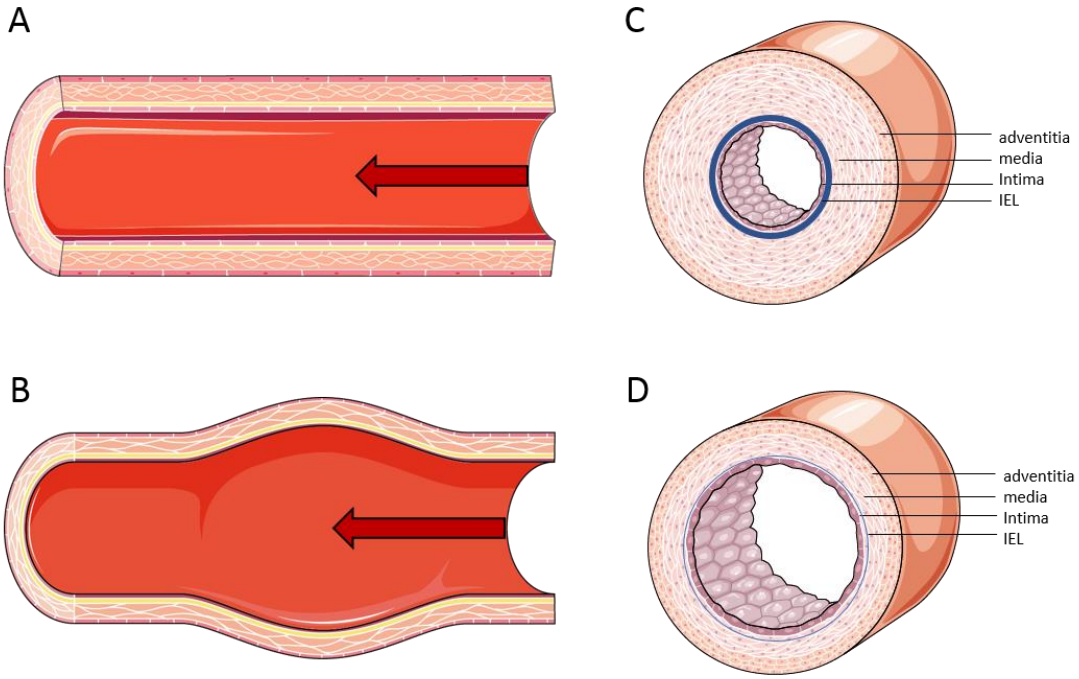

Figure 1.4: Healthy aorta versus aneurysmal aorta

A Healthy artery with blood (red arrow) flowing through.
B Injured artery with blood flow (red arrow) that pushes the outside creating a bulge called an aneurysm.
C Cross-section of a healthy artery with an inner layer of endothelial cells (intima), an intact internal elastic lamina (blue), a thick medial layer and an adventitial outer layer.
D Cross-section of an aneurysmal artery, with a thin layer of endothelial cells (intima), a thinned and damaged internal elastic layer (light blue), a markedly thinned medial layer and an adventitial outer layer. Figure made using elements from https://smart.servier.com/

Aneurysms are a multifactorial disease in which both genetic and environmental factors play a prominent role [12]. Although the specific cause of arterial aneurysms is uncertain, a number of factors could contribute to weaken a portion of the arterial wall increasing an individual's risk of developing an aneurysm. Men are around four times more likely to be diagnosed with an aneurysm than women, and this risk increases by 40% every five years after the age of 65 years [13]. Moreover, a study revealed aneurysms are more prevalent among whites than blacks, Asians, and Hispanics [14]. Smoking is also considered a strong risk factor for the initiation and progression of aneurysms, attributed to alterations in the inflammatory response of the aorta wall, alongside increased matrix degradation due to an imbalance between proteases (such as matrix metalloproteinases (MMPs) and protease inhibitors (for example α1 antitrypsin) [15]. Moreover, there is an association of both smoking duration and amount with the prevalence of aneurysms [16]. Other aneurysm-associated risk factors include atherosclerosis, hypertension, hyperlipidaemia, and family history of the disorder [17]. In particular, it has been shown that people with a family history of aneurysms have a 30% increased risk of developing aneurysms and have a higher risk of aneurysm rupture and developing an aneurysm at a younger age [18]. Furthermore, another study revealed that the growth rate of small aneurysms in patients with a family history of aneurysm is doubled compared to patients with no evidence of family history [19] [20]. Thoracic arterial aneurysms (TAAs) display cystic medial degeneration alongside inflammation, proteolysis, reduced survival of VSMCs and elastic fibre degeneration, leading to damage and destruction of the arterial wall and aneurysm progression. Medial degeneration is involved in certain connective tissue disorders such as Marfan syndrome or Familiar TAA syndrome [21] [22]. Ascending arterial aneurysms are associated with bicuspid arterial valve (BAV) which is a congenital heart deformity. Different groups have showed the presence of cystic medial necrosis in patients with BAV disease, which is characterised by VSMC apoptosis, elastic fibre fragmentation, and accumulation of inflammatory cells [23]. In addition, a mutation in fibrillin 1 (FBN1), a gene required for microfibril formation and elastin deposition, underlies Marfan syndrome, patients of which prematurely develop aneurysms and is also linked to increased risk of BAV [23]. Inflammatory conditions, such as giant cell arteritis and Takayasu arteritis, may cause TAAs, as well as untreated infections, such as syphilis or salmonella [24]. Aneurysms often grow slowly and are usually silent, until they further expand and rupture, making them difficult to detect. When symptoms do arise, patients usually present with constant abdominal, back or flank pain, which lasts hours to days. Some patients report with a palpable abdominal mass. Occasionally, AAAs can cause symptoms due to local compression, inclusive of nausea, early satiety, and urinary symptoms. Moreover, aneurysms with associated symptoms have higher risk for rupture, which is then associated with high

mortality rates. Due to the asymptomatic nature of most AAAs, diagnosis is commonly a result of screening or during a routine examination with abdominal palpation. However, the sensitivity of detection depends on random criteria including examiner's experience, aneurysms size, and patient's size [25]. Unruptured intracranial aneurysms are also silent, although at times they may be associated with aspecific symptoms such as headache, migraine or seizures. Their rupture is associated with dramatic conditions such as ictus (stroke) or sudden death [7]. Aneurysms are sometimes associated with chronic infections such as syphilis (aortic aneurysms) or mycosis (cerebral aneurysms), therefore the use of antibiotics in such infective cases may be beneficial. The best screening test of choice for each anatomical type of aneurysm depends on the size and location. Ultrasound scan is an accurate way to measure the size of an aneurysm with the advantage of being inexpensive and non-invasive. Computed tomography scanning (CT scanning) also has high accuracy in determining the size and extent of an aneurysm [26]. Although largely asymptomatic, patients with TAA or AAA report: coughing, hoarseness, or difficulty breathing due to a local mass compressing the trachea or bronchus, dysphagia through oesophagus compression, and rarely chest or back pain from compression of other thoracic structures [19]. The lethal consequences of TAA are aortic dissection or rupture which induces similar symptoms as stroke, including severe chest or upper back pain, loss of consciousness, shortness of breath, sudden difficulty in speaking, loss of vision, and unilateral paralysis. A ruptured arterial aneurysm can lead to life-threatening internal bleeding [27]. In general, larger aneurysms exhibit a greater risk of rupture [28]. Similar to AAAs, diagnosis of TAAs is difficult because often there are no symptoms, and often the condition goes undiagnosed until a rupture occurs. TAAs are evident on chest x-ray, however CT scanning and magnetic resonance (MR) angiography are usually preferred [29]. Patients suspected of TAAs are subjected to a CT scan of the entire aorta, this is a robust technique to detect aneurysm size. Magnetic resonance imaging (MRI) is a valid alternative to CT in patients with high probability of harbouring a thoracic aneurysm [29].

1.2.3 Anatomical sites of aneurysm

Aneurysms are a localized bulge in the wall of a blood vessel with a diameter at least 50% greater than the normal lumen diameter of the artery. As shown in Figure 1.5 aneurysms can develop anywhere along the aorta, and are sub-divided into those located within the abdominal aorta, and those within the thoracic aorta [30]. Abdominal aneurysms are the most common aneurysm, with a prevalence of 5-6% for men and 1-2% for women, in people older than 65 years, whereas the prevalence of thoracic aneurysms is five-fold lower [31]. Thoracic aneurysms are observed within the aortic root, ascending aorta, the aortic arch, and the descending aorta. Sixty percent of TAA develop in the aortic root and ascending aorta, 40% cover the descending aorta whereas only 10% involve the arch and the thoracic-abdominal region [19]. AAAs are located within the supra-renal region where they involve the visceral arteries, para-renal area if they develop at the beginning of the renal arteries, and finally infra-renal if they begin lower than the renal arteries [12]. The pathogenesis of AAAs and TAAs is distinct.

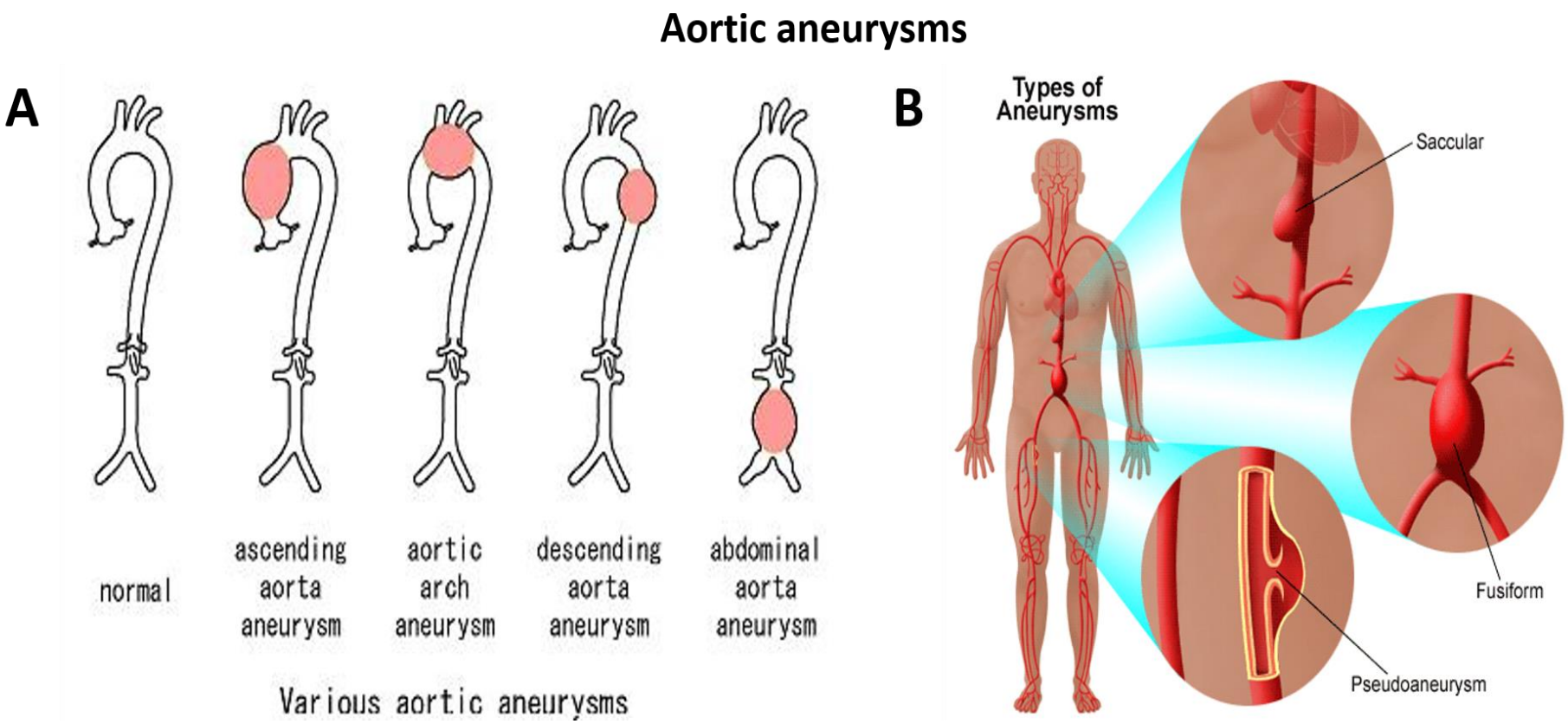

Figure 1.5: Anatomy of thoracic and abdominal aorta and type of aneurysm

A Normal aorta versus thoracic aorta aneurysm (ascending aortic arch and descending aorta), and abdominal aorta aneurysm.
B Type of aneurysm: saccular aneurysm that appears on one side of the aorta, fusiform aneurysm that appear as symmetrical bulges around the circumference of the aorta and pseudoaneurysm (also known as a false aneurysm) where the dilatation does not involve all the layer.

1.2.4 Current therapies

Therapies for aneurysms depend on a range of factors such as size and location and patient-specific factors including age, other risk factors, or additional existing conditions that could increase the risk during surgical intervention. Small aneurysms (less than 5.5 cm in diameter) are classified as low risk for rupture, and therefore classically treated with medicines which reduce shear stress within the aorta and control blood pressure [32]. For example, beta-blockers can decrease the rate at which aneurysms grow by reducing blood pressure and the contractility of the left ventricle [32]. Statins are also considered a good therapy due to their anti-inflammatory affects, as well as their ability to reduce the expression of MMPs, proteases capable of reducing the integrity of the arterial wall during the pathogenesis of aneurysms [6]. Additionally, antibiotic therapy has also been evaluated for reducing aneurysm expansion rate by through actions which inhibit proteases and inflammation [16]. Moreover, a current treatment for several cardiovascular disease, including AAA, is the use of angiotensin-converting enzyme-inhibitors (ACE-inhibitors) and Ang II receptor blockers (ARBs) [6, 32]. A study conducted by Vorkapic and colleagues demonstrated the use of Imatinib, a selective inhibitor of several tyrosine kinase enzymes, as a potential drug for aneurysm treatment due to its ability to reduce vascular inflammation within the aortic wall, in particular they showed a significant decrease in the aortic diameter and wall thickness in mice treated with the drug compared to controls [33]. A previous study showed that zinc can increase the expression of zinc finger protein A20, whose expression was lower in aneurysm models compared to controls [34]. Moreover, zinc can perturb nuclear factor kappa-light-chain-enhancer of activated B cells (NF-κB) activation by reducing the expression of the subunit NF-κB p65; it can also reduce inflammation, aortic dilation, and prevent the degradation of elastin, suggesting a new approach to treat aneurysms [34]. Finally, lifestyle changes have been proposed to prevent aneurysm progression and rupture. As mentioned above, smoking is considered a risk factor for aneurysm progression, and guidelines of the American College of Cardiology/American Heart Association (ACC/AHA) in 2005 recommended smoking cessation for people with a positive family history of aneurysm [35].

1.2.5 Surgical and percutaneous interventions of aneurysms

Repair of aortic or cerebral aneurysms is indicated when there is an obvious dilatation of the arterial diameter. This can be adjudged through a cut off >5.5cm in aortic aneurysms. For cerebral aneurysms this is more challenging as the critical difference between health and risk of rupture may be in the order of 1-2mm only. Currently, two methods of elective/urgent intervention are available for aortic and cerebral aneurysms including either open surgery or a percutaneous endovascular approach (Figure 1.6). Surgical repair is adopted when the diameter of the aorta is greater than 5.5 cm as the risk of rupture outweighs the complications of surgery. Currently two main methods of elective intervention are used; open repair and endovascular surgery (as shown in Figure 1.6). Open surgery repair (OS), involves a large incision in the chest (for TAA) or in the abdomen (for AAA), after which the damaged section of the aorta is removed and replaced with a graft which is a synthetic tube. This allows blood to flow through the graft, reducing pressure on the damaged wall of the aorta by bypassing the area of the aneurysm [14]. This procedure requires a recovery period of 2–3 months and it is associated with a higher risk of mortality [35]. On the other hand, endovascular repair (EVAR), involves repair of the aneurysm from the inside of the damaged blood vessel, through the insertion of a graft within the aneurysm via incisions in the groin and using X-rays to guide the graft into place. This is considered a less invasive procedure because it does not interfere with the circulation as much as open surgery, and importantly the recovery period is greatly reduced [16]. Considering outcomes, a study involving patients undergoing AAA repair involving 50 different surgeons within 11 different hospitals from 2003 to 2007, analysed the predicted mortality, depending on several risks presented. One-year mortality rates after open repair covered a wide range from 1% to 67%, due to the accumulation of risk factors [36]. Similarly, mortality rates in patients that underwent endovascular repair ranged from 3.6% to 23% [36]. Another study showed that long term survival (ten years after surgical repair) after open repair was 59% [37]. Comparably, long-term survival rates after open and endovascular procedures were similar, taking associated risk factors such as age, anticoagulation therapies, and statin use into account, whereas short-term survival linked to EVAR was higher within the first 2 years of repair [37]. Importantly, the treatment modality (EVAR or OS) did not influence long-term clinical outcome, however the mortality rates remain high and account for 2% of all deaths within the UK [36]. Overall, both procedures are associated with high mortality risk, therefore treatments that attenuate aneurysm progression and rupture would dramatically reduce the mortality rate related to both surgical procedures alongside the aneurysm itself.

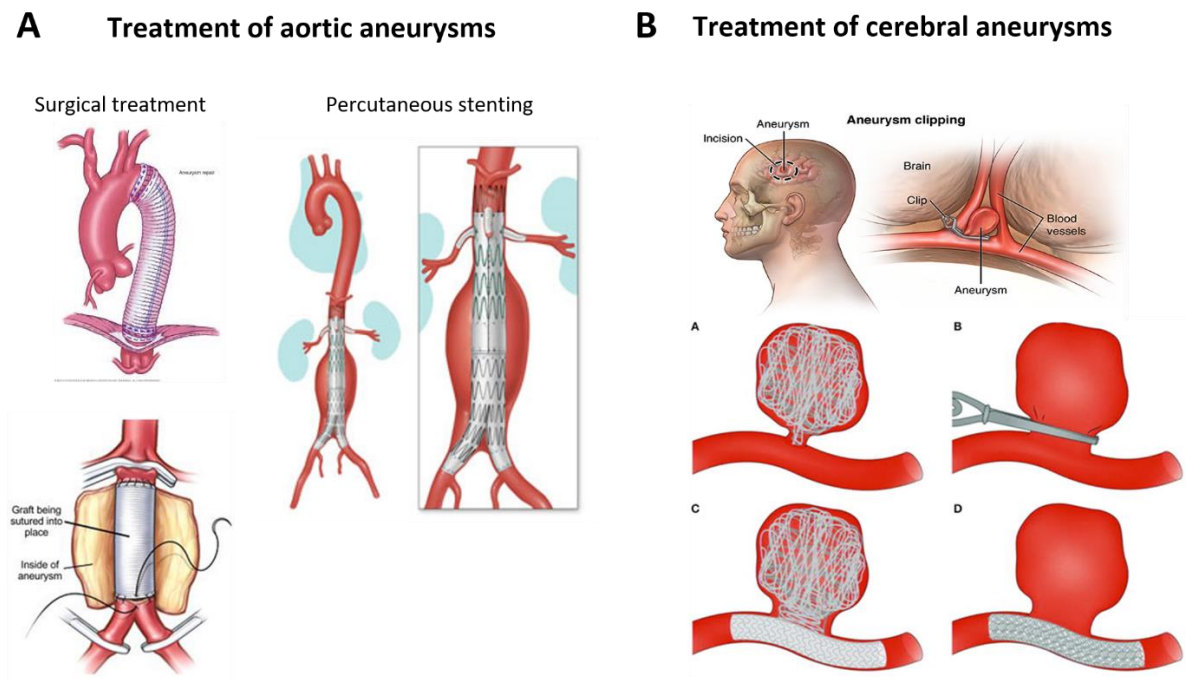

Figure 1.6: Two main methods of elective intervention for aneurysm repair

(A) On the left-side two methods of intervention for aortic aneurysms including either surgical treatments or percutaneous endovascular approach
(B) On the right-side, Surgical and endovascular treatments for cerebral aneurysm thrombosis.
A: Endovascular coiling of the aneurysm sac.
B: Surgical clipping of the aneurysm neck.
C: Endovascular treatment combining use of coils and a stent.
D: Endovascular treatment with a flow diverter. Taken from Perrone et al. (2015).

1.3 Pathogenesis and composition

Aneurysms are characterised by structural disintegration of the aortic wall, consequent gradual aortic dilatation and ultimately rupture (as summarised in Figure 1.7). Multiple factors are implicated in the pathogenesis of aortic aneurysms, which cause destructive changes to the connective tissues of the media and adventitia of the aortic wall, driving aneurysm formation and eventually rupture. In the first instance, the link between aneurysm formation and rupture is influenced by factors such as aneurysm size, expansion rate, gender, age, smoking, and family history [16]. Nonetheless, the major processes implicated in the development of aneurysms are extracellular matrix (ECM) degeneration through degradation of elastin and collagen, the accumulation of inflammatory cells throughout all layers of the aortic wall, and associated secretion of inflammatory factors including cytokines, immunoglobulins and chemokines. In most cases of aneurysmal disease, the pathogenesis is further characterised by medial neovascularization and reduced VSMC number through apoptosis [38]. MMPs and other proteases are produced from macrophages and VSMCs and can influence all the aforementioned processes. Lastly, calcification also predominates within aneurysms and represents a manifestation of inflammation of the aortic wall [39] .

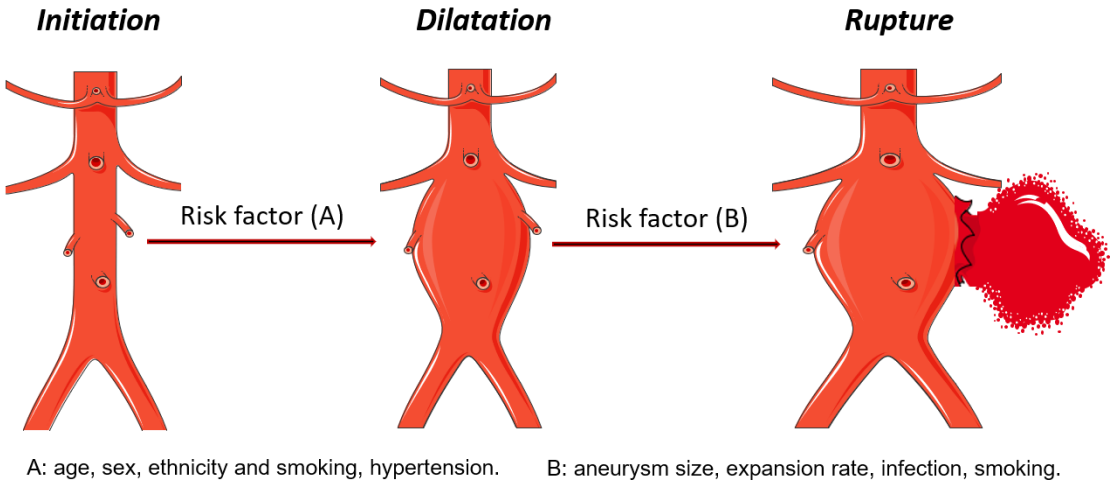

Figure 1.7: Schematic diagram of aneurysm pathogenesis

The pathogenesis of an aneurysm (initiation-progression-rupture) is affected by several risk factors and biological processes. A, the risk of AAA formation is increased with age, smoking hypertension and Caucasian ethnicity. B, the risk factors linked to further dilatation and consequently rupture depends on aneurysm size, rate of expansion, infection and smoking.
Figure made using elements from https://smart.servier.com/

1.3.1 Elastin and collagen

Elastin and collagen are the most abundant ECM proteins within the blood vessel wall and they impart the elastic properties, strength and mechanical resistance to the vessel wall [40]. Collagen is the principal structural protein present in the connective tissue and it is an aggregate of three parallel polypeptide strands in a left- hand helix conformation, termed alpha chains, and are stabilised by hydrogen bonds that form a structure called tropocollagen [41]. Collagen fibrils are stable structures formed by the aggregation of several subunits of tropocollagen which are approximately 300nm long and 1.5nm in diameter. Twenty-nine types of collagen have been identified in humans, although 80–90% of the collagen within the body consists of types I, II, and III [41, 42]. In particular, in the aortic wall collagen I, which represents 70% of the total collagen content, is predominantly expressed in the adventitia and intima, whereas type III collagen is found in the media and tends to be deposited along the elastic lamina [43]. Several studies have demonstrated decreased collagen content within aortic aneurysms, and therefore collagen loss is considered to contribute to the instability of the aorta wall. ECM degradation is prevalent during aneurysm formation and progression, driven by a localised increase in protease expression including MMPs and cysteine proteinases which can directly cleave collagens I and III, permitting further proteolysis by other proteases targeting denatured collagen. Increased collagen degradation combined with a reduction in collagen synthesis and deposition have been linked to aneurysm progression. Products released during collagen catabolism have been purported as aneurysm biomarkers, in particular PIIN, the amino terminal pro-peptide of type III procollagen. Indeed, serum from patients with aortic aneurysms contained significantly elevated PIIN levels compared to control subjects, although the serum level of PICP, the carboxyterminal pro-peptide of type I procollagen, was similar between groups [42]. A further study suggested that structural alteration within the aortic wall may be related to ageing, as collagen III levels were reduced in the abdominal aorta of older subjects compared to younger controls, whereas the quantity of collagen I was unchanged [40].

Elastin as its name suggests, is a highly elastic protein of the connective tissue usually organized in elastic fibres within the medial layer of the aortic wall. The interaction between elastic fibres, collagen and VSMCs provides a solid structure called the lamellar unit, which is necessary for the biomechanical and elastic properties of the arterial wall [44]. This structure can become unstable and weaken with ageing, hypertension and aneurysm progression, releasing elastin-derived peptides into the circulation via the action of elastin proteolysis [42] A screening study revealed that patients with aneurysms greater than 6cm in diameter which have undergone rupture, exhibit higher levels of elastin-derived peptides compared to

aneurysms with no rupture, implying that increased elastin degradation is strongly linked to aneurysm rupture. The primary proteolytic enzyme responsible of elastin degradation is family of genes which are collectively called elastases, whose activity is inhibited by alpha-1 anti-trypsin (A1AT). It has been shown that serum levels of A1AT are higher in aneurysm patients compared to those with aortic occlusive disease, considered a response to counter increased elastase activity [42]. A proof-of-principle *in vivo* rat model of aortic aneurysm was induced by perfusing a segment of abdominal aorta with pancreatic elastase, and demonstrated that elastase perfusion generated aneurysms exhibiting marked loss of elastin content, and showed elastase concentration positively correlated with aneurysm size [45]. In summary, alterations in the quantity or architecture of elastin and collagen (in part through increased degradation), promotes aneurysm formation and progression. Moreover, aortic dilatation is linked to loss of elastin, whereas aortic rupture is predominantly associated with collagen loss [40] [46].

1.3.2 MMPs and TIMPs

MMPs, also called matrixins, are a family of enzymes that proteolytically degrade various components of the ECM. MMPs are involved in several physiological processes including morphogenesis, tissue repair and remodelling, while also playing a crucial role in pathological diseases such as atherosclerosis, post-myocardial infarction (MI) remodelling and aneurysm formation, progression and rupture [47]. In addition to degradation of ECM components, MMPs have the ability to influence the behaviour of macrophages, VSMCs, ECs and other inflammatory cell types [48]. MMPs are zinc-containing and calcium-dependent endopeptidases that are synthesised as pro-MMPs, inactive zymogen forms that require activation to exert functionality [42]. Due to the abundance and variation in forms of ECM proteins and in order to maintain an equilibrium between synthesis and degradation, the synthesis, activation and expression balance relative to their inhibitors is tightly regulated [49]. The activity of MMPs is closely regulated by the endogenous tissue inhibitors of MMPs (TIMPs). Moreover, other non-specific inhibitors such as tissue-factor pathway inhibitor-2 (TFPI-2), the pro-collagen C-terminal proteinase enhancer (PCPE), and the plasma protein α2-macroglobulin, have been shown to exert MMP inhibitory actions. Twenty-three members of the MMP family have been commonly identified, which share structural similarities consisting of a pro-domain, a catalytic domain, a hinge region and a hemopexin domain (as shown in Figure 1.8). MMPs are included within the Metzincin family together with ADAMs (a disintegrin and MMPs family) and ADAMTSs (ADAM with thrombospondin motifs) [47, 50]. Four TIMPs (TIMP-1, TIMP-2, TIMP-3, and TIMP-4) have been identified in vertebrates, which collectively reversibly inhibit all MMPs via binding the catalytic domain of MMPs through

residues present on their N terminal domain. Some of the TIMPs can also inhibit members of ADAM and ADAMTS family. Further detail on MMPs and their involvement in aneurysms is provided later within the Introduction (see section1.5-1.5.6).

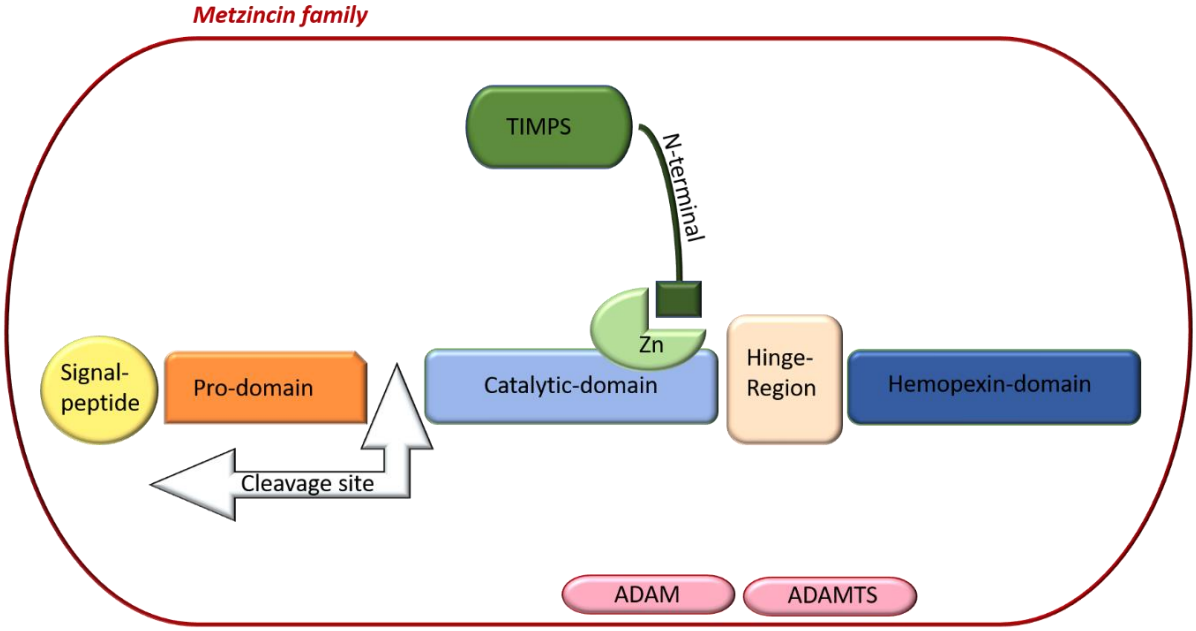

Figure 1.8: Domain structure of MMPs

MMPs are members of the Metzincin family together with ADAMs and ADAMTSs, and share structural similarity. General domain structure includes the signal peptide (yellow), pro-domain (orange) after which there is a cleavage site (white), catalytic domain (light blue) with the active-zinc binding site (green), the hinge domain (cream), and the hemopexin domain (dark blue). Figure made using elements from https://smart.servier.com/

1.3.3 Vascular smooth muscle cells

VSMCs are a type of smooth muscle cell found within, and composing the majority of the blood vessel wall. VSMCs are spindle-shaped cells, 20-30 µm long by 4 µm wide at the centre, concentrically layered around the vessel. Under physiological conditions, VSMCs are the only cells present within the medial layer of the vessel wall. They play an important role maintaining the structure of blood vessels such as the aorta, through the production of elastin, collagen, an array of other ECM proteins, numerous proteases and their inhibitors, so as to provide structural integrity to the vessel while also regulating the vessel diameter through contraction and relaxation in response to specific stimuli [51]. VSMCs regulate the contractile tone of the vessel alongside the secretion of ECM proteins, these two functions highlight the existence of different VSMC phenotypes, synthetic and contractile [52]. In healthy blood vessels the predominant VSMC phenotype is the contractile form, highlighted by the limited secretion of ECM proteins and abundant myofilament production to allow regulation of blood vessel flow and its diameter. During pathological conditions due to tissue injury or repair induced pathways such as the oxidative stress response, the switching of the contractile VSMC phenotype to a synthetic form is induced, which is characterised by increased protease production (such as MMPs), which degrade ECM proteins including elastin and collagen [38, 53]. The diversity of the two VSMC phenotypes can be further delineated by changes in their morphology, expression levels of specific VSMC marker genes, and their proliferative and migratory properties (as shown in Figure 1.9). Contractile VSMCs display an elongated morphology and are mainly composed of contractile apparatus and limited synthetic organelles in the perinuclear area of the cell. Synthetic VSMCs exhibit a cobblestone morphology, a high concentration of synthetic organelles and limited contractile filaments [54]. Studies have shown that select marker genes are associated with the phenotypic modulation of VSMCs, allowing the recognition of VSMC phenotypic state. Contractile markers include the well-characterised proteins smooth muscle α-actin (SMα-actin), smooth muscle myosin heavy chains SM-1 and SM-2, calponin, SM-22α, and smoothelin. Markers of the synthetic VSMC phenotype include caldesmon and vimentin but have been less characterised in the literature, accordingly it is the loss of contractile VSMC markers after an injury/insult which are commonly used as indicators of a switch to a synthetic phenotype [52][66]. During an inflammatory response numerous factors such as cytokines, chemokines, leukotrienes, reactive oxygen species and immunoglobulins are secreted, which have been shown to induce VSMC proliferation and migration in order to facilitate healing. Synthetic VSMC modulation and associated heightened proliferative and migratory capacity represents a critical step which promotes vascular remodelling and aneurysm formation [55]. Migration and proliferation are important mechanisms during the arterial response to an injury and increased MMP

expression is also involved in this process. MMP-dependent remodelling of the ECM controls VSMC migration through multiple mechanisms. First of all, MMP-mediated breakdown of the VSMC basement membrane and immediate surrounding ECM permit their motility and migration into the intima [56]. VSMCs are also anchored to the ECM in part by integrins and a high concentration of integrins is associated with slow migration rate [55]. Specific MMPs are able to cleave integrins and liberate VSMCs from their adhesive state [55]. Furthermore, VSMC migration can be stimulated by growth factors including platelet-derived growth factor-BB (PDGF-BB), which are liberated from the ECM by MMPs to enable their interaction with VSMCs [48, 51]. Ang II is a hormone and part of the angiotensin-renin system, it can regulate the proliferation, migration and survival of VSMCs. Mechanisms involved in the formation and inhibition of Ang II can be modulated by MMPs, and consequently increased exposure of VSMCs to Ang II increases their migratory and proliferative rates [55]. Taken together, it is apparent that targeting MMPs may serve as an efficient strategy to reduce VSMC migration and proliferation. Increased MMP expression is also associated with heightened VSMC proliferation, similarly through multiple mechanisms. A direct mechanism includes the MMP-dependent cleavage and processing of latent growth factors into their active forms (such as transforming growth factor beta), while indirectly MMPs can release ECM-bound growth factor [57]. MMPs have also been linked to cadherin cleavage which stimulates beta-catenin signalling and influences VSMC proliferation [57].

VSMC apoptosis is also contributing factor to the pathogenesis of aneurysms. A study analysing the relationship between VSMCs and aneurysm degeneration showed that the density of VSMCs is dramatically reduced in aneurysms compared to control normal aorta, due to increased VSMC apoptosis. The same study also demonstrated that VSMCs within aneurysms display increased production of p53, which is a pro-apoptotic protein member of the Bcl-2 family [58]. MMPs can affect VSMC apoptosis through cleavage of apoptotic receptors and their ligands including tumour necrosis factor alpha (TNF-α) and Fas-Ligand, as well as the degradation of pro-survival cell–matrix contacts [56]. Furthermore, a study demonstrated that MMP-7 is involved in the cleavage of the survival molecule N-cadherin, triggering VSMC apoptosis [59]. Finally, a member of the tissue inhibitor of metalloproteinase family, TIMP-3, can promote VSMC apoptosis when over-expressed at non-physiological levels, while TIMP-1 and TIMP-2 exert pro-survival actions [60].

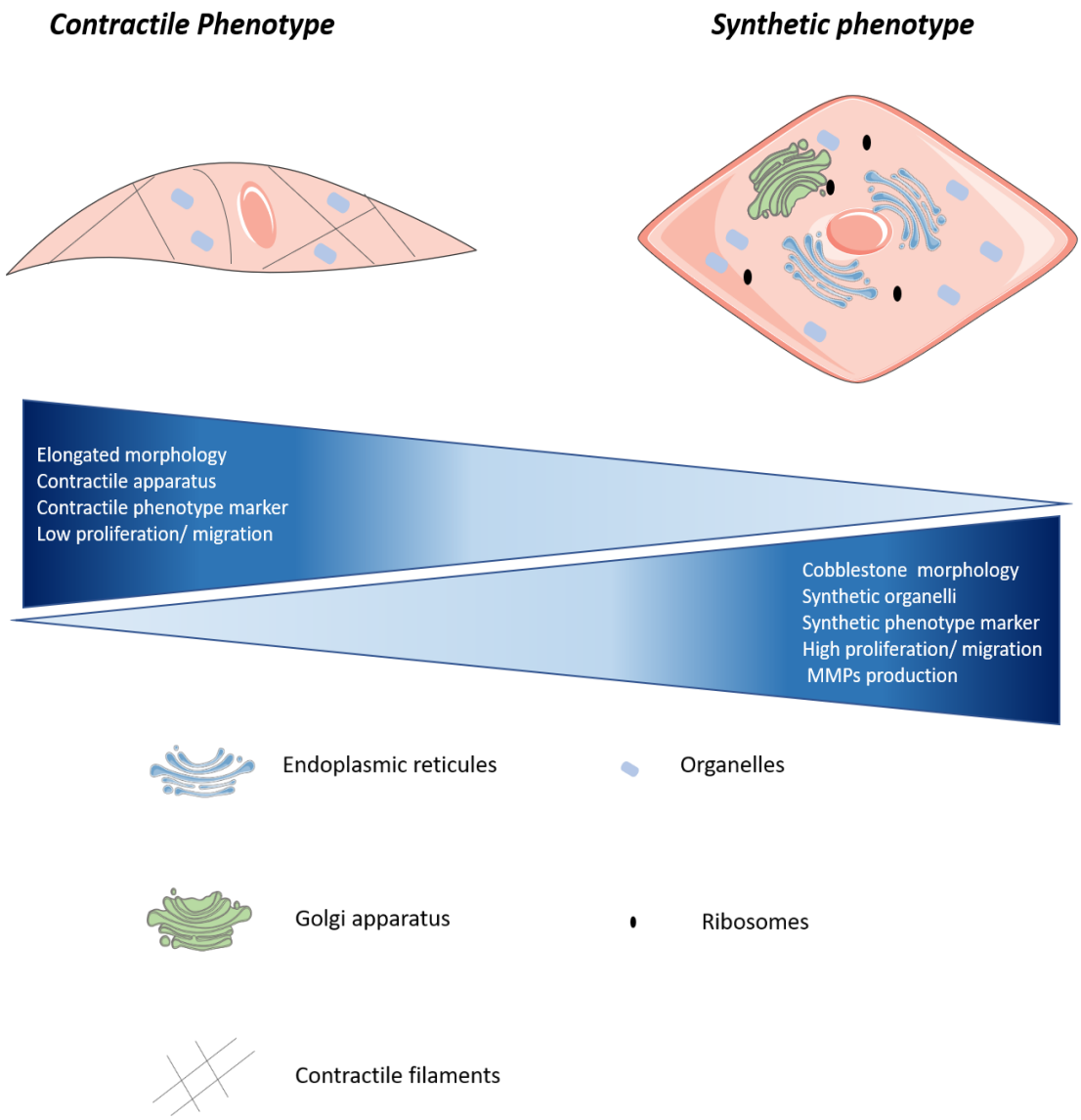

Figure 1.9: Characteristics of contractile and synthetic VSMC phenotypes

VSMCs can exist in contractile (on the left side) and synthetic phenotypes (on the right side). Contractile VSMCs (left side) are elongated and are mostly composed of contractile apparatus, they display a high concentration of contractile proteins and have a low proliferation and migration rate.
Synthetic VSMCs (right side) have a cobblestone morphology and are mostly composed of synthetic organelles, furthermore they display a high concentration of synthetic proteins and have high proliferation/migration rates alongside heightened MMP production. Figure made using elements from https://smart.servier.com/ and information from Tuqa Saleh et al 2015 [61].

1.3.4 Endothelial cells

ECs are of the dominant cell type within the inner surface of the vessel wall, the intima. ECs are typically organised in a single and continuous layer of cells and contribute to multiple major homeostatic functions within the vessel wall [61]. ECs have an important role in barrier function between the circulating blood and the vessel wall by regulating the exchange of solutes and fluids. Moreover, ECs are also involved in the regulation of blood pressure through the release of specific mediators such as nitric oxide (NO) and prostacyclin (PGI2), as well as vasoconstrictors, including endothelin (ET) and platelet-activating factor (PAF) [62]. Similarly to VSMCs, ECs have been proposed to play an important role in the pathogenesis of AAA. Rateri and colleagues examined the response of ECs to Ang II. Interestingly, they found that mice deficient for the Ang II receptor type 1 (AGTR1) in VSMCs or monocytes developed AAAs, whereas mice with AGTR1 deletion only in ECs had no increase in abdominal aorta diameter [63]. This important study suggests that Ang II primarily affects ECs which subsequently modulates VSMC behaviour, however the direct underlying mechanisms are yet to be elucidated. As such ECs are stimulated during AAA formation and subsequently release different growth factors and enzymes that modulate the ECM composition as well as the behaviour of other cells. Haemodynamic changes and inflammatory stimuli are associated with increasing the susceptibility of ECs to apoptosis alongside altering EC-VSMC communications resulting in promotion of a synthetic VSMC phenotype [64]. Ramella *et al* demonstrated that silencing MMP-9 in ECs resulted in suppressed NF-κB activation and retarded their ability to migrate [65]. Furthermore, MMP-9 knockdown in ECs altered their ability to modulate VSMC function [65]. EC telomerase activity has also been explored in AAA patients as telomerase protects chromosomes from DNA damage, and telomerase loss is correlated with cardiovascular diseases, cell ageing and oxidative stress. A recent study revealed reduced telomerase activity in human AAA tissues when compared to healthy control samples, suggesting changes in telomerase activity may serve as a novel biomarker of AAA [66]. ECs are characterised by cell-cell interactions which are necessary for maintaining barrier function and modulating immune responses. Adherens junctions represent major adhesive cell–cell junctions in ECs, and as shown in Figure 1.10 the transmembrane component of endothelial adherens junction is VE-cadherin, which through its cytoplasmic domain interacts with adaptor proteins, including p120-catenin, β-catenin, and plakoglobin. Interestingly, under specific conditions p120-catenin and β-catenin can translocate to the nucleus and regulate gene expression [67]. Ang II had been shown to induce EC dysfunction, through dephosphorylation of VE-cadherin and subsequently increasing cell permeability, compromising endothelial barrier function [68]. As previosly mentioned, ECs are predominant within the intima of healthy blood vessels and in direct contact with the blood, and are therefore

sensitive to changes to shear stress and pressure. Shear stress had been described as the tangential force of the blood that flows over the endothelial surface within a blood vessel. As such, changes in shear stress dynamically alter the function and behaviour of ECs and has therefore been proposed play a fundamental role in cardiovascular disease development [69].

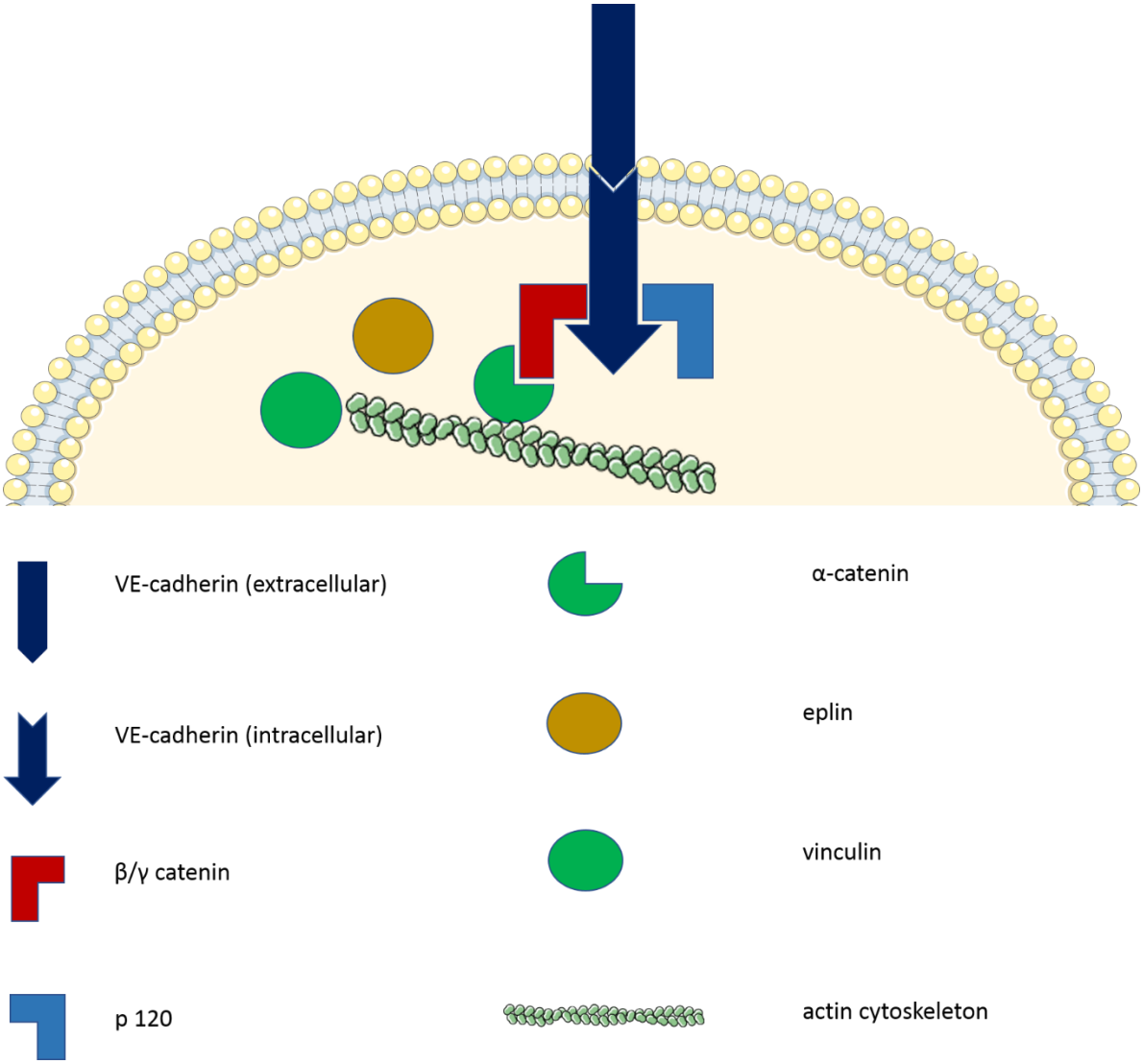

Figure 1.10: VE-cadherin signal pathway

VE-cadherin is a transmembrane protein in endothelial cells (dark blue); its cytoplasmic domain interacts with p120-catenin, β/γ catenin. These proteins are able to further interact with α-catenin, eplin and vinculin which connect to the actin cytoskeleton.

1.3.5 Inflammation

Inflammation has been postulated to play a pivotal role in the pathogenesis of aneurysms. Notably cells such as neutrophils, T cells, B cells, macrophages, mast cells and natural killer cells (NK) accumulate within the aortic wall, and are associated with increased expression of pro-inflammatory cytokines, chemokines, immunoglobulins and leukotrienes. Furthermore, VSMC, ECs and monocyte/macrophage MMP expression can be regulated by chemokines and perpetuate ECM degradation and subsequent weakening of the aortic wall during aneurysm progression [70, 71]. A diagram summarising the proposed role of inflammation in AAA pathogenesis is shown in Figure 1.11. Cytokines are key molecules within the immune system which regulate inflammation, haematopoiesis, cellular and humoral responses, and wound healing [72]. Prevalent inflammatory cells found within aneurysms include cluster of differentiation 4+ (CD4+) T cells, B cells and macrophages. CD4+ type 1 T helper cells (Th1) and CD8+ T-cytotoxic type-1 (Tc1) cells produce interferon gamma (IFN-γ), interleukin-2 (IL-2) and tumour necrosis factor (TNFα), whereas type 2 T helper cells (Th2) and type 2 cytotoxic cells (Tc2) secrete interleukin-4, interleukin-5 ,interleukin-10 and interleukin-13 (IL-4, IL-5, IL-10 and IL-13), which are also produced by B cells, macrophages, NK cells and ECs. Tumour necrosis factor alpha (TNFα) has a main role in the inflammatory process due to its role in the activation and recruitment of immune cells to sites of inflammation, the secretion of other pro-inflammatory cytokines and MMPs, and inducing VSMC death [70] [73]. A study by Xiong and colleagues in rodent models of aneurysm demonstrated that messenger RNA (mRNA) and protein levels of TNFα are increased in aneurysmal tissue, and injection of a TNFα-binding protein reduced elastase levels, suggesting an important role for TNFα in the pathogenesis of aneurysms [74]. Moreover TNFα can induce macrophage cytokine release and protease productions, including heightened MMP-9 expression [75]. IFN-γ is predominantly produced by activated Th1 cells and NK cells, and there is conflicting evidence on the role of IFN-γ in aneurysm progression. Increased levels of IFN-γ alongside IL-1, IL-6 and TNFα have been detected in aneurysmal vessels compared to controls, and IFN-γ can dampen VSMC collagen production [76]. Conversely, a study showed that blocking the IFN-γ receptor accelerated aneurysm formation [77]. A possible reason for this discrepancy can be attributed to the divergent roles of IFN-γ, as it can exert pro-inflammatory and anti-inflammatory effects, which are dependent on the pathology and the cytokines involved. Another protein known to alter the structure and composition of the ECM and proposed to play an important role in vascular remodelling is transforming growth factor beta (TGF-β). TGF-β is secreted by many cell types and contributes to processes including proliferation, angiogenesis, differentiation, apoptosis, inflammation, and wound healing. Similarly to IFN-γ, divergent roles have been proposed for TGF-β in numerous cardiovascular diseases. With regards to aneurysms, reduced TGF-β

were detected in aneurysm patients and correlated with low levels of cystatin C, a cysteine protease inhibitor [78]. TGF-β has also been demonstrated to retard the expression and activity of select MMPs (such as MMP-12) in mouse models of aneurysm, and therefore inhibit disease progression [79]. Conversely, AAA formation has been associated with increased TGF-β activity, while functional blocking of TGF-β reduced aneurysm formation [80, 81]. Habashi *et al*., demonstrated that neutralising the activity of TGF-β in a mouse model of Marfan syndrome prevented aneurysm formation, which was comparable to treatment with the Ang II type 1 receptor inhibitor Losartan [80]. Human genetic studies showed that single nucleotide polymorphisms in two TGF-β receptors (TGFBR1 and TGFBR2) which are responsible for Marfan syndrome type II and Loeys-Dietz syndrome and associated with TAA dissection, positively correlate with AAA severity [82].

In addition to TGF-β, other cytokines have also been implicated in aneurysm pathology, including macrophage migration inhibitory factor (MIF) which was originally classed as a lymphokine, is derived from activated T-cells, and proposed to inhibit macrophage migration. However, it is now considered a pleiotropic protein, involved in inflammatory and immune responses, stimulating angiogenesis and regulating proliferation [15]. MIF also regulates the production and activation of T and B cells as well as modulating proteolysis through the regulation of MMP expression, and activation of both the urokinase plasminogen activator (uPA) and tissue plasminogen activator (tPA) [73]. Similarly, osteoprotegerin (OPG) is a glycoprotein which belongs to the TNF receptor superfamily, and is expressed by osteoblasts, ECs, VSMCs, dendritic cells, lymphocytes, and plasma cells, and can act as a decoy receptor for the receptor activator of nuclear factor kappa B ligand (RANKL). Previous studies showed that OPG is linked to vascular disease [83, 84], while others show a link between the elevated serum concentrations of OPG with aneurysm disease [85]. Moran and co-workers, compared OPG levels in biopsies of aneurysm subjects and normal individuals, confirming OPG concentration was increased in aneurysm patients [86]. Interleukins are a large cytokine family with specific immunomodulatory functions, including cell proliferation, maturation, migration and adhesion. Interleukins are also involved in differentiation and activation of immune cells. Previous studies showed significantly higher concentrations of IL-1β, IL-2 and IL-6 in patients with AAA compared to control subjects [87].

Elevated plasma levels of C-reactive protein (CRP) is considered an indicator of systemic inflammation and is associated with cardiovascular events, and Vainas *et al.* found high levels of serum CRP in patients with increased aortic diameter [88]. Patients with symptomatic or ruptured AAAs also showed higher circulating levels of CRP, and the concentration of CRP correlated with the size of the aneurysm [88].This relationship between CRP and aneurysm size was confirmed in a further study which demonstrated CRP levels were greater in patients

with large AAAs, compared to small ones, and a marked difference between AAA patients and healthy controls [89]. Homocysteine (Hcy) is an intermediate product of methionine metabolism, and homocysteine is primarily recycled through a transmethylation reaction involving vitamin B12 and folic acid while a smaller amount is metabolised by transulphuration involving vitamin B6; these mechanisms underlie why dietary folate and vitamin B supplementation can normalise Hcy levels [90]. Raised circulating levels of Hcy have been linked to coronary artery disease [91]. Previous studies have also identified increased levels of Hcy as a risk factor of AAA. Brunelli *et al.* showed that Hcy plasma levels were significantly higher in AAA patients than in control subjects [89]. Furthermore, Cao *et al.* performed a meta-analysis of previous studies and confirmed an association between Hcy and AAAs, however further studies are required to determine causality [90]. Infectious diseases have been linked to numerous cardiovascular diseases, in particular Chlamydia pneumoniae has been associated with atherosclerosis, myocardial infarction, and aortic aneurysms. Karlsson *et al.* demonstrated the presence of Chlamydia pneumoniae in the aortic wall of patients with AAAs, with at least 80% of patients testing positive for Chlamydia pneumoniae [92]. Finally, serum-tissue levels of a phosphorylated acidic glycoprotein called osteopontin (OPN), which is produced by VSMCs, ECs and macrophages, and linked to inflammatory processes such as lymphocyte survival and chemotaxis of macrophages and T cells, was shown to positively correlate with human AAAs [93].

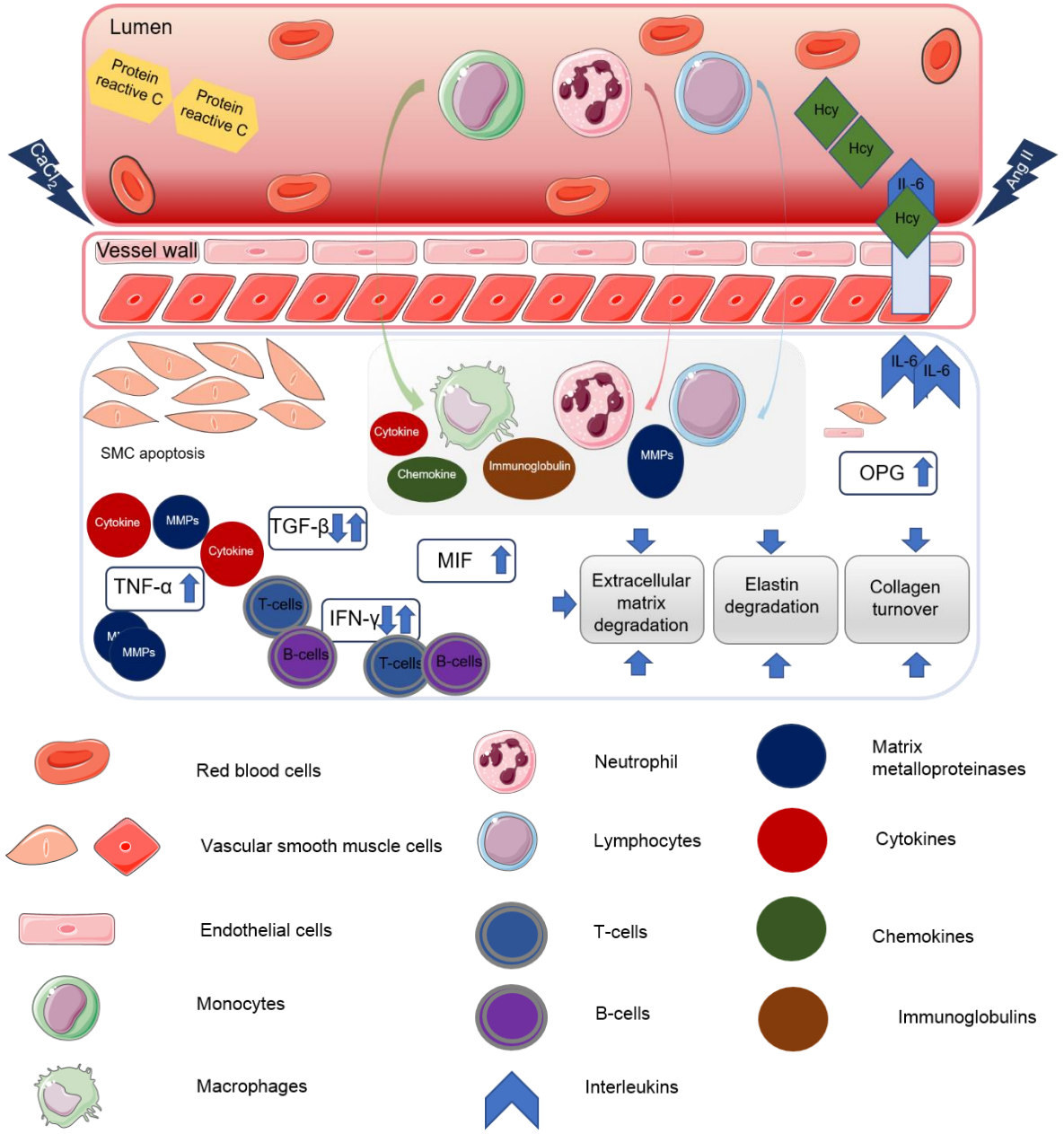

Figure 1.11: Schematic diagram of the major signalling pathways involved in aneurysm formation.

In response to an injury or aneurysm-inducing agents (such as Ang II or calcium chloride) cells including neutrophils, T or B cells, macrophages, mast cells and natural killer cells (NK) accumulate within the aortic wall. There is an accompanying increased expression of pro-inflammatory cytokines, chemokines, immunoglobulins and leukotrienes. Tumour necrosis factor alpha (TNF-α) facilitates further recruitment of immune cells to the already inflamed area, perpetuating pro-inflammatory cytokine and MMP expression, alongside induction of VSMC death. Interferon gamma (IFN-γ) and transforming growth factor beta (TGF-β) have been reported to exert both beneficial and detrimental roles in aneurysm formation. Migration inhibitory factor (MIF) is a pleiotropic protein, involved in inflammatory and immune responses, stimulating angiogenesis and regulating proliferation. Osteoprotegerin (OPG) is glycoprotein also linked to vascular disease. Collectively, these factors can directly influence extracellular matrix degradation, elastin loss and collagen turnover, subsequently contributing to aneurysm formation and rupture.

1.3.6 Calcification

Abdominal aortic calcification (AAC) is commonly observed in advanced atherosclerosis, with many studies showing an association between calcification and risk of cardiovascular events, supporting its use as a potential biomarker [94, 95]. Calcification is considered an inflammatory process within the arterial wall and often classified as; intimal calcification which occurs in association with atherosclerosis and is associated with lipid deposition, macrophage infiltration, and VSMC proliferation; medial calcification can exist independently of atherosclerosis and is usually associated with elastic fibres; calcification can also occur as the result of a genetic disorder [96]. Arterial calcification causes a reduction in the elasticity of the vessel wall which increases its risk of rupture during aneurysm development and progression [39, 97]. Considering vascular calcification represents a risk factor for aortic aneurysms, Buijs *et al.* assessed 334 AAA patients, some with ruptured aneurysms, some with symptomatic non-ruptured aneurysms, and some with elective surgery, and revealed that marked calcification associated with large vessel diameters in ruptured and symptomatic patients, compared to patients receiving surgical therapy [39]. Du Kim *et al.* demonstrated that lifestyle risk factors such as age, dyslipidaemia and exercise correlated with AAC, while an association with smoking was found in male subjects, and diabetes and hypertension were linked to calcification in female subjects [98]. A proteomics study revealed 138 and 134 proteins differentially expressed in calcified AAAs (CAAs) and calcified TAAs (CTAs) respectively, in contrast to healthy aortic tissue, in particular type I collagen α-1 and type III collagen α-1 chains were increased in CAA, whereas type XIV collagen α-1 was decreased [93]. Furthermore, levels of ECM proteins such as fibulin-5 were decreased in CTA patients [99]. Fibulin-5 is an integrin-binding matricellular protein which plays a role in EC adhesion and is therefore considered important for preserving aortic wall stability [100]. Finally, a recent imaging study utilised the ability of Fluorine-18–sodium fluoride (18F-NaF) uptake to delineate active calcification in AAA patients and revealed increased 18F-NaF signal in AAA regions compared to non-AAA used as control. This study suggested that 18F-NaF can potentially be used as a surrogate marker of aneurysm progression [95].

1.3.7 Angiogenesis/neovascularisation

Angiogenesis involves the formation of new blood vessels from pre-existing vessels and is a fundamental process involved in embryogenesis, inflammation, tissue development and repair [101]. Normally the process of the angiogenesis starts with ECM degradation followed by activation of vascular ECs, with their subsequent increased proliferation and migration fundamental for new blood vessel formation. Under physiological conditions the right balance between pro- and anti-angiogenic factors is maintained, whereas in pathological disorders there is an imbalance that favours the accumulation of pro-angiogenic factors [102]. Angiogenesis is associated with the destructive processes which occur within the AAA wall and therefore proposed to play a key role in aortic aneurysm development and rupture [103]. It should also be noted that within aneurysms (and atherosclerotic lesions), the formation of new blood vessels is termed neovascularisation rather than angiogenesis, and consequently within the literature these two terminologies are used interchangeably. Under hypoxic and/or inflammatory conditions multiple pro-angiogenic factors are released, including: vascular endothelial growth factor (VEGF), platelet derived growth factor, basic fibroblast growth factor (b-FGF), monocyte chemotactic protein-1 (MCP-1), as well as numerous proteases such as chymase, tryptase, and MMPs [104]. The development of an intimal thickening is a pathological characteristic of aneurysms and angiogenesis represents an adaptive response to the hypoxic environment rendered through the formation of a thickened intima. For example, hypoxia inducible factor-1α is an angiogenic factor which is increased within aneurysmal aortae. VSMCs are able to produce angiogenic factors including VEGF, nitric oxide synthase and cyclo-oxygenase-2 (COX-2) within hypoxic environments [105]. In particular, angiogenesis within the media of the aortic wall is a prominent feature of AAA and is thought in part to be driven by increased MMP expression and activity [106]. Supporting a causal role for angiogenesis to AAA progression, Choke *et al.* revealed that micro-vessel density was increased within the medial layer of ruptured aneurysms, which was associated with increased expression of VEGF, VE-cadherin, MCP-1, and vimentin [106]. A similar study demonstrated neo-vessel density was significantly increased in aortic aneurysmal tissue compared to non-aneurysmal atherosclerotic aortas [101]. A mouse study using the Ang II-infusion model demonstrated combined administration of bexarotene (a ligand for retinoid X receptors and exerting anti-angiogenic activity) and rosuvastatin (statin member) blunted aneurysm formation which was associated with decreased production of pro-angiogenic chemo-attractants and VEGF alongside perturbed inflammation and neovascularisation [107]. In addition to AAA, neo-vessel formation is increased within TAAs, including patients with bicuspid aortic valve or Marfan syndrome, although no relationship with changes in hypoxia or VSMC phenotype have been reported [108]. Taken together, the above findings suggest

that the deployment of anti-angiogenic therapies such as those used in cancer, might be effective at preventing AAA expansion and rupture [104, 107].

1.3.8 Atherosclerosis

The pathology of atherosclerosis is characterised by thickening of the arterial wall due to the accumulation of lipids, vascular and inflammatory cells, and the deposition of various ECM proteins within the tunica intima [109]. Briefly, the atherosclerotic process starts with the retention and modification of low-density protein (LDLs) within the intima due to dysfunctional ECs at athero-prone regions of the arterial tree which are pre-disposed to altered haemodynamic flow patterns. Dysfunctional ECs and phenotypically altered VSMCs which are found at athero-prone sites and termed adaptive intimal thickenings [110], release cytokines and express adhesion molecules (such as MCP-1 and vascular cell adhesion protein-VCAM-1, respectively) which facilitate monocyte recruitment and accumulation. Within the intima, monocytes differentiate into macrophages and express scavenger receptors, permitting their uptake of modified lipoproteins and their transformation into foam cell macrophages. Foam cell macrophages undergo apoptosis and necrosis resulting in the development of a lipid-rich necrotic core within the deeper aspects of the intima and delineated from the lumen by a VSMC- and ECM-rich fibrous cap [111]. During the progression of atherosclerosis, the fibrous cap becomes thinner and weakened due to proteolytic activity of enzymes such as MMPs and VSMC apoptosis, which render the plaque vulnerable and susceptible to rupture [109, 112]. Atherosclerosis and AAAs share multiple risk factors including smoking, hypertension, diabetes mellitus, obesity, and genetic predisposition [113]. In particular, smoking has been recognised as a strong risk factor linked to atherosclerosis progression and AAA frequency [114]. Both cardiovascular pathologies involve remodelling of the arterial wall but affecting different layers, the media for AAAs and the intima for atherosclerosis [115]. Several studies have revealed a strong association between atherosclerosis and aneurysm formation, notably atherosclerosis is often considered a risk factor for subsequent aneurysm formation [116]. However, it is still unclear if these two pathologies are linked through sharing common risk factors or exert direct causal effects. In the past different concepts have been proposed to explain the link between AAAs and atherosclerosis, with the general consensus agreeing aneurysms are caused by atherosclerosis and are therefore termed atherosclerotic aneurysms, which typically occur in the abdominal aorta [117]. It has been proposed that luminal narrowing of the aorta typical of atherosclerosis formation, induces modification and remodelling of the medial wall in order to compensate for the loss of lumen patency, involving ECM remodelling to ‘normalise’ the vessel diameter but inadvertently induces medial thinning, typical of AAA development. Subsequently, protease-mediated degradation of ECM proteins, and in particular elastin fragmentation, result in the generation of chemotactic small peptides

which alongside the release of pro-inflammatory factors from inflammatory cells present in the overlying atherosclerotic lesion, drive further disease progression [113]. A second model postulates that AAAs and atherosclerosis are two independent pathologies with different aetiologies, but however share risk factors including smoking, hypertension, and hypercholesterolemia which are linked with both diseases. A final concept suggests that AAAs or atherosclerosis can develop first and consequently encourage the development of the other. Interestingly, Golledge *et al.* stated that AAA and atherosclerotic plaque formation are induced via several independent mechanisms, which vary from patient to patient, and therefore a broad standardised therapeutic approach would not be successful [113].

1.3.9 Aortic dissection

Aortic dissection is commonly a lethal condition in which the inner layer of the aorta initially tears resulting in blood pushing through the tear, separating the middle layer of the wall from the outer layer and creating a new lumen, that is commonly termed a false lumen (as illustrated in Figure 1.12) [118]. Dissections can create several problems including the reduction of blood flow and limiting oxygen supply to tissues [118]. In some cases, the dissection will cross all three layers of the aortic wall and cause immediate rupture and almost certain death [119, 120]. Dissections have been reported to occur at multiple vascular sites, such as in the thoracic and abdominal aorta, carotid arteries and coronary arteries. Several underlying conditions can alter and weaken the aorta wall and subsequently predispose people to aortic dissection, including; hypertension, atherosclerosis, disorders of the connective tissue (Marfan Syndrome, Ehlers-Danlos Syndrome), genetic disorders (familial TAA disorder), or trauma which can damage the aorta wall so as to cause a dissection (such as a road traffic accident) [121]. Based on their anatomic distribution, aortic dissections are categorised using the DeBakey or Stanford classification schemes, with the Stanford classification serving as most popular. Stanford divided them into: Type A which includes dissection of the ascending aorta, and possibly the arch and descending aorta; and Type B which involves dissection of the descending aorta only [122] [123]. The DeBakey schema classifies aortic dissections into; Type I which originates within the ascending aorta and propagates into the arch and often the descending aorta; Type II dissections are limited to the ascending aorta; and Type III are located only within the descending aorta [118, 122, 124]. Aortic dissections can be further characterised through the presenting clinical symptoms including pain in the chest or back, while others can suffer pain in the arms and legs and loss of consciousness, and rarely a heart attack. The phenotypic modulation of VSMCs has been proposed to play a prominent role in the susceptibility to aortic dissection. Polycystin 1 (PKD1) is a glycoprotein and kinase which can modulate cell behaviour including migration, proliferation and apoptosis [118], changes in its abundance are associated with aortic disease. Feng *et al.* demonstrated that aortic dissections displayed medial thinning, reduced VSMC density, and increased collagen deposition compared to healthy aortae, which associated with reduced PKD1 mRNA and protein expression [125]. Further *in vitro* mechanistic findings demonstrated that loss of VSMC PKD1 expression promoted VSMC modulation to a synthetic phenotype in an ERK-dependent manner, as evidenced by loss of protein expression for the contractile phenotype proteins [125]. In an attempt to elucidate whether circulating pro-inflammatory molecules can serve as biomarkers for aortic dissection, Vianello and colleagues proposed evaluation of CD40 ligand (CD40L), myeloperoxidase (MPO), MMP-1 and TIMP-1 may act as a diagnostic panel for aortic dissection patients, depicting active structural changes within the aortic wall [126].

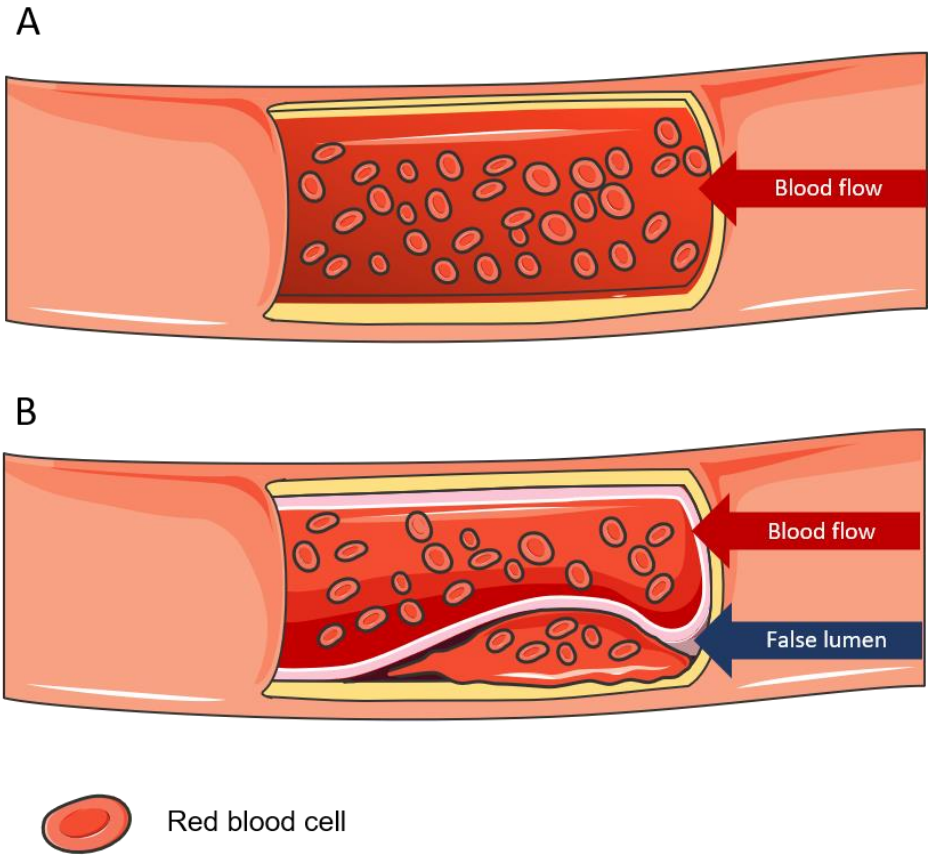

Figure 1.12: Aortic dissection

A, Normal blood vessel with unidirectional blood flow passing through the lumen
B, Aortic dissection is a tear in the inner layer of aortic wall, that allows blood to separate the wall layers, creating a second lumen called a false lumen and resulting in vessel expansion.

1.4 Animal models of aneurysm

Aortic aneurysm is a degenerative disorder commonly associated with aortic rupture that can commonly result in sudden death; current therapies are limited to open surgical repair of the aorta and endovascular repair. Accordingly, a number of different animal models have been developed with the purpose of studying the pathogenesis of AAAs and elucidating the biochemical and cellular mechanisms underlying this disease [127]. A large range of animal models has been developed across a variety of species including; pig, sheep, dogs, rabbits, rodents and primates. Similar to humans, dogs have comparable sized arteries and are able to endure prolonged anaesthesia. Pigs also show a high level of similarity in the morphology of the arteries to humans, whereas in sheep the mechanism of coagulation is similar to humans. Finally, primates share a high level of similarity with humans especially within the fibrinolytic system. However, due to the maintenance costs and ethical concerns derived from large animal usage, their deployment in aneurysm studies has been limited. The mouse is the most commonly used species to model experimental AAAs, due to their small size, relatively low maintenance costs, and the ability to genetically modify their genome in order to overexpress or delete specific genes [128]. There are several classes of experimental AAA models which can be divided into three categories: genetically predisposed animal models, surgical models; and chemical induction. Within the chemical induction category there are three methods including localised perfusion of elastase, application of $CaCl_2$ to the adventitia of the aorta, or systemic infusion of Ang II [129]. The most commonly used animal model of aneurysm is the Ang II infused mouse model, which involves the sub-cutaneous implantation of osmotic mini-pumps into male or female apolipoprotein-E-deficient (Apoe−/−) mice, in order to deliver Ang II (between 500-1000 ng/kg/min) and to induce suprarenal aneurysm formation between 3 and 14 days after implantation [130-132]. Such mice show increased atherosclerosis when combined with high-fat feeding, and aneurysm formation at the suprarenal portion of the aorta alongside medial degeneration, inflammation and thrombosis. Moreover, whilst modest hypertension is sometimes observed, aneurysm formation in this Apoe−/− model is not always characterized by changes in blood pressure. After Ang II infusion macrophage aggregation occurs within the medial wall, increased elastin degradation, incidence of aortic dissection and vascular haematomas, alongside adventitial ECM deposition and infiltration of other inflammatory cell types. During the later stages of the aneurysm, super-imposed foam cell macrophage-rich atherosclerotic lesions are also observed [127, 129].

The application of $CaCl_2$ solution is another method of aneurysm formation. This method was first applied to rabbit aortas, and subsequently mice and involves the application of 0.25-1

molar $CaCl_2$ to the adventitia layer of the abdominal aorta, using a soaked swab or directly in solution [133]. Results illustrated an increase in the aortic diameter by 64% after 2 weeks of application and up to 110% 3 weeks after treatment. Moreover, the aneurysms which form in this mouse model show an increased inflammatory response and medial disruption [121]. The $CaCl_2$ model has been used to assess the role of MMPs in AAA formation, demonstrating that mice deficient for MMP-2 or MMP-9 did not develop aneurysms, while MMP-12-deficeint mice had smaller aneurysms [122]. Surprisingly, $CaCl_2$ application in TIMP-2 deficient mice also resulted in reduced aneurysm formation compared to wild-type control animals, although this may be due to the ability of TIMP-2 to activate MMP-2 [122]. Collectively these findings highlight the importance of interaction between MMPs and TIMPs, and their contributory role to the pathogenesis of aortic aneurysms within mouse models [8]. The intra-luminal infusion of elastase is also an additional model used to study the pathogenesis of aneurysms. This method requires the use of a catheter inserted into the infrarenal portion of the abdominal aorta and the further isolation of a segment of the abdominal aorta by placement of a distal suture and subsequent intra-luminal perfusion of elastase. This model results in medial destruction, dilatation of the aorta and consequent aneurysm formation between 2-4 weeks after infusion [129].

A wide range of studies conducted on mice genetically modified for an array of differing genes have reported spontaneous aneurysm formation. Mice deficient for select individual MMPs and TIMPs display spontaneous thoracic and abdominal aneurysm development and dissection [134], while mice rendered hyperlipidaemic through deficiency of either apolipoprotein E (Apoe) or the low density lipoprotein (LDL) receptor, can also naturally develop abdominal aortic aneurysms [127]. Mice with reduced levels of lysyl oxidase due to a mutation on the X chromosome which limits copper-mediated activation of lysyl oxidase, have an inability to crosslink both elastin and collagen and are predisposed to aneurysm formation [127].

1.4.1 Mechanism of Angiotensin II induced aneurysm formation

As mentioned above, the Ang II-induced mouse AAA model represents the most widely used model as it is relatively simple to perform and reproduce, and as it shares several common features with the human disease. Ang II is a hormone and is part of the renin-angiotensin system and proposed to play a pathological role in both atherosclerosis, and in the progression of aortic aneurysms [86] [130]. There are two angiotensin II receptors, Ang II type 1 (AT1R) and type 2 (AT2R) receptors, and Ang II preferentially interacts with AT1R. [135, 136]. Ang II can induce and up-regulate the expression of numerous MMPs through distinct pathways (see Figure 1.13), precipitating matrix degradation, in particular elastin degradation and therefore driving aortic aneurysm formation [137]. The main Ang II signalling pathways proposed to underlie its pro-aneurysmal effects are; the NFκB-IL-6 signalling pathway which has been shown to regulate monocyte activation and recruitment, and the TGF-β-Smad2 pathway which modulates VSMC differentiation and T lymphocyte differentiation. The NFκB-IL-6 pathway involves activation of RhoA/Rho kinase (Ras homolog gene family, member A/Ras homolog gene family) complex through interaction of Ang II with its cognate type I receptor. Specifically on binding Ang II to AT1R, Rho guanine exchange factor (Rho-GEF) catalyses the activation of Rho by replacing GDP (guanosine diphosphate) with GTP (guanosine triphosphate) [137]. Rho activation then induces activation of NFκB which is a transcription factor involved in the regulation of many genes involved in multiple mechanisms related to aneurysm formation including; MMPs, pro-inflammatory molecules, cytokine expression, stress regulation, cell division and transformation [138]. Ang II can induce Smad signalling through interaction with its type II receptor and subsequent down-stream phosphorylation of Smad-2 and -3, or through activation of latent TGF-β and its association with the TGF-β receptor, resulting in Smad-2/-3 phosphorylation [139]. After translocation to the nucleus, the Smads act as transcription factors by binding to genes with a Smad-responsive binding element, inducing the expression of key genes considered pro-aneurysmal, such as MMPs [140].

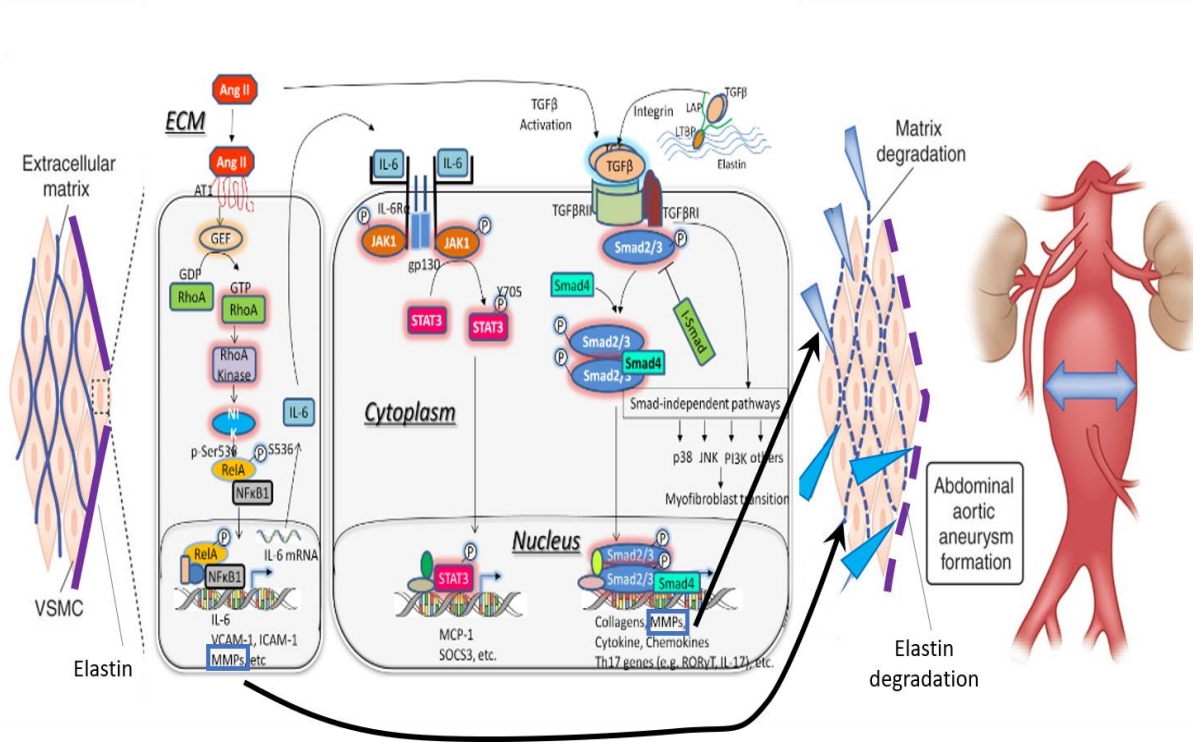

Figure 1.13 : Proposed mechanisms of angiotensin II signalling on abdominal aortic aneurysm formation and progression

Ang II interacts with its receptors AT1 to activate two divergent signalling pathways: the nuclear factor-κB (NF-κB)-interleuchin-6 (IL-6) pathway, and the transforming growth factor (TGF-β)-Smad pathway, both can induce MMP expression and consequently increase ECM degradation. Figure adapted from Brasier et al. 2011 [141].

1.4.2 Mechanism of calcium chloride induced aneurysm formation

The application of calcium chloride ($CaCl_2$) solution to arteries promotes accelerated aneurysm formation, as observed by increased aorta diameter by 64% after 2 weeks application, and by 110% after 3 weeks treatment [127, 129]. The initial action of $CaCl_2$ application on the aorta is considered to be increased EC permeability and induction of VSMC apoptosis. The VSMCs also increase their production of select MMPs and decrease their synthesis of collagen and elastin, both characteristics of aneurysm formation. Moreover, the application of $CaCl_2$ increases inflammatory cell recruitment and accumulation, giving rise to the heightened production of pro-inflammatory cytokine such as IL-1β, IL-6, TNFα, as well as an additional source of MMP secretion and activity, promoting degradation of collagen and elastin and thus further compromising the stability of the aortic wall. The signalling pathways through which $CaCl_2$ exerts down-stream effects on aneurysm biology are varied and the underlying mechanisms have achieved limited attention. Nonetheless, $CaCl_2$ application has been shown to promote phosphorylation of c-Jun N-terminal kinases (JNKs) and subsequent activation of c-Jun, and pharmacological inhibition of JNK reversed $CaCl_2$-induced aneurysm formation which was associated with reduced MMP-2 and MMP-9 expression and increased lysyl oxidase levels which is important for collagen and elastin deposition [127, 133]. Hamblin *et al.* showed that peroxisome proliferator-activated receptor-γ (PPAR-γ) may play a protective role in $CaCl_2$ -induced aneurysm formation, as PPAR-γ deficient mice displayed increased elastin degradation (due in part to increased cathepsin-S activity) increased macrophage infiltration, and marked vessel dilatation [142]. A number of chemokines have also been linked to $CaCl_2$-induced aneurysm formation. Specifically, the interaction of MCP-1 with its C-C chemokine receptor type 2 (CCR2) is associated with the inflammatory response observed in this model, as CCR2-deficient mice exhibit decreased aneurysm formation alongside less inflammation and reduced MMP-2 and MMP-9 levels [133]. The group X secretory phospholipase A2 (sPLA2-X) specifically in neutrophils has also been proposed to play a pathogenic role in $CaCl_2$-induced aneurysm formation through the use of sPLA2-X deficient mice, which exhibit diminished elastin degradation and vessel dilatation [129] [143]. Finally, plasminogen which can facilitate matrix degradation through plasmin-mediated MMP activation, has also been demonstrated to exert a detrimental role in $CaCl_2$-induced aneurysm formation, as shown by attenuated vessel dilatation and associated inflammation in plasminogen-deficient mice, which was MMP-9 dependent [144]. Finally, administration of $CaCl_2$ in mice reduced expression of the antioxidant enzyme catalase (that should protect cells from oxidative damage), therefore mice were more susceptible to AAA formation [145, 146].

1.5 Matrix metalloproteinases & their endogenous tissue inhibitors (TIMPs)

Matrix metalloproteinases, commonly called matrixins, are a family of proteases which can degrade proteins of the ECM including collagen and elastin [147]. It is important to underline that ECM integrity is necessary for physiological cell function during morphogenesis, angiogenesis, and wound repair. Furthermore, degradation of the ECM is associated with the development and further progression of cardiovascular diseases such as atherosclerosis, restenosis and aneurysms [148]. In addition to degrading ECM proteins, MMPs can also target non-ECM molecules, including cell-cell and cell-matrix connections and therefore affect cell behaviour directly [149]. In particular, MMPs are capable of modulating migration, proliferation and apoptosis of VSMCs, ECs, and macrophages, which are the key cell types connected to pathophysiological processes of vascular remodelling [144, 150]. MMP activity is tightly regulated during their transcription, activation, and through their interaction with endogenous inhibitors (such as TIMPs). However during pathological conditions, one or several of these processes become dysregulated, resulting in increased or reduced MMP activity [48].

1.5.1 MMP classification, structure and function

The MMP family in humans consists of 23 MMP proteins [47]. They belong to the Metzincin family together with ADAMs (a disintegrin and metalloproteinase family) and ADAMTS (ADAM with thrombospondin motifs), bone morphogenetic protein 1 (BMP1) tolloid-like protein 1 (TLL1), and meprins [151]. MMPs are multi-domain proteins that consist of a pro-peptide domain, a catalytic domain, a linker named hinge region, and a hemopexin-like domain [147]. MMPs are usually synthesised as a zymogen, linked to a pro-peptide and accordingly kept inactive through binding between cysteine, contained in the pro-peptide, and zinc ions within the active site, which prevent substrate interaction and subsequent activation. The activation of MMPs through pro-domain cleavage represents an important step in their activity. Stepwise activation of secreted MMPs requires their destabilisation, followed by cleavage of the pro-domain by plasma proteinases or bacterial proteinases, and can additionally be cleaved by other activated MMPs [47, 152]. Transmembrane type MMPs (MT-MMPs, such as MMP-14), together with MMP-11, MMP-23 and MMP-28 are activated intracellularly by pro-protein convertases such as furin and either then localise to the membrane (MT-MMPs) or are secreted (MMP-11) as active enzymes into the extracellular space [47] [153]. The activity of MMPs is endogenously regulated by TIMPs; four members of the TIMP family have been identified in vertebrates; TIMP-1, TIMP-2, TIMP-3, and TIMP-4 [154]. TIMPs are secreted proteins with a C-terminal domain that can bind the hemopexin-like domain of MMPs,

rendering them inactive. However, TIMPs present divergent inhibitory specificity towards the numerous MMPs, for example the inhibitory actions of TIMP-1 are more restricted than other TIMPs, presenting low affinity for the MT-MMPs (MMP-14, -16, -19, and -24). In addition, TIMP-1 preferentially targets MMP-3 compared to TIMP-2 and -3, whereas TIMP-3 has a wide inhibitory effect on ADAM and ADAMTS family members [155]. Other endogenous inhibitors are able to interact and inactivate MMPs, such as α2-macroglobulin, the serine protease tissue factor pathway inhibitor-2 (TFPI-2) and the reversion-inducing-cysteine-rich protein with Kazal motif (RECK), although the mechanism of their inhibitory interaction with MMPs is poorly studied [147]. As previously mentioned, the MMPs share structural homology (a pro-domain, catalytic domain, a hinge region and a hemopexin-like domain), however they can be sub-classified into six groups on the basis of variations to their domain structure and their biological properties (as shown in Figure 1.14).

- Collagenases (MMP-1, MMP-8, MMP-13, MMP-18) display the characteristic structure of soluble MMPs and degrade interstitial collagens (type I, II and III) at a specific site generating ¼ and ¾ fragments. In addition collagenases have the ability to catabolise other ECM and non-ECM molecules [147].

- The two gelatinases MMP-2 and MMP-9, also commonly called gelatinase A and B, can digest denatured collagens and gelatins. Within their catalytic domain, gelatinases A and B have three fibronectin type II repeats that are necessary to bind denatured collagen and gelatin [147, 156].

- The stromelysins MMP-3 and MMP-10, also named stromelysin 1 and 2, share a similar structure to the collagenases and can degrade an array of ECM components including gelatin, fibronectin, laminin and aggrecan, although they are unable to digest collagens [156]. The stromelysin MMP-11, also named stromelysin 3, has a similar structure to the other stromelysins but its activation is intracellular and proposed to have a weak proteolytic activity towards ECM proteins [152][61].

- The matrilysins MMP-7 and MMP-26 are also termed matrilysin 1 and 2, and have broad substrate specificity, perhaps due in part to their lack of a hinge region and hemopexin-like domain [139].

- The six membrane-type MMPs, MMP-14, MMP-15, MMP-16, MMP-17, MMP-24, and MMP- 25, are also named MT1-MMP to MT6-MMP, respectively. The MT-MMPs are further divided in two groups including four transmembrane type I proteins (MMP-14, -15, -16 and -24) plus two glycosylphosphatidylinositol-anchored MMPs (MMP-17 and -25). They are able to digest several ECM components, and in particular MMP-14 is able to degrade collagen type I, II, and III. With the exception of MMP-17 and MMP-25, they also contain a COOH-terminal cytoplasmic tail [157].

- There are seven further MMPs which do not fall into the above categories including; MMP-12, -20 and -27 which share structural similarity to stromelysins members, and MMP-12 has been shown to play an important role during macrophage migration. MMP-19 has a broad substrate specificity, but in contrast to most other MMPs, is not able to activate latent MMPs. MMP-20 is also called enamelysin due to its ability to degrade enamel-specific proteins [139]. MMP-21 and MMP-23 lack a cysteine switch in their pro-domain and also lack a hemopexin domain, but instead contain a cysteine-rich immunoglobulin-like domain. Lastly, MMP-28 is also known as epilysin and is mainly expressed by keratinocytes [147].

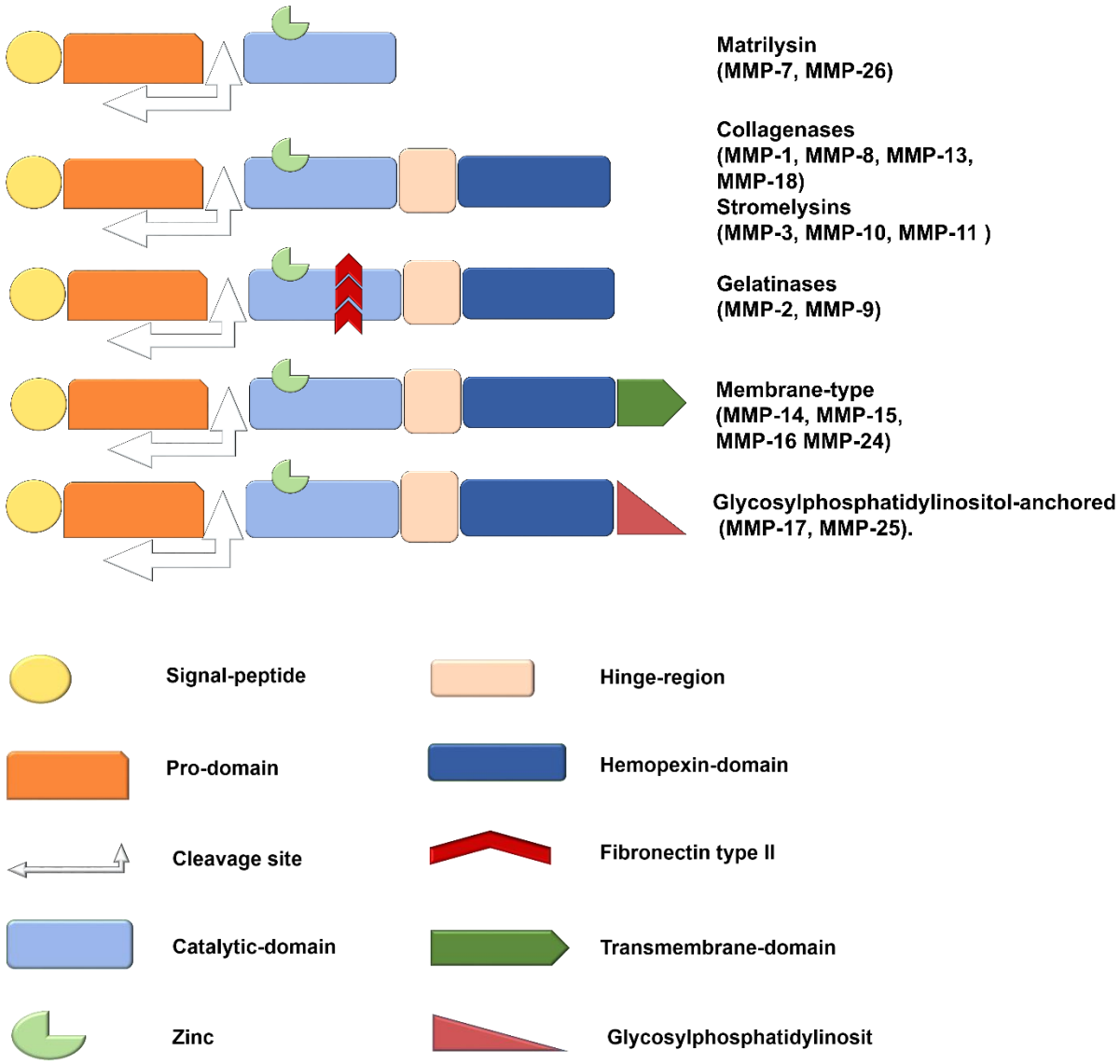

Figure 1.14 : Classes of MMPs and their structure

MMPs share structural homology and are classified into six classes on the basis of their structure. A signal peptide (yellow), a pro-domain (orange), a catalytic domain (light blue) containing the catalytic zinc (light green); a cleavage site (white arrow) between pro-domain and catalytic domain is really important for their activation; these structures are characteristic for members of the Matrilysin family. A linker called hinge region separates the catalytic domain (pink) from the hemopexin-like domain (blue) for members of the collagenase and stromelysin families. Three fibronectin type II repeats in the catalytic domain (red) are present within members of the gelatinases. Membrane-type MMPs also contain a transmembrane domain and a cytoplasmic tail (green) which is linked to the cell membrane. Two members of membrane-type MMPs are glycosylphosphatidylinositol-anchored MMPs (light red).

`

1.5.2 MMP domains

As previously mentioned, MMPs are proteins composed of several domains including a signal peptide followed by a pro-peptide domain then a catalytic domain and finally a hemopexin domain linked by hinge region. Moreover MT-MMPs and gelatinases contain an additional -COOH at their N-terminal domain, and in MT-MMPs only, the -COOH is followed by a trans-membrane domain and a cytoplasmic tail, whereas in gelatinases there are three fibronectin repeats within their catalytic domain. The differing domain structures within MMPs and their associated functions are discussed within this section.

The signal sequence is a short peptide, of 18-30 residues, present at the NH2-terminal sequence. This peptide is hydrophobic and is therefore able to direct the MMPs to the cell membrane, and is cleaved during secretion [47, 152].

The pro-peptide domain is composed of 80 amino acids, organised into three alpha-helices. The pro-peptide domain contains the cysteine-switch which is characterised by a PRCG (V/N) PD amino acid sequence that is a conserved sequence amongst all MMPs. The cysteine domain is necessary to interact with the active site zinc ion in order to maintain MMPs in an inactive form [147]. The initial activation of MMPs can be induced through a number of different mechanisms including separation of the pro-domain, or conformational change of this region [158].

The catalytic domain is composed of 165 amino acid residues and contains a zinc-binding sequence, HEXXHXXGXXH, where three residues of conserved histidine coordinate the active zinc ion [158]. In addition, a region called the loop region contains a conserved methionine “Met-turn” and provides a hydrophobic base for the zinc-binding site. In addition MMP-2 and MMP-9 contains three fibronectin type II repeats [47] [158].

The hinge region is a peptide linker located after the catalytic domain and just before the hemopexin-like domain. This region can adopt a different length between 2 and 72 amino acids, it is particularly long in collagenases, which also display a high concentration of proline residues which may benefit their collagenolytic activities [152].

The hemopexin-like domain (PEX) represents the COOH-N terminal of MMPs and is composed of about 200 amino acids. The structure of this domain consists of four β-sheets linked by disulfide bonds with a central core consisting of Ca+2 Cl- ion [47, 152].

1.5.3 Role of MMPs in inflammation

MMPs play a significant role in tissue remodelling which can be associated with various physiological or pathological processes such as morphogenesis, angiogenesis, tissue repair, inflammation and metastasis. In particular, MMPs are involved in the regulation of cell barrier integrity and also stimulate cell migration, proliferation and lastly apoptosis. Studies showed that MMPs can regulate the permeability of the endothelial barrier and this allows leukocytes to reach areas of damage. MMP-7 harbours the ability to cleave VE-cadherin while MMP-2 and MMP-9 can degrade endothelial tight junctions within the blood brain barrier [159]. MMP-14 is considered a marker of monocyte invasion during atherosclerotic plaque progression, as studies have shown that the expression and further activity of MMP-14 is increased in atherosclerosis and this fosters macrophage accumulation, while limiting MMP-14 activity can retard atherosclerotic plaque progression [160, 161]. Furthermore TIMP-2 (which can inhibit MMP-14), but not TIMP-1 (which cannot inhibit MMP-14) has been linked with decreased macrophage migration, increased macrophage apoptosis, and consequent retardation of atherosclerotic lesion progression [162]. Another important function that MMPs exert during inflammation is their ability to modulate the activities of inflammatory mediators including an array of chemokines, cytokines and growth factors. The activity of specific MMPs increase the concentration of pro-inflammatory cytokines such as TNF-α [163]. For instance, MMP-7 can increase the release of TNF-α from macrophages. MMP-2, -3, and -9 can contribute to the activation of IL-1β from its inactive form, although MMP-1, -2 and -9 have also been linked to IL-1β degradation, indicative of the multiple and varied roles of MMPs during inflammatory processes [159]. Chemokines are important during inflammation; their production is regulated in several steps including biosynthesis, processing and mobilisation, and MMPs can regulate them during all these phases [163]. MMPs can also generate a chemotactic concentration gradient which directs leukocyte migration, for example MMP-7 can cleave a domain of CXCL1 creating a CXCL1 chemotactic gradient [159]. In addition to their role during inflammation, MMPs play a prominent role in vascular remodelling [144]. In particular, the regulation of hemodynamic changes, oxidative stress, and hypoxia-related responses linked to pathological angiogenesis are influenced by MMPs. MMPs can also regulate the migration, proliferation and apoptosis of VSMC [48, 56].

1.5.4 MMP and TIMP expression in human aortic aneurysms

ECM remodelling is a characteristic feature associated with degeneration of the aortic wall during the pathogenesis of aortic aneurysms [164]. Increased MMP activity alongside reductions in TIMP levels can induce ECM degeneration as well as disruption of elastin and collagen, and consequently aneurysm formation. Accordingly, the measurement of circulating MMP and TIMP levels has been proposed as a predictive tool to assess aneurysm progression [165]. Several studies have shown that in aneurysm tissues the expression and the activity of many MMPs is linked to changes in the proliferation, migration, and apoptosis of inflammatory cells within the vessel wall. Davis *et al.* focused their study on expression of MMP-2 and MMP-9 in tissue samples from aorta in AAA, atherosclerotic and health control tissue and demonstrated both MMPs are elevated in aortic disease; however increased MMP-2 levels were characteristic of AAA and co-localised prominently with VSMCs [166, 167]. Elmore *et al.* assessed the expression of MMP-2, -9, TIMP-1 and TIMP-2 in AAA and control samples and found significantly increased in MMP-9 expression within AAA tissues compared to control aorta, while MMP-2 was unchanged, concluding that MMP-9 but not MMP-2 contributes to aneurysm formation [167]. Regarding the TIMP expression, no changes were observed in TIMP-1 and TIMP-2 expression between the groups [167]. MMP-9 is largely expressed by macrophages and its activity, assessed by zymography, is increased in ruptured compared to intact large aneurysms (diameter between 5 and 7 cm) [150]. Furthermore, levels of total and active MMP-8 are elevated in human AAAs when compared with un-diseased aortic tissue [168]. Recently Alonso *et al.* suggested a protective role for MMP-17 (also named MT4-MMP) in TAA progression due to the fact that a missense mutation in MMP-17 predisposes patients to TAA [169]. MMP-14, better known as MT1-MMP, has been detected in VSMCs within aneurysm tissue, and thought to promote aneurysm progression through its ability to convert pro-MMP2 to its active form [170]. Newman *et al.* demonstrated that MMP-3 and MMP-9 are significantly increased in aneurysms; the active form of MMP-3 can activate MMP-9 which can degrade collagens, elastin and other ECM components, underlying their potential causal role in aneurysm development [171]. MMP-12 is predominantly expressed by infiltrating-macrophages within the media of aneurysmal areas of the abdominal aorta [172]. MMP-12 was found increased in mice after $CaCl_2$ application compared to wild type (WT) mice, furthermore MMP-12 expression was significantly increased within the vessel wall after stimulation with nicotine [173]. Conversely, TIMP-1 and -2 which are necessary to counter aberrant MMP activity, are reduced in human aneurysms compared to control tissues [174]. However increased TIMP-3 expression was observed in patients with aneurysms, although this may reflect a feedback response to negate elevated MMP activity [175, 176]. Lastly, the

expression of TIMP-4 protein is significantly lower in aneurysmal aortic tissue and plasma of patients with bicuspid aortic valve disease compared to healthy controls [177].

Numerous studies have been conducted in animal models of aneurysm development to elucidate the pathophysiological role of MMPs. Such models should display degradation and loss of collagen and elastin in order to reduce the stability of aortic wall. The three most utilised models of aneurysm formation involve systemic administration of Ang II, aortic intra-luminal elastase-infusion, and peri-aortic $CaCl_2$ application, commonly in mice [129]. Using the elastase-induced AAA model, Pyo *et al.* showed that administration of a MMP-9 inhibitor suppressed aneurysm formation, supporting a deleterious role for MMP-9 in aneurysmal disease [178]. Similarly, genetic deficiency of MMP-9 in the $CaCl_2$ model, afforded protection from aneurysm development [177]. Furthermore, mice deficient for both MMP-2 and MMP-9 showed no aneurysm formation compared to WT controls [179]. Moreover, add-back experiments using competent MMP-9 expressing macrophages and MMP-2 expressing mesenchymal cells demonstrated that these two MMPs from specific cellular compartments are necessary for aneurysm induction in the $CaCl_2$ model of AAA [179]. In order to assess the contribution of VSMC phenotypic modulation to aneurysm development, Mao *et al.* deployed a peri-adventitial elastase application rat model to induce VSMC phenotypic switching [180]. Animals in this model displayed aortic dilatation alongside low expression of the contractile VSMC phenotype markers smooth muscle myosin heavy chains (SMMHC) and α-SM actin, and high expression of MMP-2 and MMP-9. MMP-12 (also known as macrophage metalloelastase) has also been proposed to contribute to aneurysm formation. Wang *et al.* showed that MMP-12 promotes Ang II-induced aneurysm formation through the use of MMP-12 deficient mice, while additionally demonstrating that the protective effect of TGF-β on aneurysm formation in this model is in part via suppression of MMP-12 activity [79]. Increased expression of MMP-14 has also been associated with the development of AAAs and TAAs. In particular, using bone marrow transplantation from MMP-14 deficient mice into WT animals using the $CaCl_2$ model, aneurysm development was reduced and could be reversed through the re-introduction of MMP-14 expressing macrophages [181]. As previously mentioned, MMP activity is tightly regulated at the transcriptional and translational levels, notably the most effective post-translational regulation involves the action of the four TIMPs. Accordingly, depletion of TIMP-1, either in WT or Apoe-deficient mice, increased aortic aneurysm development [182]. Moreover, VSMC-restricted overexpression of TIMP-1 in a rat xenograft model of reduced aneurysm formation by reducing elastin degradation and activity of MMP-2 and MMP-9 [183]. Zhao *et al.* demonstrated that local intra-luminal delivery of an adenovirus carrying the TIMP-2 gene into the aorta of rats previously subjected to elastase-induced aneurysm induction, reduced ECM degradation and suppressed the formation of AAAs [179].

Supporting studies in atherosclerosis mouse models have also demonstrated that elastin degradation and 'pseudo-aneurysm' formation are increased in mice deficient for TIMP-1 or TIMP-2 [184]. Two independent studies have demonstrated a protective role of TIMP-3 in the formation of aortic aneurysms using the Ang II-induced model. Basu and colleagues showed that TIMP-3 retards AAA formation in part through inhibiting MMP-2 activity, while also noting that the increase in TIMP-3 expression observed in aneurysmal tissues indicates a compensatory mechanism in response to heightened MMP activity [185]. Di Gregoli and co-workers showed similar findings in TIMP-3 deficient mice additionally lacking either Apoe or Ldlr and subjected to Ang II-infusion [186]. Moreover, this study revealed that aneurysm formation was increased within the ascending, thoracic and abdominal aorta of TIMP-3 deficient animals, and this could be countered through restoration of TIMP-3 expression by inhibiting a specific microRNA (miR-181b) that targets TIMP-3 [186]. No animal study addressing the role of TIMP-4 in aortic aneurysm development and rupture has been conducted to date.

1.5.5 MMP pharmacological intervention in animal models of AAA

Until recently, the dogma existed that all MMPs played deleterious roles in atherosclerosis and by association aneurysms, as in concert they can degrade the ECM components elastin and collagen. As such strategies for the therapeutic treatment of aortic aneurysms included the broad-spectrum inhibition of MMP activities in order to preserve the aortic wall. Doxycycline is an antibiotic of the tetracycline class that has the ability to non-specifically inhibit MMPs. It was demonstrated that e*x vivo* culturing of human AAA tissue with Doxycycline at concentrations of 2.5 to 40 µg/mL for 10 days, inhibited expression and activity of MMP-2 and MMP-9 [187]. In addition, a study conducted in the rat intra-luminal elastase-induced AAA model, demonstrated that daily administration of Doxycycline inhibited aortic dilatation in a dose-dependent effect, attributable to decreased MMP-9 activity and increased elastin content within the aortic wall [172]. Similar results were obtained in the mouse Ang II-induced AAA model, where Doxycycline (administered within the drinking water) significantly reduced aneurysm development from 86% (in controls) to 35%, although interestingly Ang II-induced atherosclerosis was unaffected [188]. Broad-spectrum MMP inhibition achieved through administration of hydroxamate-based compounds has also shown favourable results. Subcutaneously systemic delivery of RS 132908 in the mouse intra-luminal elastase-induced AAA model, suppressed aortic dilatation and associated elastin degradation, consistent with a direct inhibitor action on various MMPs [189]. In agreement, Bigatel *et al.* showed that daily administration of BB-94 (also known as Batimastat) in the rat intra-luminal elastase-induced

AAA model displayed reduced aortic dilatation alongside decreased elastin fragmentation and inflammatory cell accumulation [190].

1.5.6 MMP inhibitors in clinical trials

Supported by the favourable observational studies in animal models of aneurysm highlighting the potential therapeutic effect of Doxycycline, several clinical trials have been performed in humans to assess the therapeutic efficacy of Doxycycline treatment. A study on 32 patients with existing large AAA was performed. Patients were randomly selected to receive Doxycycline or placebo therapy for 3 months, and showed a significant reduction in aneurysm expansion in the Doxycycline treated group [191]. Furthermore, a group of 60 patients elected for aneurysm repair were randomly selected for short term treatment (two weeks) with differing doses of Doxycycline (50, 100, or 300 mg/d, respectively) or no medication, and treated patients showed a reduction of MMP-9 expression alongside lowered inflammatory cell numbers within the diseased aortic wall, independent of drug dose [192]. A longer-term (six months) randomised placebo-controlled trial similarly demonstrated that administration of Doxycycline reduced MMP-9 levels in treated patients after aneurysm repair and was associated with reduced aortic diameter compared to placebo-treated controls [193]. Assessment of AAA tissues removed from patients that were previously treated with Doxycycline (100mg/twice daily/for seven days) when compared to untreated controls, showed reduced MMP-9 mRNA and protein expression alongside blunted MMP-2 and MMP-9 activity [178]. However, a similar study giving Doxycycline daily at the same dose but for a month, showed no change in the expression or activity of MMP-2 and MMP-9 [194, 195]. Comparably, long term Doxycycline administration (100mg/twice daily/for six months) had no effect on AAA diameter or expansion alongside a modest reduction in plasma MMP-9 levels [195]. As such, further studies are required to robustly assess the therapeutic potential of non-selective MMP inhibitors such as Doxycycline in patients with existing aneurysms, while the mechanism by which Doxycycline may affect aneurysm expansion and MMP mRNA expression also needs further elucidation.

1.6 Animal models of aneurysm and the 3Rs

In order to further elucidate the appropriateness of new and existing therapies aimed at inhibiting select, classes, or all MMPs for retarding the progression of aneurysms, it is clearly evident that multiple experiments in large groups of animals raises ethical considerations. Within the most commonly used mouse models of aneurysm formation, pronounced AAAs are observed after 28 days, although approximately 15% of animals also suffer from aortic dissections and subsequent sudden death in the first 7-10 days [130]. The patho-physiological processes in these animal models are similar (although obviously accelerated) to that observed in humans [181]. Accordingly, mouse models of aneurysm formation/development have afforded numerous mechanistic and proof-of-principle studies to be conducted, in an attempt to reveal potential therapeutic targets and identify prospective biomarkers. However, the number of *in vivo* mouse experiments appears to be increasing and are regularly published in high impact factor journals such as *J Clin Invest, J Exp Med, PNAS, Circulation, Circ Res* and *ATVB*. Accordingly, the quantity of animals used for aneurysm research shows no signs of reducing, and with the advent of large animal models of aneurysm such as those developed in rabbits and pigs, in vivo aneurysm studies show no signs of abating [181, 196]. Indeed, within the last five years there have been 835 original articles published that use mouse models of aneurysm formation. Counting that each study, on average, use three experimental groups with nine mice per group, we can assume that around 22,545 mice have been used in the last five years for aneurysm studies. Furthermore, the use of Ang II in high-doses (1000 ng/kg/min) results in at least 15-20% of those animals suffering from aortic dissection and subsequent sudden death. The 3Rs (**R**eplacement, **R**eduction, and **R**efinement) were devised over 50 years ago in an attempt to detail criteria for performing more humane animal research. More recently, the 3Rs have served as a bedrock of national and international legislation and regulation for the use of animals in scientific procedures. Moreover, this framework has moulded the policies of organisations that fund or conduct research in animals, such as the National Centre for the Replacement, Refinement and Reduction of Animals in Research (NC3Rs). Taking the 3Rs into account, there is therefore a need to develop and characterise a potential reproducible *ex vivo* human model of aneurysm, to serve as a suitable replacement for mouse models of aneurysm development, progression and rupture. Such a model should mimic the current *in vivo* animal models to become a suitable replacement with similar cellular and morphological features such as altered expression of MMPs and their TIMPs, loss of elastin and associated vessel dilation, and differences in VSMC phenotypic markers. A suitable *ex vivo* aneurysm model utilising human tissue will be applicable for the testing of new therapeutics and has the potential to supplant the need for animal models, although a small number of studies may still be required for *in vivo* validation.

1.7 Aims

The over-arching aim of this research was to develop and characterise a potential reproducible *ex vivo* human model of aneurysm, to serve as a suitable replacement for mouse models of aneurysm development, progression and rupture.

1.8 Hypothesis

Human umbilical cord artery subjected to aneurysm-associated stimuli in an *ex vivo* flow model, induces characteristics associated with aneurysm formation in mouse models and human disease, supporting its use for aneurysm studies.

CHAPTER 2

2 Materials and Methods

2.1 *In vitro* studies

2.1.1 Cell culture media

2.1.1.1 Dulbecco's Phosphate Buffered Saline (DPBS)

Dulbecco sterile Phosphate Buffer Saline (sPBS) without calcium and magnesium was used and stored at room temperature (Sigma, D8537).

2.1.1.2 Smooth Muscle Cell Growth Medium 2

Smooth muscle cell growth medium 2 was obtained from Promo Cell (Promo Cell, C-22062). The Medium Kit included a 500 ml bottle of medium and a growth supplement mix (Promo Cell, C-39267) containing the components as listed in Table 2.1. All supplements were added using a syringe filter to prevent infection, mixed well and finally stored at 4°C.

Table 2.1: Media composition for Smooth Muscle Cell Growth Medium 2

Reagent	Final Concentration	Supplier
Foetal Calf Serum	0.05 ml/ml	Promo Cell, C-39267
Epidermal Growth Factor (recombinant human)	0.5 ng/ml	Promo Cell, C-39267
Basic Fibroblast Growth Factor (recombinant human)	2 ng/ml	Promo Cell, C-39267
Insulin (recombinant human)	5µg/ml	Promo Cell, C-39267
Gentamicin	400 µl/500 ml	PAA (P11-040)
Penicillin & Streptomycin	100 Ul/ml &100 µl/ml	PAA (P11-010)
L-glutamine	2Mm	PAA (M11-004)

2.1.1.3 Serum free Dulbecco's modified Eagle's Medium (SFM)

Dulbecco's modified Eagle's Medium (DMEM) was obtained from Sigma (PAA, E15-005) and it was supplemented as in Table 2.2. All supplements were added using a syringe filter to prevent infection, mixed well and finally stored at 4°C.

Table 2.2: Media composition for Serum Free DMEM

Reagent	Final Concentration	Supplier
Gentamicin	400 µl/500 ml	PAA (P11-040)
Penicillin & Streptomycin	100 Ul/ml &100 µl/ml	PAA (P11-010)
L-glutamine	2Mm	PAA (M11-004)

2.1.1.4 10% FBS/DMEM Culture media

Serum free DMEM was supplemented with 50 ml foetal bovine serum (FBS) gold (Thermo Fisher Scientific,10500-064) to obtain 10% FBS/DMEM. All the components of 10% FBS/DMEM are listed in Table 2.3. FBS was added using a syringe filter to prevent infection, mixed well and finally stored at 4°C

Table 2.3: Media composition for 10% FBS/DMEM

Reagent	Final Concentration	Supplier
Foetal Calf Serum	10%	PAA (A11-151)
Gentamicin	400 µl/500 ml	PAA (P11-040)
Penicillin & Streptomycin	100 Ul/ml &100 µl/ml	PAA (P11-010)
L-glutamine	2Mm	PAA (M11-004)

2.1.1.5 Endothelial Cell Medium

Endothelial cell growth medium was obtained from Promo Cell (Promo Cell, C-22010). The Medium Kit included a 500 ml bottle of endothelial cell growth medium and a growth supplement mix (Promo Cell, C-39210) containing the components as listed in Table 2.4. All supplements were filtered using a syringe filter to prevent infection, mixed and finally stored at 4°C.

Table 2.4: Media composition for Endothelial Cell Medium

Reagent	Final Concentration	Supplier
Foetal Calf Serum	0.02 ml / ml	Promo Cell (C-39215)
Endothelial Cell Growth Supplement	0.004 ml/ml	Promo Cell (: C-39215)
Epidermal Growth Factor (recombinant human)	0.1 ng / ml	Promo Cell (C-39215)
Basic Fibroblast Growth Factor (recombinant human)	1 ng / ml	Promo Cell (C-39215)
Heparin	90 µg / ml	Promo Cell (C-39215)
Hydrocortisone	1 µg / ml	Promo Cell (C-39215)
Gentamicin	400 µl/500 ml	PAA (P11-040)
Penicillin & Streptomycin	100 Ul/ml &100 µl/ml	PAA (P11-010)
L-glutamine	2mM	PAA (cat No: M11-004)

2.1.1.6 Endothelial Cell 2% FCS Medium

Endothelial Cell Basal Medium was obtained from Promo Cell (Promo Cell, C-22210) and was supplemented as in Table 2.5. All supplements were filtered using a syringe filter to prevent infection, mixed and finally stored at 4°C.

Table 2.5: Media composition for Endothelial Cell Medium

Reagent	Final Concentration	Supplier
Foetal Calf Serum	2%	PAA (A11-151)
Gentamicin	400 µl/500 ml	PAA (P11-040)
Penicillin & Streptomycin	100 Ul/ml &100 µl/ml	PAA (P11-010)
L-glutamine	2mM	PAA (M11-004)

2.1.1.7 Hepes-buffered RPMI 1640 for saphenous vein

25 mM Hepes-buffered Roswell Park Memorial Institute (RPMI) 1640 was obtained from Gibco (Gibco, 42401-018) and supplemented as in Table 2.6. All supplements were filtered by using a syringe filter to prevent infection, mixed and finally stored at 4°C.

Table 2.6: Media composition for Hepes-buffered RPMI

Reagent	Final Concentration	Supplier
Gentamicin	8 µg/ ml	PAA (cat No: P11-040)
Penicillin & Streptomycin	100 Ul/ml &100 µl/ml	PAA (cat No: P11-010)
L-glutamine	2Mm	PAA (cat No: M11-004)

2.1.2 Cell culture

2.1.2.1 Human arterial VSMC isolation

Human umbilical cords were obtained from St. Michael's Maternity Hospital (Bristol) covered under existing ethical approval (Research Ethics Committee reference: E5431) and stored at 4°C after delivery. Under sterile conditions, human umbilical cord was placed into a silicon dish, the two arteries were isolated from human umbilical cord by dissection and stored at 4°C. Arteries were then micro-dissected, cleaned of blood, and then cut into approximately 2mm x 2mm explants under a laminar flow-hood. The explants were placed into 75 cm^3 flasks by standing the flask on its end, and incubated at 37°C, 5% CO_2 for at least 2 hours or overnight in 10ml of 10% FBS/DMEM media to facilitate explant adhesion. The following day a further 5ml of 10% FBS/DMEM was added to cover the explants and re-incubated at 37°C, 5% CO_2. Fresh media was added every 4/5 days until cells reached confluence. For cell characterisation see section 2.1.4.3).

2.1.2.2 Passaging of arterial VSMC

Once VSMCs had reached 70-90% confluency, they were washed twice with PBS and then incubated at 37°C, 5% CO_2 for 5 minutes with 0.5% trypsin-EDTA until detached from the flask surface. Cells were visually checked under a microscope to confirm detachment. Equal volume of 10% FBS/DMEM was then added to neutralise the trypsin and remaining adherent cells were gently scraped from the bottom of the flask into the media using a cell scraper. The cell suspension was transferred to a Falcon tube and then centrifuged at 1500 rpm for 5 minutes. After centrifugation the supernatant was discarded, and the cell pellet (located at the base of the tube), was re-suspended in 1ml of 10% FBS/DMEM. The cells were then reseeded in a new flask.

2.1.2.3 Seeding of arterial VSMCs

Confluent VSMCs isolated from human umbilical cord arteries were trypsinised, pelleted, then re-suspended in 1-7ml of 10% FBS/DMEM, dependent on pellet size. Cells were then counted using a Neuberger haemocytometer and the cell density calculated using the following formula:

Number of cells/ml = Average number of cells per $1mm^2$ x 10^4

Cells were seeded at the required density and then incubated overnight in 10% FBS/DMEM.

2.1.2.4 Cell stimulation

After 24 hours incubation, adherent cells were washed in sPBS and subsequently incubated in SFM for 24 hours to quiesce them. VSMCs were then treated either continuously with 5 µmol/L of Ang II (Enzo Life Science, ALX-151-039-M025) or pre-treated for 15 minutes with

$CaCl_2$ (250mM and 500 mM). RNA was collected after 6 hours and cell lysates/condition media after 24 hours. The concentrations of Ang II and $CaCl_2$ were chosen based on doses used in the associated experimental mouse models.

2.1.2.5 Cryopreservation and resuscitation

The process of cryopreservation is used to enable stocks of cells to be stored; cells were trypsinised as in 2.1.2.2 and re-suspended in 1ml 10% (v/v) dimethyl sulphoxide (DMSO) and then pipetted into cryovials (Nalgene). Cryovials were immediately stored at -80°C in a freezing container that freezes cells at a rate of -1°C to -3°C /minute; the following day, cells were transferred into liquid nitrogen for indefinite periods providing a temperature of less than -135°C.

For resuscitation, cryovials of cells were retrieved from liquid nitrogen storage, and in order to reduce the number dying cells and associated debris, the cells were gently transferred to a Falcon tube and then centrifuged at 1500 rpm for 2 minutes. After centrifugation the supernatant was discarded, and the cell pellet (located at the base of the tube), was re-suspended in 1ml of endothelial cell growth medium and then transferred into 24ml of pre-warmed 10% FBS/DMEM and incubated at 37°C in 5% CO_2. Media was then replaced every 4/5 days.

2.1.2.6 Human Umbilical Vein Endothelial Cells

For all *in vitro* experimental conditions, we used Human Umbilical Vein Endothelial Cells (HUVECs), which were isolated from vein of umbilical cord. The cells were purchased from Promo Cell (Promo Cell, C-12203). Each vial contained 500,000 cryopreserved cells isolated in standard Endothelial Cell Growth Medium from single donors or from four pooled donors. Media was replaced with fresh media every three days until the cells reached the required confluency.

2.1.2.7 Passaging of HUVECs

Once HUVECs had reached 70-90% confluency, they were washed twice with PBS and then incubated at room temperature with 0.5% Trypsin-EDTA until detached from the flask surface. Cells were visually checked under a microscope to confirm that they had detached. Endothelial cell growth medium was then added to neutralise the trypsin, and cells were gently transferred to a Falcon tube and then centrifuged at 1200 rpm for 4 minutes. After centrifugation the supernatant was discarded, and the cell pellet was re-suspended in 1ml of endothelial cell growth medium. The cells were then reseeded in a new flask.

2.1.2.8 Seeding of HUVECs

Confluent HUVECs isolated from human umbilical vein were trypsinised, pelleted, then re-suspended in 1-7ml of endothelial cell growth media, dependent on pellet size. Cells were then counted using a Neuberger haemocytometer and the cell density calculated using the following formula:

Number of cells/ml= Average number of cells per $1mm^2 \times 10^4$

Cells were seeded at the required density and then incubated overnight in endothelial cell growth media.

2.1.2.9 Cell stimulation

After 24 hours' incubation, cells were washed in PBS and subsequently incubated in 2% FBS endothelial cell growth media for 24 hours to quiesce them. HUVECs were then treated with either Ang II (5 µmol/L), Ang II + recombinant human TIMP 3 (rTIMP-3) (5nM), or Ang II + losartan (25µM), or unstimulated.

2.1.2.10 HUVEC seeding for the in vitro flow

Cells were seeded at $1x10^5$ on four well glass chamber slides (Thermo Fisher, 154526) and incubated overnight. Before the seeding process, chamber slides were pre-coated with collagen (sigma, C3867, 4mg/ml) for 1 hour at room temperature to improve cell adhesion. After 1-hour, residual collagen solution was aspirated, and chambers washed with 2 changes of PBS.

2.1.2.11 HUVEC stimulation for in vitro flow experiments

The next day, cells were placed on a laboratory rocker (Grant Instruments Grant Bio PMR-30 Compact Fixed-Angle Platform Rocker Platform Style. Fischer Sci Warehouse 12965501) in order to enable cells to experience a form of haemodynamic flow for 24 hours, following which HUVECs were treated with Ang II (5µM), Ang II (5µM) + rTIMP-3 (5nM), or Ang II (5µM) + Losartan (25µM), or unstimulated (control) for 24h or 72h (as shown in Figure 2.1). Losartan is an antagonist of the Ang II receptor type 1 (AT1R) and is currently used clinically to treat hypertension. The following day cells were fixed with 3% PFA and subjected to immunocytochemistry (ICC) for VE-cadherin (see section 2.1.4.2 for more details).

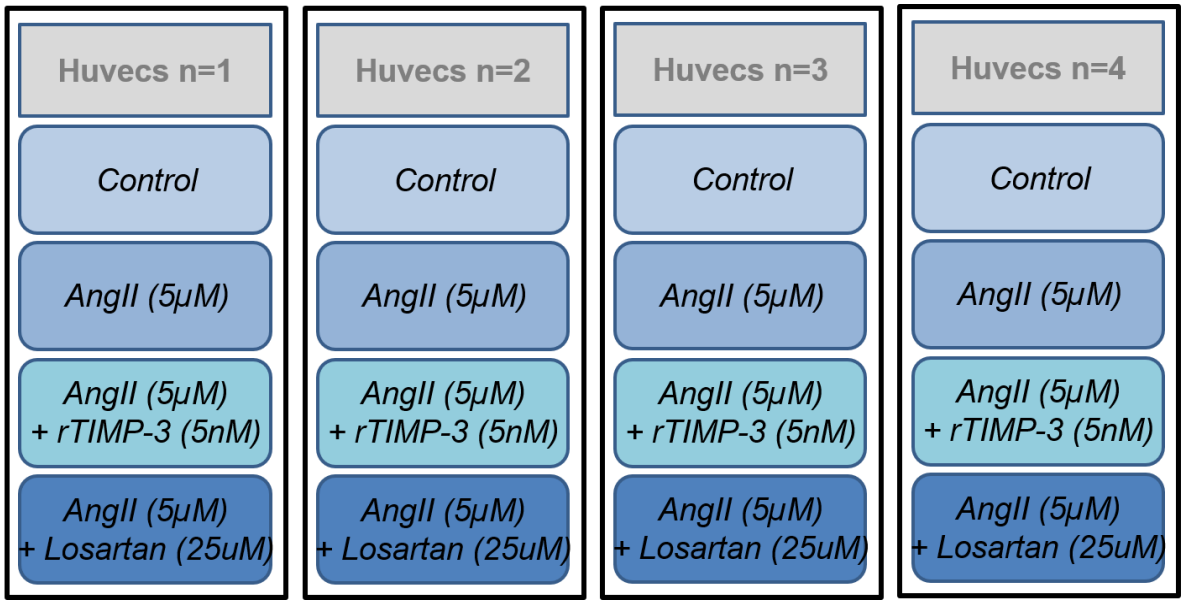

Figure 2.1: Schematic representative of four-chamber slide experimental set-up

HUVECs were treated with Ang II (5μM), Ang II (5μM) + rTIMP-3(5nM), Ang II (5μM) +Losartan (25μM), or unstimulated (control) for 24h or 72h. n=4 different HUVECs donors were used for this experiment.

2.1.3 Polymerase Chain Reaction (PCR)

2.1.3.1 Cell lysis for RNA extraction

First, cells were washed twice in PBS (1ml), then 350µl of Buffer RLT (from the Qiagen RNeasy Mini Kit (Qiagen, 74104) containing 10% β-mercaptoethanol was added. The barrel of a 1ml syringe was used to facilitate cell detachment and lysis, and the lysate was transferred into a DNAse/RNAse-free eppendorf and stored at -80°C until RNA purification.

2.1.3.2 Tissue lysis for RNA extraction

The mirVana PARIS kit (ThermoFisher, AM1556) was used to enable the isolation of both RNA and protein from of the same piece of arterial tissue. Pieces of human umbilical cord (2cm in length) were cut into 4 equal pieces, placed in different 2ml sterile and RNA free tubes prefilled with ceramic beads (cat.no. 91-PCS-CK14S PEQLAB) and then 300µl of cell disruption buffer added. Tubes were then placed in a Bertin Minilys tissue homogenizer (3 cycles at full power for 10 seconds with 30 seconds rest in between cycles). Subsequently, 250µl of tissue lysate was kept on ice for 30 minutes and then centrifuged at 10,000 rpm for 10 minutes at 4^0C. The supernatant was collected and split for RNA isolation and protein analysis or stored at -20^0C.

2.1.3.3 RNA extraction from cell lysates

Using the Qiagen RNeasy Mini Kit (Qiagen, 74104), cells lysates were transferred to a gDNA eliminator spin column and centrifuged for 30 seconds at 8000 g (10,000 rpm) in order to remove genomic DNA, and then 350 µl of 70% ethanol was added to each sample and mixed well by pipetting. After that the entire sample (350µl) was added to a RNeasy column and centrifuged for 15 seconds at 8000 g (10,000 rpm); following this step, three washes (one with 700 µl Buffer RW1 and two with 500 µl Buffer RPE) were performed. The RNeasy spin column was placed in a new 2 ml collection tube. Finally, in order to elute and collect the RNA 30µl RNAse-free water was added and centrifuged for 1 minute at 8000 g (10,000 rpm). The columns were discarded, and the RNA was stored at -20°C.

2.1.3.4 RNA extraction from tissue lysates

Using the mirVana PARIS kit (ThermoFisher, AM1556), tissue lysates (50µl) were mixed with denaturing solution (50µl) and then an equal volume of chloroform (100µl) was added to each sample. The mixture was vortexed for 30 seconds and then centrifuged at 10,000g at room temperature in order to separate the aqueous and organic phases. Following, the upper aqueous phase was collected and transferred to a new-labelled RNAse free eppendorf. Then,

1.25 volume of 100% ethanol was added to each sample and mixed by pipetting. Samples were then transferred to a filter cartridge/column and centrifuged for 30 seconds at 10,000g. The flow through was discarded and 700µl of washing solution 1 was added to the column, which was then centrifuged for 15 seconds at 10,000g. Following, the flow through was discarded and 500µl of washing solution 2 was added and centrifuged for 15 seconds at 8,000g (this step was repeated 2 times). An additional spin for 1minute at 10,000g was performed to remove additional fluids. The filter cartridge/column was then transferred to a fresh RNAse free eppendorf tube. To elute and collect the RNA extract, 50µl of pre-heated nuclease free water was applied to the centre of the column directly on the membrane and then a centrifugation for 30 seconds at 10,000g was performed to recover the RNA. The column was discarded, and the RNA stored at -20°C or quantified immediately.

2.1.3.5 RNA quantification

Total RNA was quantified using a NanoDrop ND-1000 spectrophotometer. The RNA sample (1.5µl) was added to the NanoDrop and the RNA concentration (ng/ml) was obtained by measuring absorbance at 230nm, 260nm and 280nm. Samples with a 260/280 ratio <1.8 (contamination with ethanol or phenol) or a 260/230 ratio >2.2 (contamination with nucleic acid) were excluded from further analysis.

2.1.3.6 Reverse transcription PCR (RT-PCR)

Reverse transcription was performed using the QuantiTect Reverse transcription kit (Qiagen, 205310). All the reagents were placed on ice. Firstly, RNAse free water was used to normalize RNA levels at the same concentration, then 2 µl of genomic-DNA wipeout buffer was added to each sample and incubated for 2 min at 42°C. Samples were then placed on ice. Secondly, 6 µl of master mix (in accordance with the manufacturers data sheet) was added to the samples which were then incubated at 42°C for 30 minutes followed by 95°C for 3 minutes and finally cooled to 4˚C. The cDNA samples were stored at -20°C for future QPCR analysis.

2.1.3.7 Quantitative PCR (QPCR)

Quantitative PCR was performed using a LightCycler 480 PCR Platform (Roche) alongside SYBR Green I Master kit (Roche, 04707516001) or QuantiTect SYBR Green PCR Kit (Qiagen, 204145). Firstly, 9µl of a SYBR Green Mastermix (containing 5µl SYBR green, 3µl PCR grade water and 1µl primers) was added to each well, secondly 1µl of cDNA (previously normalised at the same concentration) was added to a 96 well QPCR plate. Each sample was analysed in duplicate. As negative controls, a blank RT reaction sample was used for each primer. The plates were sealed using plastic plate sealers (Greiner Bio-One, 676040) and then centrifuged at 2,500rpm for 30 seconds using an MPS-1000 mini-plate spinner (Labnet). PCR program conditions were as shown in Table 2.7:

Table 2.7: Programme used for RT-QPCR reaction

	Temperature (C°)	***Time***
Initial denaturation	95	15
Denaturation	94	15
Annealing	60	20
Extension	72	2
Final extension	72	10
Melting curve	From 95 to 72	0.05 (°C/sec)

The expression intensity of a certain gene from a sample under specific biological conditions was expressed in Cycles to Threshold (C_T) of PCR. This value corresponds to the number of cycles whereby the amplified cDNA template reaches a linear detection threshold and is therefore only a relative measure of amplicon concentration. These $C_{T\ values}$ were used for calculating fold changes in mRNA expression. As cDNA samples were run in duplicate, two C_T values were generated per sample which were averaged to give a mean C_T value for each sample. Primers used for QPCR were designed using the primer blast programme on the Sigma website and purchased from Sigma. Table 2.8 and Table 2.9 below shows their characteristics;

Table 2.8: List of primers used for QPCR

Gene	Left/right	Primer sequence
MMP-2	*Forward*	CCATTGAACAAGAAGGGGAACTTG
	Reverse	GGATACCCCTTTGACGGTAAGGAC
MMP-3	*Forward*	CGCCTGTCTCAAGATGATATAAAT
	Reverse	CTGACAGCATCAAAGGACAA
MMP-9	*Forward*	AAGGATGGGAAGTACTGG
	Reverse	GCCCAGAGAAGAAGAAAAG
MMP-10	*Forward*	CAAAATCTGTTCCTTCGGGATCTG
	Reverse	GATGCCTCTTGGATAACCTGCTTG
MMP-12	*Forward*	TTACCCCCTTGAAATTCAGCAAGA
	Reverse	CGTGAACAGCAGTGAGGAACAAGT
MMP-14	*Forward*	GGAGACAAGCATTGGGTGTT
	Reverse	GGTAGCCCGGTTCTACCTTC
TIMP-1	*Forward*	GATACTTCCACAGGTCCCACAACC
	Reverse	CAGCCAACAGTGTAGGTCTTGGTG
TIMP-2	*Forward*	GAAGGAAGTGGACTCTGGAAACGA
	Reverse	ATGAAGTCACAGAGGGTGATGTGC
TIMP-3	*Forward*	CTTCCGAGAGTCTCTGTGGCCTTA
	Reverse	CTCGTTCTTGGAAGTCACAAAGCA
TIMP-4	*Forward*	AGATGTTCAAAGGGTTTGAGAAAG
	Reverse	GTAGTTGCACAGATGGATGAAGAC
36B4	*Forward*	GCCCAGGGAAGACAGGGCGA
	Reverse	GCGCATCATGGTGTTCTTGCCCA
GAPDH	*Forward*	GACCTGACCTGCCGTCTAGAAAAA
	Reverse	TGCTGTAGCCAAATTCGTTGTCAT
ELF1	*Forward*	TATTAGGACTATACAGGCT
	Reverse	GTTACTGTATGCAACTGCTG

Table 2.9: List of quantitec primers used for QPCR

Gene	Catalogue number	Company
α-SM actin (ACTA2)	*QT02407307*	Quantitec (QUIAGEN)
Caldesmon (CALD1)	*QT00070021*	Quantitec (QUIAGEN)
Tangelin (TAGLN)	*QT00072247*	Quantitec (QUIAGEN)

2.1.3.8 Western Blotting

2.1.3.9 Cell lysis

Cells were treated for 24 hours, washed 2 times with PBS and were then lysed and collected using the barrel of a 1ml syringe alongside addition of 120µl of SDS lysis buffer (5% SDS, 50mM Tris hydrochloric acid (HCL pH 6.8, 10% glycerol). The lysate collected was passed through a 200µl pipette and pipetted up and down 10 times to shear DNA. The lysates were then centrifuged at 13,000g for 5 minutes and stored at -20°C until analysis.

2.1.3.10 Protein assay (Protein quantification)

The Bicinchoninic Acid (BCA) Protein Assay Kit (Thermo Scientific, 23235) in 96-well plates is a colorimetric test to estimate protein concentrations. Firstly, 140µl of HPLC grade water was added to a 96-well plate (to the appropriate wells). Bovine serum albumin (BSA) at concentrations of 0, 0.1, 0.25, 0.5, 1.0, 2.5, 5.0 and 10mg/ml were used for the production of a standard curve. Then, 5µl per well of sample followed by 150µl/well of BCA reaction mix solution (composed of 50% reagent A, 48% reagent B and 2% reagent C) was added to the appropriate wells. All samples and standards were conducted in duplicate. The plate was incubated at 37°C for 1 hour and was then read at 560nm using an ELISA plate reader (LabTech; model number: LT-5000MS). A standard curve was calculated by plotting the 560 nm reading for each BSA standard versus its concentration in µg/mL (already known). The standard curve was used to calculate the protein concentrations of samples from their 562 nm reading.

2.1.3.11 Gel electrophoresis

Cell lysates were previously diluted in HPLC (high pressure liquid chromatography) water to standardise volume and protein concentration to ensure equal loading, then 1.5µl of Bromothenol blue and 1.5µl of β-mercaptoethanol were added to all samples. Samples were heated to 95˚C for a maximum 10 minutes in order to denature or unfold the protein, then

briefly centrifuged. Subsequently samples were loaded into precast Mini-PROTEAN® TGX Stain Free Gels (Bio-Rad, 456-8024_7.5% polyacrylamide gels, or 456-8084_4-15% polyacrylamide gels) and run in a Mini-PROTEAN® Tetra Cell (BIO-RAD, 165-8004) filled with 10% running buffer (BIO-RAD 161-0732) for 30 minutes at 200V. Alongside the samples, a protein marker (Geneflow Limited, S60024) was also loaded as a molecular weight marker. Relevant recombinant proteins were also used as positive controls.

2.1.3.12 Stain-free gels

After the 30 min of electrophoresis, precast gel packs were opened, placed into the ChemiDoc MP System and exposed to UV light for 5 minutes The principle of stain free gel is based on interaction between trihalo compounds (present in the precast gel) and tryptophan residues (present in the protein). This interaction results in a fluorescent signal, that is visible when the precast gels are activated by UV light. These images were used as a control to calculate the total protein amount loaded.

2.1.3.13 Protein transfer and detection

Straight after electrophoresis, the separated proteins are transferred onto 0.2µM nitrocellulose Transfer Packs (BIO-RAD, 170-4158 (mini format) or 170-4159 (midi format) by using the Trans-Blot® Turbo™ System (Bio-Rad). After which, the membrane was washed in 5% milk solution in TBS-T (tris-buffered saline-tween) (20Mm Tris,137Mm NaCl, 0.1% (v/v) Tween-20, ph 7.6) for 45 minutes to block nonspecific binding of antibodies with the membrane. Following, membranes were incubated with the relevant primary antibodies diluted in SignalBoost™ Immunoreaction Enhancer Kit#A (Merck Millipore, 407207) for 1 hour at room temperature or overnight (16-18 hours) at 4°C (see list of antibodies used in Table 2.10). The following day, blots were washed two times briefly and once for 30 minutes using TBS-T with 5% skimmed milk powder, then blots were incubated at room temperature with relevant HRP-conjugated secondary antibodies diluted 1:1000 in SignalBoost Immunoreaction Enhancer Kit#B (Merck Millipore, 407207) for one hour (see list of antibodies used in Table 2.11). Blots were then washed in TBS-T for three times briefly, then one long wash of 30 minutes, and finally 3 more washes of 5 minutes. Luminata Forte Western horseradish peroxidase (HRP) substrate (Millipore, WBLUF0500) was used to detect luminescence by using the ChemiDoc MP imaging system (Bio-Rad).

2.1.3.14 Densitometry

Band density (densitometry) was determined using Image Lab software (Bio-Rad) which was then normalised to the stain free gel for final analysis and interpretation.

Table 2.10: List of primary antibodies used for western blotting

Antibody	Species	Dilution Used	Molecular weight	Catalogue number	Company
MMP-2	Mouse	1/500	72kD	902	R&D
MMP-3	Rabbit	1/500	54kD	53015	Abcam
MMP-9	Mouse	1/500	100kd	AF909	R&D
MMP-10	Mouse	1/500	55kD	9101	R&D
MMP-12	Mouse	1/500	54kD	56305	Abcam
MMP-19	Goat	1/250	50-57kD	AF6790	R&D
SMMHC-11	Rabbit	1/1000	22kD	53219	Abcam
Transgelin	Mouse	1/500	18/24kD	mab78861	R&D
Anti-Actin, α-Smooth Muscle	Mouse	1/500	22kD	A2547	SIgma
Calmodulin	Rabbit	1/500	16kD	ab45689	Abcam
B-actin	Mouse	1/10000	42kD	A5316	Sigma
GAPDH	Mouse	1/5000	37kD	Mab 374	Millipore

Table 2.11: List of secondary antibodies used for western blotting

Secondary Antibodies	Species	Working Concentration	Company	Catalogue Number
Anti-Rabbit HRP	Goat	WB 1/1000	DAKO	P0217
Anti-Goat HRP	Rabbit	WB 1/1000	DAKO	P0449
Anti-Mouse HRP	Goat	WB 1/1000	DAKO	P0447

2.1.4 Cell Behaviour Studies

2.1.4.1 Proliferation Assay on VSMCs – EdU Labelling

VSMCs were seeded at a density of $2x10^4$ cells/ml in 24-well cell culture plates containing 13mm circular glass cover slips, at 37°C under a 5% CO_2 atmosphere. After 24 hours or when cells had reached desired confluence, cells were incubated with EdU (EdU-Click 488 Kit, Sigma, BCK-EDU488) in SFM (1/1000 of 10mM EdU stock) for 24 hours. All volumes used for the 24 well plates were between 250 and 500µl per well. The following day cells were fixed with 3% paraformaldehyde/PBS for 10 minutes at room temperature and then washed three times with PBS. Cells were then subjected to immunocytochemistry or plates stored in the fridge. Cells were washed twice with 3% PBS/BSA and permeabilised with 0.5% Triton/PBS, at room temperature for 20 minutes. During these 20 minutes 1x EdU-Click buffer additive was prepared by diluting 10x solution (1/10 in deionised water) and EdU-Click Plus cocktail was prepared according to the manufacturer's datasheet (see Table 2.12). After 20 minutes incubation, 0.5% Triton/PBS solution was removed, and cells were washed twice with 3% BSA/PBS. 500 µl of EdU-Click reaction cocktail was added to each well and incubated for another 30 minutes in the dark at room temperature. Cells were washed once in 3% BSA/PBS and then once in PBS. Nuclei were stained by 30 minutes incubation with Hoechst 33342 in PBS on a rocker at room temperature. Subsequently, the samples were washed 3 x 3 minutes with PBS, then the coverslips carefully removed and mounted on glass slides with Prolong gold anti-fade reagent containing DAPI (Invitrogen, P36931). VSMCs were then visualised under a fluorescent microscope and x 10 magnification fields acquired. The proliferation rate was determined by quantifying positive-labelled cells and expressed as percentage of all nucleated cells positively labelled for EdU.

Table 2.12 : EdU-Click 488 Kit ® reaction cocktails.

Reaction components	Number of coverslips			
	1	2	4	5
1x EdU-Click reaction buffer	430µl	860µl	1.8ml	2.2ml
$CuSO_4$	200µl	40µl	80µl	100µl
Alexa Fluor azide	1.2µl	2.5µl	5µl	6µl
Reaction buffer additive	50µl	100µl	200µl	250µl
Total volume	500µl	1ml	2ml	2.5ml

2.1.4.3 Immunocytochemistry for VE-cadherin and F-actin

HUVECs between passage 2 and 7 were seeded at a density of 1 x 10^5 in multi-chamber glass slides (Millipore, PEZGS0816). After 24 hours, when the cells had reached the desired confluency, slides were placed on a laboratory rocker for 24 hours to simulate shear stress, then treated with Ang II +/- inhibitors for 24 or 72 hours. After this time, the cells were washed twice in PBS and fixed in 250µl 3% paraformaldehyde/PBS for 10 minutes at room temperature. After two more washes in PBS, cells were permealised with 0.5% Triton/PBS and then incubated with 250µL 20% goat serum/PBS for 30 minutes at room temperature. The goat serum was removed and then the anti-VE-cadherin antibody was added overnight at 4ºC (details are given in Table 2.13). The following day, cells were washed in PBS (3 x 2 minutes) and incubated with DyLight-conjugated secondary antibody (1:200 in PBS) for 1 hour in the dark (details are given in Table 2.13). Cells were washed three more times in PBS and then incubated with Alexa flour 594 conjugated phalloidin. Cells were visualised under a fluorescent microscope and x 20 magnification fields acquired. VE-Cadherin was visualised as green fluorescence (at 24 hours) and as a red fluorescence (at 72 hours). VE-cadherin positive cells-defined as staining of the membrane along with intracellular expression of VE-cadherin was quantified at 24 hours exposure. The same parameters were counted at 72 hours treatment. In addition, F-actin positive cells (phalloidin colour) were also quantified.

2.1.4.2 Immunocytochemistry for β-catenin

HUVECs between passage 2 and 7 were seeded at a density of 1 x 10^5 in multi-chamber glass slides (Millipore, PEZGS0816). After 24 hours, when the cells had reached the desired confluency, slides were placed on a laboratory rocker for 24 hours to simulate shear stress, then treated with Ang II +/- inhibitors for 72 hours. After this time, the cells were washed twice in PBS and fixed in 250µl 3% paraformaldehyde/PBS for 10 minutes at room temperature. After two more washes in PBS, cells were permealised with 0.5% Triton/PBS and then incubated with 250µL 20% goat serum/PBS for 30 minutes at room temperature. The goat serum was removed and then the anti-β-catenin antibody was added overnight at 4ºC (details are given in Table 2.13). The following day, cells were washed in PBS (3 x 2 minutes) and incubated with DyLight-conjugated secondary antibody (1:200 in PBS) for 1 hour in the dark (details are given in Table 2.13). Cells were washed three more times in PBS and then were visualised under a fluorescent microscope and x20 magnification fields acquired. β-catenin was visualised as red fluorescence. Intracellular expression of β-catenin was quantified at 72 hours exposure.

2.1.4.3 Immunocytochemistry on VSMC

VSMCs isolated from human umbilical cord arteries and were seeded at a density of 1 x 10^4 in multi-chamber glass slides (Millipore, PEZGS0816) and then incubated for 24 hours in 10% FBS/DMEM. After 24 hours, when the cells had reached the desired confluency the cells were washed twice in PBS and fixed in 250µl 3% paraformaldehyde/PBS for 10 minutes at room temperature. After two more washes in PBS, cells were permealised with 0.2% Triton/PBS and then incubated with Image IT Signal Enhancer (Invitrogen) was for 30 minutes to eliminate non-specific binding of antibodies and fluorescent dyes to the cells. After removing liquid carefully α-SM actin, caldesmon, SMMHC11 and VE-caderin antibodies were added overnight at 4ºC (details are given in Table 2.13 A). The following day, cells were washed in PBS (3 x 2 minutes) and incubated with the appropriate DyLight-conjugated secondary antibody (1:200 in PBS) for 1 hour in the dark (details are given in Table 2.13 B). Cells were washed three more times in PBS and then were visualised under a fluorescent microscope and x10 magnification fields acquired and data presented as percentage of immune-labelled positive nucleated cells.

Table 2.13: List of the antibodies (A primary, B secondary) for fluorescent ICC

A

Antibody	Species	Dilution Used	Catalogue number	Company
α-SM actin	Mouse	1/200	Clone1A4-M0851	Dako
Caldesmon	Rabbit	1/50	D5C8D	Cell Signalling
SMMHC11	Rabbit	1/400	ab53219	Abcam
VE-cadherin	Rabbit	1/400	D87F2	Cell Signalling
B-catenin	Rabbit	1/500	D2U8Y	Cell Signalling

B

Secondary Antibodies	Species	Working Concentration	Company	Catalogue Number
Anti-Rabbit Dylight 488	Horse	1/200	Vector Laboratories	DI-1088
Anti-Rabbit Dylight 594	Horse	1/200	Vector Laboratories	DI-1094
Anti-Mouse Dylight 488	Horse	1/200	Vector Laboratories	DI-2488
Phalloidin DyLight 488 Conjugated	_	1/200	Thermo Fisher	21826
Phalloidin DyLight 594 Conjugated	_	1/200	Thermo Fisher	21833

2.1.4.4 Apoptosis Assay – Cleaved Caspase-3 immunofluorescence

HUVECs between passage 2 and 7 were seeded at a density of 1 x 10^5 in multi-chamber glass slides (Millipore, PEZGS0816). After 24 hours, when the cells had reached the desired confluency, slides were placed on a laboratory rocker for 24 hours (to simulate shear stress) then treated with Ang II +/- inhibitors for 24 or 72 hours. All volumes added within the multi-chamber glass slides were between 200 and 300µl per well. Cells were fixed with 3% paraformaldehyde, and then washed with PBS. The day after, cells were washed twice with 3% PBS/BSA, permeabilised with 0.2% Triton/PBS, at room temperature (3 x 5 minutes) and then washed with PBS. Goat serum (Vector Lab, S-1000-20) was used for 30 minutes to eliminate non-specific binding of antibodies and fluorescent dyes to the cells. Cells were then incubated with 1µg/mL anti-cleaved caspase-3 (CC3) antibody (details are given in Table 2.14 A).) at 4°C overnight. Following, cells were washed three times with PBS and then incubated with biotinylated goat anti-rabbit IgG (details are given in Table 2.14 B) diluted 1:200 in PBS for one hour at room temperature. The cells were then washed twice in PBS and treated with 250 µL per well of DyLight594-conjugated Streptavidin (Vector Laboratories, DI-1088) diluted 1:200 in PBS for 1 hour. After washing twice in PBS, coverslips were applied with Prolong gold antifade reagent containing DAPI (Invitrogen, P36931) and stored at 4°C. Cells were then visualised under a fluorescent microscope and x 20 magnification fields acquired. CC3 positive cells (red) and negative cells (blue only) were counted and the number of CC3 positive cells (apoptotic cells) was expressed as a percentage of the total number of cells.

Table 2.14: List of the antibodies (A primary, B secondary) CC3

A

Primary Antibody	Species	Dilution Used	Catalogue number	Company
Cleaved Caspase-3	Rabbit	1/400	D175	Cell signalling

B

Secondary Antibody	Species	Working Concentration	Company	Catalogue Number
Anti-Rabbit Dylight 594	Horse	1/200	Vector Laboratories	DI-1088

2.1.4.5 Senescence assay- β-galactosidase labelling

A Senescence Cells Histochemical Staining Kit (Sigma, CS0030) contains all the reagents required for identifying senescent cells. VSMCs isolated from human umbilical cord arteries were cultured at a density of $2x10^4$ cells per well in 24-well plates on glass-coverslips in 10% FBS/DMEM overnight at 37°C, 5% CO_2 for 24 hours, then quiesced in SFM and incubated with $CaCl_2$ (250mM) for 15minutes or Ang II (5µM) for 24 hours. All the volumes used for the 24 well plates were between 250 and 500 µl per well the day after, cells were washed with PBS and fixed using a filtration buffer (Cat No. F1797) for 6-7 minutes at room temperature. Cells were then washed three times with PBS and subsequently incubated with a staining mixture solution (for 10ml staining mixture: 1 ml of Staining Solution, 125 ml of Reagent B, 125 ml of Reagent C ,0.25 ml of X-gal Solution, 8.5 ml of ultrapure water) at 37°C and without CO_2 overnight. The plate was sealed with parafilm to prevent cells from drying out. This staining protocol employs the β-galactosidase substrate X-gal, which when cleaved produces a blue precipitate, to detect senescence-specific β-galactosidase activity at pH 6.0. VSMCs were visualised under a bright field inverted microscope and x10 magnification fields acquired. B-galactosidase positive cells (blue stained cells) and negative cells (no blue) were counted, and the number of B-galactosidase positive cells (senescence cells) was expressed as a percentage of total cells number.

2.2 *Ex vivo* studies

2.2.1 Development of an *ex vivo* model of aneurysm

2.2.1.1 Human umbilical cord dissection and isolation of arteries

In electing to use the human umbilical arteries we balanced out the pro and cons of some peculiar aspects of the feto-placental circulation and in particular the fact that *in vivo* the umbilical arteries carry de-oxygenated blood with poor nutrients from the foetus to the placenta (see Figure 2.2) instead of what occurs in a typical artery transporting nutrients, oxygen and hormones. Our decision was based on the practical aspect of using the arteries *ex vivo* in a bioreactor with no blood and most of all on the need to utilise several segments at one time from the same artery for control vs intervention experiments. Moreover, harvesting both umbilical arteries from the same human cord greatly facilitated quantitation and associated statistical analysis as paired experiments were conducted, making my comparative experiments more robust. Human umbilical cords were obtained from St. Michael's Maternity Hospital (Bristol) covered under existing ethical approval (Research Ethics Committee reference: E5431) and stored at 4°C straight after delivery (Figure 2.3 a). Umbilical cord samples were processed as soon as possible and no more than two hours after delivery. A tissue culture laminar flow-hood was cleaned with 70% ethanol, followed by Milton sterilising solution. The average length of an umbilical cord is 50 cm, however the length of cord received varied from donor to donor (Figure 2.3 b). Human umbilical cords contain two arteries and one vein surrounded by Wharton jelly, and under sterile conditions, and within a silicon dish, the arteries were identified by observing a cross-section of the umbilical cord (Figure 2.3 c). The cord was then partially opened and pinned down on the dish in order to get a flat surface to work on. Subsequently, arteries were micro-dissected under phosphate-buffered saline (PBS, pH 7.4) containing penicillin 100 U/mL and streptomycin 100 mg/mL at 4^0C, (Figure 2.3 d, e) and flushed with PBS to remove any possible blood clots before being transferred into SFM at 4°C (Figure 2.3 f). The excised arteries were then used as soon as possible after the dissection in order to preserve vessel integrity and maintain consistency.

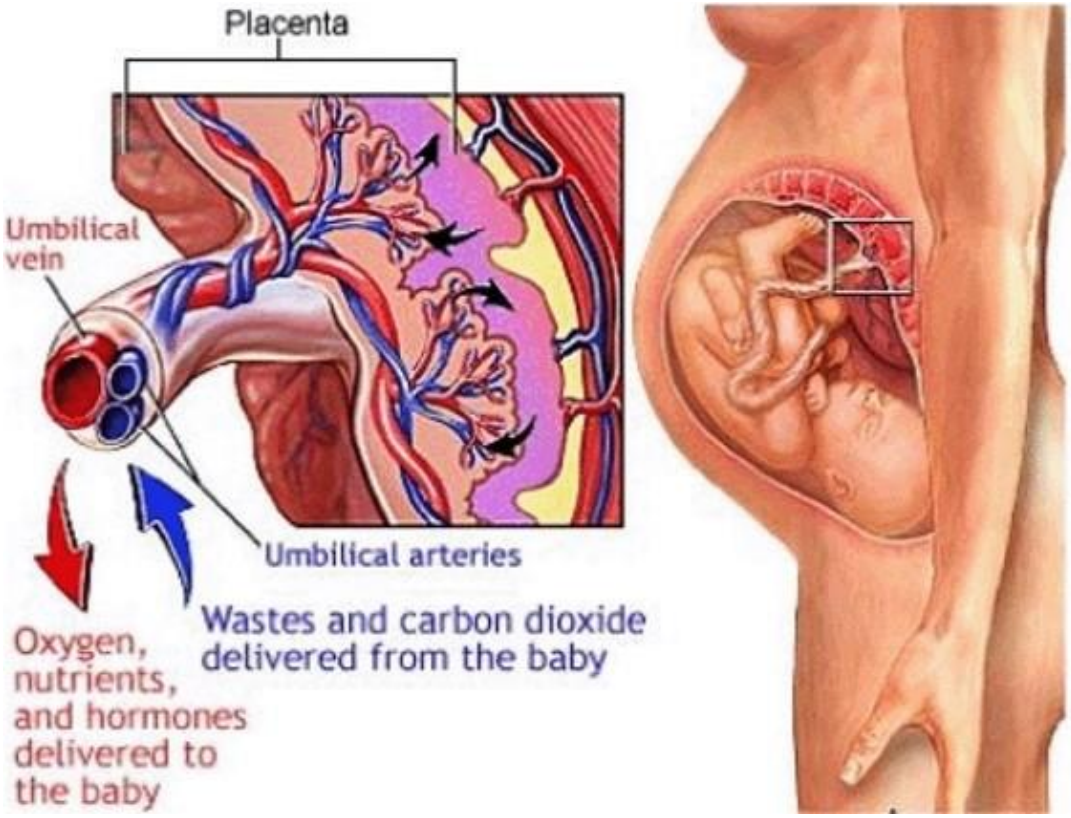

Figure 2.2: Foeto-placental circulation

The umbilical cord contains one vein (the umbilical vein displayed in red) and two arteries (the umbilical arteries displayed in blue). The umbilical vein carries oxygenated, nutrient-rich blood from the placenta to the foetus, whereas the umbilical arteries carry deoxygenated, nutrient-depleted blood from the foetus to the placenta. The umbilical cord serves as a connection between the placenta and the foetus.

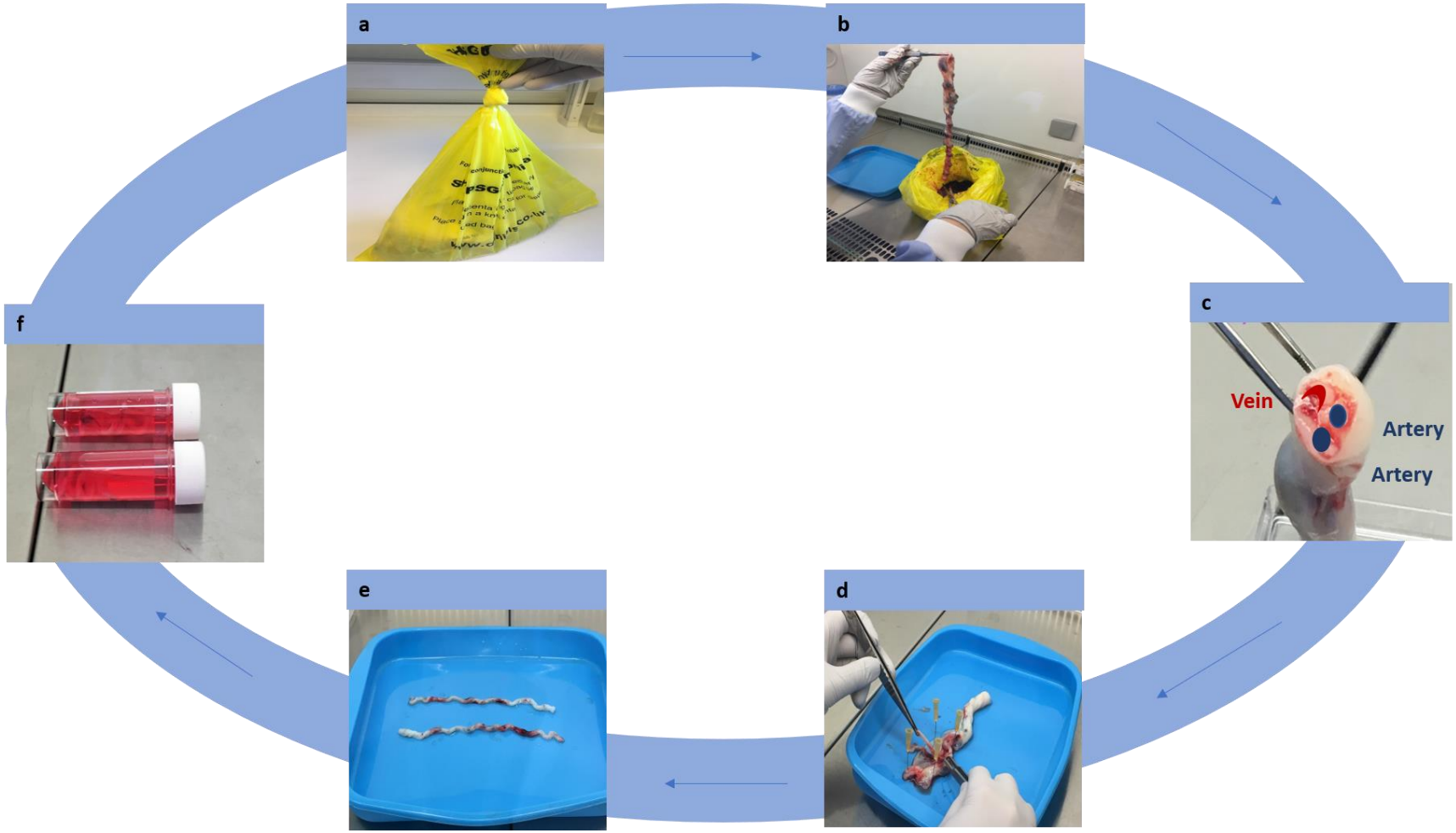

Figure 2.3: Human umbilical cord dissection and isolation of arteries

a) *Umbilical cords were collected from St. Michael's Maternity Hospital; b) length of the umbilical cord was checked to ensure an appropriate amount was available with no signs of damage; c) arteries and vein were identified in a cross-section; d) arteries were micro-dissected from human umbilical cord; e) arteries were cleaned of possible blood clots; f) arteries were stored in serum free media at 4°C.*

2.2.1.2 Ex vivo model of aneurysm

Tissue culture hoods were sterilised with a Milton sterilising solution, similarly bio-reactor chambers were placed for at least 2 hours in Milton sterilizing solution then briefly washed in sterile water and finally placed under a tissue culture hood to dry. As described in section 2.2.1.1, arteries were micro-dissected from human umbilical cord (Figure 2.4 a) and kept in SFM at 4^0C for maximum 1 hour (Figure 2.4 b). Arteries were then cut into three equal pieces of 5 cm to be used for baseline, untreated and either Ang II or $CaCl_2$ treatment. Silicon tubing (Male Luer Fitting 1/16 ID, 13160-100) was then used to connect either ends of the bio-reactor chamber (Figure 2.4 c).

As shown Figure 2.4 d, arteries were mounted between two small cannulae (Male Luer Fitting 1/16 ID, 13160-100) and sutures (Sofsilk, VS-870) were used to tie the artery to the cannulae. Each cannula was connected to silicon tubing (228-1094; Tubing Ssil. Wacker, ID 3,18MM, OD 6,35MM) and then placed inside a supporting bio-reactor chamber. The silicon tubing was filled with 10%FBS/DMEM (Figure 2.4 e) and passed through a peristaltic pump (Watson-Marlow Sci-Q 300 Series Peristaltic Pump, ThermoFisher,14-284-118) to close the system and permit the induction of laminar flow within an incubator (Figure 2.4 f).

As summarised in Figure 2.5, the chamber and the silicon tubing were filled with 80ml of 10% FBS/DMEM. The medium was flushed into the input cannula, passed through the arterial lumen and out through the distal cannula and into the chamber (as showed by the arrows). Each chamber was subjected to identical flow conditions with a flow rate of 6.5 dynes/cm^2 in order to closely mimic abdominal aortic *in vivo* conditions, at 37°C, 5% CO_2 for 72 hours. In control untreated chambers, 80 ml of 10% FBS/DMEM alone was used. For Ang II treated arteries, media was supplemented with 5µM Ang II. For $CaCl_2$-treated arteries, vessels were pre-soaked with 250mM $CaCl_2$ for 15 minutes then placed within the chamber with 80ml of 10% FBS/DMEM as usual. After 72 hours of flow within the bio-reactor chambers, arteries were carefully removed, the proximal section was fixed in 10% formalin and prepared for histology, and the distal segment was stored in a -80^0C freezer awaiting further analysis.

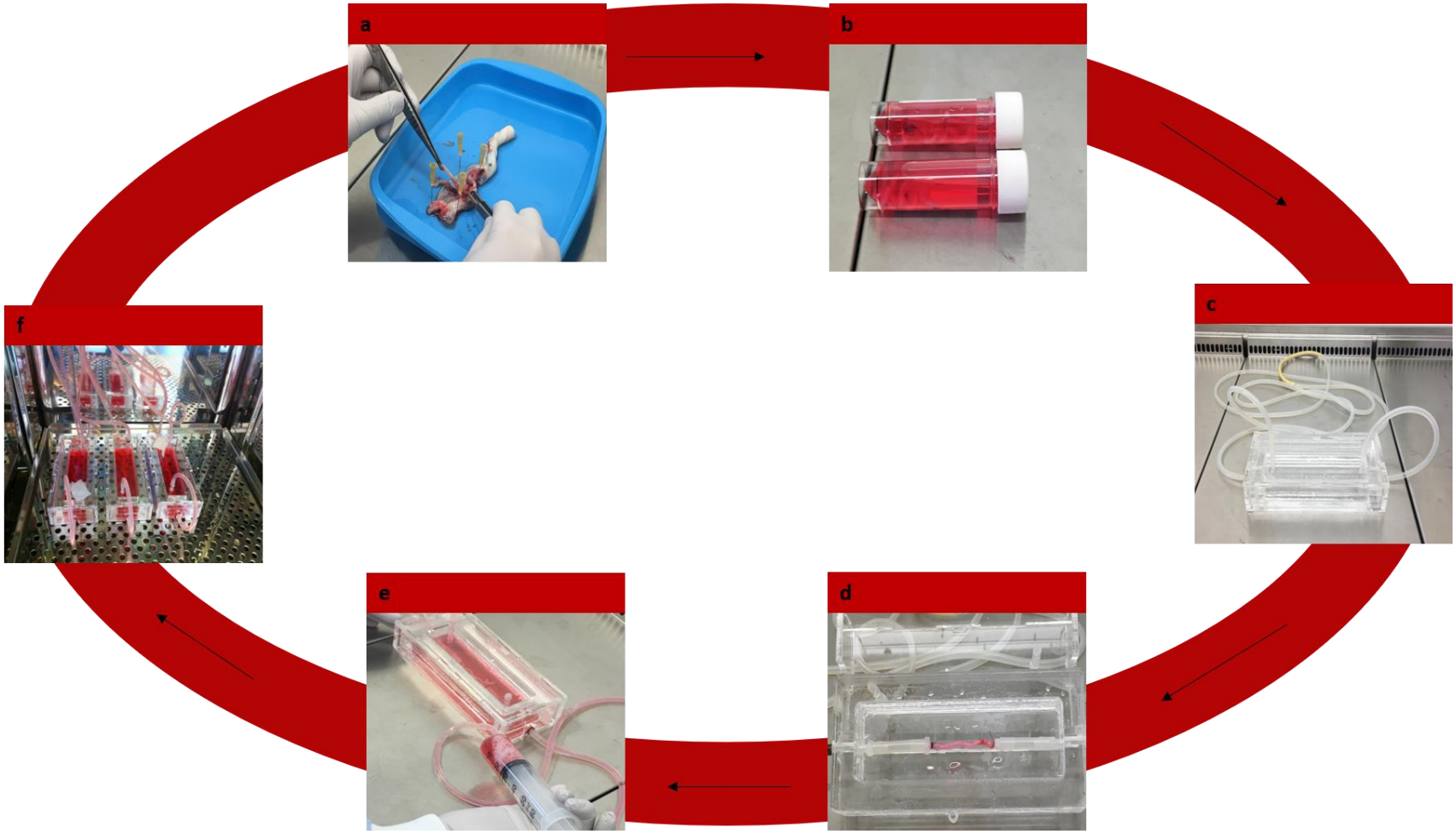

Figure 2.4: Arterial placement within the bio-reactor system

a) Arteries were dissected from human umbilical cords; b) arteries were stored in serum free media at 4^0C; c) a bio-reactor chamber was connected to a silicon tubing; d) arteries were mounted between two small cannulae within the bio-reactor chamber; e) silicon tubing was filled with 10%FBS/DMEM; f) bio-reactor chambers were inserted within an incubator.

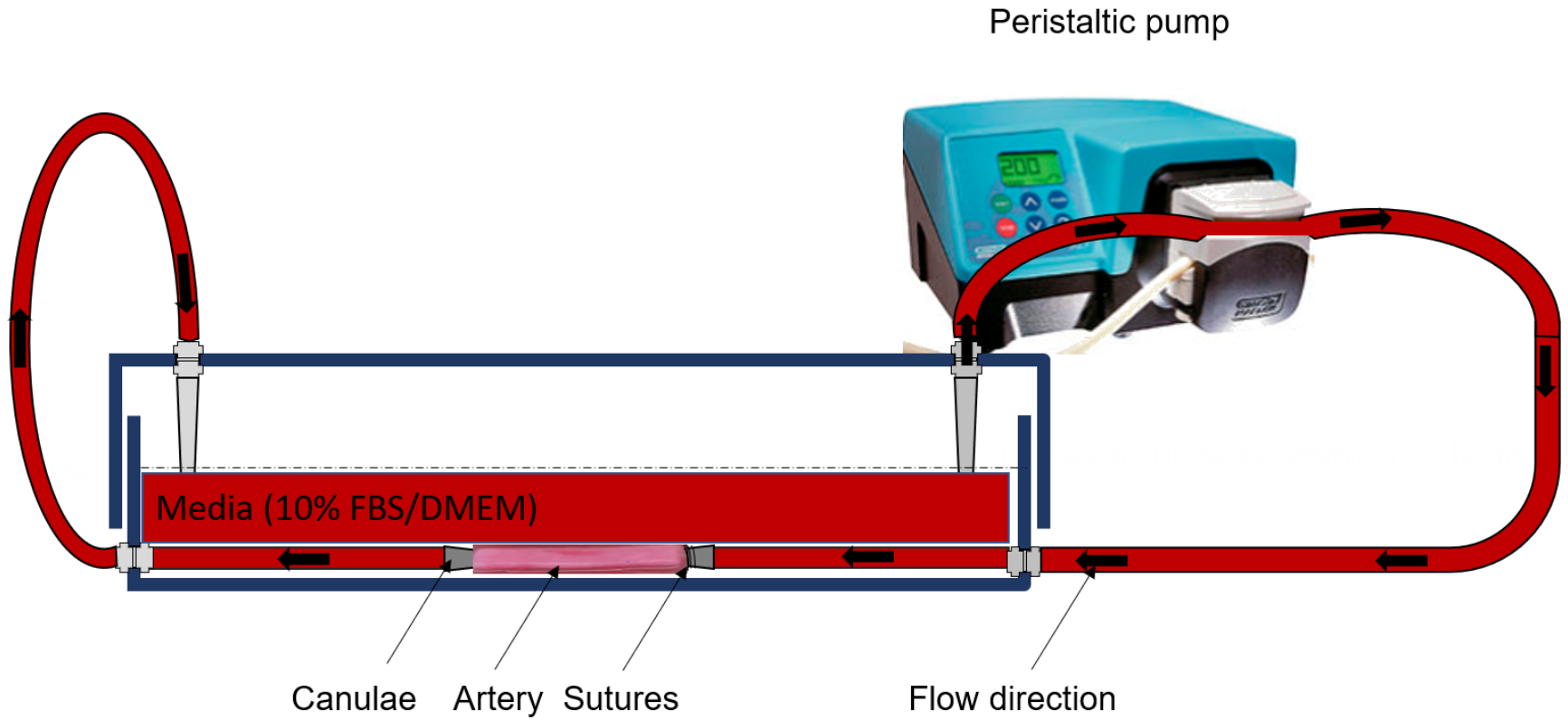

Figure 2.5: Ex vivo aneurysmal model

Arteries (pink) were mounted between two small cannulae (grey). Suture (black) was used to secure the artery to the cannulae. Each cannula was connected to silicon tubing and then placed inside a supporting bio-reactor chamber (blue). A long silicon tube (red because filled of media) was connected to either end of the bio-reactor and passed through a peristaltic pump. The system is closed, and this permit controlled and constant induction of laminar flow. The black arrow indicates the flow direction.

2.2.1.3 Ex vivo model of aneurysm: interventions

As described in the previous section (2.2.1.2), arteries were micro-dissected from human umbilical cord and then cut into five equal pieces of 5cm in length to be used for baseline, untreated, Ang II (5µM) and Ang II plus selected interventions. For this experiment three different anti-aneurysmal interventions previously shown to effective in murine aneurysm models, were added into the bio-reactor system. These interventions included recombinant TIMP-3 (rTIMP- 3, 5nM), a transforming growth factor beta neutralising antibody (TGF-β NAb) (R&D Systems, MAB1835) at 0.25µg/ml, and a selective MMP-12 inhibitor RXP470 (10nM). Each chamber was subjected to identical conditions with a flow rate of 6.5 dynes/cm^2 in order to closely mimic in vivo conditions, at 37°C, 5% CO_2. After 72 hours of pulsatile flow within the bio-reactor chambers, arteries were carefully removed, the proximal section was fixed in 10% formalin and prepared for histology and the distal segment was stored in a -80^{0}C freezer awaiting further analysis.

2.2.1.4 Ex vivo flow model: regression

In order to assess if the aforementioned interventions altered arteries after Ang II-induced aneurysm formation, the anti-aneurysmal agents were administered 72 hours after initial Ang II addition. In brief and as described in the previous section (2.2.1.2), human umbilical cord arteries were cut into four equal 5cm lengths and cultured within a bio-reactor system at a flow rate of 6.5 dynes/cm^2 for 72 hours with Ang II (5µM) supplementation. After 72 hours of pulsatile flow within the bio-reactor chambers, flow was stopped, and the chambers placed under a tissue culture hood so the media could be replaced. The media changes were performed as follows: the first chamber was refilled with 80 ml 10% FBS/DMEM containing 5µM Ang II only, while chambers 2-4 received 80 ml 10% FBS/DMEM including either rTIMP-3 (5nM), a TGF-β NAb (0.25µg/ml), or the MMP-12 inhibitor RXP470 (10nM), respectively. After the media changes, chambers were returned to the bio-reactor and subjected to identical flow conditions as the previous 72 hours with a flow rate of 6.5 dynes/cm^2 for a further 72 hours. After the additional 72 hours of pulsatile flow within the bio-reactor chambers, arteries were carefully removed, the proximal section was fixed in 10% formalin and prepared for histology and the distal segment was stored in a -80^{0}C freezer awaiting further analysis.

2.2.1.5 Enface assessment of endothelial cells within the ex vivo model of aneurysm

In order to assess if Ang II-induced aneurysm formation affected endothelial cell function, arterial segments were obtained for en face preparation. In brief and as described in the

previous section (2.2.1.2), human umbilical cord arteries were cut into equal 5cm lengths and cultured within a bio-reactor system at a flow rate of 6.5 dynes/cm^2 for 24 hours with and without Ang II (5µM) supplementation. After 24 hours of pulsatile flow within the bio-reactor chambers, arteries were carefully removed, opened out on a silicon dish and pinned down with the endothelial layer up, fixed for 4 hours with 3% paraformaldehyde/PBS and washed three times with PBS. The *ex vivo* arterial segments were then subjected to immunocytochemistry (ICC) for VE-cadherin and F-actin (phalloidin labelling) as previously described in section 2.1.4.1. Images were then acquired using a confocal microscope (Leica SP5 AOBS, Germany)

2.2.2 Histological processing

2.2.2.1.1 Elastin van Gieson staining

Elastin van Gieson (EVG) staining was used to determine elastin content within 3µm sections from formalin-fixed paraffin-wax embedded human arterial segments. EVG staining was performed using a Shandon Varistain 24-4 Automatic Slide Stainer (Thermo Scientific, 74200103). The protocol details are shown in Table 2.15. Following the staining, slides were mounted in DPX mounting medium (Thermo Fisher Scientific, 10050080) and then slides were visualized under a bright field microscope within x 20 magnification fields acquired. The relative amount of elastin (which appears as black under light microscopy) was determined using a computerised image analysis program (Image Pro Plus, DataCell, Maidenhead, UK) and expressed as an average percentage of the arterial cross-section.

Table 2.15: Staining protocol for EVG

Solution	Incubation time
Clearene	2 x 3 minutes
100% (v/v) alcohol (industrial methylated spirits: IMS)	2 x 3 minutes
Tap water	5 minutes
0.5% (w/v) potassium permanganate	10 minutes
Distilled water	3 minutes
1% (w/v) oxalic acid	5 minutes
Distilled water	3 minutes
70% (v/v) alcohol (industrial methylated spirits: IMS)	2 minutes
50% (v/v) Millers elastin stain (Pioneer Research Chemical Limited, PRC/R/108)	60 minutes
70% (v/v) alcohol (industrial methylated spirits: IMS)	2 minutes
Running tap water	3 minutes
Van Gieson stain (Thermo Scientific, LAMB/400-D)	20 seconds
100% (v/v) alcohol (industrial methylated spirits: IMS)	2 x 5 minutes
Clearene	2x 5 minutes

2.2.2.1.2 Haematoxylin and eosin stain

Haematoxylin and eosin (H&E) staining was used to assess general tissue architecture and nucleated cells within 3µm sections from formalin-fixed paraffin-wax embedded human arterial segments. H&E staining was performed using a Shandon Varistain 24-4 Automatic Slide Srainer (Thermo Scientific, 74200103). The protocol details are shown in table 2.16. Following the staining, slides were mounted in DPX mounting medium (Thermo Fisher Scientific, 10050080) and then slides were visualised under a bright field microscope and x 20 magnification fields acquired.

Table 2.16: Staining protocol for H&E

Solution	Incubation time
Clearene	2 x 3 minutes
100% (v/v) alcohol (industrial methylated spirits: IMS)	2 x 3 minutes
Tap water	5 minutes
Haematoxylin	3 minutes
Distilled water	3 minutes
Scots Tap water	1minute
Running tap water	3 minutes
1% Eosin	80minutes
Running tap water	3 minutes
100% (v/v) alcohol (industrial methylated spirits: IMS)	2 x 5 minutes
Clearene	2x 5 minutes

2.2.2.1.3 Picrosirius Red staining

Picrosirius Red staining was used to detect collagen in our human arteries from the ex *vivo* model of aneurysm. Firstly, 3µm paraffin-wax sections were placed in a slide rack and de-waxed by placing in three changes of Clearene™ (Surgipath, 3803600E) for the duration of 5 minutes in each. Sections were then rehydrated three changes of 100% Industrial Methylated Sprits (IMS), followed by 90% IMS and lastly in 70% IMS, for the duration of 5 minutes each. Following, sections were incubated with picrosirius red solution (0.1% (w/v) Sirius Red F3B, saturated aqueous picric acid, pH 1.8-2.2) for 90 minutes at room temperature. After the incubation, sections were rinsed twice in 0.01N hydrochloric acid and then in distilled water. After, sections were allowed to air dry and placed in oven for 1 hour, rinsed in alcohol (100% IMS) and then placed in three changes of Clearene. Slides were mounted in DPX mounting medium (Thermo Fisher Scientific, 10050080) and visualised under a bright field microscope and both x4 and x10 magnification fields acquired. The relative amount of collagen (which appears as red under light microscopy) was determined using a computerised image analysis program (Image Pro Plus, DataCell, Maidenhead, UK) and expressed as an average percentage of the arterial cross-section.

.

2.3 Statistical Analysis

Statistical analysis was performed using GraphPad InStat statistical software. For experiments comparing means of more than two groups, a repeated measures ANOVA test was used with a Tukey-Kramer Multiple Comparisons post-test. If matching of samples was not effective, a Friedman (non-parametric repeated measures ANOVA) test was used with a Dunn post-test. All data is presented as mean ± standard error of the mean (±SEM). When data was presented as a fold change and compared to 1 or 100, a paired two-tailed t-test was used for normally distributed data. If data failed the normal distribution test and assumed to have different standard deviations, the alternate (Welch) t test was used. If samples still failed to display Gaussian distribution, a Mann-Whitney (non-parametric) test was used. An output of $P<0.05$ was accepted as significantly different in all statistical tests.

Chapter 3

3 Does Ang II or $CaCl_2$ induce aneurysm formation within an *ex vivo* model?

3.1 Introduction

3.1.1 Current AAA studies

AAAs are characterised by irreversible dilatation of the arterial wall and represent a leading cause of mortality worldwide accounting for 2% of all deaths in the UK [197]. The pathogenesis of AAA is asymptomatic, and therefore difficult to detect. Moreover, there are currently no preventative treatments available to halt aneurysm dilatation and subsequent rupture. In order assess the efficacy of potential new therapies several mouse models of aneurysm formation have been developed [127]. The mouse model approaches include periaortic incubation of $CaCl_2$ or subcutaneous infusion of Ang II [127, 133]. More details regarding these methods are discussed earlier in section 1.4-1.4.2. To facilitate translation, it is necessary that these animal models of aneurysm formation present cellular and biochemical characteristics of the human disease. Mouse models of aneurysm formation have several advantages such as small size, low cost and reproducibility. However, the administration of high-doses of Ang II (1000 ng/kg/min) or $CaCl_2$ (0.25-1 molar) results in the occurrence of aortic dissections and sudden death within 15-20% of mice [198]. Within the last five years there have been 835 original articles published which use mouse models of aneurysm formation. On average these studies use nine mice per experimental group, and each study averages three groups. Accordingly, this equates to approximately 22,545 mice used in the last five years alone for aneurysm studies. Considering such a large number of animals are used for such studies alongside the high sudden death rate, there is an obvious requirement to evaluate means of refining, reducing, and even replacing the number of animals used in aneurysm research (the 3Rs). One such avenue involves the development of suitable non-animal alternatives to study aneurysm pathogenesis, alongside testing of potential new therapeutics.

3.1.2 *Ex vivo* human model using umbilical cord arteries

The ability to mimic aneurysm formation within a bio-reactor system using human vessels would represent an effective strategy to potentially reduce the numbers of mice used in aneurysm research whilst also providing a greater translational perspective. The viability of *ex vivo* tissue models has been previously demonstrated in studies using porcine abdominal aorta or porcine carotid artery [199, 200]. As healthy human aortic tissue is unavailable/limited for *ex vivo* research (as is also the case for most major blood vessels) a more accessible source of conduit is required, and the human umbilical cord may harbour such a source. The umbilical cord houses two arteries which are freely available (with the appropriate ethical consent in place), and umbilical cord is accessible to most laboratories throughout the world. It was therefore hypothesised that human umbilical arteries isolated from umbilical cord may represent a novel approach to study AAA formation *ex vivo*.

The principle of the *ex vivo* aneurysm model is summarised in Figure 3.1 (A) where the flow direction is unidirectional in order to generate concentric dilatation or (B) angled flow to induce focal eccentric dilatation. Concentric dilatation is typical of fusiform aneurysm formation which in common in AAAs, whereas angled dilatation creates a bulge to one side in saccular aneurysms. In our system we tried to mimic concentric dilatation of the human artery which is more common in AAA formation and rupture (illustrated in Figure 3.1 A).

Regarding blood flow, multiple studies have been performed to understand the mechanics of blood flow within human arteries [201, 202]. The aorta, like other blood vessels is characterised by pressure that is exerted from the heart to drive systemic blood circulation. An additional mechanical force is wall shear stress which is the frictional force of blood flow upon the blood vessel in a tangential direction. Finally, due to the pulsatile nature of blood flow, the vessel wall is subjected to cyclic stretch which is a circumferential stress in contrast to shear stress [203, 204]. Shear stress differs between the artery and vein based on their flow velocity differences; 5 – 40 dynes/cm^2 and 1 – 5 dynes/cm^2, respectively [205]. With regards to the aorta, studies in young healthy individuals have shown that wall shear stress increased in the abdominal aorta from 3.5 dynes/cm^2 at rest to 6.2 dynes/cm^2 during exercise [206]. In AAA patients, exercise increased mean wall shear stress from 3.6 dynes/cm^2 at rest to 9.2 dynes/cm^2 [207]. Accordingly, a wall shear stress of 6.5 dynes/cm^2 in a laminar flow direction was used within *ex vivo* model, to ensure similar haemodynamic conditions as that observed in mouse models, and importantly the abdominal segment of the human aorta. To further develop the model, molecules/compounds previously shown to promote or exacerbate aneurysm formation in mouse models were selected for incorporation into the *ex vivo* system. Specifically, Ang II or $CaCl_2$ were used which have both been shown to induce AAA formation

in mice and were therefore selected for use in the *ex vivo* model [130, 133]. There is substantial literature supporting the role of Ang II and $CaCl_2$ in aneurysm formation. For instance, *in vitro* studies have shown that human and mouse aortic VSMCs stimulated with Ang II increased the production of MMPs, in particular MMP-2 [208, 209]. Similarly, *in vitro* $CaCl_2$ stimulation of VSMCs increased expression of MMP-2 and MMP-9 [210]. Finally, *in vivo* infusion of Ang II in male apolipoprotein E (Apoe)- and LDL receptor (Ldlr)-deficient mice increased aortic lumen diameter and promoted aneurysm formation after 28 days administration [211]. Analogous *in vivo* studies with $CaCl_2$ application in C57Bl/6 wild-type mice increased VSMC apoptosis and promoted aneurysm formation [133]. Furthermore, human studies showed increased mRNA expression of MMP-19 in tissue of dilated aorta compared to non-dilated segments [212]. In addition, in both human and mouse aneurysmal tissues there is dysregulated ECM degradation due to an imbalance between expression and activity of MMPs and TIMPs, alongside increased inflammatory cell accumulation which further exacerbates irreversible remodelling of the ECM [213].

Vessel dilatation in conjunction with heightened MMP expression/activity is associated with thinning of the vessel media layer and destruction of the IEL, resulting in “bulge formation” typical of aneurysm development. Elastin and collagen represent the main structural proteins within the arterial wall which provide strength and elasticity to the vessel wall [40, 214]. Mouse models of aneurysm formation are linked to an increased turnover of collagen [215]. In addition, histopathological studies of human aneurysmal tissue obtained during surgery for AAA and compared to non-AAA patients showed increased collagen degradation in tissues from AAA patients which was further heightened in AAA patients with aortic rupture [216]. As evidenced above, morphological and compositional changes typical of aneurysm formation have been widely characterised, therefore a good model for aneurysm studies should display most of these characteristics. In this thesis, a novel experimental model was used to induce aneurysm formation in human umbilical arteries with the aim of replicating the disease development induced in murine models of aneurysm formation.

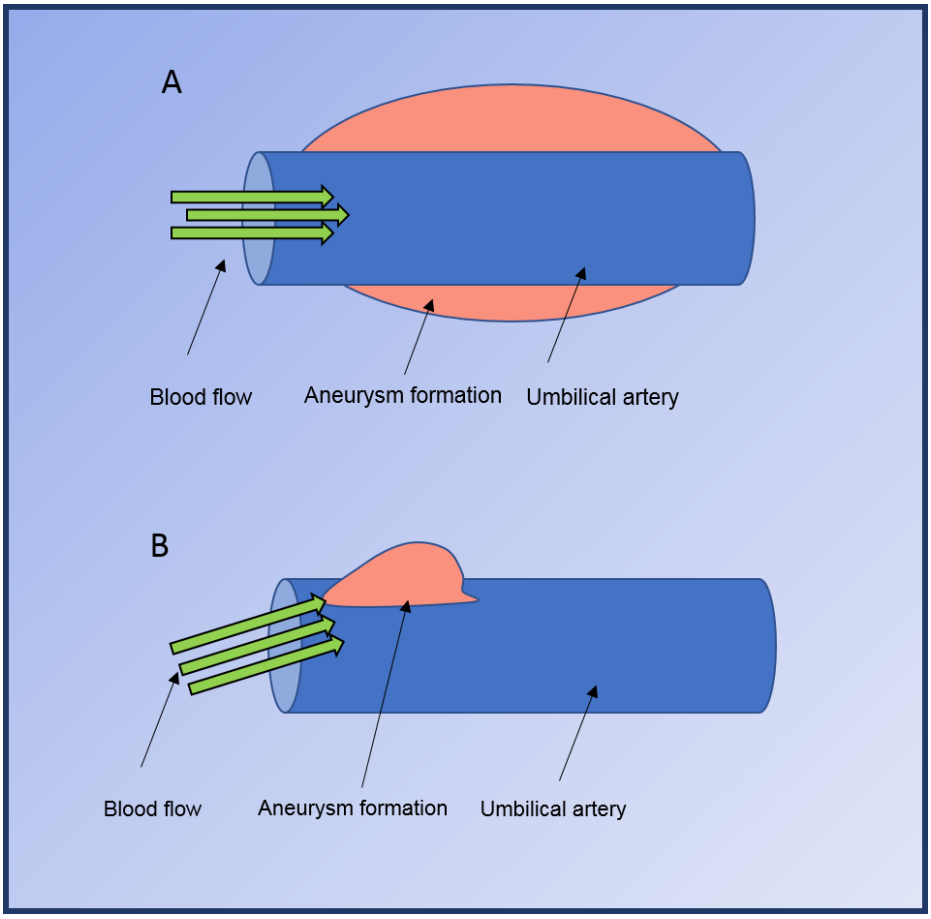

Figure 3.1: Diagram of the ex vivo aneurysm model

Aneurysm development was induced in human umbilical arteries placed in a bio-reactor through the addition of Ang II or $CaCl_2$.
(A) Laminar flow conditions (green arrow) to generate concentric dilatation (pink)
(B) Angled flow condition (green arrow) to generate focal eccentric dilatation (pink).

3.2 Aim of this chapter

The aim of this chapter was to develop an *ex vivo* human model of aneurysm with the intention of reducing and replacing (two of the 3Rs) the number of animals used in scientific research through the creation of a new suitable alternative to the animal models currently utilised to study aneurysm pathogenesis and progression. As the Ang II-infusion and $CaCl_2$ application mouse models are the most commonly used in animal aneurysm studies, the ability of Ang II or $CaCl_2$ to induce aneurysm formation in a novel *ex vivo* model by using arteries isolated from human umbilical cords, inserted within a bio-reactor and exposed to Ang II or $CaCl_2$ under laminar flow was examined. To determine whether the model accurately reflected disease characteristics observed in animals, multiple morphological and cellular changes such as medial thinning, elastin degradation, vessel dilatation and VSMC apoptosis were assessed.

3.3 Results

3.3.1 Effect of the laminar flow on morphological and compositional parameters in *ex vivo* bio-reactor cultured human umbilical cord arteries

Firstly, to evaluate solely the effect of laminar flow in my *ex vivo* model of aneurysm formation, human umbilical cord arteries were isolated and cut into two equal lengths. One portion was inserted into the bio-reactor system for 72 hours at 6.5 dynes/cm^2 whereas the other portion of umbilical artery was only washed and soaked with PBS and not subjected to laminar flow. As shown in Figure 3.2, arteries placed in a bio-reactor for 72 hours (called untreated bio-reactor) showed significantly decreased medial thickness when compared to baseline arteries, ($P<0.05$; n=5). However, assessment of arterial wall elastin content revealed no changes in the medial elastin content in untreated bio-reactor arteries compared to baseline control arteries, as illustrated in Figure 3.3 (n=5). Similarly, image analysis of EVG-stained sections to quantify total vessel area as an indicator of arterial dilatation demonstrated total vessel area was not statistically different between untreated bio-reactor umbilical arteries and baseline native arteries (Figure 3.4, $P>0.05$; n=5).

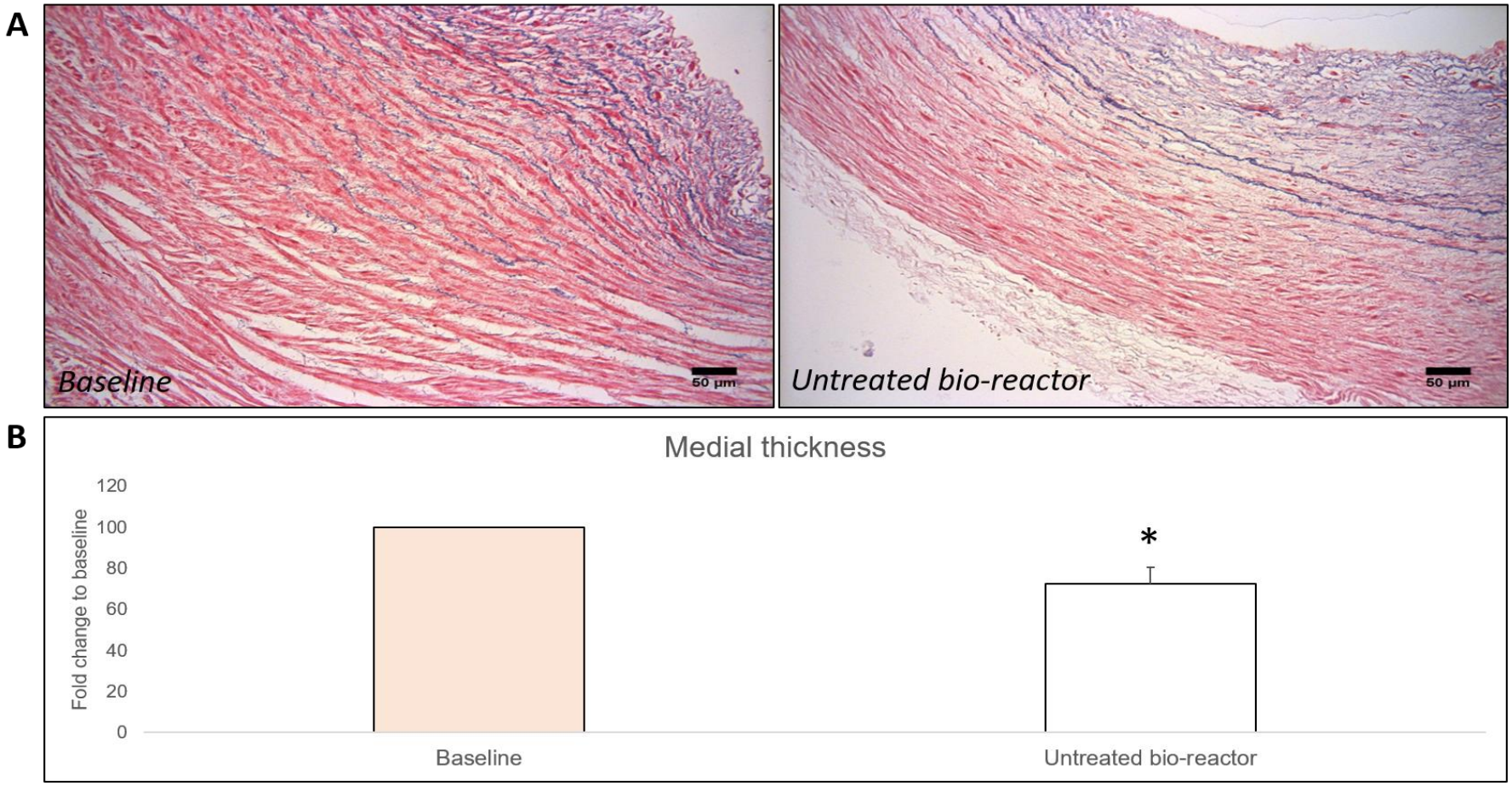

Figure 3.2: Laminar flow decreases umbilical cord artery medial thickness

*Representative images (A) and quantification (B) of medial thickness assessed in x20 magnification fields of EVG stained sections from human umbilical cord arteries only washed with PBS and not subject to laminar flow (baseline) and human umbilical cord arteries after insertion within a bio-reactor for 72 hours (untreated bio-reactor). Data is expressed as a fold change in medial thickness of the untreated bio-reactor compared to native baseline vessels (mean±SEM; n=5). * denotes p<0.05 versus control, 2-tailed Student paired t test. Scale bars represent 50 µm.*

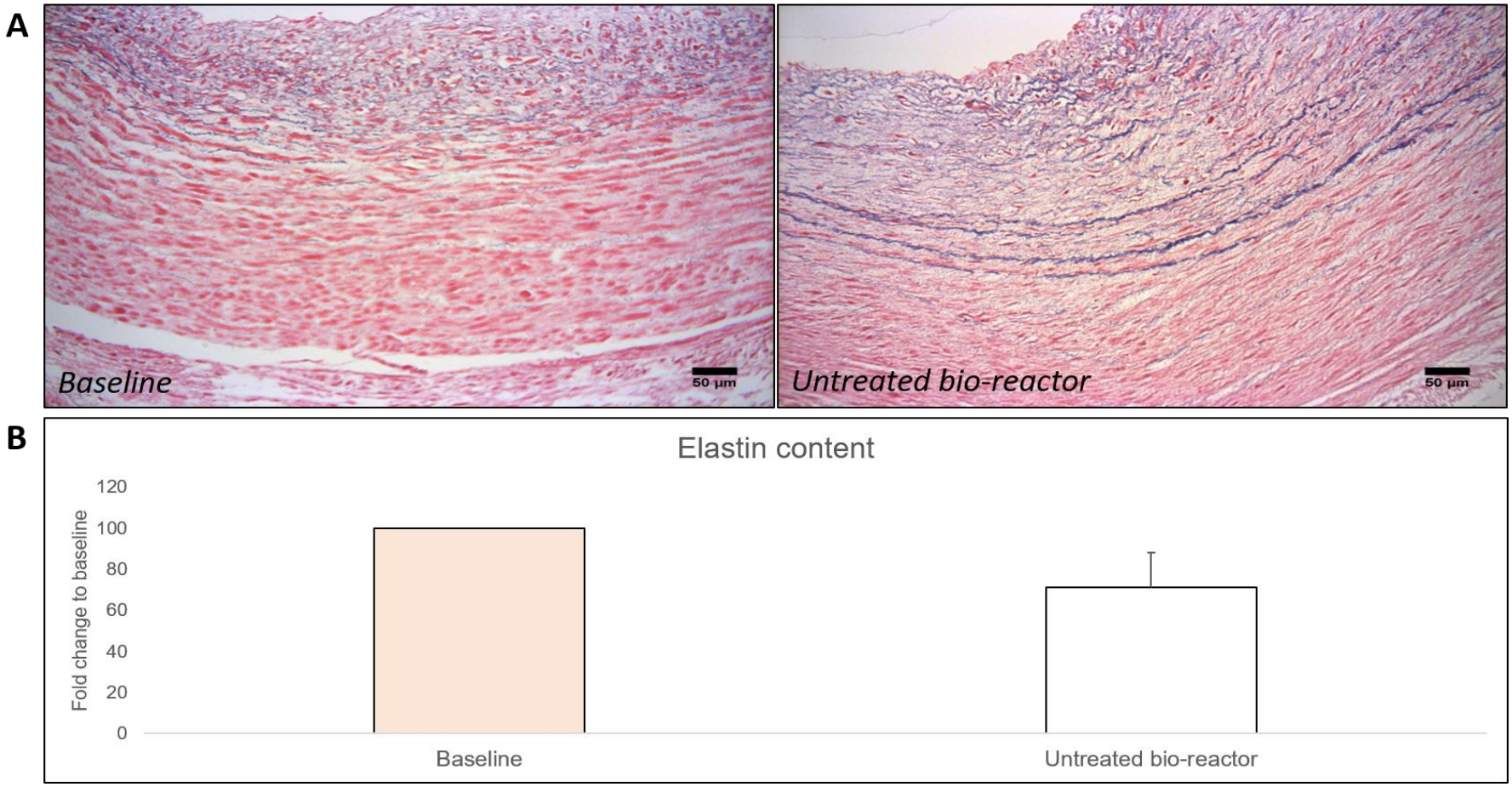

Figure 3.3: Laminar flow does not affect human umbilical cord artery elastin content

Representative images (A) and quantification (B) of elastin content assessed in x20 magnification fields of EVG stained sections from human umbilical cord arteries only washed with PBS and not subject to laminar flow (baseline) and human umbilical cord arteries after insertion within a bio-reactor for 72 hours (untreated bio-reactor). Data is expressed as a fold change in elastin content of the untreated bio-reactor compared to native baseline vessels (mean±SEM; n=5). 2-tailed Student paired t test. Scale bars represent 50 µm.

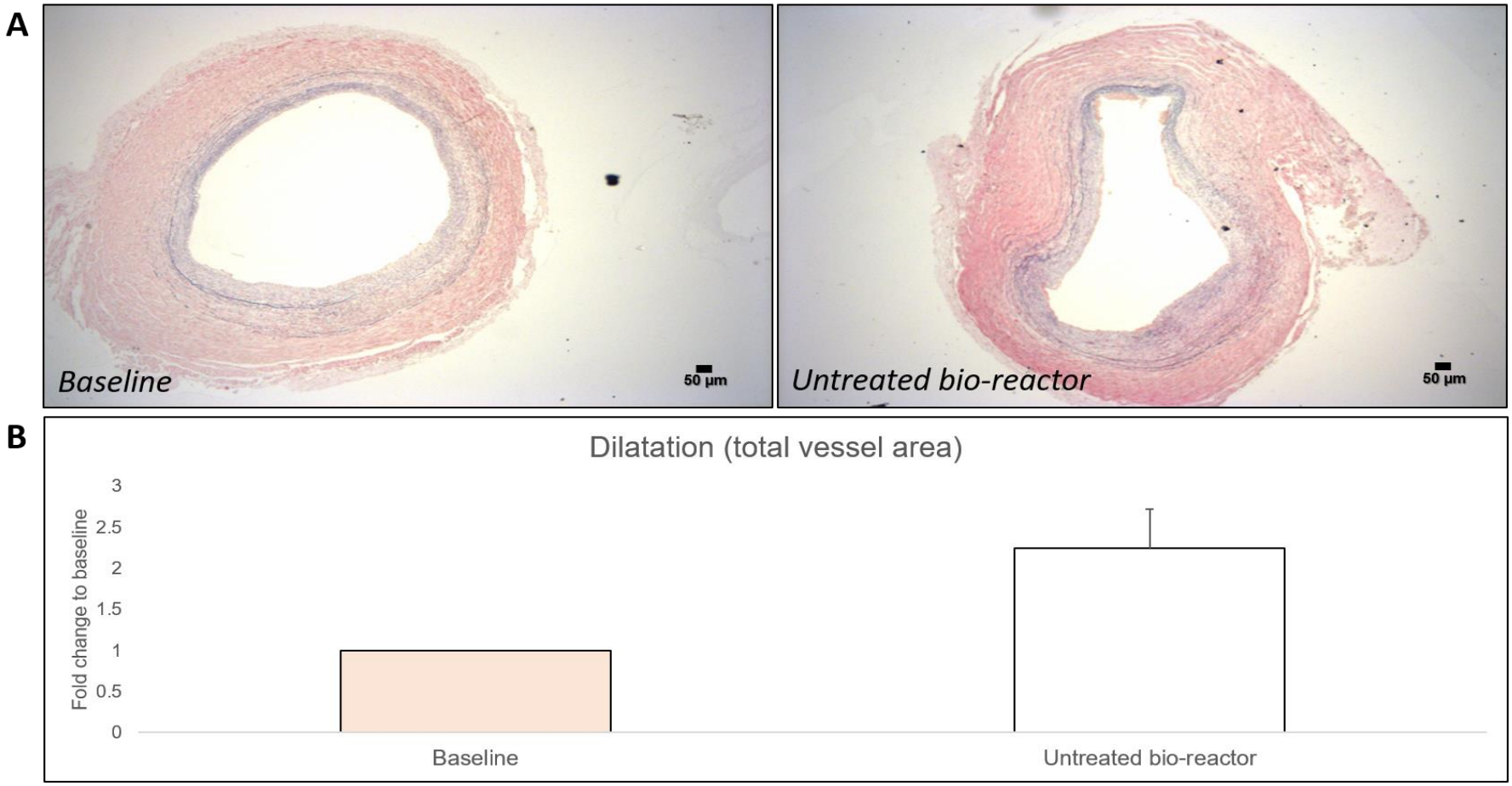

Figure 3.4: Laminar flow does not affect human umbilical cord artery total vessel area

Representative images (A) and quantification (B) of total vessel area in x 4 magnification fields of EVG stained sections from human umbilical cord arteries only washed with PBS and not subject to laminar flow (baseline) and human umbilical cord arteries after insertion within a bio-reactor for 72 hours (untreated bio-reactor). Data is expressed as a fold change in dilatation (total vessel area) of the untreated bio-reactor compared to native baseline vessels (mean±SEM; n=5). 2-tailed Student paired t test. Scale bars represent 50 µm.

3.3.2 Effect of $CaCl_2$ pre-treatment on morphological and compositional parameters associated with aneurysm formation in *ex vivo* bio-reactor cultured human umbilical cord arteries

To evaluate the effect of $CaCl_2$ in my *ex vivo* model of aneurysm formation, human umbilical cord arteries were isolated and cut into two equal lengths. One portion was soaked for 15 minutes in $CaCl_2$ (0.25 mM) then washed with PBS, before insertion into the bio-reactor system for 72 hours at 6.5 dynes/cm^2, whereas the other portion of umbilical artery was washed and soaked with PBS only, before insertion within the bio-reactor system and served as a paired control. As shown in Figure 3.5 $CaCl_2$-treated arteries after 72 hours within the bio-reactor showed decreased medial thickness when compared to untreated controls, (34%; $P<0.05$; n=6). Assessment of elastin content within EVG-stained sections from arteries within the *ex vivo* aneurysm model revealed significantly decreased elastin content in $CaCl_2$ pre-treated arteries compared to untreated controls (as shown in Figure 3.6) (26%; $P<0.05$; n=6).

Finally, total vessel cross-sectional area was quantified to determine effects on vessel dilatation, given that dilatation is triggered through thinning of the medial layer and degeneration of the internal elastic lamina during aneurysm formation [16]. However, no change in total vessel area was observed between $CaCl_2$ pre-treated arteries and control vessels within the *ex vivo* aneurysm model (Figure 3.7).

It has been previously demonstrated that VSMC apoptosis within the arterial wall is associated with aneurysm formation [217]. In particular, in mouse models the application of $CaCl_2$ to the adventitia of the aorta increased the number of apoptotic cells within the medial layer compared to vessels from untreated control mice [218]. The density of VSMC was altered by placing umbilical cord artery within the bio-reactor for 72 hours, by comparing to paired arteries which were not placed within the bio-reactor (Figure 3.8). However, as shown in Figure 3.9 medial cell density was significantly reduced in $CaCl_2$ pre-treated umbilical arteries after 72 hours within the bio-reactor compared to untreated control arteries (53%; $P<0.05$; n=6).

To summarise, 15-minute pre-treatment with $CaCl_2$ reduced medial thickness, elastin content, and number of cells per cross-sectional area of human umbilical arteries, therefore promoting changes associated with aneurysm formation in mouse models and humans. However, $CaCl_2$ pre-treatment did not induce vessel dilatation, a key feature of aneurysm formation. Therefore, *ex vivo* culture of human umbilical cord artery with $CaCl_2$ pre-treatment cannot be considered an appropriate model to replace the current $CaCl_2$ pre-treatment mouse model.

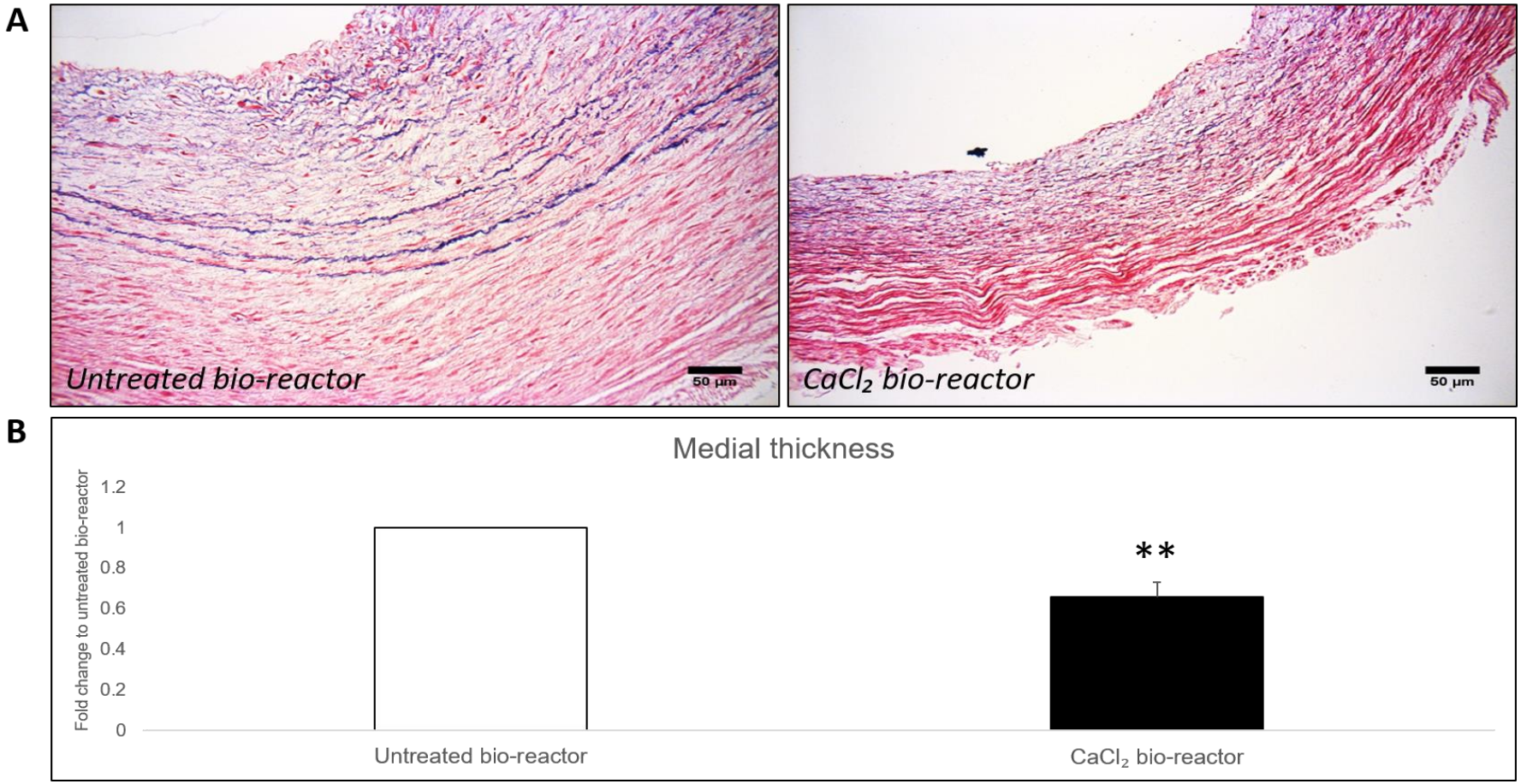

Figure 3.5: $CaCl_2$ pre-treatment significantly reduced medial thickness

*Representative images (A) and quantification (B) of medial thickness assessed in ten x20 magnification fields of EVG stained sections from human umbilical cord arteries after insertion within a bio-reactor for 72 hours without $CaCl_2$ (untreated bio-reactor) and with $CaCl_2$ ($CaCl_2$ bio-reactor) pre-treatment for 15 minutes. Data is expressed as a fold change in medial thickness of the $CaCl_2$ pre-treated arteries compared to control (untreated) vessels (mean±SEM; n=6). ** denotes $p<0.01$ versus control, 2-tailed Student paired t test. Scale bars represent 50 µm.*

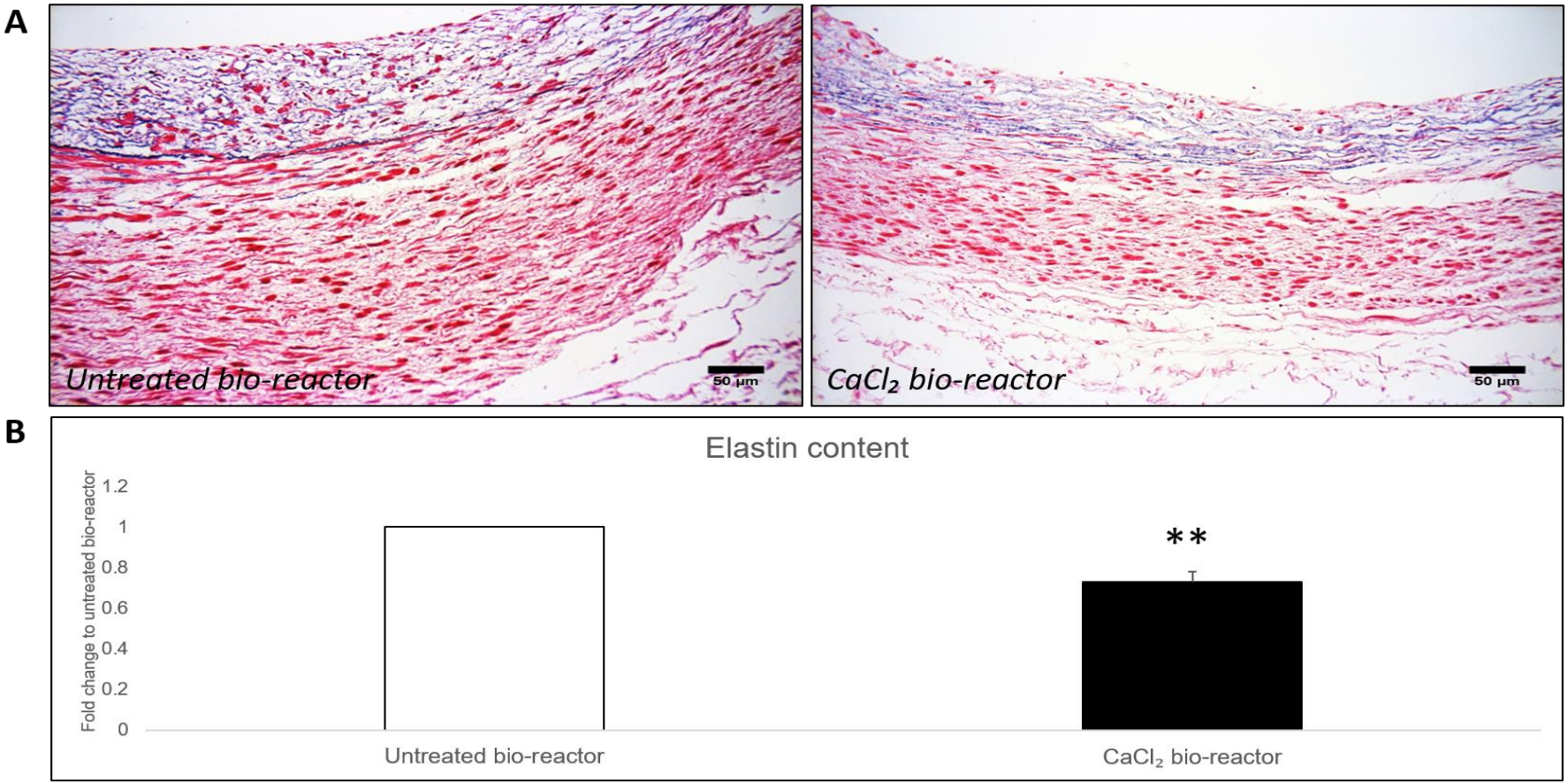

Figure 3.6: $CaCl_2$ pre-treatment significantly reduced elastin content

*Representative images (A) and quantification (B) of elastin content assessed in ten x20 magnification fields of EVG stained sections from human umbilical cord arteries after insertion within a bio-reactor for 72 hours without $CaCl_2$ (untreated bio-reactor) and with $CaCl_2$ ($CaCl_2$ bio-reactor) pre-treatment for 15 minutes. Data is expressed as a fold change in elastin content of the $CaCl_2$ pre-treated arteries compared to control (untreated) vessels (mean±SEM; n=6). ** denotes p<0.01 versus control, 2-tailed Student paired t test. Scale bars represent 50 µm.*

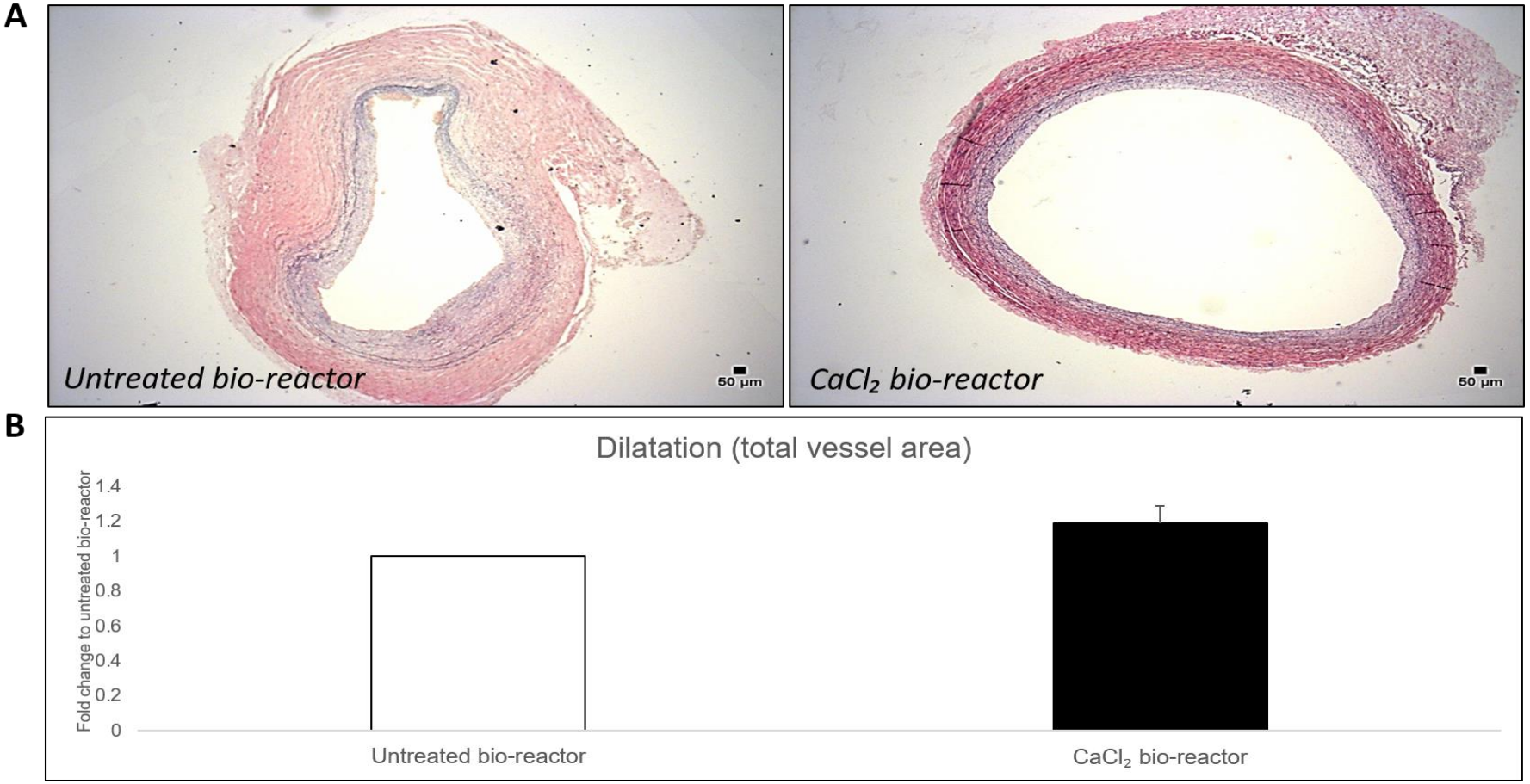

Figure 3.7: $CaCl_2$ pre-treatment does not increase total vessel area

Representative images (A) and quantification (B) of total vessel area (dilatation) assessed in ten x20 magnification fields of EVG stained sections from human umbilical cord arteries after insertion within a bio-reactor for 72 hours without $CaCl_2$ (untreated bio-reactor) and with $CaCl_2$ ($CaCl_2$ bio-reactor) pre-treatment for 15 minutes. Data is expressed as a fold change percentage in total vessel cross-sectional area of the $CaCl_2$ pre-treated arteries compared to control (untreated) vessels (mean±SEM; n=6). 2-tailed Student paired t test. Scale bars represent 50 µm.

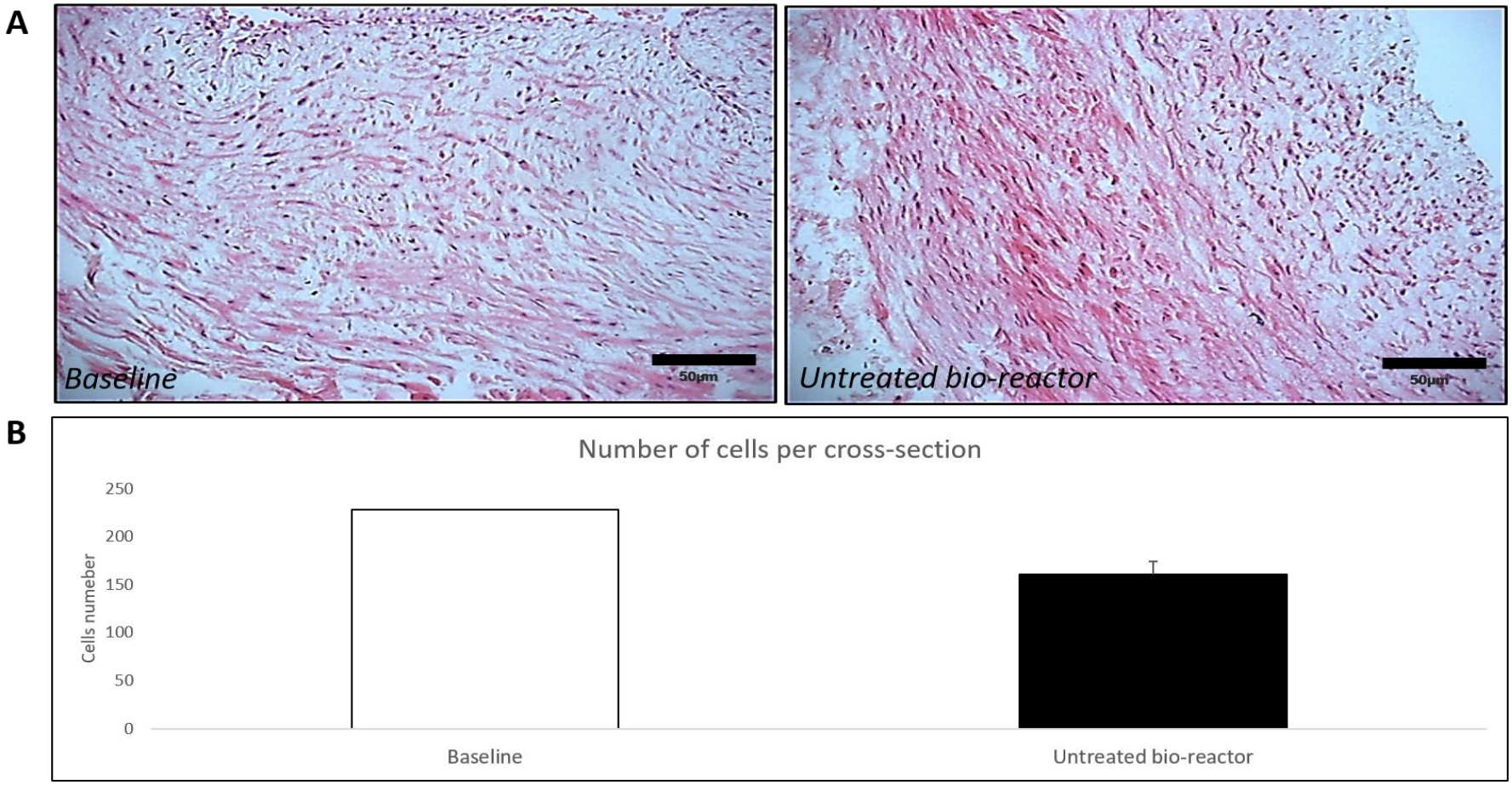

Figure 3.8: Insertion of umbilical cord arteries within a bio-reactor for 72 hours does not alter cell density

Representative images (A) and quantification (B) of medial cell content assessed in ten x20 magnification fields of H&E stained sections from human umbilical cord arteries before placement in an ex vivo bio-reactor system (termed baseline) and after insertion within a bio-reactor for 72 hours (untreated bio-reactor). Data is expressed as a number of cells per arterial cross-section (mean±SEM; n=6). 2-tailed Student paired t test. Scale bars represent 50 µm.

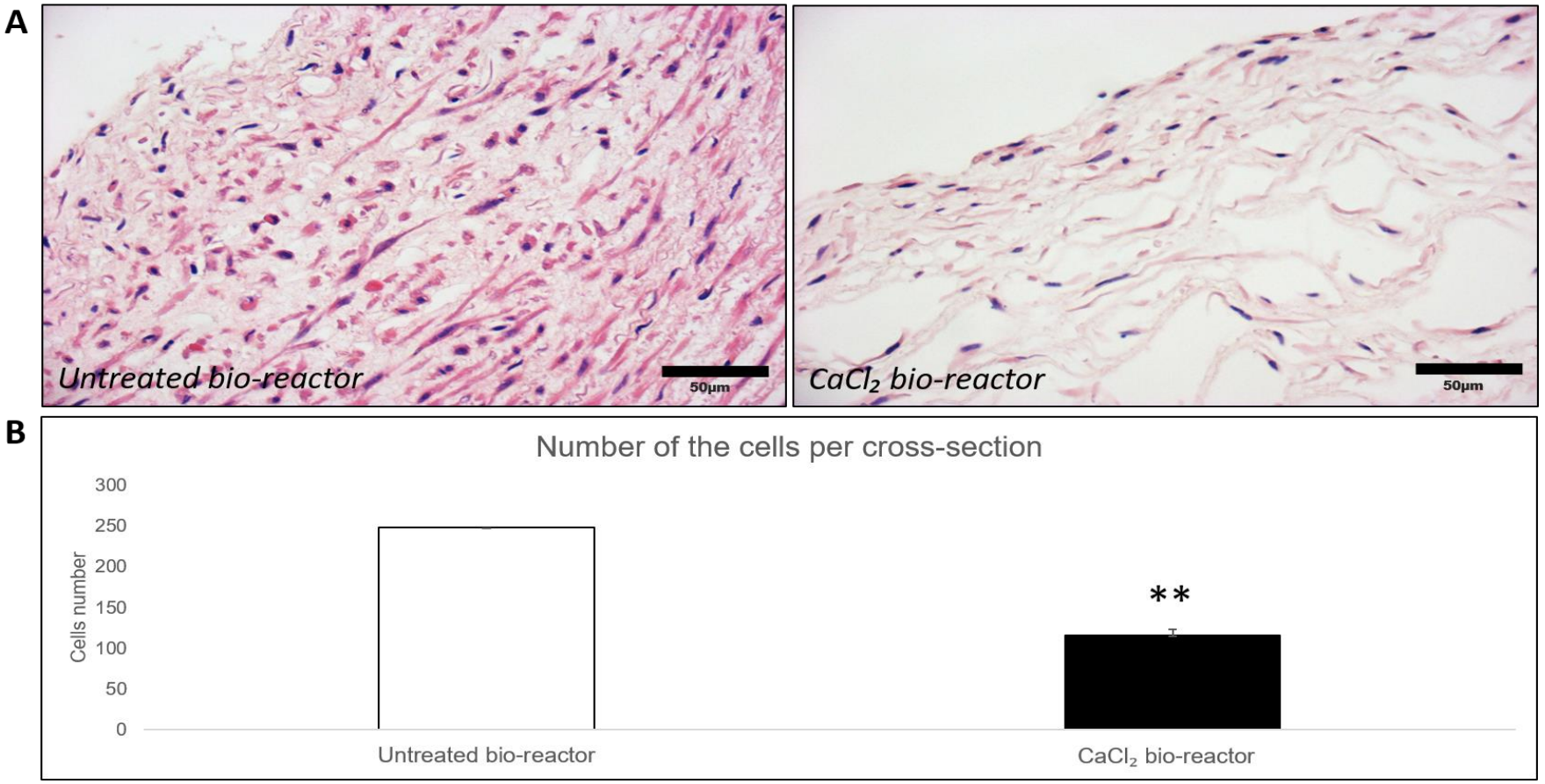

Figure 3.9: $CaCl_2$ pre-treatment significantly reduced human umbilical cord artery cell density

*Representative images (A) and quantification (B) of medial cell content assessed in ten x20 magnification fields of H&E stained sections from human umbilical cord arteries after insertion within a bio-reactor for 72 hours without $CaCl_2$ (untreated bio-reactor) and with $CaCl_2$ ($CaCl_2$-bio-reactor) pre-treatment for 15 minutes. Data is expressed as a number of cells per arterial cross-section (mean±SEM; n=6). ** denotes p<0.01 versus control2-tailed. Student paired t test. Scale bars represent 50 µm.*

3.3.3 Effect of Ang II administration on morphological and compositional parameters associated with aneurysm formation in *ex vivo* bio-reactor cultured human umbilical cord arteries

To evaluate the effect of Ang II in our *ex vivo* model of aneurysm formation, human umbilical cord arteries were isolated and cut into two equal lengths. One portion was flushed with PBS and inserted within a bio-reactor system at 6.5 dynes/cm^2 using media containing 5μM Ang II in order to mimic the mouse model of aneurysm formation [130, 219]. Untreated control human umbilical cord artery was placed in the bio-reactor system for 72 hours at 6.5 dynes/cm^2 with media alone and served as a paired control. As shown in Figure 3.10 A, umbilical cord artery treated with Ang II for 72 hours showed macroscopically visible dilatation compared to a paired untreated control vessel. Similarly, marked dilatation in Ang II-infused arteries were visible through macroscopic visualisation of H&E-stained paraffin-wax sections (Figure 3.10 B). Although the observation that macroscopic differences in arterial dilatation were seen with Ang II stimulation were encouraging, further robust quantitative examination was required to further validate the *ex vivo* model.

To ensure that the macroscopic changes were indicative of dilatation, further histological examination was performed. As previously mentioned, principle morphological and compositional characteristics associated with aneurysm formation were assessed, including arterial dilatation, elastin loss linked to proteolytic degradation, medial thinning and decreased VSMC density.

Firstly, as shown in Figure 3.11 Ang II stimulation (5μM) for 72 hours significantly reduced umbilical artery medial thickness compared to untreated paired control artery segments (49%; $P<0.05$; n=6). Secondly, assessment of arterial wall elastin content revealed decreased medial elastin content in Ang II-treated umbilical arteries (60%; $P<0.05$; n=6), compared to untreated control arteries (Figure 3.12). Thirdly, image analysis of EVG-stained sections to quantify total vessel area as an indicator of arterial dilatation, demonstrated total vessel area was significantly increased in Ang II-treated umbilical arteries (90%; $P<0.05$; n=6) compared to untreated control arteries (Figure 3.13). Lastly, as shown in Figure 3.14 medial cell density was significantly reduced in Ang II treated umbilical arteries after 72 hours within a bio-reactor compared to untreated control arteries (32%; $P<0.05$; n=5). In summary, the above observations illustrate the novel *ex vivo* bio-reactor system employing arteries retrieved from human umbilical cord and subjected to Ang II administration, displays morphological and compositional changes associated with aneurysm formation in mice and humans.

Several studies have shown increased collagen turnover during AAA formation, most commonly presented as a reduction in arterial wall total collagen content [216, 220]. Accordingly, Picrosirius red stained sections were analysed to quantify total fibrillar collagen content within umbilical cord arteries before and after 72 hours within the *ex vivo* bio-reactor system. As shown in Figure 3.15 culture of human umbilical cord artery within a bio-reactor for 72 hours had no significant effect on fibrillar collagen content. However, the administration of Ang II significantly reduced total collagen content when compared to untreated control arteries (32%; $P<0.05$; n=5; Figure 3.16). Taken together these findings suggest that our *ex vivo* bio-reactor without aneurysm inducers such as Ang II, does not consistently affect key elements associated with aneurysm formation, such as collagen turnover or medial cell density, whereas addition of Ang II within the *ex vivo* model does induce collagen loss, alongside changes of other key aspects.

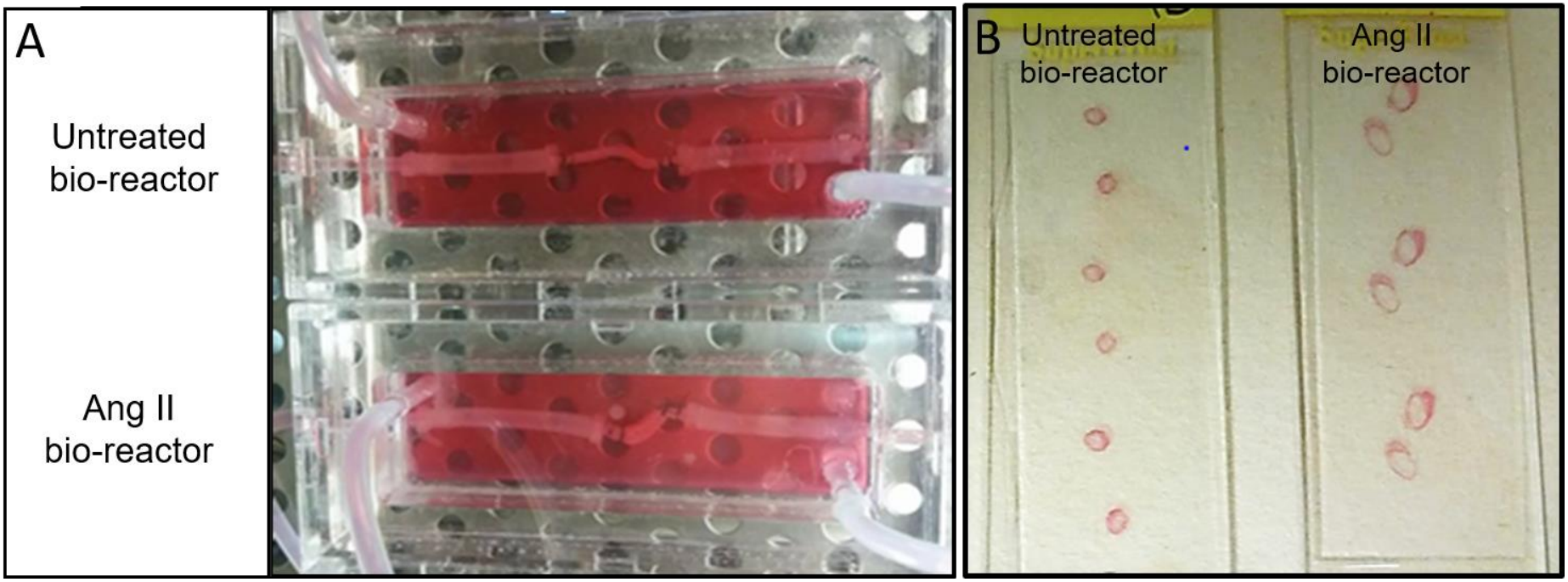

Figure 3.10: Representative images of ex vivo Ang II-infusion aneurysm model after 72h within a bio-reactor

Macroscopic changes in vessel dilatation were observed after 72h within a bio-reactor plus angiotensin II infusion compared to untreated control paired artery, assessed (A) while still within the bio-reactor, or (B) after histological sectioning and H&E staining.

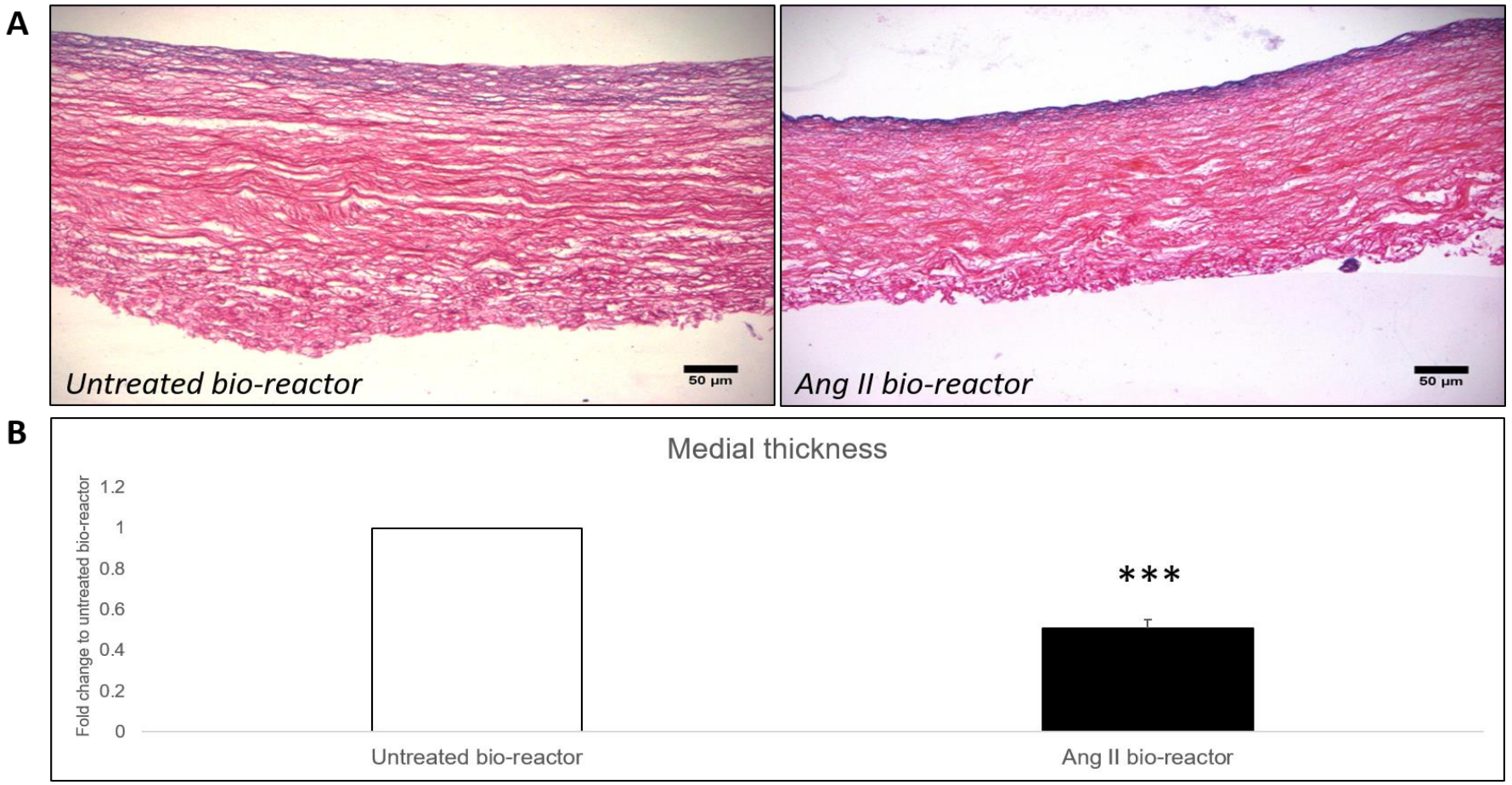

Figure 3.11: Ang II administration significantly reduced human umbilical cord artery medial thickness

*Representative images (A) and quantification (B) of medial thickness assessed in ten x20 magnification fields of EVG stained sections from human umbilical cord arteries after insertion within a bio-reactor for 72 hours without Ang II (control) and with Ang II (Ang II). Data is expressed as a fold change percentage in medial thickness of the Ang II-infused arteries compared to control (untreated) vessels (mean±SEM; n=6). *** denotes p<0.001 versus control, 2-tailed Student paired t test. Scale bars represent 50 µm*

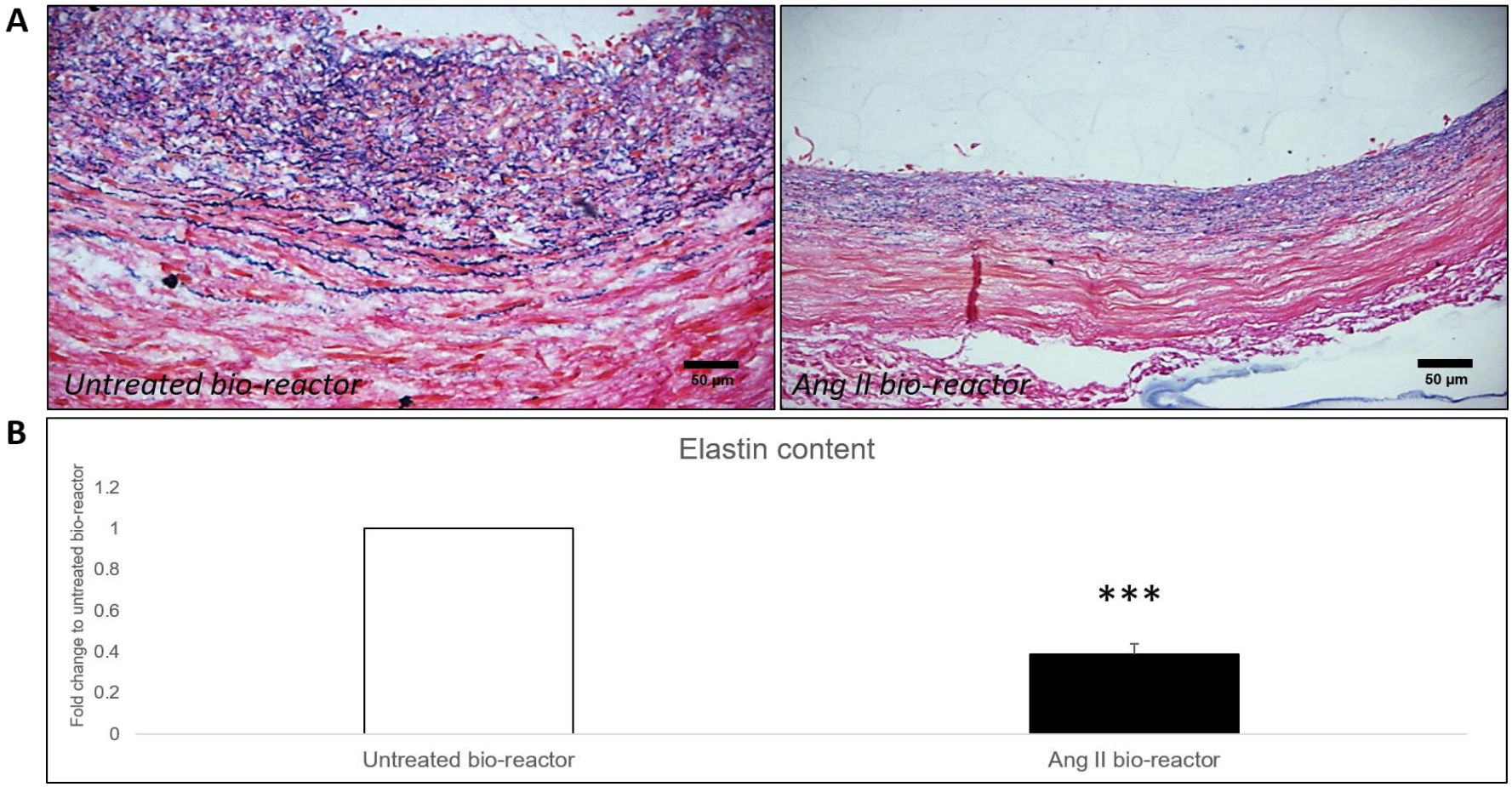

Figure 3.12: Ang II administration significantly reduced human umbilical cord artery elastin content

*Representative images (A) and quantification (B) of elastin content assessed in ten x20 magnification fields of EVG stained sections from human umbilical cord arteries after insertion within a bio-reactor for 72 hours without Ang II (untreated) and with Ang II (Ang II). Data is expressed as a fold change percentage in elastin content of the Ang II-infused arteries compared to control (untreated) vessels (mean±SEM; n=6). *** denotes p<0.001 versus control, 2-tailed Student paired t test. Scale bars represent 50 µm.*

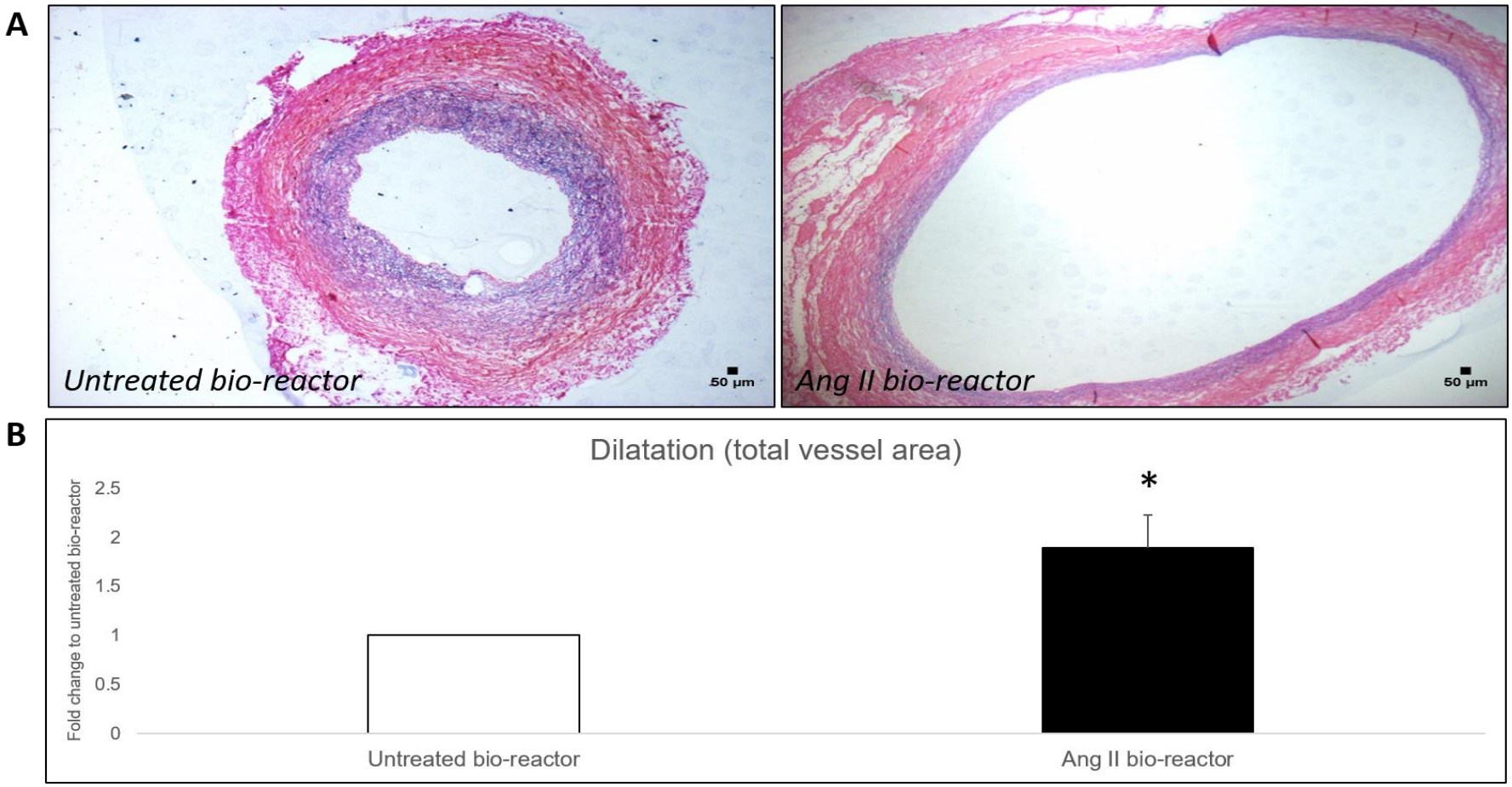

Figure 3.13: Ang II administration significantly increased human umbilical cord artery total vessel area

*Representative images (A) and quantification (B) of total vessel area (dilatation) assessed in ten x20 magnification fields of EVG stained sections from human umbilical cord arteries after insertion within a bio-reactor for 72 hours without Ang II (untreated) and with Ang II (Ang II). Data is expressed as a fold change percentage in elastin content of the Ang II-infused arteries compared to control (untreated) vessels (mean±SEM; n=6). * denotes $p<0.05$ versus control, 2-tailed Student paired t test. Scale bars represent 50 µm.*

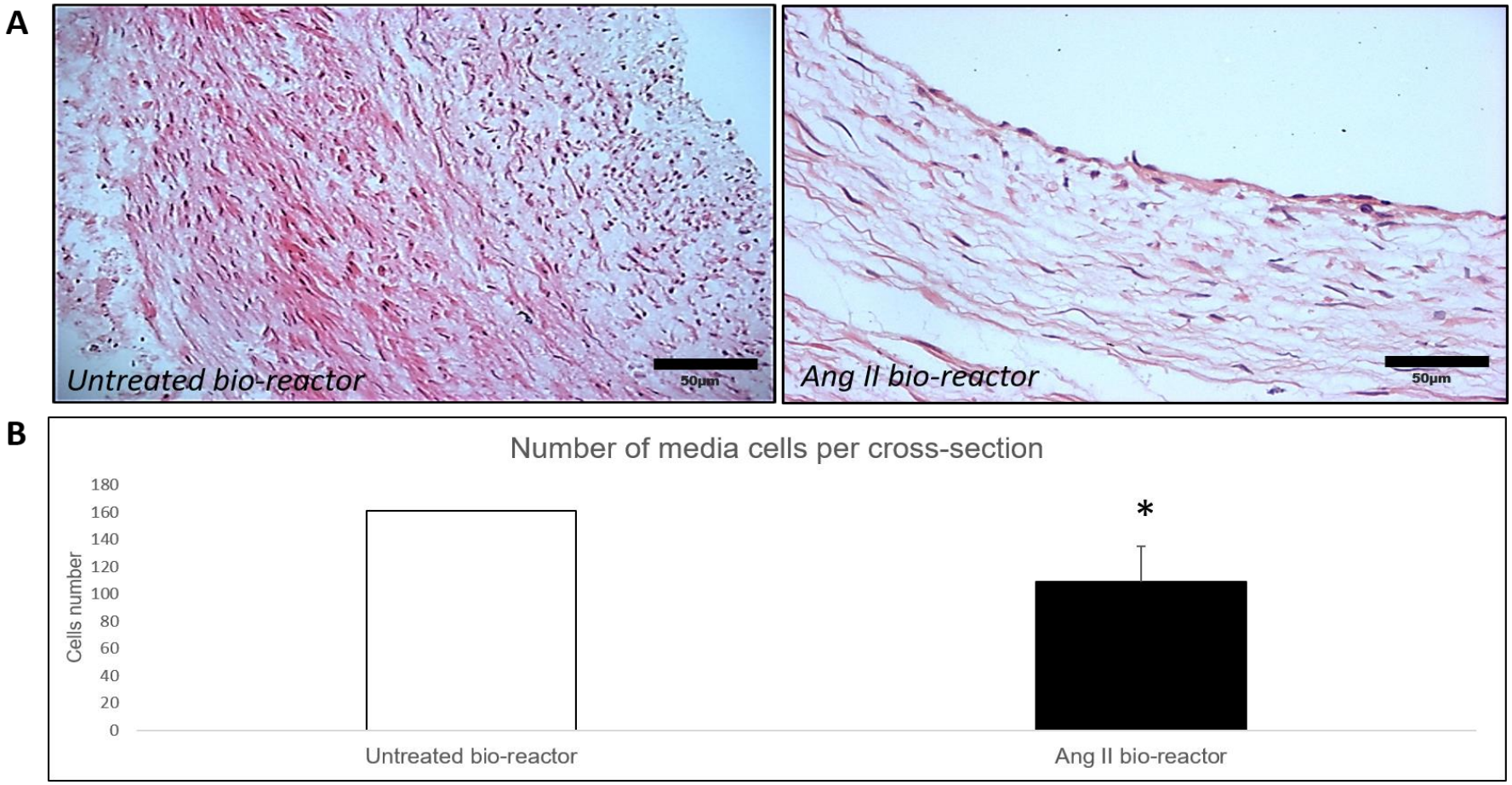

Figure 3.14: Ang II administration significantly decreased human umbilical cord artery medial cell content

*Representative images (A) and quantification (B) of medial cell content assessed in ten x20 magnification fields of H&E stained sections from human umbilical cord arteries after insertion within a bio-reactor for 72 hours without Ang II (untreated) and with Ang II (Ang II) administration. Data is expressed as number of cells per arterial cross-section (mean±SEM; n=6). * denotes $p<0.05$ versus control, 2-tailed Student paired t test. Scale bars represent 50 µm.*

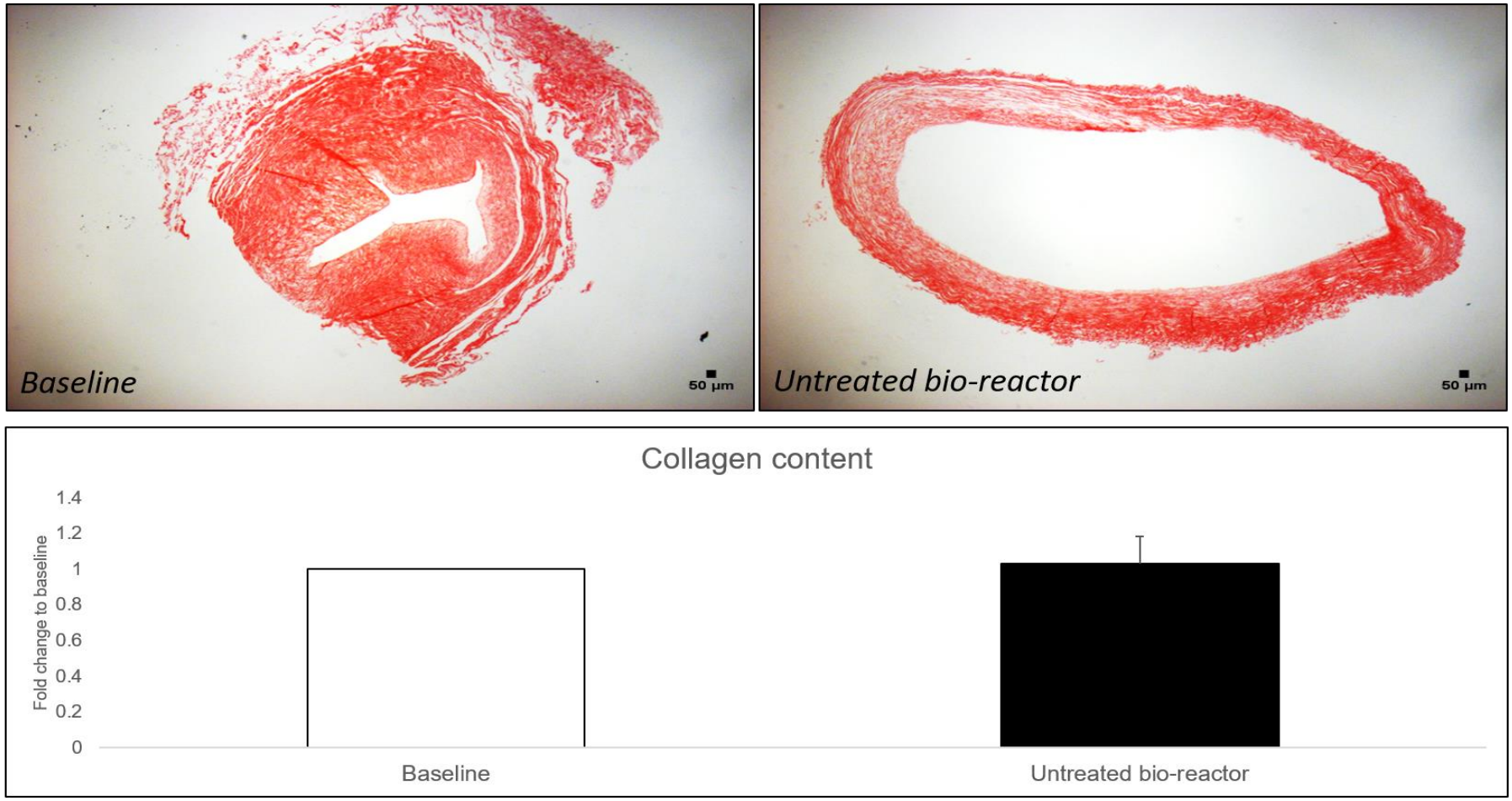

Figure 3.15: Insertion of umbilical cord arteries within a bio-reactor for 72 hours does not affect fibrillar collagen content

Representative images (A) and quantification (B) of collagen content assessed in ten x20 magnification fields of Picrosirius red stained sections from human umbilical cord arteries before placement in an ex vivo bio-reactor system (termed baseline) and after insertion within a bio-reactor for 72 hours (untreated bio-reactor). Data is expressed fold change in collagen content in the bio-reactor 72 hours artery (untreated bio-reactor) compared to native baseline vessels (mean±SEM; n=6). 2-tailed Student paired t test. Scale bars represent 50 µm.

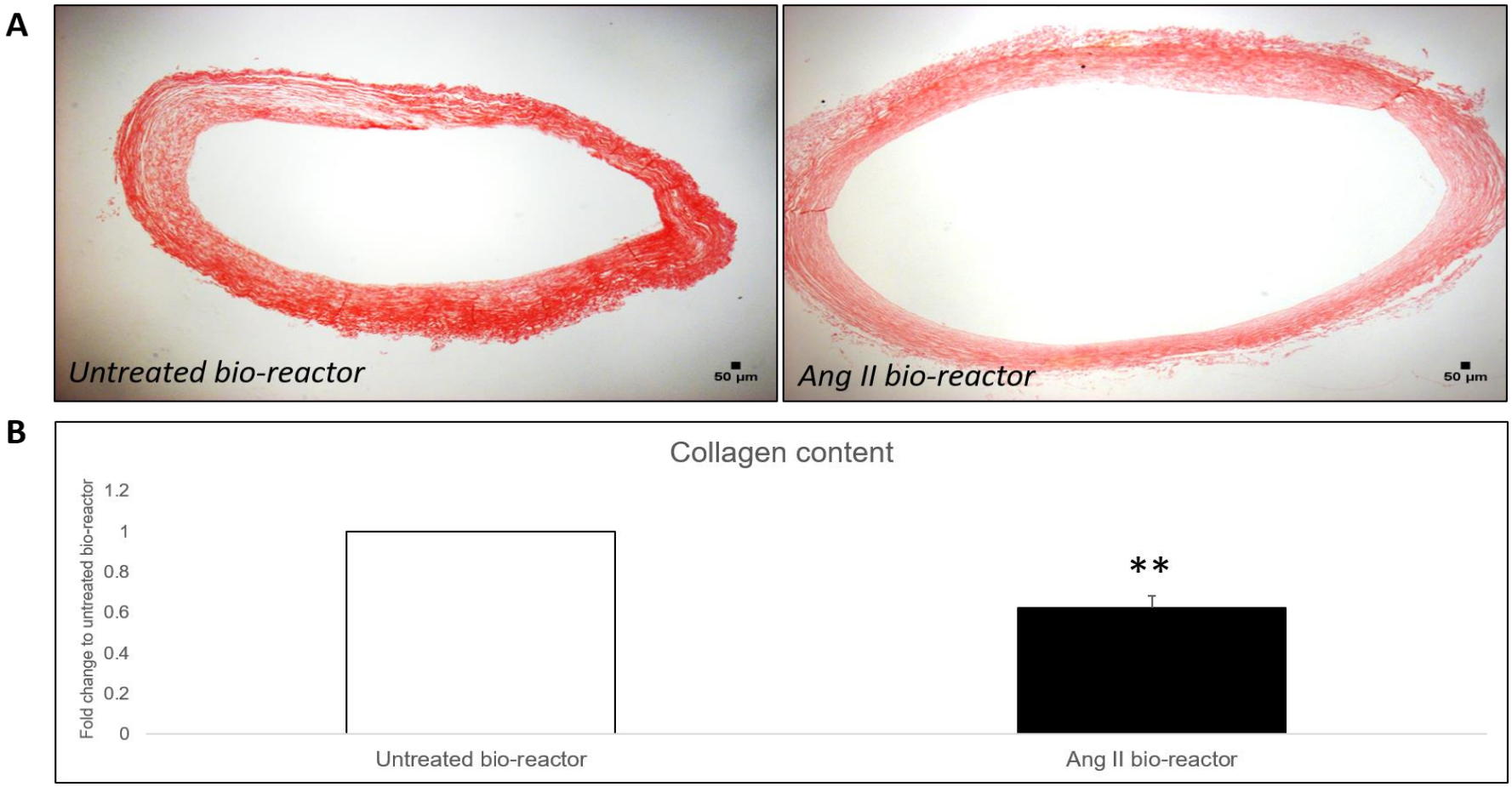

Figure 3.16: Ang II administration significantly reduced human umbilical cord artery fibrillar collagen content

*Representative images (A) and quantification (B) of total fibrillar collagen content assessed in ten x20 magnification fields of Picrosirius red stained sections from human umbilical cord arteries after insertion within a bio-reactor for 72 hours without Ang II (control) and with Ang II (Ang II). Data is expressed as a fold change percentage in total collagen content of the Ang II-infused arteries compared to control (untreated) vessels (mean±SEM; n=6). ** denotes p<0.01 versus control, 2-tailed Student paired t test. Scale bars represent 50 µm.*

3.3.4 Effect of Ang II administration on MMP expression in *ex vivo* bio-reactor cultured human umbilical cord arteries

Evidence has implicated that MMPs and TIMPs play a fundamental role in aneurysm formation, progression, and propensity to rupture [164, 179]. MMPs have been considered the main proteases driving extracellular matrix degradation within the aneurysm wall. In view of this, the effect of placing human umbilical cord arteries within a bio-reactor for 72 hours alongside administration of Ang II on the expression of select MMPs was assessed. As shown in Figure 3.17 and Figure 3.18 subjection of human umbilical cord arteries to bio-reactor conditions for 72 hours significantly decreased MMP-3 protein expression (76%; $P<0.01$; n=5), and increased levels of MMP-9 (42-fold; $P<0.05$; n=5) and MMP-12 (7.5-fold; $P<0.05$; n=5), whereas expression of MMP-10 and MMP-19 were unaffected, when compared to baseline artery segments (not placed within a bio-reactor). Conversely, in response to Ang II-infusion the protein expression of MMP-3, MMP-9, and MMP-12 did not change when compared to control arteries maintained within a bio-reactor for 72 hours (Figure 3.17). However, significantly increased expression of MMP-10 (2.4-fold; $P<0.05$; n=5) and MMP-19 (2.7-fold; $P<0.05$; n=5) were observed in umbilical cord arteries exposed to Ang II relative to control arteries (Figure 3.18). In all instances, a protein assay was performed in order to ensure equal loading and a stain free gel was used to normalise protein expression.

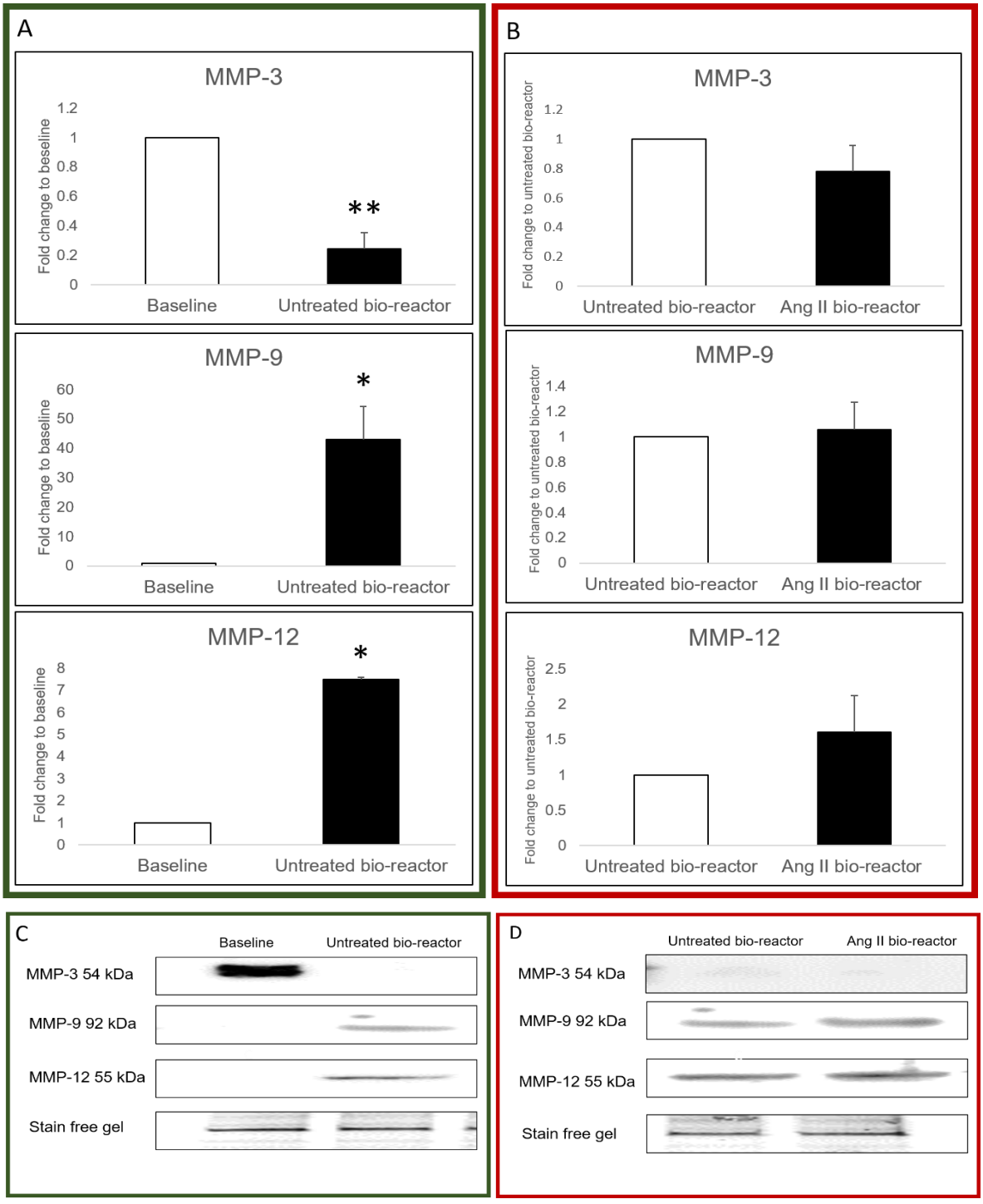

Figure 3.17: Effect of umbilical cord artery insertion within a bio-reactor for 72 hours with and without Ang II-infusion, on the expression of MMP-3, MMP-9 and MMP-12

*Densitometric quantification (A and B) and representative western blots (C and D) of MMP-3, MMP-9 and MMP-12 protein expression in tissue lysates from human umbilical cord arteries before (baseline) and after insertion within a bio-reactor for 72 hours (A and C, within green box), or without Ang II (control) and with Ang II (B and D, within red box). Data is expressed as fold change against baseline (A) or against control (untreated) vessels (B) (mean±SEM; n=5). * denotes p<0.05 and ** denotes p<0.01 versus baseline. Associated stain free gels are shown as a loading control.*

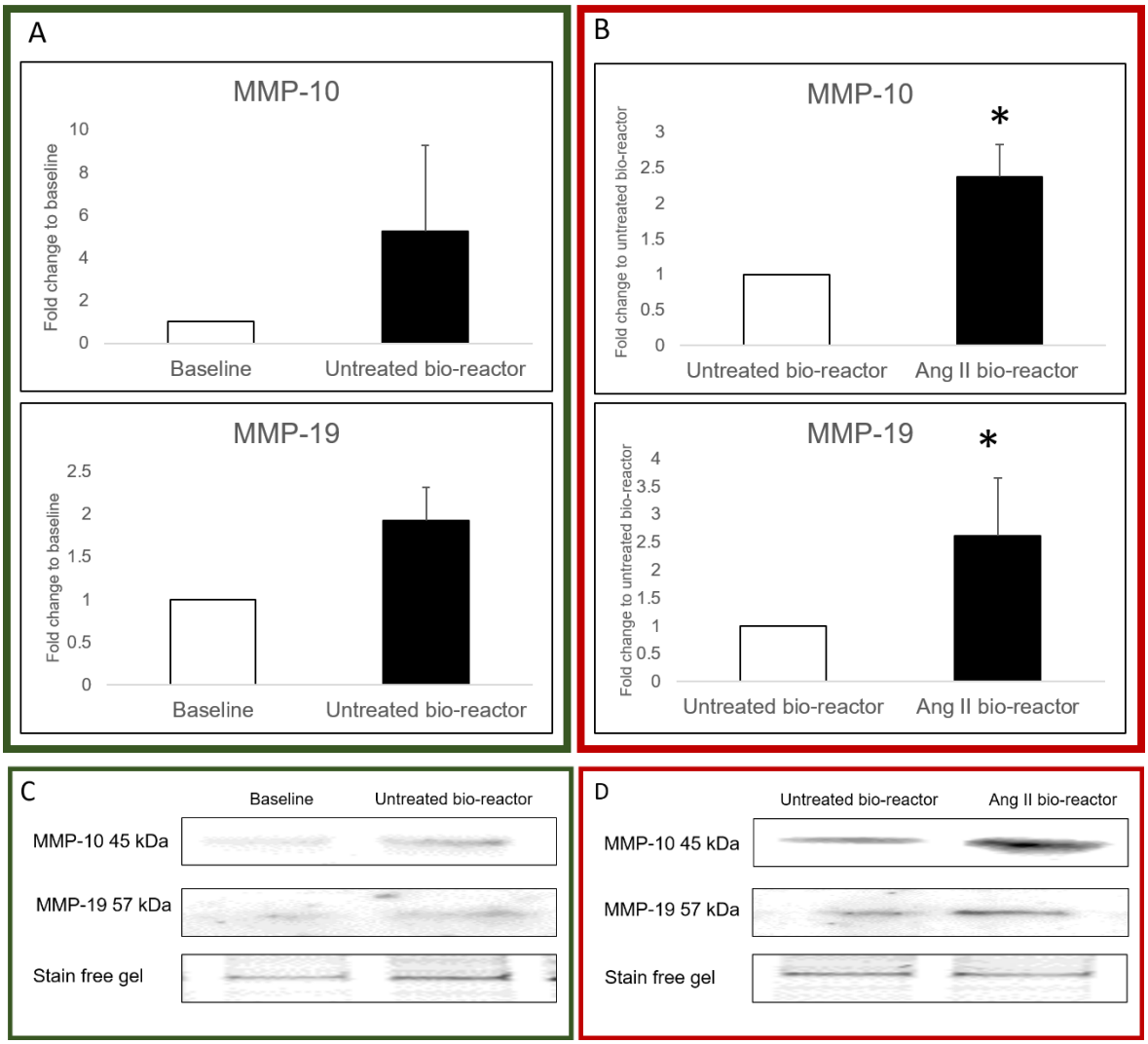

Figure 3.18: Effect of umbilical cord artery insertion within a bio-reactor for 72 hours with and without Ang II-infusion, on the expression of MMP-10 and MMP-19

*Densitometric quantification (A and B) and representative western blots (C and D) of MMP-10 and MMP-19 protein expression in tissue lysates from human umbilical cord arteries before (baseline) and after insertion within a bio-reactor for 72 hours (A and C, within green box), or without Ang II (control) and with Ang II (B and D, within red box). Data is expressed as a fold change against baseline (A) or against control (untreated) vessels (B) (mean±SEM; n=5). * denotes p<0.05 versus control (untreated) vessels. Associated stain free gels are shown as a loading control.*

3.4 Conclusion

The first aim of this chapter was to determine the effect of peri-vascular $CaCl_2$ application or Ang II-infusion within a potential novel *ex vivo* model of aneurysm formation. Firstly, $CaCl_2$ application for 15 minutes followed by 72 hours within a bio-reactor significantly decreased umbilical artery medial thickness, reduced elastin content, and induced medial cell loss. However, arterial dilatation (assessed through changes in total vessel area) was unchanged with $CaCl_2$ administration; therefore, it cannot be considered a replacement for mouse aneurysm studies. In contrast, Ang II stimulation for 72 hours within a bio-reactor significantly increased arterial dilatation alongside reductions in medial thickness and cell density, and reduced elastin and collagen content. The observed morphological and compositional changes induced by Ang II within the *ex vivo* model are consistent with aneurysm formation in mouse models and patients (see Figure 3.19), and were associated with increased expression of two understudied proteases, MMP-10 and MMP-19, both of which have been associated with the progression of cardiovascular diseases in humans.

Collectively, these findings demonstrate the potential of the *ex vivo* human umbilical cord artery bio-reactor system as a model for aneurysm formation and therefore possibly reducing the number of animals used in aneurysm studies and a potential replacement for mouse models, fulfilling two of the key principles of the 3Rs. These findings support its use as a reproducible model for aneurysm studies and supplanting the need for ethically challenging animal experiments.

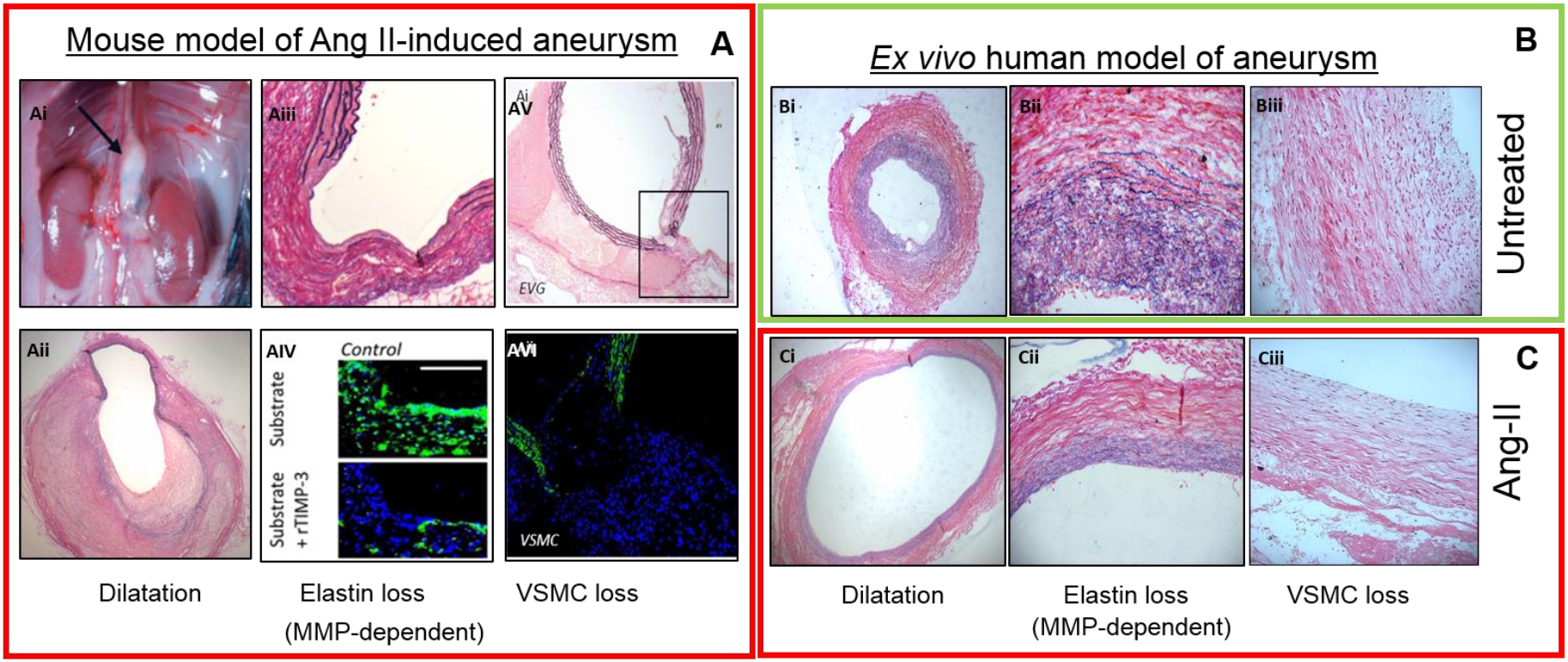

Figure 3.19: Comparison between the Ang II mouse model of aneurysm and the novel ex vivo human model of aneurysm

(A) The Ang II-infusion (via osmotic mini-pump) mouse model of aneurysm is characterised by dilatation of the aorta, elastin fragmentation (which is dependent on MMP activity), and loss of VSMC density.

(B) Placement of untreated umbilical cord arteries within a bio-reactor and subjected to laminar pulsatile flow at 6.5 dynes/cm^2 for 72 hours, did not induce arterial dilatation, elastic fragmentation, or VSMC loss.

(C) The ex vivo flow model of aneurysm using umbilical cord arteries infused with angiotensin II under laminar pulsatile flow at 6.5 dynes/cm^2 for 72hours, showed dilatation of the artery, elastin fragmentation and loss of VSMC density, similar to observations within the mouse model.

Ai, dilatated mouse aorta

Aii, section of dilatated mouse aorta with Ang II
Aiii, mouse aorta displaying elastin fiber
Aiv, immunofluorescent staining of mouse aorta displaying the proteolytic activity in green that is reduces using an inhibition of MMP- pathway
Av, section of mouse aorta
Avi, area of mouse aorta in panel Av depicted by box, immunolabelled for VSMCs (α SMactin, green) and nuclei (blue, showing loss of VSMCs at site of rupture
Bi, Native human umbilical cord artery
Ci, Dilatated human umbilical cord artery treated with Ang II
Bii, Elastin content (purple) within native human umbilical cord artery
Cii, Elastin content (purple) within Ang II-treated human umbilical cord artery
Biii Nuclei per cross-section in native human umbilical cord artery
Ciii, Nuclei per cross-section in Ang II-treated human umbilical cord artery

3.5 Discussion

There have been limited attempts to develop and deploy *ex vivo* models for aneurysm research studies, which have been restricted to the use of porcine carotid arteries or porcine abdominal aortae [199, 200]. One of the novel aspects of the model developed during this study is the use of arteries of human origin, greatly adding to the translational potential of studies conducted using this model. Moreover, as the arteries are isolated from human umbilical cord, this represents a resource which is normally discarded as waste tissue and is freely available to researchers around the globe (taking ethical permissions into consideration), increasing the applicability of this model.

This chapter was undertaken to assess the effect of $CaCl_2$ application or Ang II-infusion within a novel *ex vivo* bio-reactor system using human umbilical cord arteries to determine whether aneurysm formation could be reproducibly modelled. It was proposed that an umbilical cord artery *ex vivo* model of aneurysm formation could serve as a potential replacement of mouse models of AAA studies and concomitantly reduce the number of mice used within aneurysm research. The use of current mouse models of AAA is increasing, and their use raises ethical concerns and poor public perception due to the increasing number of mice which suffer sudden death due to acute aortic rupture. In order to characterise and validate the *ex vivo* model, it needs to display distinct morphological and cellular changes which are observed in mouse models of aneurysm formation alongside human aneurysms. Moreover, any model should be relatively easy to set-up, reproducible and therefore accessible to a wide range of researchers globally

3.5.1 The use of $CaCl_2$ application in an *ex vivo* model of aneurysm

Previous studies have shown that peri-vascular $CaCl_2$ application to the aorta of mice for 15 minutes induced histological changes such as vessel dilatation, elastin loss and medial thinning, when the animals were analysed 28-days later [40, 133, 221]. Furthermore, increased MMP expression, along with elevated levels of pro-inflammatory cytokines was also observed within the dilated aortic tissue. Similarly, in the *ex vivo* model deploying peri-vascular application of $CaCl_2$ to human umbilical cord arteries for 15 minutes, reduced elastin content and decreased medial thickness were detected, indicating dysregulated proteolysis and medial thinning, both considered underlying mechanisms of aneurysm formation and associated vessel dilatation. However, using total cross-sectional vessel area as a measure of dilatation, no effect of $CaCl_2$ application on this salient parameter was detected. The exact mechanisms causing aneurysm formation and further rupture is still not well understood but

there are potential mechanisms behind it. In human aneurysms there is a correlation between AAA diameter and the extent of adventitial inflammation [222] including the presence of macrophages and mast cells [223]. However, this *ex vivo* aneurysmal model is lacking inflammation, therefore it is possible inflammation is required to induce vessel dilatation. Moreover, the findings imply that VSMC-driven proteolysis and apoptosis is not sufficient to drive dilatation, in the umbilical cord artery bio-reactor system at least.

Nonetheless, in this study $CaCl_2$ application did induce morphological and compositional changes within the arterial wall. The potential mechanisms linked with $CaCl_2$ application include an increase of calcium deposition within the vessel wall and subsequent increased calcification and destruction of elastic fibres resulting in reduction in the elastin content [221]. Furthermore, $CaCl_2$ application is associated with VSMC apoptosis in mouse models of the of $CaCl_2$ application as well as in the *ex vivo* model of aneurysm [133]. It is well known that maintenance of calcium ion channel homeostasis within cells is necessary for cellular function including hormone secretion, myofilament contraction and metabolite modulation. Ion channels are involved in apoptosis with their main role to reduce cell damage [224]. Consequently, a possible mechanistic action $CaCl_2$ stimulation may be the alteration of calcium concentration within the cells resulting in increased apoptosis [225].

As mentioned in section 1.4.2, several molecular mechanisms have been proposed for $CaCl_2$ application-induced AAA formation, including reduction of the antioxidant enzyme catalase and activation of specific kinases and subsequent MMP induction, Nonetheless, such mechanisms rely on high concentrations of $CaCl_2$. Analysis of pertinent published *in vivo* studies using $CaCl_2$ application revealed the use of $CaCl_2$ concentrations of ranging between 0.1 and 0.68M [133], with 0.25M as the most commonly used concentration (in 56% of studies). Based on the above meta-analysis, 0.25M was selected as the optimal concentration of $CaCl_2$ for use in the *ex vivo* aneurysm model. Interestingly, the physiological extracellular concentration of calcium in humans is around 0.0015-0.002M, and concentrations above this are considered toxic. An *in vivo* study showed that low concentrations of $CaCl_2$ (between 0.1M and 0.2M) applied for 15 minutes to the mouse aortic wall generated vessel wall calcification, but did not induce aneurysm formation [221], demonstrating the need for $CaCl_2$ concentrations in excess of 0.2 M to induce aneurysms and supporting the use of 0.25M in the current *ex vivo* model. However, it should be noted that as the $CaCl_2$ mouse models relay upon supra-physiological concentrations of $CaCl_2$, the translational relevance of such models should be questioned.

3.5.2 The use of Ang II administration in an *ex vivo* model of aneurysm

This chapter demonstrated that infusion of Ang II to human umbilical cord arteries for 72 hours within a bio-reactor induced aneurysm formation. Multiple studies have demonstrated that Ang II administration to wild-type mice and hypercholesterolaemic mouse models significantly increased vessel area, decreased elastin content and induced medial thinning alongside increased VSMC apoptosis [63, 130, 219, 226]. Similar morphological and cellular changes within the *ex vivo* model with infusion of Ang II at a concentration of 5µM were observed. The concentration of Ang II was established on the basis of previously published Ang II-infusion mouse model studies and as importantly, according to the range detected in human aneurysmal disease. The circulating Ang II level within healthy human subjects is between 4 and 15 pg/ml whereas AAA patients display plasma Ang II levels of 20-85 pg/ml. Within the *ex vivo* bio-reactor model a concentration of 65 pg/ml was used, which is within the range detected in AAA patients. However, the Ang II-infusion mouse model of AAA predominantly relies upon plasma concentrations of 250pg/ml, which is obviously markedly higher compared to levels in AAA patients, raising possible translational concerns. Although, it has recently been demonstrated that 125 pg/ml Ang II concentrations are still effective in mice for inducing AAA formation [186], a concentration which is closer to that used within the *ex vivo* model detailed in this thesis.

Nonetheless, evidence from the Ang II-infusion model and human aneurysm pathological studies show that AAA formation and development are characterised by loss of medial thickness, collagen and elastin content, alongside depletion of VSMCs, all associated with vessel dilatation. In developing and characterising the *ex vivo* Ang II-infused human umbilical cord artery model of aneurysm similar changes are observed, supporting the use of this novel model for future aneurysm studies.

3.5.3 Morphological changes

The dominant feature of aneurysm formation in humans is vessel dilatation, and it is therefore paramount that this pathological adaptation is present within the *ex vivo* umbilical cord artery aneurysm model. An increase in vessel area implies a reduction of elasticity of the aortic wall, permitting dilatation to take place. One of the preliminary effects observed was dilatation of umbilical cord arteries subjected to Ang II-infusion, which was even visible macroscopically. Notably, the effect of the dilatation was due primarily to a direct effect of Ang II administration and not insertion within the bio-reactor system, as arterial dilatation was only significantly increased in Ang II-infused arteries compared an untreated paired control vessel segments,

whereas no significant difference in total vessel area was detected between umbilical cord artery segments before and after placement in the bio-reactor system for 72 hours. Potential mechanisms for Ang II-induced vessel dilatation are through induction of VSMC apoptosis, destruction of elastin and extracellular matrix degradation that therefore lead to vessel dilatation and rupture.

Under physiological conditions, a dynamic balance between mechanical or chemical stimuli and biological responses is preserved to maintain homeostatic conditions [224]. A perturbation of this balance with mechanical stimuli that is too high or too low can either lead to physiological adaptation or possibly disease of the vessel wall [227]. An important advantage of the *ex vivo* model is a single umbilical cord can generate multiple segments to enable paired statistical analysis, such as with and without Ang II administration, whereas in the mouse experiments a single mouse is required for each condition and paired statistical analysis in not achievable, increasing inter-subject variability and reducing statistical power and therefore increasing the number of mice required per condition.

Concerning the key developmental proprieties of the *ex vivo* model, two key criteria are the AAA inducers deployed and haemodynamic considerations. Systemic blood pressure in human arteries is 140-110mmHg during systole and 80-75mmHg at diastole. Considering the blood pressure experienced within the human umbilical cord arteries is approximately 50mmHg [228], a similar pressure was used within the bio-reactor set-up resulting in a pulsatile laminar wall shear stress of 6.5 dynes/cm^2, which is similar to that observed within the aorta of AAA patients [207]. This ensured the changes within the vessel were more reproducible as they relied primarily upon Ang II infusion, as opposed to exposing human umbilical cord artery to dramatic changes in pressure which could cause acute damage and not permit long-term assessment of the vessels, for example in regression studies to validate the model.

3.5.4 Medial cell loss

Medial cell loss was observed in both $CaCl_2$ and Ang II treated umbilical cord arteries in our *ex vivo* bio-reactor model compared to paired untreated arterial segments. However, when comparing baseline (before placement in the bio-reactor) and running within the bio-reactor for 72 hours, no difference was detected in medial cell density. These findings indicate that observed cell depletion is due directly to $CaCl_2$ or Ang II treatment, as opposed to placement within a bio-reactor under the selected haemodynamic conditions.

The observed depletion of medial cells, assumed to be VSMCs, can be ascribed to heightened VSMC apoptosis which is a known effect of Ang II administration *in vitro* and *in vivo* [229]. Apoptosis is a form of cell death that produces nuclear and cytoplasmic condensation; it is usually associated with specific stimuli, including endogenous mediators (including death factors and its receptors) [230] and is associated with specific patterns of cell degradation through the degradation of specific proteases (such as caspases) and nuclease enzymes. Apoptosis of VSMCs has been associated with the development of human atherosclerosis and aortic aneurysm formation [139, 231].

Apoptosis of VSMCs induced by peri-vascular $CaCl_2$ application or Ang II infusion, is thought to be essential during aneurysm formation in rodent models of aneurysms. For example, i*n vivo* studies performed on rat blood vessels showed increased apoptosis with Ang II infusion [232]. Furthermore, Yangxin Li *et al.* demonstrated that human VSMCs stimulated with Ang II had a reduction in their viability but not in their proliferation [229]. Moreover, *Lopez-Candales et al* compared cell density in 21 human abdominal aortic tissue samples from healthy individuals compared to AAA patients and reported cell density was decreased in AAA tissues compared to control samples due to heightened VSMC apoptosis [233]. It is therefore most likely that the medial cell depletion observed within treated arteries in the *ex vivo* aneurysm model is specifically due to apoptosis. Nevertheless, to confirm this postulation, further investigation by Western blotting alongside immunohistochemistry for an apoptotic marker such a cleaved caspase-3 would be necessary.

3.5.5 Extracellular matrix proteins and MMPs

The architecture of the blood vessel wall is of primary importance for the stability of blood vessels during physiological and pathophysiological conditions (such as cardiovascular diseases) and is maintained through the deposition of structural extracellular matrix proteins, principally collagens and elastin within the aorta [234]. Elastin is an important structural protein of the aorta, responsible for stability and elasticity of the aortic wall, and therefore elastin loss is linked to vessel wall instability and aneurysm formation [46]. Validating the *ex vivo* model of aneurysm, a sizeable reduction in umbilical cord artery elastin content was observed with Ang II infusion and associated with decreased medial thickness. Similarly, a substantial reduction in the collagen content was also observed after Ang II infusion, suggesting increased collagen turnover in response to the Ang II stimulation.

Excessive and dysregulated degradation of the ECM is linked to the formation and progression of multiple cardiovascular diseases including atherosclerosis and aneurysms [148]. Evidence obtained from human pathological studies and those utilising well-established mouse models

of aneurysms, have demonstrated a major role for MMPs in the pathogenesis of aortic aneurysms [235] [127]. Additionally, MMPs have been shown to drive the remodelling processes involved in coronary and carotid atherosclerosis, and restenosis subsequent to clinical interventions including coronary artery bypass grafting and stent deployment [236]. A closer examination of the substrates of the MMP family member's reveals that many of them can target collagens and elastin, implying their active role in the changes in collagen and elastin content observed within the Ang II-infused umbilical cord artery samples, or in response to running untreated artery segments within the *ex vivo* bio-reactor system.

3.5.5.1 MMP-3

MMP-3 protein expression was down-regulated in human umbilical cord artery segments after running within a bio-reactor for 72 hours compared to baseline segments, whereas Ang II infusion had no effect, suggesting haemodynamic alterations were responsible for altered MMP-3 levels. The expression of MMP-3 has been assessed in many cardiovascular diseases [237]. MMP-3 belongs to the stromelysin family of MMPs and can activate others MMPs including MMP-9 during VSMC behavioural changes [238], suggesting MMP-3 plays a central role in tissue remodelling [239]. Studies focusing on the role of MMP-3 in AAA have shown that MMP-3 expression was increased in 36 aneurysmal arteries from patients presenting with several cardiovascular risk factors compared to mammary arteries used as a control [240]. Following, Newman *et al.* demonstrated increased MMP-3 and MMP-9 levels in aortic segments from patients with aneurysms supporting their role in ECM destruction and AAA formation [171]. Additionally, in another study the expression of MMP-3 was found increased in AAA wall [241]. Another study assessed blood levels of MMP-3 in AAA patients elected for either endovascular grafting or open surgical repair and revealed MMP-3 plasma levels were higher in both groups of AAA patient compared to healthy individuals. Interestingly, MMP-3 levels significantly decreased after endovascular grafting or open surgical repair [242]. Finally, assessment of MMP-3 expression within infra-renal aortic biopsies from patient undergoing aneurysm repair demonstrated MMP-3 levels were significantly decreased in patients which also received statin-treatment, further validating a deleterious role for MMP-3 in AAA formation [243].

3.5.5.2 MMP-9

The results from the *ex vivo* model experiments demonstrated that the expression of MMP-9 in freshly isolated human umbilical arteries (baseline) is negligible but is markedly induced after 72 hours within the bio-reactor with or without Ang II infusion. In support of this finding Galis *et al*. showed that MMP-9 expression was low/absent in healthy arteries but was induced

within atherosclerotic arteries, inferring that MMP-9 is only induced during vascular remodelling, such as subjection to altered haemodynamics, and is therefore flow-sensitive [244]. Indeed, Richard Magid at el demonstrated elevated MMP-9 mRNA and protein expression in endothelial cells subjected to unidirectional flow at 15 dynes/cm^2 compared to static cells [245], in line with the observations within the *ex vivo* model of aneurysm. Future experiments to assess MMP-9 localisation within the umbilical cord arteries alongside determining the effects of altered haemodynamic flow on endothelial cell expression of MMP-9 would be informative in this respect. Another study within the rat model of TAA induced by $CaCl_2$ showed increased expression of MMP-9 in the $CaCl_2$ treated mice compared to untreated animals. This study was performed using immunohistochemistry for MMP-9 on rat aortic tissue sections [21].

3.5.5.3 MMP-10

MMP-10 protein expression was increased in the *ex vivo* model in response to Ang II infusion when compared to control untreated arteries. MMP-10 is also known as stromelysin-2 and has been afforded a role during wound repair and vascular remodelling [246]. As a member of the stromelysin sub-family of MMPs, MMP-10 shares structural similarity with MMP-3 [47], although they differ in their activation and tissue distribution and are therefore proposed to play differing roles. With regards to cardiovascular diseases, MMP-10 levels were found upregulated in human atherosclerotic plaques compared to healthy arteries, with increased endothelial cell MMP-10 expression particularly evident in atherosclerotic plaques [247]. Additionally, increased circulating levels of MMP-10 within 400 patients identified at cardiovascular risk were associated with accumulating number of atherosclerosis risk factors [240].

The role of MMP-10 had been tested by Krampert *et al*. using transgenic mice that were expressing a mutant MMP-10 in keratinocytes (which results in more MMP-10) and they showed a reduced deposition of new matrix and increased cell apoptosis in the wound healing epithelium [248]. These studies, together with my findings might suggest a prominent role of MMP-10 in AAA formation, although there are no published studies directly assessing the effect of MMP-10 modulation on aneurysm formation/progression. Therefore, more studies are required to elucidate the possible pro-aneurysmal role of MMP-10, and based upon my findings, the *ex vivo* model represents a robust test-bed for potential MMP-10 inhibitors before pre-clinical testing in animals.

3.5.5.4 MMP-12

MMP-12 is mainly expressed by macrophages and plays an active role in elastin degradation and proteolysis of other extracellular matrix proteins [47]. However, similar to the expression profile of MMP-9, MMP-12 protein levels are low in freshly isolated human umbilical arteries (baseline) but markedly induced after 72 hours within the bio-reactor with or without Ang II infusion. In support of these findings, MMP-9 and MMP-12 levels were found decreased after 1 week in the $CaCl_2$ induced mouse model of aneurysm [249]. Although, in the same study the expression of MMP-9 and MMP-12 was increased 4 and 8 weeks after $CaCl_2$ application [249]. Therefore, it is clear that MMP induction/expression can change over time during aneurysm formation and progression. However only one-time point (72 hours) was assessed within the *ex vivo* model of aneurysm, and perhaps if longer-term experiments were conducted a different pattern of MMP-12 expression may have been observed. There is also an absence of inflammatory cells within the *ex vivo* model and it is plausible the increased MMP-12 detected in the *in vivo* study and human samples was due to inflammatory cell (macrophage) accumulation. Indeed, MMP-12 has been shown to serve as a key factor in monocyte/macrophage invasion [160, 250] and macrophage MMP-12 expression is associated with the progression of atherosclerosis in mice and humans [160, 251-253]. Nonetheless, VSMCs have also been shown to express MMP-12 which can cleave non-matrix substrates (including N-cadherin) to alter VSMC behaviour [254]. Indeed, serum MMP-12 activity is increased in patients with aortic dissection (a VSMC-related pathology) compared to coronary artery disease patients [Yi Song 2013]. In contrary to the findings from the *ex vivo* model, several studies have demonstrated a detrimental role for MMP-12 in AAA formation. For instance, Longo *et al*. used the $CaCl_2$ mouse model of AAA in MMP-12 knock out (KO) mice and revealed that MMP-12 deficiency attenuated aneurysm development which was associated with reduced macrophage recruitment [179]. Additionally, it has been shown that MMP-12 activity is required for aneurysm development and rupture within the Ang II-infusion mouse model of AAA formation in normocholesterolemic C57BL/6 mice [79].

3.5.5.5 MMP-19

Similar to MMP-10, MMP-19 protein expression was increased in the *ex vivo* model in response to Ang II infusion when compared to control untreated arteries. MMP-19 together with MMP-20 are the most recently identified MMPs [255]. MMP-19 is a potent basement membrane-degrading enzyme which is highly expressed by endothelial cells, modulates their behaviour, and may play a role in tissue remodelling, but remains understudied in cardiovascular diseases [255]. Nonetheless, a study examining the expression of all MMP family members in aortic tissue samples from 109 patients identified a change in the

expression of only two MMPs: MMP-14 and MMP-19, which were therefore postulated to play a causal role in AAA development [212], supporting the findings presented within this chapter. Taken together, the published findings and the *ex vivo* model of aneurysm data warrant further studies into the role of MMP-19 in AAA formation and rupture.

3.5.6 Other mouse models of aneurysm formation

In addition to the $CaCl_2$ peri-vascular application and Ang II-infusion approaches tested in this thesis, another commonly used animal model of aneurysm development is the elastase-perfusion model [45]. Elastase was not considered as an inducer for the *ex vivo* model as a key molecular effector pathway of aneurysm generation is dysregulated proteolysis, including increased MMP expression/activity, which the elastase model would circumvent as elastase is a member of the protease family [256]. Accordingly, there are less publications employing the elastase-perfusion model compared to $CaCl_2$ application and Ang II infusion as regulation of proteolysis is usually a main area of interest within aneurysm studies. Taken together the results presented within this chapter demonstrate that the Ang II-infusion umbilical cord artery *ex vivo* model displays similar pathogenic characteristics of AAA formation and progression to current mouse models and the human pathology. Therefore, to further characterise and validate the model, assessment of therapeutic interventions shown effective in mouse models should be tested within the *ex vivo* model.

Chapter 4

4 Effects of aneurysm-inducers on vascular smooth muscle cell function in vitro

4.1 Introduction

4.1.1 A comparison of aortic and umbilical cord artery VSMCs

VSMCs are the predominant cell type within the wall of arterial vessels [51]. Under physiological conditions, VSMCs are the only cells present within the medial layer of the vessel wall. The vital function of VSMCs is to produce elastin, collagen and other extracellular matrix proteins which are important for the integrity of the vessel wall. In addition, VSMCs play a role in regulating vessel diameter and homeostasis through active contraction and relaxation [257]. The contractile machinery of a VSMC consists of two filaments, α-actin-2 (ACTA2) and myosin-11 (MYH11), specifically, VSMC contraction is regulated by the sliding of myosin along the actin filaments [258]. Actin filaments are connected to integrins through intermediate filament proteins such as α-actinin, talin, and filamin, which serve as a mechanotransduction complex linking the ECM to the actin cytoskeleton and contractile machinery [259]. In the same manner as the human aorta, the human umbilical cord represents a valid source of VSMCs which can be used to study biological mechanisms. Like other arteries, the human umbilical cord artery has an intima, media and adventitia. VSMCs are located within the medial layer and are involved in the control of vascular tone [260]. VSMCs have been shown to have similar growth rates and morphological characteristics to saphenous vein VSMCs, which are often used for experimental studies[261]. Together this evidence suggests that VSMCs from umbilical cord arteries could be a good source for AAA-related VSMC *in vitro* studies.

4.1.2 The effect of Ang II or $CaCl_2$ on VSMC

Ang II-infusion and $CaCl_2$ peri-vascular application and are widely used *in vivo* mouse models of aneurysm [130, 133]. To better interrogate cell signalling pathways involved in AAA, *in vitro* studies are required. Ang II is a hormone, part of the renin-angiotensin system which has been proposed to play an important role in the pathogenesis of AAA [262]. Ang II can regulate a

wide range of cellular functions including cell growth, apoptosis and migration, alongside modulating inflammatory responses and vascular remodelling [263]. Ang II interacts with two cognate receptors, type 1 AGTR1 and type 2 AGTR2 receptors, binding both receptors with high affinity [135, 136, 264]. Studies have revealed that Ang II can act as vasoconstrictor via interaction with AGTR1s which are widely distributed throughout the body. On the other hand, AGTR2 have a limited distribution pattern and are less well characterised, although their interaction with Ang II can induce vasodilatation and the receptor is implicated in cardiovascular function [263, 265, 266]. However, Daugherty *et al.* showed that blocking of AGTR1 in an *in vivo* mouse model of aneurysm reduced aneurysm formation. Surprisingly, the authors showed that blocking AGTR2 accelerated AAA development, suggesting a protective effect of this receptor in AAA formation [264]. Therefore, more studies are needed to better understand the role of these receptors in aneurysm development. Both receptors are members of the seven transmembrane G protein receptor (GPCR) family. Interaction between Ang II and AGTR1 can activate molecular pathways involved in VSMC remodelling, including the phospholipase C (PLC), phospholipase D (PLD) and phospholipase A_2 (PLA_2) signalling pathways [267]. These signalling pathways imply the activation of protein kinase C (PKC) and the ERK pathway [268, 269]. In addition, interaction between Ang II and AGTR1 can activate the NF-κB-IL-6 signalling pathway in VSMCs, subsequently increasing MMP production [135].

In addition, both receptors are known to activate a G protein signalling, but AGTR2 can activate three different pathways including activation and phosphorylation of protein phosphatases, regulation of the nitric oxide (NO)–cGMP system; and finally, stimulation of phospholipase A2 (PLA2) and release of arachidonic acid [270]. Ang II/AGTR2 interaction can also activate the TGF-β-Smad-2 signalling pathway AGTR2 directly leading to phosphorylation of Smad-2/-3 and its subsequent nuclear translocation and induction of MMP gene expression [139, 140].

Compared to Ang II, mechanistic insight into the pro-aneurysmal effects of $CaCl_2$ have been less well characterised. Addition of $CaCl_2$ to VSMCs has been show to increase apoptosis susceptibility [221], and increase the expression of select MMPs dysregulated during aneurysm formation [271]. In addition, a study showed decreased antioxidant enzyme activity, such as catalase activity, after $CaCl_2$ application that is linked to vessel wall damage and AAA formation[145]. A further possible mechanism of $CaCl_2$ includes the activation of c-Jun N-terminal kinase (JNK) and subsequent repression of genes involved in ECM biosynthesis such as members of the lysyl hydroxylase family. Additionally, JNK signalling is associated with increased expression of MMPs and inflammatory molecules, further implying a contribution to the disruption of the ECM within the vessel wall during aneurysm formation [272]. However,

further elucidation of the molecular mechanisms underlying these signalling pathways is important for the identification of novel therapeutic targets.

4.1.3 MMP expression in aneurysmal VSMCs

Damage to the vessel wall during pathological conditions principally affects VSMCs, commonly resulting in a shift of their phenotype from a contractile state to a synthetic form [55]. When synthetic, VSMCs increase their production of proteases including MMPs which are involved in degradation of ECM proteins, including elastin and collagen. [38, 53]. *Wang et al.* demonstrated Ang II induced a dose-response increase in human aortic smooth muscle cell MMP-2 expression [273]. Similarly, MMP-2 mRNA expression was found increased in murine VSMCs stimulated with Ang II [208]. Newman *et al.* demonstrated MMP-3 activated MMP-9 and both were increased in human aortic tissue from patients with aortic occlusive disease [171]. *In vivo,* mice receiving $CaCl_2$ application showed increased MMP-12 expression within the aneurysmal aorta [179]. MMP-10 belongs to the stromelysin family and is involved in the degradation of ECM proteins including collagen III, IV, V and fibronectin [274] and can activate other MMP family members [274], including MMP-9 and MMP-7, but not MMP-2 or MMP-3 [274].

In order to maintain proteolytic homeostasis, vascular cells including VSMCs secrete TIMPs, which are specific endogenous inhibitors of MMPs and include TIMP-1, TIMP-2, TIMP-3 and TIMP-4. Evidence suggests that an imbalance between MMPs and TIMPs is linked to aortic dilatation typical of AAA [275]. For example, TIMP-1 was found to be reduced in rat aortic VSMCs after treatment with Ang II [276], and TIMP-1 levels are reduced in aneurysmal tissue compared to healthy vessels [175]. Conversely, Lipp *et al.* found the expression of TIMP-3 to be increased in human aneurysmal tissue compared to controls, although this is proposed to be a compensatory response to combat increased MMP activity. Finally, the protein expression of TIMP-4 was significantly lower in aneurysmal aortic tissue and plasma of patients with bicuspid aortic valve disease compared to healthy controls [177].

4.1.4 Phenotype markers in aneurysmal VSMCs

As previously mentioned, VSMCs are characterised by phenotypic plasticity, being able to shift from a contractile state to a synthetic phenotype, frequently termed phenotypic modulation [52]. In a healthy blood vessel VSMCs are in a contractile phenotype with limited secretion of ECM proteins and abundant myofilament production to allow regulation of blood vessel diameter and blood flow. In response to pathological conditions such as tissue injury, VSMCs can switch their phenotype towards a synthetic form, associated with increased

protease production (such as MMPs), facilitating the degradation of ECM proteins including elastin and collagen [38]. Contractile VSMCs are usually elongated in shape and they have more contractile apparatus than synthetic organelles [54]. Synthetic VSMCs display a cobblestone morphology, and conversely have a high concentration of synthetic organelles and reduced number of contractile filaments [54]. Furthermore, synthetic VSMCs have a high rate of proliferation and migration compared to contractile VSMCs, in part related to increased MMP production which permits liberation from the restrictive cell-ECM and cell-cell contacts [277]. Commonly, the diversity of the two VSMCs phenotypes can be delineated by assessing the expression of VSMC phenotype-related marker genes. Contractile VSMCs express abundant levels of specific genes including alpha smooth muscle actin (αSM-actin), smooth muscle myosin heavy chains SM-1 (SMMHC11) and SM-2, calponin, caldesmon, transgelin (SM22α), and smoothelin [52]. Synthetic VSMC phenotype markers such as vimentin or tropomyosin-4 are less well-characterised and therefore not routinely used in published studies. Accordingly, loss of contractile VSMC markers after an injury are usually used at an indicator of a switch from a contractile state to a synthetic phenotype [52]. With regards to aneurysms, VSMC phenotypic modulation represents a critical step which promotes vascular remodelling and aneurysm formation [55].

4.2 Aim

The first aim of this chapter was to isolate and characterise VSMCs from human umbilical cord arteries in order to investigate the *in vitro* effects of Ang II and $CaCl_2$ on the expression of select MMPs and TIMPs in conjunction with VSMC phenotypic modulation. In addition, the second aim was to characterise VSMC phenotype markers in the *ex vivo* aneurysm model.

4.3 Results

4.3.1 Characterisation of VSMCs isolated from human umbilical cord arteries

To verify the efficiency of the explant model used in this study and therefore the purity of the arterial VSMCs isolated from human umbilical cord arteries, fluorescence ICC was performed using antibodies specific for either VSMC or EC marker proteins. Quantification of fluorescent images demonstrated that 99.3% of the isolated cells were labelled positive for α-smooth muscle actin (αSM actin), 89.7% for smooth muscle myosin heavy chain 11 (SMMHC11) and 98.7% for calmodulin (Figure 4.1). The use of an antibody directed to the endothelial marker VE-cadherin revealed that the isolated cells showed no positivity (Figure 4.1), strongly indicating that the isolated cells were VSMCs.

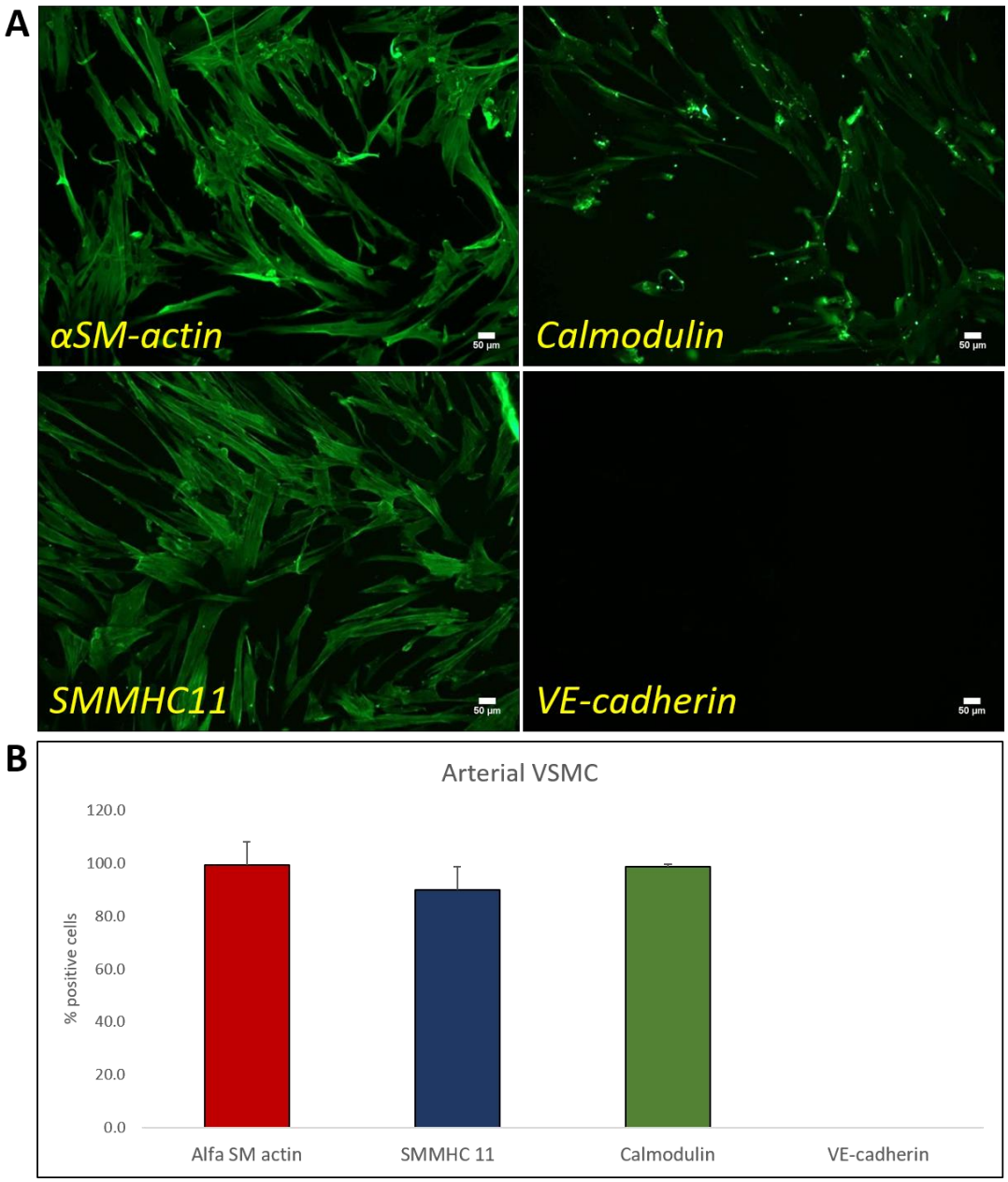

Figure 4.1: VSMC phenotype marker expression.

A: Representative images of ICC for VSMC phenotype markers
human umbilical cord artery VSMCs were subjected to fluorescence immunocytochemistry analysis for three phenotypic markers of VSMCs (αSM-actin, SMMHC 11 and calmodulin) and an endothelial cell marker (VE-cadherin) as a control.
B: Quantification of ICC for VSMC phenotype markers
Immunopositivity of the selected markers were counted within eight random x10 magnification fields and expressed as a percentage of positive nucleated cells. Data is presented as mean±SEM; n=4.

4.3.2 VMSC morphology

The findings within Chapter 3 showed that stimulation of human umbilical cord arteries with Ang II or $CaCl_2$ induced characteristics of aneurysm formation. Therefore, to determine whether Ang II or $CaCl_2$ affected VSMC morphology, human umbilical cord artery VSMCs were stimulated with these two experimental aneurysm inducers. As shown in Figure 4.2, human umbilical cord artery VSMC morphology was not affected by Ang II. However, $CaCl_2$ stimulation induced a marked change in cell shape and cells were inclined to form clumps (as shown in Figure 4.2).

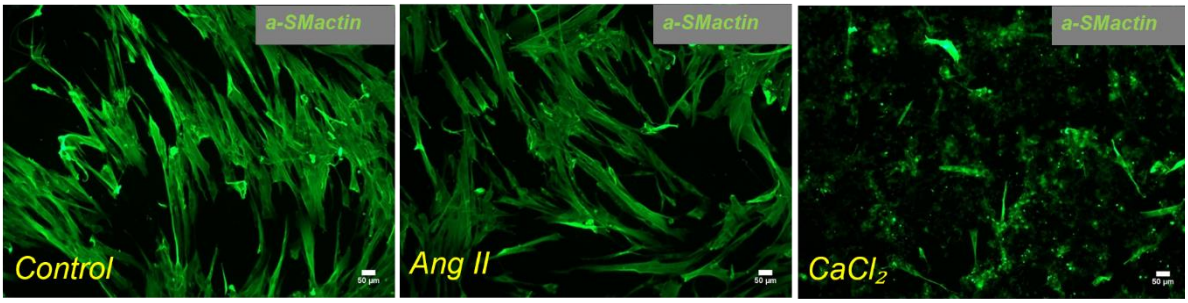

Figure 4.2: Human umbilical cord artery VSMC morphology in response to Ang II or CaCl2

Representative images of fluorescent ICC for αSM-actin (to assess cell morphology) on human umbilical cord artery VSMCs either untreated or treated with Ang II (5µM) or $CaCl_2$ (250mM) for 24h. Cells were visualised at x10 magnification.

4.3.3 VSMC senescence

To further investigate the effect of $CaCl_2$ on VSMCs, VSMCs from umbilical cord arteries were stimulated with different concentrations of $CaCl_2$ and the susceptibility to senescence was assessed. Cellular senescence was evaluated by measuring expression of β-galactosidase activity and the incidence of senescence was elevated in VSMCs treated for 15 minutes with $CaCl_2$. Additionally, augmented senescence was observed with increasing concentrations of $CaCl_2$ (as illustrated in Figure 4.3).

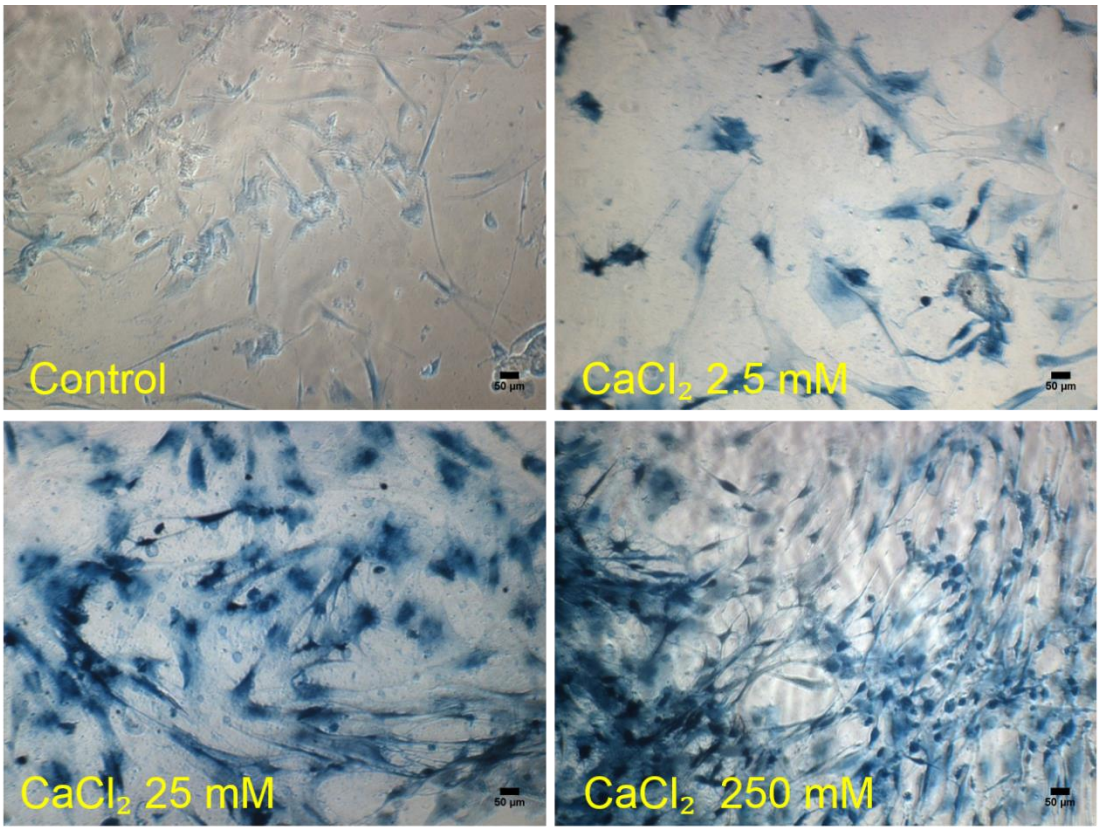

Figure 4.3: $CaCl_2$ induced senescence of human umbilical cord artery VSMCs

Representative images of histochemical staining for β-galactosidase activity (as a marker of cellular senescence) on human umbilical cord artery VSMCs treated with $CaCl_2$ at different concentrations (untreated, 2.5mM, 25mM and 250mM). Blue stained cells (senescent cells) were visualised at x10 magnification.

4.3.4 Effect of Ang II or $CaCl_2$ stimulation on human umbilical cord artery VSMC MMP and TIMP mRNA expression

Data presented within Chapter 3 revealed that human umbilical cord arteries stimulated *ex vivo* under flow with and without Ang II stimulation display differing expression patterns for the investigated MMPs. In order to examine effects explicitly on VSMCs, isolated human umbilical cord artery VSMCs were stimulated *in vitro* with Ang II (5μM) or $CaCl_2$ (250mM) in order to determine whether these aneurysm inducers affect the expression of select MMPs and TIMPs. As shown in Figure 4.4 MMP-2 mRNA expression was significantly up-regulated in human umbilical cord artery VSMCs treated with Ang II (1.5-fold; $P<0.05$; n=4), but unaffected by $CaCl_2$ treatment. Conversely, MMP-3 mRNA expression was significantly up-regulated in $CaCl_2$ stimulated VSMCs (4.3-fold; $P<0.05$; n=4; Figure 4.4) but not Ang II stimulation. MMP-10 mRNA expression was significantly up-regulated in VSMCs treated with either Ang II or $CaCl_2$ (3.0-fold & 5.2-fold respectively; $P<0.05$; n=4; Figure 4.4), whereas MMP-12 mRNA expression was significantly down-regulated in human umbilical cord arteries VSMCs treated with $CaCl_2$ (74%; $P<0.05$; n=4; Figure 4.4), but unaffected by Ang II stimulation. Lastly, MMP-14 and MMP-9 expression were not significantly altered by either treatment. With regards to TIMP expression, $CaCl_2$ treatment did not affect the mRNA expression of any TIMP investigated in human umbilical cord arteries VSMCs, while Ang II increased the mRNA expression of TIMP-1, TIMP-2 and TIMP-3 (1.8-fold, 1.5-fold and 1.3-fold; respectively; $P<0.05$; n=4; Figure 4.5) but not TIMP-4.

With regards to mRNA normalisation, the expression of two housekeeping genes was assessed, 36B4 and ELF1. Using a time response to Ang II stimulation at 6,12 and 24 hours, no significant change in mRNA expression of these genes was observed (Figure 4.6).

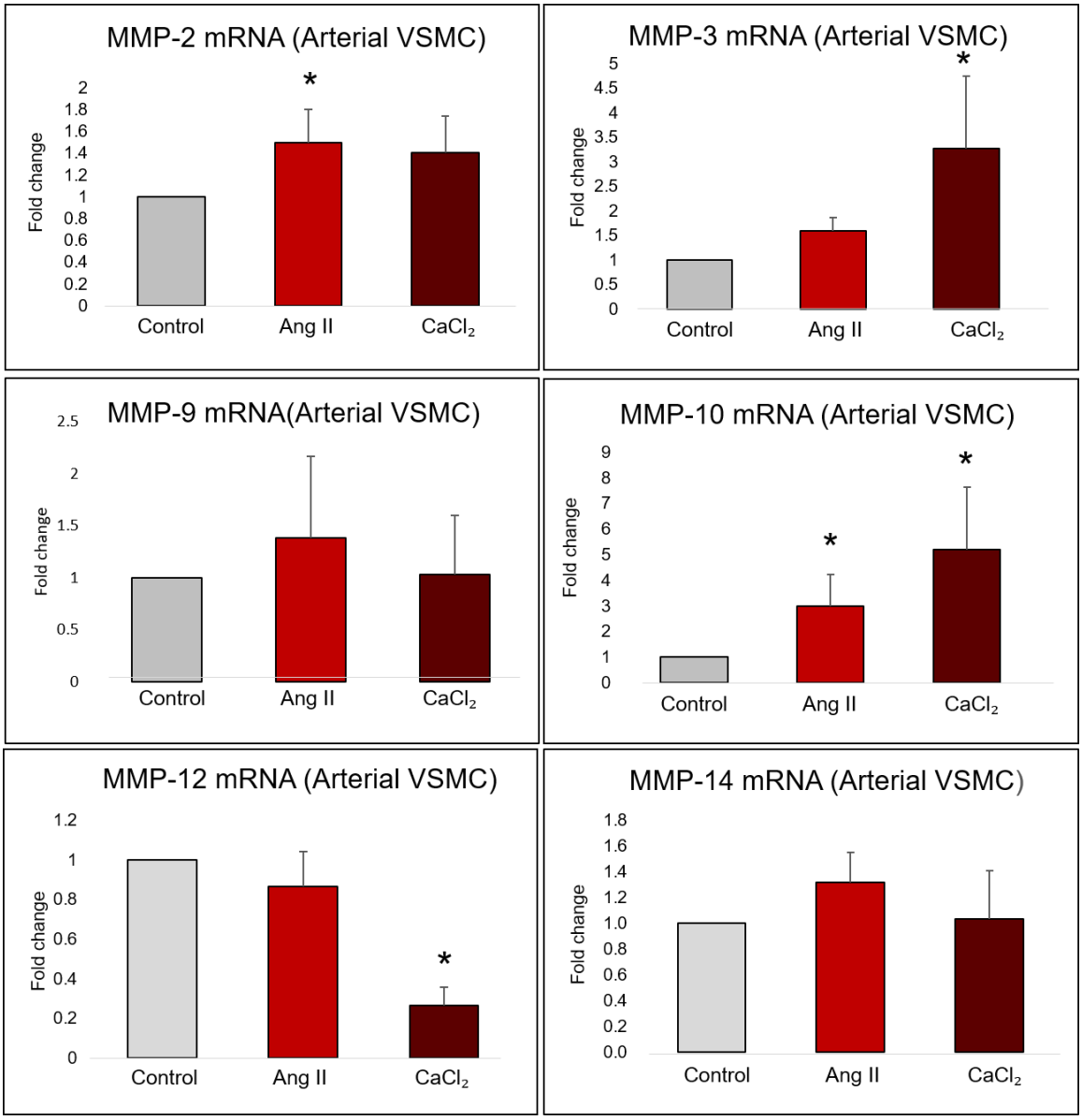

Figure 4.4: Effect of Ang II or $CaCl_2$ on mRNA expression of MMPs in human umbilical cord artery VSMCs

*RT-QPCR for MMP-2, MMP-3, MMP-9, MMP-10, MMP-12 and MMP-14 mRNA expression in human umbilical cord artery VSMCs treated with Ang II (5μM) or $CaCl_2$ (250mM). Data expressed as fold change (mean±SEM; n=5, * P<0.05 denotes significant difference from treated cells compared to control untreated cells).*

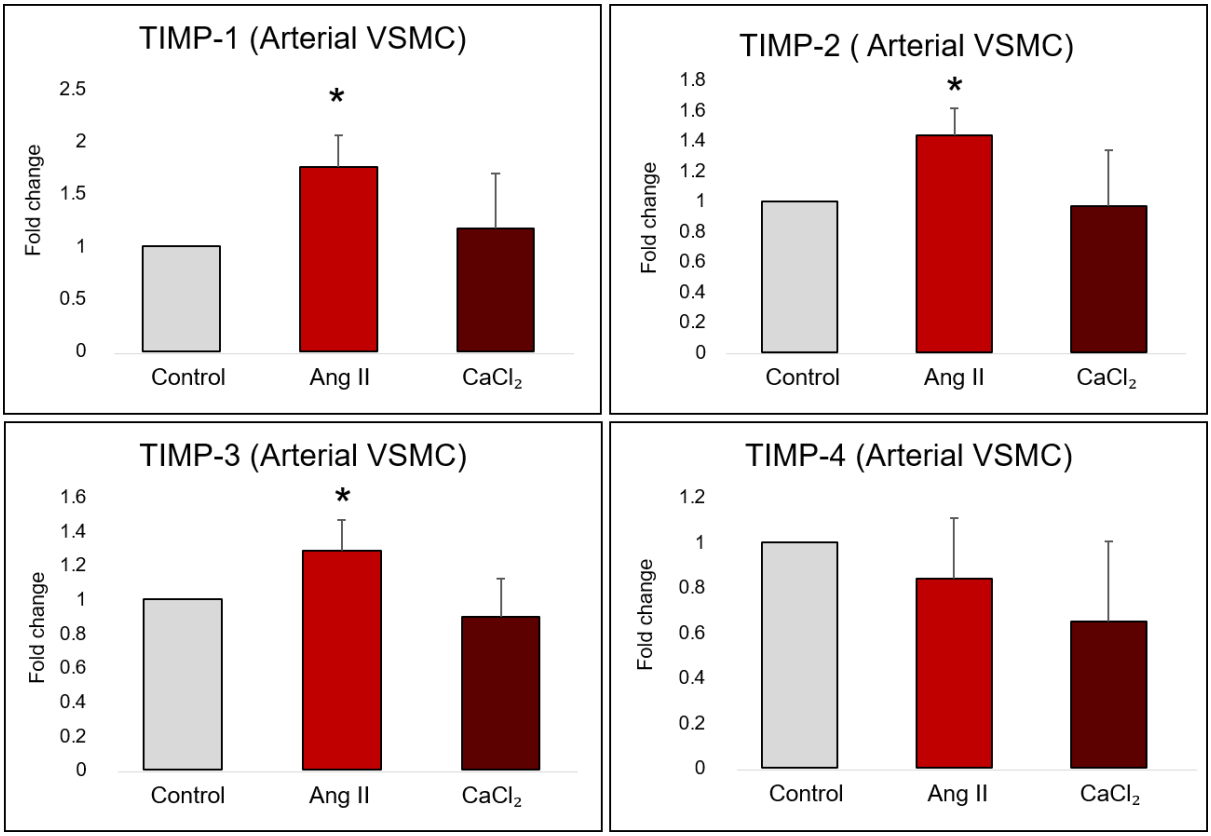

Figure 4.5: Effect of Ang II or $CaCl_2$ on mRNA expression of TIMPs in human umbilical cord artery VSMCs

*RT-QPCR for TIMP-1, TIMP-2, TIMP-3 and TIMP-4 mRNA expression in human umbilical cord artery VSMCs treated with Ang II (5μM) or $CaCl_2$ (250mM). Data expressed as fold change (mean±SEM; n=5, * P<0.05 denotes significant difference from treated cells compared to control untreated cells).*

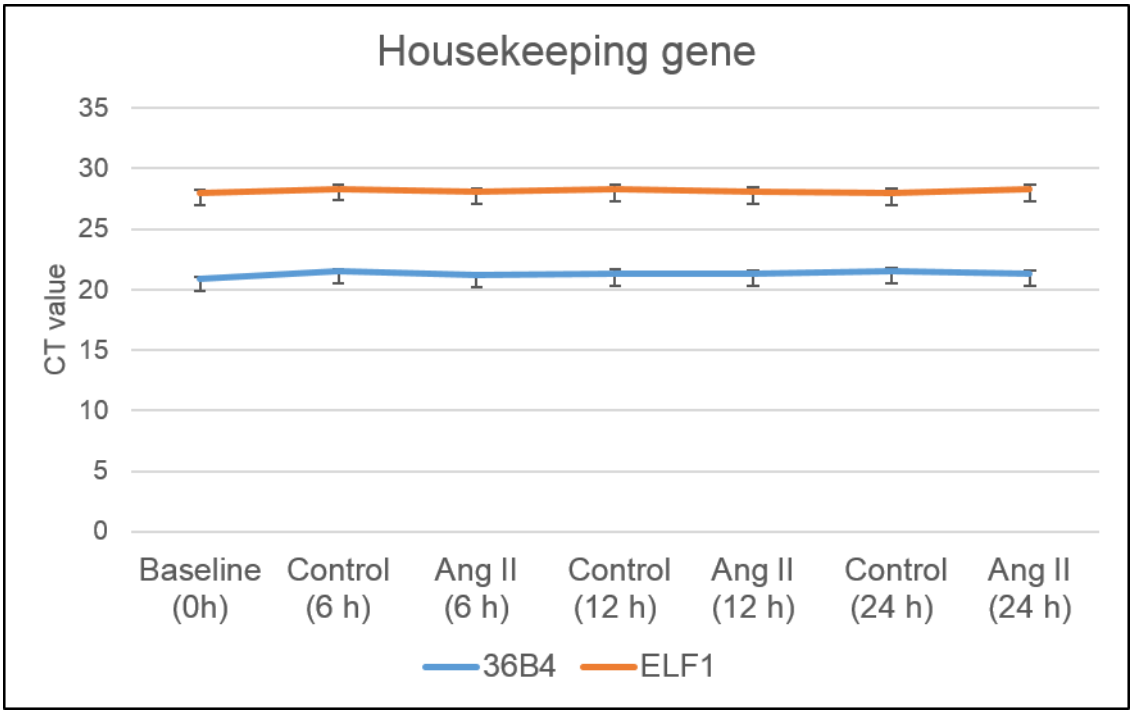

Figure 4.6: Effect of Ang II on mRNA expression of 36B4 and ELF1 in human umbilical cord artery VSMCs

RT-QPCR for mRNA expression of the two housekeeping genes 36B4 and ELF1 in human umbilical cord artery VSMCs treated with Ang II (5µM) or untreated VSMC (control) after 6 hours, 12 hours and 24 hours stimulation relative to baseline VSMCs (0 hours) Data expressed as CT value (mean±SEM; n=5).

4.3.5 Effect of Ang II or $CaCl_2$ stimulation on human umbilical cord artery VSMC MMP and TIMP protein expression

In order to validate the findings observed at the mRNA level, Western blotting was performed to assess MMP-2, MMP-3, MMP-10 and MMP-12 protein expression using human umbilical cord VSMC lysates. In all instances, a protein assay was performed to ensure equal loading. MMP-2 and MMP-12 protein expression was significantly increased in VSMCs stimulated with Ang II (2.5-fold & 2.6-fold respectively; $P<0.05$; n=4; Figure 4.7). Meanwhile, both Ang II and $CaCl_2$ stimulation induced a decrease in MMP-3 protein expression (Figure 4.7). Lastly, MMP-10 protein expression was decreased in response to $CaCl_2$ treatment but not affected with Ang II (Figure 4.7).

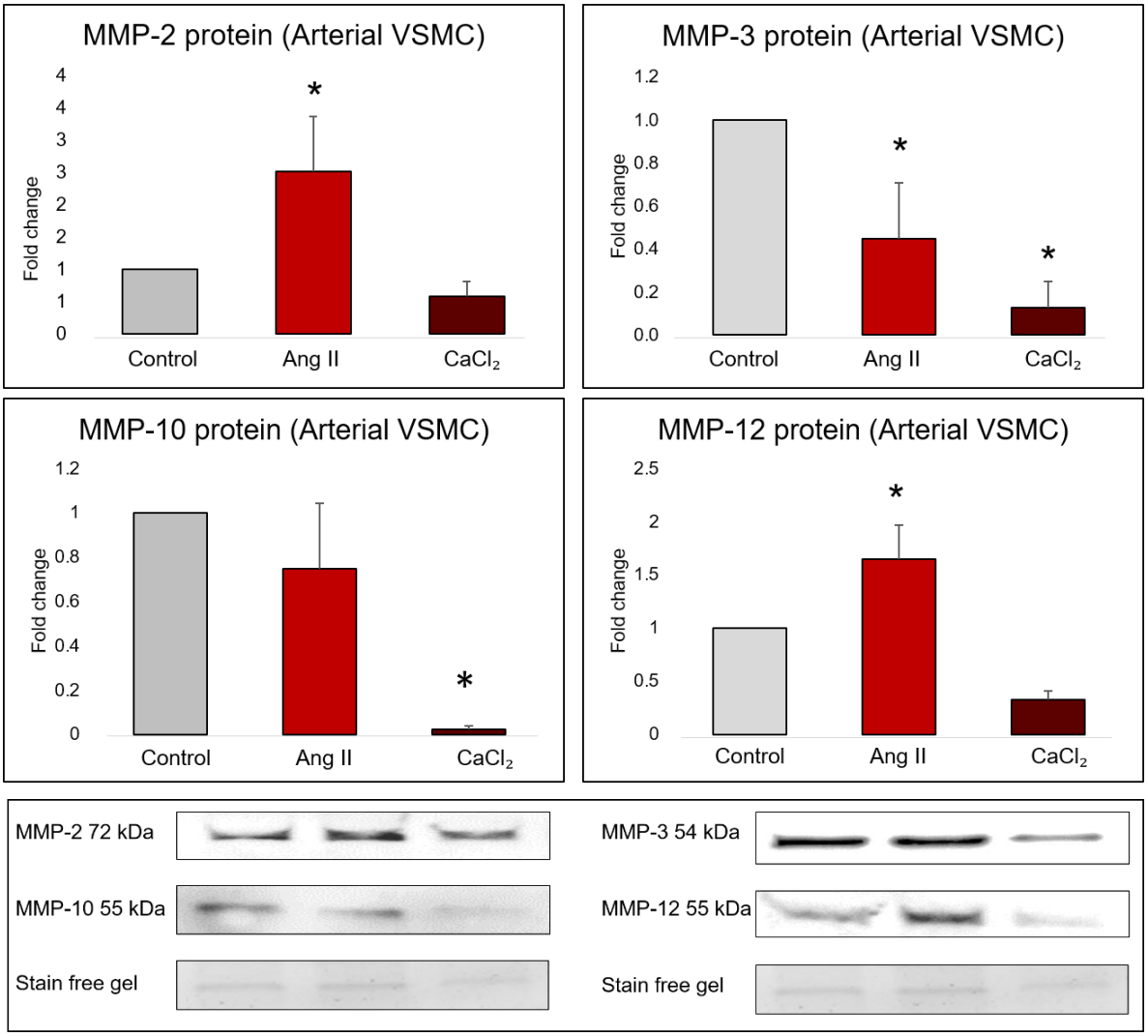

Figure 4.7: Effect of Ang II or $CaCl_2$ on MMP protein expression in human umbilical cord artery VSMCs

*Quantification and representative western blots for MMP-2, MMP-3, MMP-10 and MMP-12 expression in human umbilical cord artery VSMCs treated with Ang II (5µM) or $CaCl_2$ (250mM). Images from stain free gels are shown as loading controls. Data is expressed as a fold change against untreated control cells and * P<0.05 denotes significant difference from untreated control cells, (mean±SEM; n=4).*

4.3.6 Effect of Ang II or $CaCl_2$ stimulation on human umbilical cord artery VSMC phenotypic markers

VSMCs have the capability to change their phenotype (a process termed phenotypic modulation) in response to injury, transitioning from a contractile state to a synthetic phenotype [38]. Accordingly, human umbilical cord artery VSMCs were stimulated with Ang II (5μM) or $CaCl_2$ (250mM) to investigate changes in phenotype markers in response to these treatments. As shown in Figure 4.8 Ang II and $CaCl_2$ significantly decreased mRNA levels of the well-characterised contractile VSMC phenotypic markers αSM-actin, calmodulin, transgelin (TAGLN), alongside protein expression of SMMHC11 (P<0.05; n=4/5).

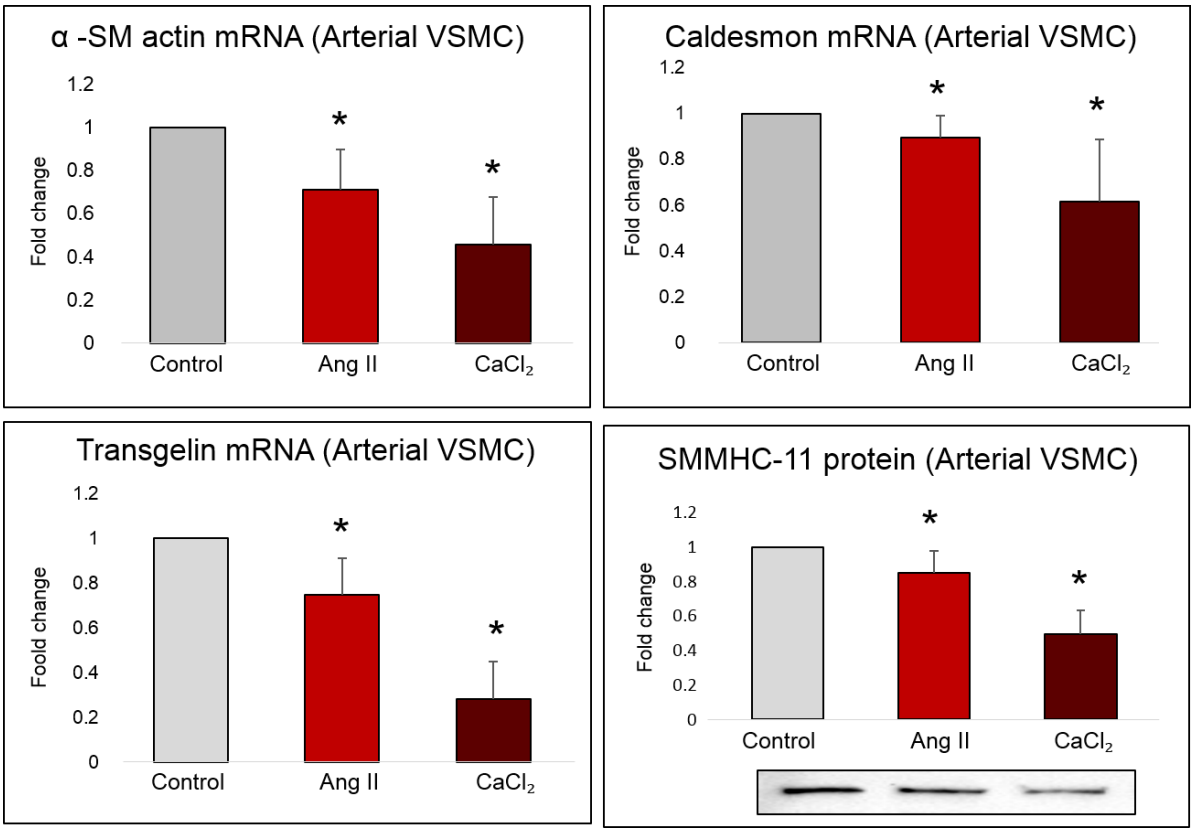

Figure 4.8: Effect of Ang II or $CaCl_2$ on VSMC phenotypic marker expression in human umbilical cord artery VSMCs

*RT-QPCR for ACTA2 (αSM-actin), CALM1 (calmodulin) and TAGLN (transgelin) mRNA expression in human umbilical cord artery VSMCs treated with Ang II (5μM) or $CaCl_2$ (250mM). Quantification and representative western blot for SMMHC11 protein expression in human umbilical cord artery VSMCs treated with Ang II (5μM) or $CaCl_2$ (250mM). Data is expressed as a fold change against untreated control cells and * P<0.05 denotes significant difference from untreated control cells, (mean±SEM; n=4).*

4.3.7 Validation of *in vitro* phenotypic modulation within the *ex vivo* aneurysm model

Evidence has implicated that the wall stress typical of aneurysm formation is linked with a transition in VSMC phenotype, shifting from a contractile state toward a synthetic phenotype [38, 278]. The data above demonstrates that administration of the aneurysm induces Ang II or $CaCl_2$ can individually decrease VSMC contractile marker expression in human umbilical cord VSMCs *in vitro*. In view of this, the effect of placing human umbilical cord arteries within a bio-reactor for 72 hours alongside administration of Ang II on the expression of select VSMC phenotype markers was assessed. As shown in Figure 4.9, subjection of human umbilical cord arteries to bio-reactor conditions for 72 hours significantly decreased calmodulin protein (70%; $P<0.05$; n=5), and transgelin protein expression (70%; $P<0.05$; n=5) compared to baseline artery segments (not placed within a bio-reactor). Whereas Ang II treatment did not further affect either calmodulin or transgelin protein expression (Figure 4.9). Conversely, the protein expression of αSM-actin and SMMHC11 within a bio-reactor for 72 hours did not change when compared to control arteries (Figure 4.10). However, a significant decrease in the expression of αSM-actin (30%; $P<0.05$; n=5) and SMMHC11 (50%; $P<0.05$; n=5) was observed in umbilical cord arteries exposed to Ang II relative to control arteries (Figure 4.10).

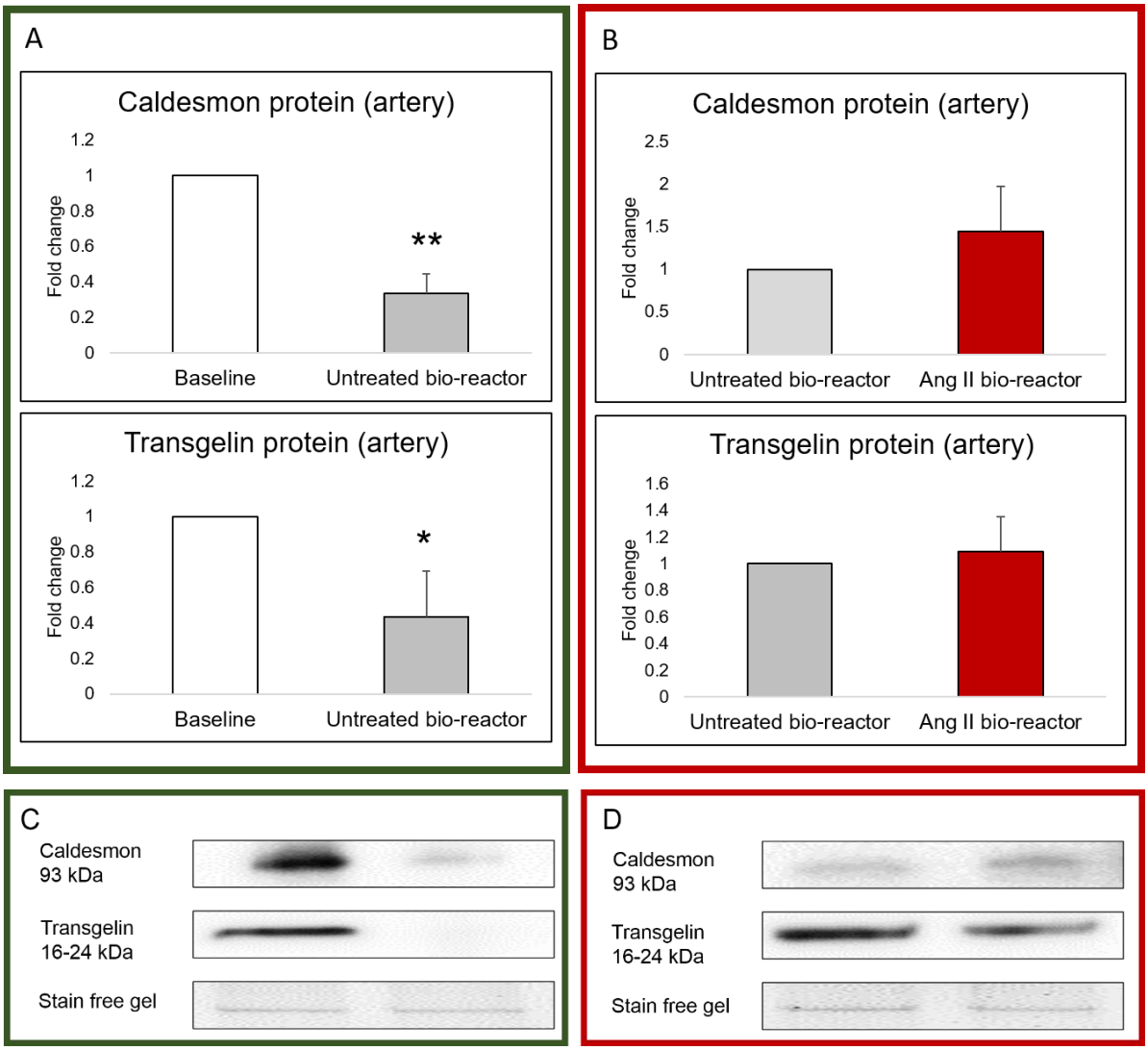

Figure 4.9: Effect of ex vivo flow and Ang II-infusion on human umbilical cord artery protein expression of the VSMC phenotypic markers caldesmon and transgelin

*Densitometric quantification (A and B) and representative western blots (C and D) for caldesmon and transgelin protein expression in human umbilical cord arteries before (baseline) and after insertion within a bio-reactor for 72 hours (A within green box), or without Ang II (untreated bio-reactor) and with Ang II-infusion (B, within red box). Data is expressed as a fold change against baseline (A) or against untreated bio-reactor vessels (B) (mean±SEM; n=5). * denotes p<0.05 and ** denotes p<0.01 versus untreated bio-reactor. Associated stain free gels are shown as a loading control.*

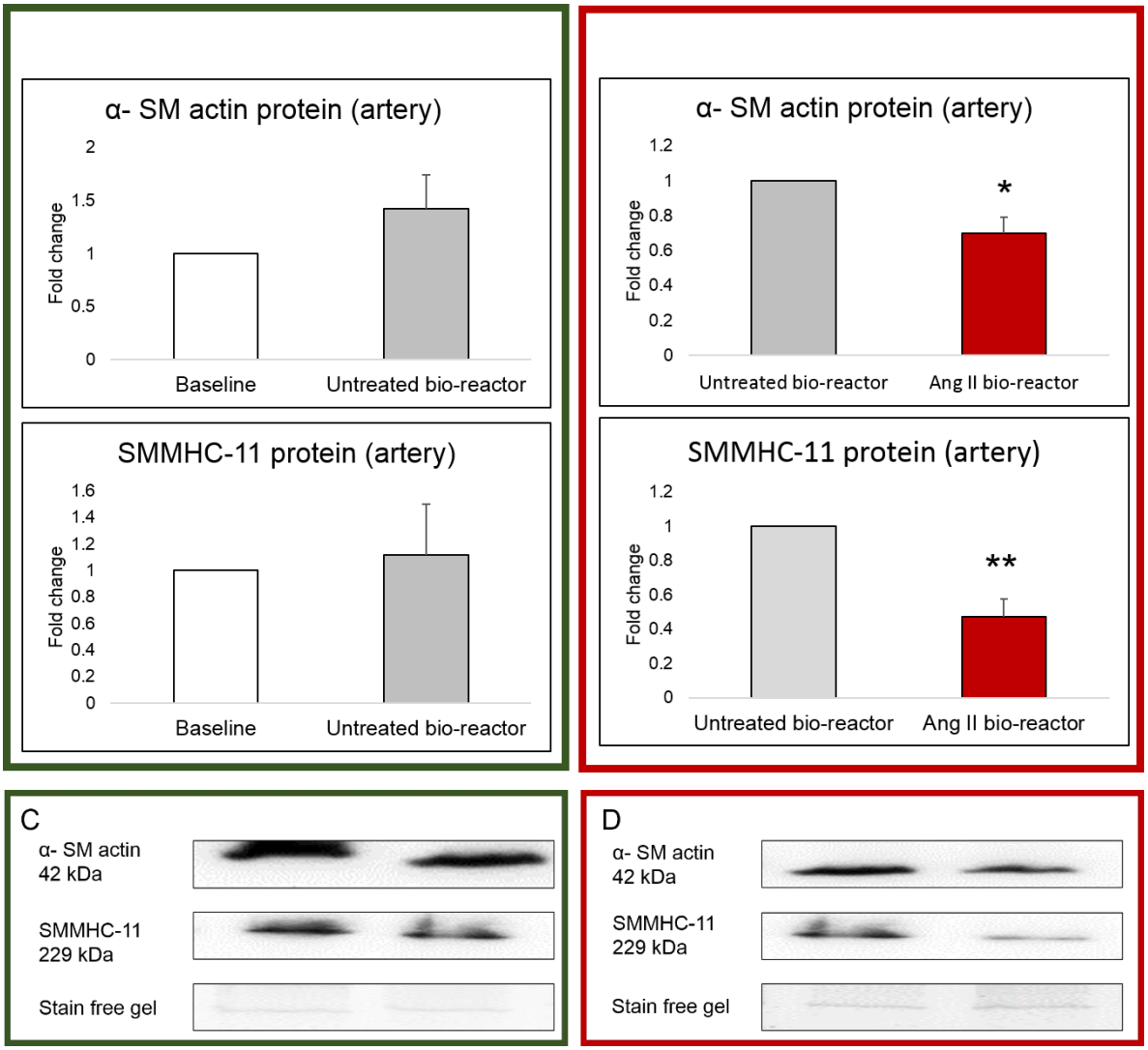

Figure 4.10: Effect of ex vivo flow and Ang II-infusion on human umbilical cord artery protein expression of the VSMC phenotypic markers αSM-actin and SMMHC11

*Densitometric quantification (A and B) and representative western blots (C and D) for αSM-actin and SMMHC11 protein expression in human umbilical cord arteries before (baseline) and after insertion within a bio-reactor for 72 hours (A within green box), or without Ang II-infusion (untreated bio-reactor) and with Ang II (B, within red box). Data is expressed as a fold change against baseline (A) or against untreated bio-reactor vessels (B) (mean±SEM; n=5). * denotes p<0.05 and ** denotes p<0.01 versus untreated bio-reactor. Associated stain free gels are shown as a loading control.*

4.4 Conclusion

The findings within this chapter demonstrate that pure VSMC preparations can be isolated from human umbilical cord arteries and that they share properties similar to those of VSMCs isolated from more commonly used conduits. As such, these observations show that the VSMCs within umbilical cord arteries, and therefore the arteries themselves, are not that far removed from vessels such as the aorta, supporting its use as a conduit within an *ex vivo* model of aneurysm for mechanistic studies and testing of potential therapeutics. Moreover, the abundant source of VSMCs within umbilical cord arteries alongside the relative ease with accessing such tissue (taking ethical permission into account), highlight such VSMCs as a viable replacement or addition to currently used VSMCs in cardiovascular research.

During the validative studies within this chapter and considering the similarities of the umbilical cord artery VSMCs to other arterial VSMCs, some novel findings were revealed. Firstly, divergent effects of Ang II stimulation on the mRNA and protein expression of several MMPs (MMPs-3, -10, and -12) were observed, suggesting involvement of a post-transcriptional regulatory mechanism such as microRNAs. There have been multiple reports of microRNAs fine tuning vascular cell MMP expression and activity, alongside regulating aspects of VSMC behaviour such as phenotypic modulation [279]. Secondly and in relation, an inferred bi-phasic effect on VSMC phenotypic modulation was revealed in umbilical cord arteries subjected to flow with and without Ang II-infusion. While expression of the contractile VSMC phenotypic markers transgelin and caldesmon were decreased in arteries after subjection to flow, infusion of Ang II was additionally required to induce suppression of αSM-actin and SMMHC11, transgelin and caldesmon, suggesting a shift towards a fully synthetic phenotype requires synergism between two complimentary pathways, such as cyclic stretch and Ang II signalling. The observed effects on the mRNA and protein expression of MMPs, TIMPs and contractile VSMC phenotype markers are summarised in the below tables (Table 4.1, Table 4.2 and Table 4.3). Collectively, aneurysm formation within the Ang II-infusion *ex vivo* model developed during this PhD, is characterised by VSMC phenotypic modulation alongside up-regulation of select MMPs, features commonly reported within the Ang II-infusion mouse model of aneurysm, and importantly human aortic aneurysms. Taken together, these findings support the applicability of the *ex vivo* model of aneurysm for future studies.

Table 4.1 Table summarising the QPCR and Western blotting data from human umbilical cord artery VSMCs

Red boxes indicate MMPs/TIMPs that were significantly increased whereas green boxes indicate decreased expression, following Ang II or $CaCl_2$ treatment compared to untreated VSMC. Grey boxes denote no change in mRNA/protein expression.

	Ang II	$CaCl_2$
MMP-2 (mRNA)		
MMP-3 (mRNA)		
MMP-9 (mRNA)		
MMP-10 (mRNA)		
MMP-12 (mRNA)		
MMP-14 (mRNA)		
TIMP-1 (mRNA)		
TIMP-2 (mRNA)		
TIMP-3 (mRNA)		
TIMP-4 (mRNA)		
MMP-2 (protein)		
MMP-3 (protein)		
MMP-10 (protein)		
MMP-12 (protein)		

No change in expression

Increased expression

Decreased expression

Table 4.2: Table summarising the QPCR and Western blotting data from human umbilical cord artery VSMCs (in vitro)

Green-filled boxes indicate decreased expression in human umbilical cord artery VSMCs following Ang II or $CaCl_2$ treatment in comparison to untreated VSMCs.

	Ang II	$CaCl_2$
α-SM actin		
SMMHC11		
Transgelin		
Caldesmon		

Decreased expression

Table 4.3:Table summarising the Western blotting data from human umbilical cord artery (ex vivo)

Green-filled boxes indicates decreased expression in untreated or Ang II-infused umbilical cord arteries after 72 hours within a bio-reactor relative to baseline tissues. Grey boxes denote no change in protein expression.

	Untreated bio-reactor	Ang II bio-reactor
αSM-actin		
SMMHC11		
Transgelin		
Caldesmon		

No change in expression

Decreased expression

4.5 Discussion

VSMCs isolated from mouse and human tissues are widely used for *in vitro* studies to understand molecular mechanisms behind AAA formation and rupture [176, 280]. In particular, elucidating the processes affecting VSMC phenotypic modulation and dysregulated proteolysis are commonly undertaken with relevance to aneurysms. The findings presented in Chapter 3 demonstrate marked changes in markers of contractile VSMCs and numerous MMPs within human umbilical cord arteries subjected to Ang II-infusion. To validate whether these observations are through direct effects on VSMCs, the current chapter examined whether $CaCl_2$ or Ang II treatment alters the expression of contractile VSMC phenotype markers and select MMPs in human umbilical cord artery VSMCs. In addition, although VSMCs isolated from mouse vessels and human arteries retrieved during surgery represent a valuable source of cells, such sources are not accessible to everybody due to the low availability of fresh human aortic tissue and the cost and ethical implications linked to experimental mouse models. As such, VSMCs isolated from human umbilical cord arteries, which is a waste tissue and is usually discarded, may overcome such limitations. Accordingly, having a plentiful supply of VSMCs from a waste tissue could represent an invaluable resource worldwide for researchers interested in VSMC biology. In order to validate whether cord artery VSMCs are suitable for *in vitro* studies, the function and behaviour of the VSMCs isolated from this tissue require assessment. As such, the results within this Chapter demonstrate that VSMC-pure preparations can be isolated from umbilical cord arteries as confirmed using three phenotype markers of VSMCs, including αSM-actin, calmodulin and SMMHC11, alongside exclusion of EC cell contamination as assessed by immunolabelling for the endothelial marker VE-cadherin, which was completely absent in all cell preparations. As such, VSMCs isolated from human umbilical cord arteries were considered a suitable test-bed for assessing the effect of Ang II or $CaCl_2$ treatment *in vitro* on VSMC expression profiles of proteins associated with aneurysmal characteristics, notably, changes in MMPs and TIMPs alongside VSMC phenotype markers.

4.5.1 VSMC morphology in response to Ang II or CaCl2

VSMCs are found within the medial layer of arteries and veins, and function to regulate vascular tone and blood pressure [281]. VSMCs are regularly isolated from arteries and veins for in vitro studies, especially the differing regions of the aorta, coronary and carotid arteries, the internal mammary artery, and the saphenous vein. However, there is scant information on the behaviour and function of VSMCs isolated from umbilical cord arteries. Accordingly, assessment of VSMCs isolated from human umbilical cord arteries revealed they exhibited an

elongated shape, the characteristic morphology for VSMCs. Indeed, previous evidence has shown the morphology of VSMCs isolated from vein and arteries and subjected to tissue culture attach to plastic surfaces (tissue culture flask for example) within two hours and their morphology transitions from rounded to spindle-shaped [282]. Furthermore, the ability of VSMCs to acquire an elongated spindle-shape allows them to be easily discernible from other potential contaminating cell types, such as endothelial cells [282]. In addition, VSMCs isolated from human umbilical cord artery have been described to display a similar elongated morphology as VSMCs isolated from other vascular beds [260].

In this chapter, VSMCs from umbilical cord arteries were treated with two different aneurysm inducers, Ang II and $CaCl_2$, exerting similar changes in the expression patterns of selected VSMC phenotypic markers but striking differences on cell morphology. Contrary to the findings in this chapter, human aortic smooth muscle cells treated with Ang II showed an increase in cell surface area, inferring a shift towards a synthetic and therefore more proliferative phenotype [283]. However, the researchers used VSMCs at a high passage (between passage 6 and 9) and were stimulated for 9 days with Ang II. Whereas in this thesis, low passage VSMCs were used (3 to 6 passage) and stimulated with Ang II for 24 hours only [283]. To my knowledge, the report by Kuma *et al.* is the only publication reporting the differing effect of Ang II on VSMC morphology.

In opposition to the morphology of untreated and Ang II-treated umbilical cord artery VSMCs, $CaCl_2$ stimulation encouraged VSMCs to form clumps, which could be indicative of nodular-type calcifications [284], and the $CaCl_2$-induced mouse model of AAA is characterised by marked medial calcification [133]. In support of this observation, a study using bovine aortic VSMCs stimulated to induce calcification through the use of media supplemented with calcium, displayed calcifying collagen fibrils and deposits of extracellular calcification adjacent to VSMCs typically nodular in morphology [285], similar to the nodular calcification observed within atherosclerotic plaques and aneurysms.

4.5.2 MMP mRNA and protein expression in response to Ang II or $CaCl_2$

A primary feature associated with aneurysm formation is an increase of proteases that degrade the ECM, in particular MMPs, that are involved in vascular remodelling and aneurysm formation. Previous studies have reported increase expression and activity of MMP-2 in human aortic VSMCs treated with Ang II [273], along with an increase of MMP-9 in rat aortic VSMCs [286]. Furthermore, increased levels of MMP-3 are linked to VSMC migration and

plaque stabilisation [287]. Interestingly, the expression of MMP-3 (which can activate MMP-9), is increased in VSMCs after vascular injury and precedes elevation in expression and activity of MMP-9 [160]. Similarly, in this chapter VSMC stimulation with Ang II increased MMP-2 mRNA and protein expression, whereas $CaCl_2$ had no effect. In support, divergent effects of Ang II and $CaCl_2$ on aneurysm formation in MMP-2 deficient mice have been reported [288]. While $CaCl_2$ application increased MMP-3 mRNA expression and Ang II treatment exerted no change, opposing both Ang II or $CaCl_2$ stimulation suppressed MMP-3 protein expression. This discord between MMP-3 mRNA and protein expression could suggest the involvement of a post-transcriptional mechanism, such as microRNA regulation, and warrants further investigation. MMP-9 mRNA expression was not affected by either Ang II or $CaCl_2$, therefore a change in protein expression was not investigated. As previously mentioned, MMP-9 can be activated by MMP-3 [289], therefore, although no change in protein expression was observed with the treatments, a difference in MMP-9 activity may be apparent given the change in MMP-3 levels. Unfortunately, MMP activity was not assessed in the current study but would be required in future studies to elucidate the contribution of VSMC-derived proteolysis to the aneurysm effects observed *in vitro* and within the *ex vivo* aneurysm model.

MMP-12, also called macrophage metalloelastase, was found increased in human AAA tissue compared to heathy tissue [172]. Similarly, in the current study, MMP-12 protein expression was increased in response to Ang II, but interestingly no increase was observed at the mRNA level. This again may suggest the involvement of a post-transcriptional mechanism and justifies further investigation. With regards to the expression of MMP-10, both Ang II and $CaCl_2$ treatment increased VSMC mRNA expression, whereas no effect or down-regulation was observed at the protein level, respectively. These findings once again suggest modification during mRNA processing of an MMP in VSMCs after stimulation with Ang II or $CaCl_2$. Indeed, future experiments to evaluate the effects of Ang II or $CaCl_2$ on microRNA regulation of VSMC MMP protein expression would be interesting. As microRNA processing relies on Dicer, knockdown or inhibition of Dicer in VSMCs and subsequent evaluation of MMP mRNA and protein expression would identify if this post-transcriptional pathway indeed regulates VSMC MMP levels in response to aneurysm inducers. Previously, MMP-10 mRNA level was found increased in macrophages and this had been linked to ECM remodelling [290], similar in my experiment MMP-10 mRNA level were found increased in VSMC and possible responsible of vascular remodelling too. Finally, MMP-14 expression was not affected by either Ang II or $CaCl_2$ treatment. MMP-14 is a membrane type MMP (MT1-MMP) and activated intracellularly by furin before translocation to the cell-surface. In the $CaCl_2$ peri-adventitial application mouse model of AAA, MMP-14 expression was increased in TAA compared to control animals, but

this change was significant only at 2 weeks and not at 4, 8 and 16 weeks [291]. However, in this thesis, only one-time point (24 hours) was assessed *in vitro*, and perhaps longer- or shorter-term experiments could be conducted to discern if a different pattern of MMP-14 expression is observed.

4.5.3 TIMPs mRNA and protein expression in response to Ang II or $CaCl_2$

TIMPs serve as endogenous inhibitors of MMPs to maintain proteolytic homeostasis, and therefore play a pivotal role in regulating ECM degradation. Under cell-free conditions, the TIMPs have been proposed to harbour the ability to inhibit all MMP family members, however the efficacy of inhibition differs between the TIMPs [154]. Notably, TIMP-1 is more efficient at inhibiting MMP-14, MMP-16, MMP-19 and MMP-24, whereas TIMP-1 and TIMP-3 preferentially retard MMP-9 activity whereas TIMP-2, TIMP-3 and TIMP-4 favour MMP-2 inhibition [60].

An imbalance of expression between MMPs and TIMPs has been linked to dilatation of the aortic wall, typifying AAA formation and progression [275]. Previous studies have shown that TIMP-2 mRNA expression was increased in AAA tissue compared to control non-diseased vessels, whereas no change in TIMP-1 mRNA was detected [167]. Moreover, the increased expression of TIMP-1, TIMP-2 and TIMP-3 in cord artery VSMCs in response to Ang II stimulation may represent a compensatory feedback response to counter heightened MMP activity. Indeed, Lipp *et al.* found increased TIMP-3 expression in AAA patients, proposed as a feedback response to increased MMP activity [175]. Furthermore, mouse studies in both the Ang II and $CaCl_2$ aneurysm models have demonstrated a protective role for TIMP-3 [185, 186]. Finally, umbilical cord artery VSMC TIMP-4 mRNA expression was unaffected by Ang II or $CaCl_2$ stimulation, although the expression of TIMP-4 protein was found significantly reduced in aneurysmal aortic tissue and plasma of patients with bicuspid aortic valve disease compared to healthy controls [177].

4.5.4 VSMC phenotype marker in response to Ang II or $CaCl_2$

VSMCs within the medial layer of the blood vessel wall can transition between contractile and synthetic phenotypes. Their diversity can be characterised by changes in their appearance and function, including differing morphology, expression of phenotype markers, and altered migration and proliferation capacities. The phenotypic modulation of VSMCs has been proposed to be an early event during the formation of aortic aneurysms, associated with a loss

in the expression of contractile VSMC marker genes/proteins [38]. Accordingly, a principle aim of this chapter was to assess the effects of Ang II or $CaCl_2$ stimulation on human umbilical cord artery VSMC phenotypic modulation.

Multiple lines of evidence support a role for VSMC plasticity and phenotypic modulation in vascular diseases, including aneurysms [51]. Specifically, Fang *et al.* demonstrated rat VSMCs stimulated with Ang II for 48-72 hours showed decreased mRNA and protein expression of αSM-actin, calponin and SM22α decreased compared to untreated cells, suggesting Ang II promoted VSMC phenotypic switching [292]. Interestingly, vascular calcification had been linked to a reduction in contractile VSMC markers including SM22α and αSM-actin alongside increased expression of osteochondrogenic markers including osteopontin and osteocalcin. [293]. Additionally, intracellular calcium accumulation is associated with VSMC phenotypic modulation [294]. With further relevance to this chapter, VSMC phenotypic modulation correlates with heightened proteolysis through the increased production and activity of MMPs [51].

The findings within this chapter demonstrate that umbilical cord artery VSMCs harbour the ability to switch their phenotype from a contractile state to a synthetic phenotype in response to Ang II or $CaCl_2$. The *in vitro* studies presented within show either treatment significantly decreased mRNA and protein expression of the well-characterised contractile VSMC phenotypic markers αSM-actin, calmodulin, transgelin, and SMMHC11. Accordingly, VSMCs isolated from umbilical cord arteries behave similarly to VSMCs from other vascular beds used for aneurysm studies, supporting their relevance and applicability for aneurysm studies. The *in vitro* studies presented within show either treatment significantly decreased mRNA and protein expression of the well-characterised contractile VSMC phenotypic markers αSM-actin, calmodulin, transgelin, and SMMHC11.

To confirm the *in vitro* observations in isolated VSMCs translate into intact tissues, the expression of VSMC phenotype markers within the *ex vivo* aneurysm model was also investigated. Similar to the *in vitro* findings, the expression of αSM-actin and SMMHC11 were downregulated in umbilical cord arteries in response to Ang II within the bio-reactor compared to untreated vessels, wherea subjection to flow alone did not affect their expression. On the contrary, running arteries within the bio-reactor alone down-regulated the expression of caldesmon and transgelin compared to baseline vessels, but Ang II stimulation did not further alter the expression of both markers. These findings imply that (using the markers employed in the current study) full VSMC phenotypic modulation is bi-phasic in nature. While subjection of umbilical cord arteries to flow and therefore cyclic strain/stretch is sufficient to down-regulate caldesmon and transgelin expression, a further stimulus such as Ang II in the current study,

is necessary to additionally suppress αSM-actin and SMMHC11 levels and permit VSMCs to fully commit to phenotype switching. Such synergistic effects of divergent pathways have previously been shown to be required for VSMC phenotypic modulation [51]. Once again, the time-point that used in this study to look at the expression of these phenotype marker was 72 hours, however earlier time points of combined exposure to flow and Ang II would permit interrogation of the above hypothesis. In addition, it would be interesting to assess whether such a bi-phasic response as reported above takes place in other arterial and venous conduits. Finally, ancillary *in vitro* studies would be useful to further elucidate if a synergistic effect of stretch and Ang II are required for contractile VSMCs to transition to a fully differentiated synthetic state.

Chapter 5

5 Effects of aneurysm-inducers on endothelial cell function *in vitro*

5.7 Introduction

Endothelial cells (ECs) are form the inner layer of the blood vessel, organised in a thin, single layer upon the internal elastic lamellae [295]. Electron microscopy studies revealed that the endothelium lining blood vessels is a continuous layer without channels through the cytoplasm [296]. The main function of ECs is to control the passage of metabolites and secretory products from the circulation through the blood vessel surface, therefore providing a barrier function [297]. Additionally, ECs regulate leukocytes passage through the endothelial barrier, and are therefore important modulator of immune responses [298]. The endothelium has the capacity to respond to different stimuli such as shear stress to increase nitric oxide (NO) production and therefore induce dilatation, or other factors including pressure, medication or temperature. ECs interact with other cells using two different types of adhesion junction called adherens and tight junctions. Adherens junctions are mainly responsible for maintaining cell-cell adhesion, remodelling of the actin cytoskeleton along with intracellular signalling. Whereas tight junctions are involved in the role of barrier function and regulate permeability [67]. VE-cadherin represents a specific endothelial cell adhesion molecule within adherens junctions, and plays a central role in cell-cell contact [299].

5.7.1 Endothelial cell dysfunction in aneurysms

Many studies have focused on the role of Ang II on VSMC function, suggesting that VSMCs harbour abundant Ang II receptor expression and are therefore the primary cell type responsible for the Ang II-mediated effects within the aortic wall during aneurysm formation. However, Rateri *et al.* showed that EC-specific deficiency of AGT1R protected Ldlr-deficient mice from Ang II-induced aortic aneurysm formation, whereas VSMC or bone-marrow-specific deficiency of AGT1R had no effect on AAA formation [63]. In addition, Franck *et al.* showed that administration of exogenous ECs in a rat xenograft model of aneurysm, reduced AAA formation and progression, due mainly to the ability of the transplanted ECs to re-establish and endothelial lining, reduce proteolysis and promote ECM deposition and VSMC growth

within the aortic wall [300]. These studies suggest a principal means of Ang II inducing aneurysm formation is through direct effects on ECs.

Alongside VSMCs, EC dysfunction has been linked to numerous cardiovascular diseases, and in particular to the pathogenesis of aneurysm [301]. Previous studies using HUVECs have shown Ang II can induce increased apoptosis, mediated through the caspase cascade, and that nitric oxide (NO) production exerts a protective role during this mechanism in order to maintain a balance, which is important during an injury response [302]. An imbalance in NO production/consumption can lead to dysfunctional endothelium and therefore damage of the endothelial layer [301]. Additionally, it has been shown that Ang II increases the production of reactive oxygen species can sequester NO, and is linked to EC dysfunction and cardiovascular disease [227]. Moreover, Ang II-induced endothelial dysfunction is also associated with hypertension during aneurysm formation, as demonstrated in a male Sprague-Dawley rat model of aneurysm [303]. Additionally, administration of the Ang II receptor antagonist losartan can reduce vascular relaxation and associated hypertension [303]. Published studies show that VE-cadherin is important for restricting EC permeability, and in response to vascular injury and EC damage the pattern of VE-cadherin expression is altered, resulting in increased permeability [304]. Furthermore, it has been shown that the phosphorylation of VE-cadherin (observed within areas of low/disturbed shear stress) can increase its internalization and subsequently increase vessel permeability [305].

Vascular endothelial permeability is also increased in HUVECs stimulated with Ang II [306], therefore assessing the effect of Ang II on umbilical cord artery EC VE-cadherin expression *ex vivo* and *in vitro*, are pertinent to this thesis. VE-cadherin is a specific endothelial marker that belongs to the super-family of cadherins which play key roles in maintaining cell junctions. Briefly, within ECs VE-cadherin binds molecules such as β- and p120-catenins (through its cytosolic tail), which are linked to the actin cytoskeleton through molecules such as α-catenin, vinculin, and epilin. [307]. Members of Wnt family can bind to cell-surface molecules termed frizzled (Fzd) receptors to modulate canonical β-catenin signalling, a potent transcription factor. Wnt ligation of Fzd results in inactivation of the β-catenin destruction complex and permits nuclear accumulation of β-catenin. Conversely, in the absence of Wnts, β-catenin becomes bound to a destruction complex and is phosphorylated, and subsequently processed for proteasomal degradation [308].

5.7.2 EC behaviour in an *in vitro* aneurysm model

AAA are characterised as focal dilatations of the aorta wall, that create a typical aneurysmal balloon like shape [309]. Hemodynamic factors including pressure, shear stress and disturbed blood flow velocity are associated with vascular pathologies, and in particular can influence aneurysm growth rate [310]. Consequently, it is important to consider these factors when attempting to simulate experimental aneurysm formation. The *ex vivo* aneurysmal model using human umbilical cord arteries described within this thesis, are subjected to pulsatile, laminar flow at 6.5 dynes/cm^2 in order to closely mimic *in vivo* conditions. However, to replicate similar conditions within an *in vitro* system is more challenging. Nonetheless, Tucker *et al.* used a six well plate on a rocker in order to reproduce an *in vitro* model of shear stress mechanotransduction. They demonstrated symmetrical fluid behaviour during each cycle and a peak of shear stress on the wall edge but overall stationary shear stress at certain value [311]. Darvik *et al.* compared laminar shear stress to orbital shear stress on EC behaviour, revealing that orbital shear stress increased cell proliferation and apoptosis compared to laminar flow. Additionally, only cells at the edge were aligned to the flow but not those within the middle [312]. Therefore, an easily reproducible and simple approach has been deployed within this chapter, using a laboratory rocker as a model of mechanotransduction to reproduce *in vitro* laminar flow compared to cells under static conditions. As described in section 2.1.2.11, glass chamber slides were pre-treated with collagen to facilitate EC adherence. The day after cells are treated with Ang II +/- inhibitors (Figure 5.1B), and consequently placed on a rocker (Figure 5.1A) for 24 or 72 hours. Due to the back-and-forth motion of the rocker, each chamber is subjected to unidirectional laminar flow (Figure 5.1C), which represents the parallel movement of liquid without turbulence. Each well is subjected to laminar flow within the middle part and oscillatory flow at the marginal sides, therefore only cells within the central part of the well (Figure 5.1D) are used for further analysis. Within this chapter, HUVECs were untreated, treated with Ang II alone, or Ang II in combination with eitherTIMP-3 or losartan, and subjected to laminar flow.

5.7.3 TIMP-3

TIMP-3 belongs to the tissue inhibitor of metalloproteinases family, with their main function to block the catalytic domain of MMPs and therefore retard their activity [50]. Our group showed that the expression of TIMP-3, which can be targeted and therefore down-regulated by the microRNA miR-181b, was downregulated in the Ang II-infusion mouse model of AAA formation and rupture. Furthermore, genetic ablation of TIMP-3 accelerated aneurysm formation, while restoring TIMP-3 expression through administration of a miR-181b inhibitor in Ang II-infused

Apoe-deficient mice reduced aortic aneurysm formation and progression [186]. Zhai *et al.* isolated VSMCs from aneurysms retrieved from a rabbit AAA model to investigate the potential beneficial effect of TIMP-3. The authors showed that TIMP-3 was able to reduce VSMC proliferation and migration alongside reduced MMP-2 and MMP-9 expression [313]. Additionally, Basu *et al.* reported reduced elastin content alongside disorganised collagen structure in TIMP-3 deficient mice compared to wild-type control mice, in response to Ang II-infusion [185]. In summary, TIMP-3 exerts a potential protective effect on aneurysms, although if the beneficial effects are in part through modulation of EC function or behaviour are yet to be fully elucidated.

5.7.4 Losartan

The renin-angiotensin system (RAS) had been implicated in the pathogenesis of cardiovascular diseases [314]. Hyperactivation of the RAS system within blood vessels results in increased Ang II concentration and can therefore induce aneurysm formation and atherosclerosis [130]. Losartan is a potent Ang II receptor inhibitor and is currently used clinically to treat hypertension [80]. Moreover, losartan administration retarded aortic dilatation and elastin fragmentation in a mouse model of Marfan syndrome, compared to control animals [80]. Additionally, Daughtery *et al.* demonstrated that losartan was able to inhibit AAA formation in the Ang II-induced mouse model [130]. Together these studies demonstrate the effectiveness of losartan to block Ang II signalling and subsequent aneurysm formation, supporting its use as a robust tool for testing the efficacy of novel models of aneurysm. Moreover, further elucidation of its effects in an *ex vivo* setting may aid the discovery and development of novel therapies for AAA progression, particularly with regards to targeting ECs.

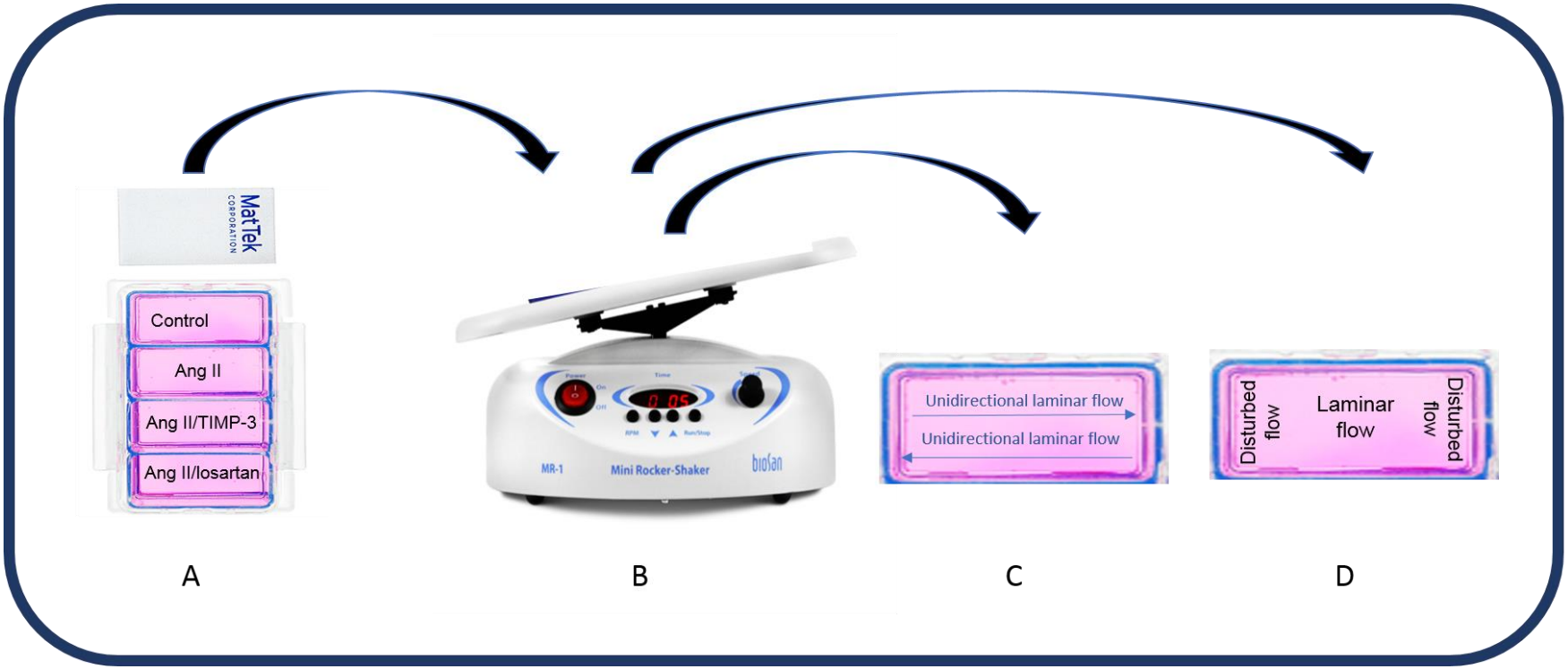

Figure 5.1: In vitro aneurysm model for evaluating EC behaviour

Endothelial cells were seeded on glass chamber slides (pre-treated with collagen), treated with Ang II +/- inhibitors (A) and were cultured for 24 or 72 hours (B). Each well of a chamber slide is subjected to unidirectional laminar flow (C). Cells within the middle section are considered to experience laminar flow and therefore used for further analysis (D).

5.8 Aim of this chapter

The aim of this chapter was to investigate the effects of Ang II on EC behaviour within the *ex vivo* aneurysm model using arteries excised from human umbilical cords. In addition, a simple *in vitro* flow model was deployed in order to assess the effect of Ang II on EC morphology and associated signalling pathways with and without inclusion of the endogenous MMP inhibitor TIMP-3, or the AGT1R inhibitor losartan.

5.9 Results

5.9.1 Effect of Ang II on endothelial cell VE-cadherin expression within an *ex vivo* aneurysm model

It has been previously demonstrated that wall shear stresses (WSS) directly affects ECs and therefore involved in arterial remodelling, such as that observed during aneurysm formation [312]. Furthermore, the use of Ang II in animal models has been associated with endothelial dysfunction and aneurysm formation [300]. Accordingly, human umbilical cord artery segments which had been within a bioreactor for 24 hours with and without Ang II were fixed and subjected to immunocytochemistry to evaluate the pattern of VE-cadherin, as assessed by confocal microscopy expression [16]. As shown in Figure 5.2A, a markedly different pattern of VE-cadherin expression was observed between untreated and Ang II-infused arteries. While endothelial VE-cadherin expression was restricted largely to the membranes and junctions of cells within untreated arteries cultured within a bio-reactor for 24 hours, Ang II-infusion resulted in intracellular accumulation of VE-cadherin expression (Figure 5.2B).

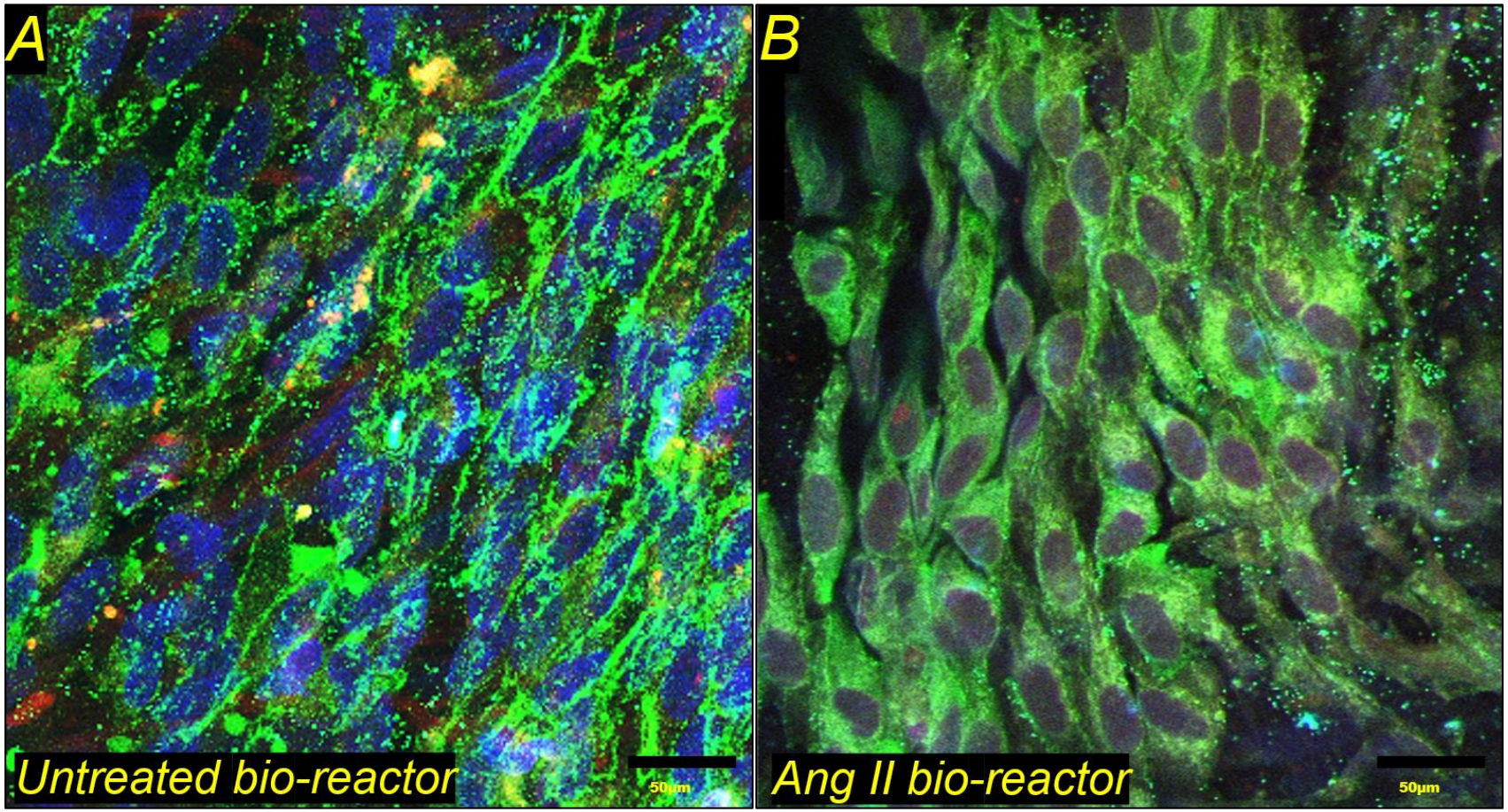

Figure 5.2: Effect of Ang II on endothelial cell VE-cadherin expression in ex vivo human umbilical cord artery

Representative confocal microscopy images of VE-cadherin immunocytochemistry of human umbilical cord arteries after insertion within a bio-reactor for 24 hours without Ang II (A untreated bio-reactor) and with Ang II (B Ang II bio-reactor). VE-cadherin (green), nuclei are stained with DAPI (blue). Scale bars represent 50 µm.

5.9.2 Effect of Ang II on endothelial cell VE-cadherin expression within an *in vitro* aneurysm model

In order to further investigate the *ex vivo* hemodynamic changes on EC VE-cadherin expression, a simplified *in vitro* flow assay was used to assess the effect of Ang II under flow on the expression of VE-cadherin on HUVECs for 24 hours (details of the method are described in paragraph 2.1.2.11). Taking the *ex vivo* observations into consideration, to evaluate hemodynamic changes the following parameters were analysed: percentage of cells with VE-cadherin positive membranes, intracellular expression of VE-cadherin, and cell area. In line with the *ex vivo* findings, the percentage of umbilical cord artery endothelial cells with VE-cadherin positive membranes was signficantly reduced in Ang II-treated cells and co-localised to the nucleus, when compared to untreated cells (66%; $P<0.05$; n=4; Figure 5.3). Interestingly, loss of membrane VE-cadherin expression was blunted when Ang II stimulated cells were co-incubated with either recombinant TIMP-3 (5nM) (65%; $P<0.05$; n=4; Figure 5.3) or losartan (25µM) (64%; $P<0.05$; n=4; Figure 5.3).

As expected given the above changes in membrane VE-cadherin expression, intracellular expression of VE-cadherin was markedly increased when cells were treated with Ang II, compared to untreated control HUVECs (89%; $P<0.05$; n=4; Figure 5.4A), which was largely reatrded through co-incubation with TIMP-3 (5nM) (94%; $P<0.05$; n=4; Figure 5.4) or losartan (25µM) (95%; $P<0.05$; n=4; Figure 5.4).

Finally, considering the assocaition of VE-cadherin expression and cell area in confluent endothelial cell monolayers [315], the effect of Ang II on HUVEC area was assessed. The area of cells treated with Ang II was significantly reduced compared to control cells (25%; $P<0.05$; n=4; Figure 5.5), which could be reversed by co-incubation with either TIMP-3 (28%; $P<0.05$; n=4; Figure 5.5) or losartan (34% $P<0.05$; n=4; Figure 5.5).

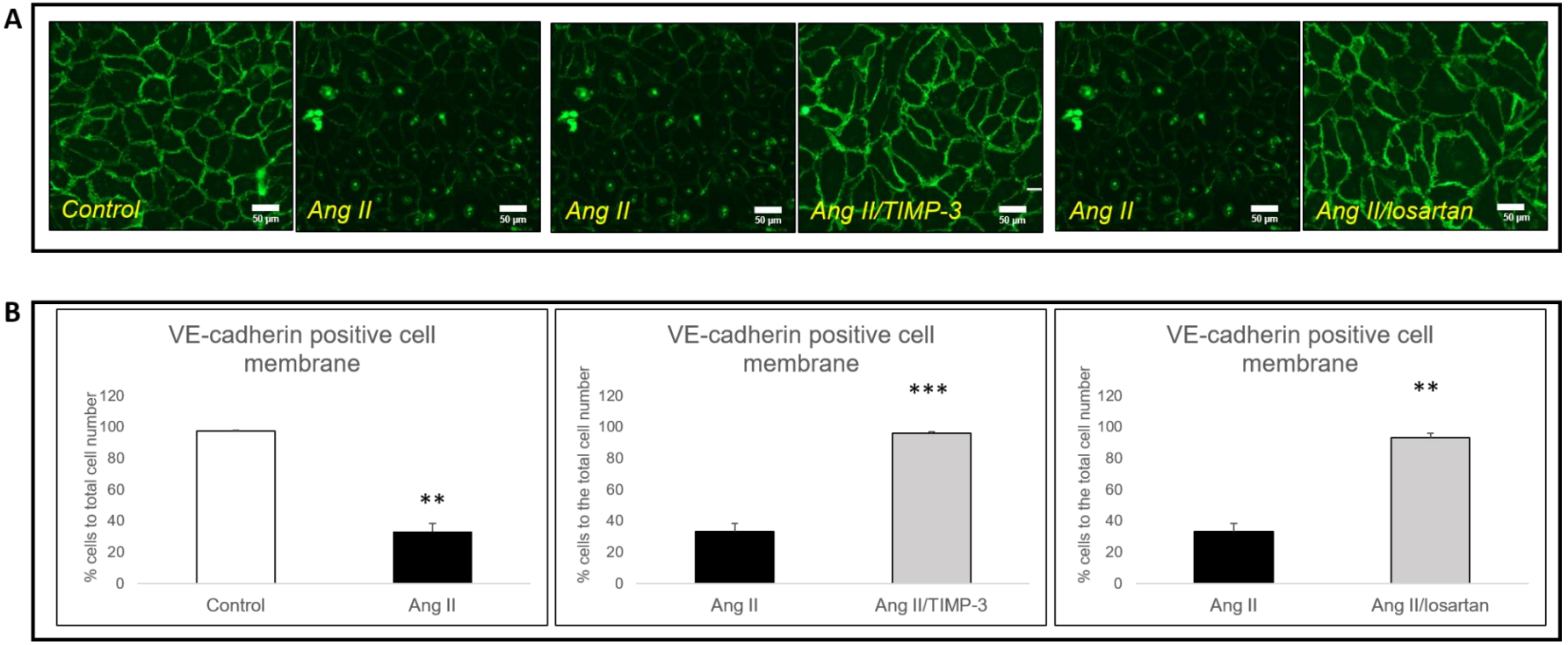

Figure 5.3: Effect of Ang II on HUVEC cell membrane VE-cadherin expression

*Representative images (A) and quantification (B) of HUVECs with VE-cadherin positive cell membranes, in x20 magnification fields of HUVECs untreated (control), Ang II treated (Ang II), or Ang II in combination with either TIMP-3 (5nM) or losartan (25µM) and subjected to laminar flow for 24 hours. Data is expressed as percentage of HUVECs with VE-cadherin positive membranes to the total cell number (mean±SEM; n=4). ** denotes p<0.01, *** denotes p<0.001, 2-tailed Student paired t test. Scale bars represent 50 µm.*

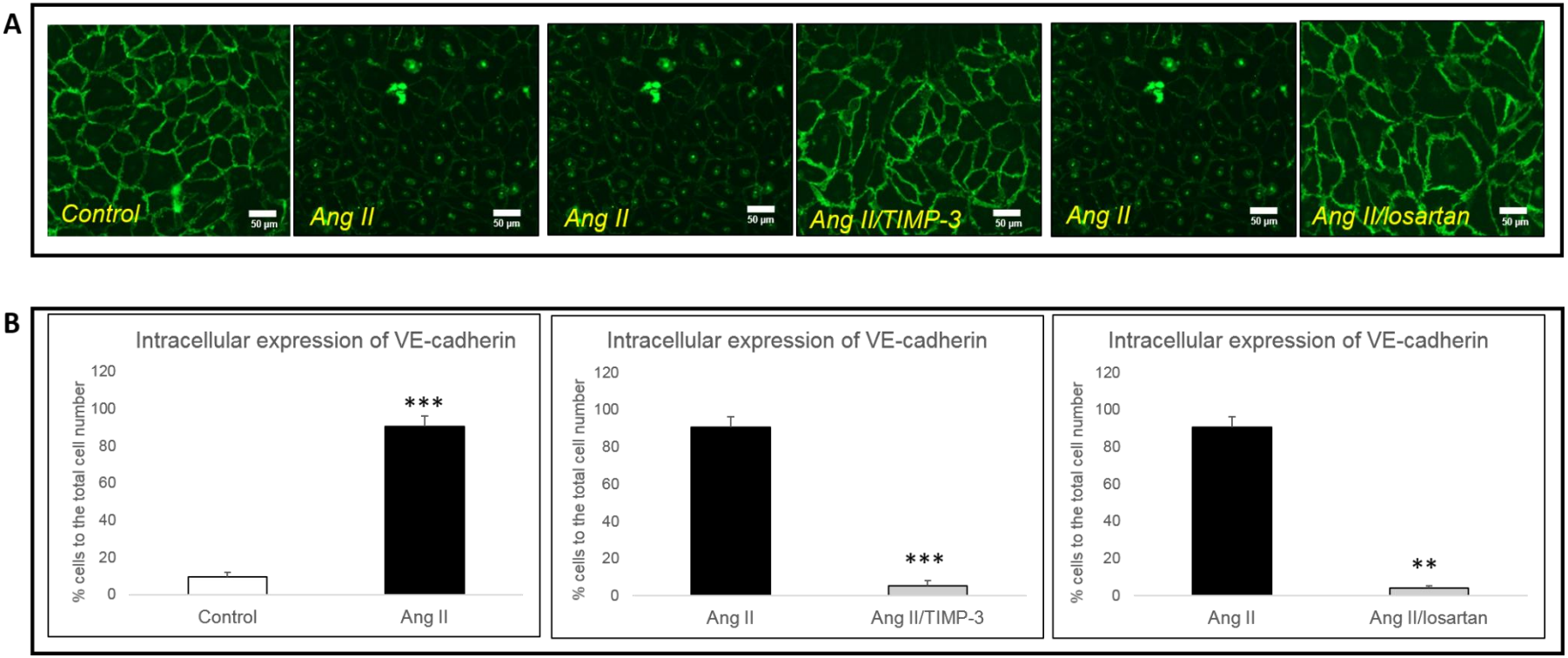

Figure 5.4: Effect of Ang II on HUVEC intracellular VE-cadherin expression

*Representative images (A) and quantification (B) of HUVEC intracellular expression of VE-cadherin, in x20 magnification fields of HUVECs untreated (control), Ang II treated (Ang II) or Ang II in combination with either TIMP-3 (5nM) or losartan (25µM) and subjected to laminar flow for 24 hours. Data is expressed as percentage of HUVECs with intracellular VE-cadherin to the total cell number (mean±SEM; n=4). ** denotes p<0.01, *** denotes p<0.001, 2-tailed Student paired t test. Scale bars represent 50 µm.*

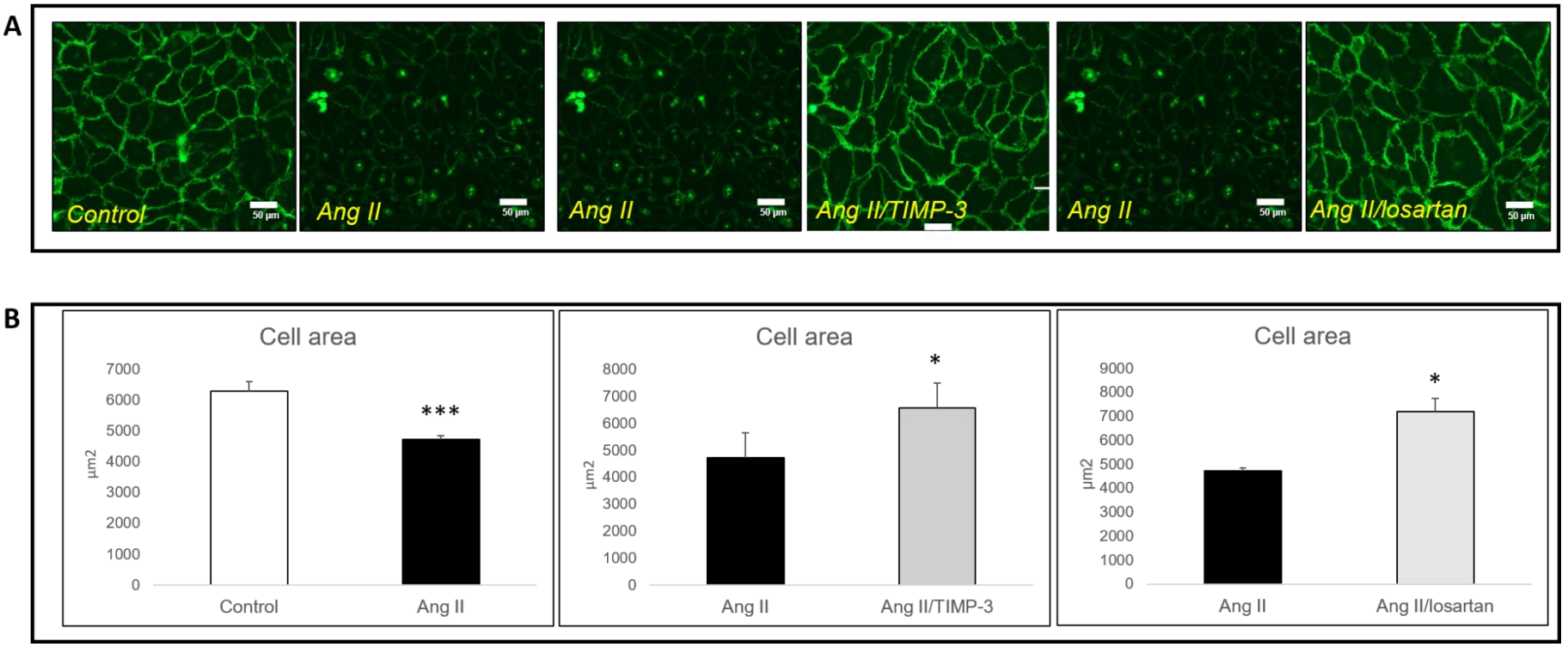

Figure 5.5: Effect of Ang II on HUVEC cell area

*Representative images (A) and quantification (B) of cell area. in VE-cadherin immuno-labelled x20 magnification fields of HUVECS untreated (control), Ang II treated (Ang II), or Ang II in combination with either TIMP-3 (5nM) or losartan (25µM) and subjected to laminar flow for 24 hours. Data is expressed as avergae cell area in µm^2 (mean±SEM; n=4). ** denotes p<0.01, *** denotes p<0.001, 2-tailed Student paired t test. Scale bars represent 50 µm.*

5.9.3 Effect of prolonged Ang II-stimulation on endothelial cell behaviour and VE-cadherin expression within an *in vitro* aneurysm model

Taking the striking effects of Ang II on HUVEC VE-cadherin expression and cell area after just 24 hours of incubation under laminar flow, effects on HUVEC cell behaviour alongside VE-cadherin expression were assessed after 72 hours Ang II stimulation under flow (to permit correlation with findings from within the *ex vivo* bio-reactor system), and also compared to cells maintained under static conditions. Specifically, HUVECs exposed to heamodynamic changes and prolonged Ang II stimulation were assessed for effects on cell proliferation, cell apoptosis, membrane VE-cadherin expression, filamentous (F)-actin expression and cell localisation, and intracellular expression of β-catenin.

5.9.3.1 Proliferation

To investigate whether basal EC proliferation rate is affected by laminar flow and/or Ang II stimulation, HUVECs were cultured in the presence of 5-ethynyl-2′-deoxyuridine (EdU), which is a thymidine analogue and is therefore incorporated into DNA during cell replication. Cells can then be subsequently subjected to immunocytochemistry to detect the presence of EdU and the percentage of proliferating cells quantified. As shown in Figure 5.6 using a repeated measures ANOVA no significant changes in proliferation rate were detected between HUVECs under static conditions or exposed to laminar flow, with and wihtout Ang II stimulation, or in the presence of either recombinant TIMP-3 or losartan. However, closer examination revelaed that proliferation rates were consistently lower in HUVECs co-incubated with Ang II and TIMP-3 compared to Ang II alone, under both static and laminar flow conditions (red box in Figure 5.6). Accordingly, a students paired t-test was performed and while no difference was detected under static conditions (Ang II 45.0±4.2 v. Ang II + TIMP-3 32.3±6.5; $P=0.095$), during laminar flow TIMP-3 co-incubation significantly reduced Ang II proliferation rates (Ang II 46.5±0.9 v. Ang II + TIMP-3 32.2±4.2; $P<0.05$).

5.9.3.2 Apoptosis

Alongside proliferation, endothelial cell loss is a hallmark of cardiovascular diseases such as aneurysms. Accordingly, the effect of laminar flow and Ang II on HUVEC susceptibility to apoptosis was assessed through immunocytochemistry for the apoptosis marker cleaved caspase-3. As illustrated in Figure 5.7 subjection of HUVECs to laminar flow had no effect on the number of cells undergoing apoptosis when compared to static cells. However, Ang II

stimulation of HUVECs significantly increased apoptotic frequencies in both static (68%; P<0.01; n=4) and laminar flow exposed cells (86%; P<0.001; n=4; Figure 5.7). However and ash shown in Figure 5.7, susceptibility to Ang II-induced apoptosis was blunted in static HUVECs in the presence of recombinant TIMP-3 (90%; P<0.001; n=4) or losartan (76%; P<0.01; n=4), and those exposed to laminar flow (80%; P<0.001; n=4, and 79%; P<0.001; n=4, respectively).

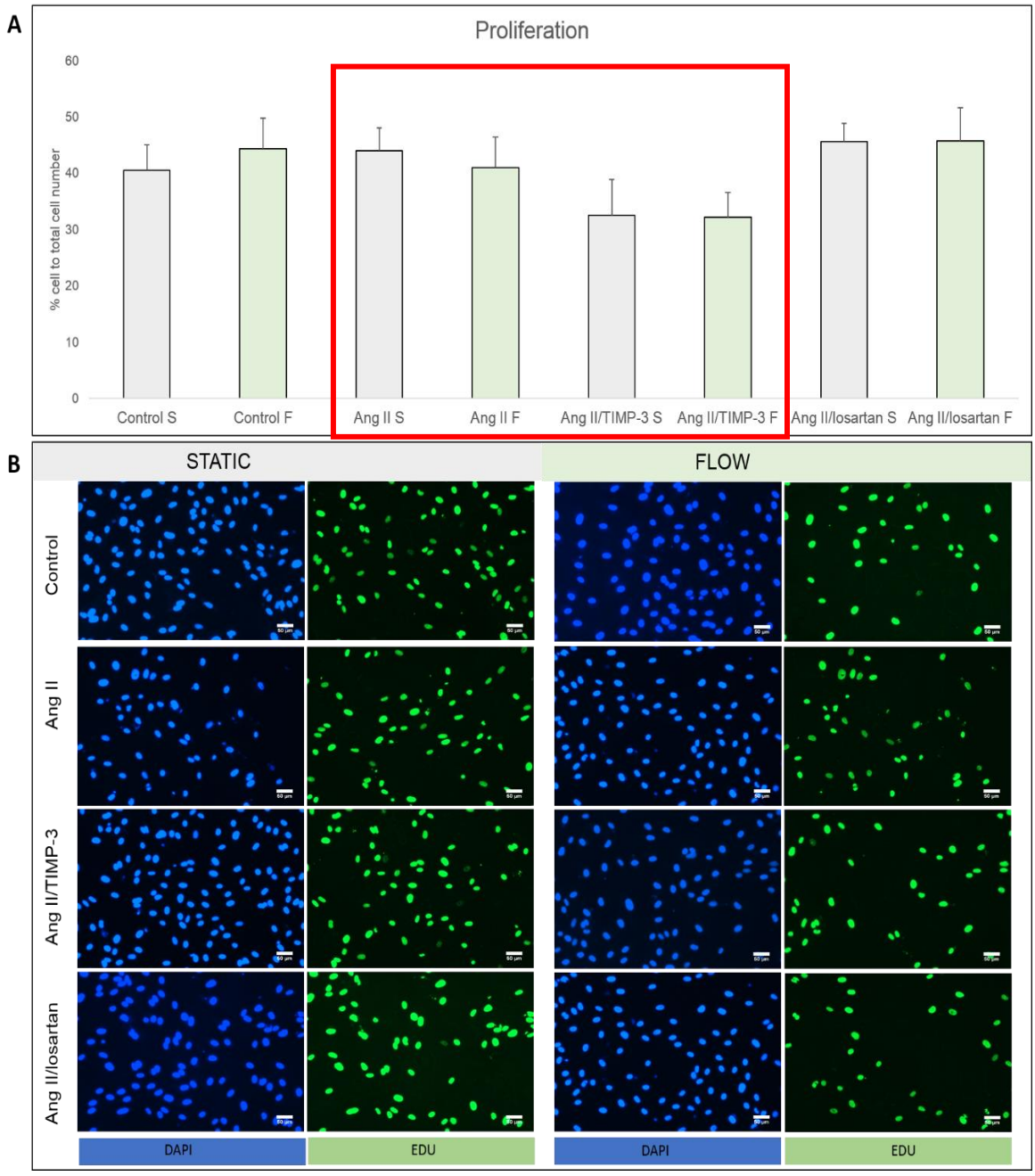

Figure 5.6: Effect of laminar flow and Ang II on HUVEC proliferation

*Quantification (A) and representative images (B) of proliferating cells (EdU positive), in x20 magnification fields of HUVECS untreated (control), Ang II treated (Ang II) or Ang II in combination with either TIMP-3 (5nM) or losartan (25µM), and subjected to either static conditions (grey columns) or laminar flow (green columns) for 72 hours. Proliferating were immuno-labelled with and anti-EdU antibody (green), and nuclei were stained with DAPI (blue). Data is expressed as a percentage of EdU positive cells to the total cell number (mean±SEM; n=4). Red box indicates data subjected to paired student t-test and * denotes $p<0.05$. S in graph indicates static and F denotes laminar flow. Scale bars represent 50 µm.*

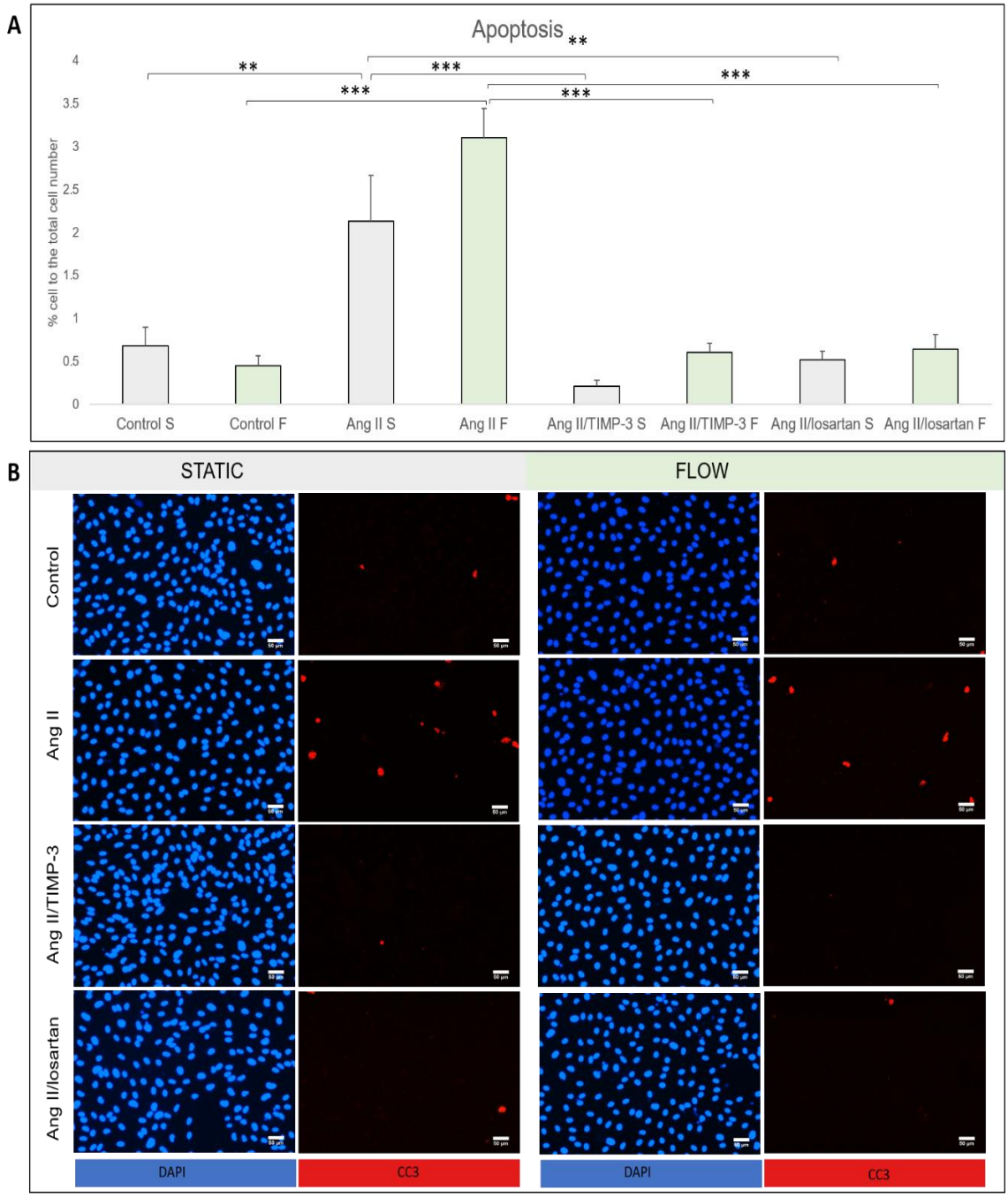

Figure 5.7: Effect of laminar flow and Ang II on HUVEC susceptibility to apoptosis

*Quantification (A) and representative images (B) of apoptotic cells (cleaved caspase-3 positive), in x20 magnification fields of HUVECS untreated (control), Ang II treated (Ang II) or Ang II in combination with either TIMP-3 (5nM) or losartan (25µM), and subjected to either static conditions (grey columns) or laminar flow (green columns) for 72 hours. Apoptotic cells were identified by immunocytochemistry for cleaved caspase-3 (red), and nuclei were stained with DAPI (blue). Data is expressed as a percentage of cleaved caspase-3 cells to the total cell number (mean±SEM; n=4). Data was subjected to repeated measures ANOVA and ** denotes p<0.01, and *** denotes p<0.001. S in graph indicates static and F denotes laminar flow. Scale bars represent 50 µm.*

5.9.3.3 VE-cadherin

Mirroring the effects observed after 24 hours incubation, HUVECs cultured for 72 hours under static conditions or laminar flow displayed a significant loss of membrane-localised VE-cadherin expression when stimulated with Ang II (static 51%; $P<0.05$; and laminar flow 40%; $P<0.001$; n=4; Figure 5.8 A and B, respectively), in comparison to untreated control cells. Also similar to the 24 hour findings, HUVEC membrane VE-cadherin expression was restored under both static culture and under laminar flow when supplemented with either recombinant TIMP-3 (static 51%; $P<0.01$; and laminar flow 42%; $P<0.01$; n=4; Figure 5.8 A and B, respectively) or losartan (static 44%; $P<0.01$; and laminar flow 37%; $P<0.01$; n=4; Figure 5.8 A and B, respectively).

Using fluorescently-conjugated phalloidin to detect F-actin expression, no significant differences were revealed between static and laminar flow exposed HUVECs, or after exposure to Ang II, although a similar trend in expression pattern to that observed for cell membrane VE-cadherin positivity was evident (Figure 5.9). Addition of recombinant TIMP-3 also showed no change, whereas losartan in Ang II stimulated HUVECs significantly increased the percentage of HUVECs expressing F-actin ($P<0.05$; n=4; Figure 5.9).

Considering the similar trend in altered F-actin expression to that detected for VE-cadherin localisation, induced by exposure to laminar flow and/or Ang II stimulation, the co-expression of F-actin and VE-cadherin was assessed. As shown in (Figure 5.10A), under either static or laminar flow conditions, the percentage of HUVECs positive for F-actin and displaying cell membrane localised VE-cadherin expression were significaintly decreased with 72 hours stimulation with Ang II compared to untreated control cells (static 53%; $P<0.01$; and laminar flow 52%; $P<0.05$; n=4; Figure 5.10 A and B, respectively). Co-incubation with recombinant TIMP-3 was able to benficially reverse this effect (static 55%; $P<0.01$; and laminar flow 52%; $P<0.05$; n=4; Figure 5.10 A and B, respectively), whilst losartan co-adminstration was only favorable under laminar flow conditions (51%; $P<0.01$; n=4; Figure 5.10B).

With regards to cell area, which was reduced by Ang II stimulation for 24 hours and reversed with TIMP-3 or losartan addition, exposure of HUVECs under either static or flow conditions to Ang II stimulation had no effect (Figure 5.11). Losartan was equally uneffective under either condition, whereas addition of recombinant TIMP-3 significantly increased cell area in HUVECs subjected to laminar flow (51%; $P<0.05$; n=4; Figure 5.11B), but not under static conditions (Figure 5.11A).

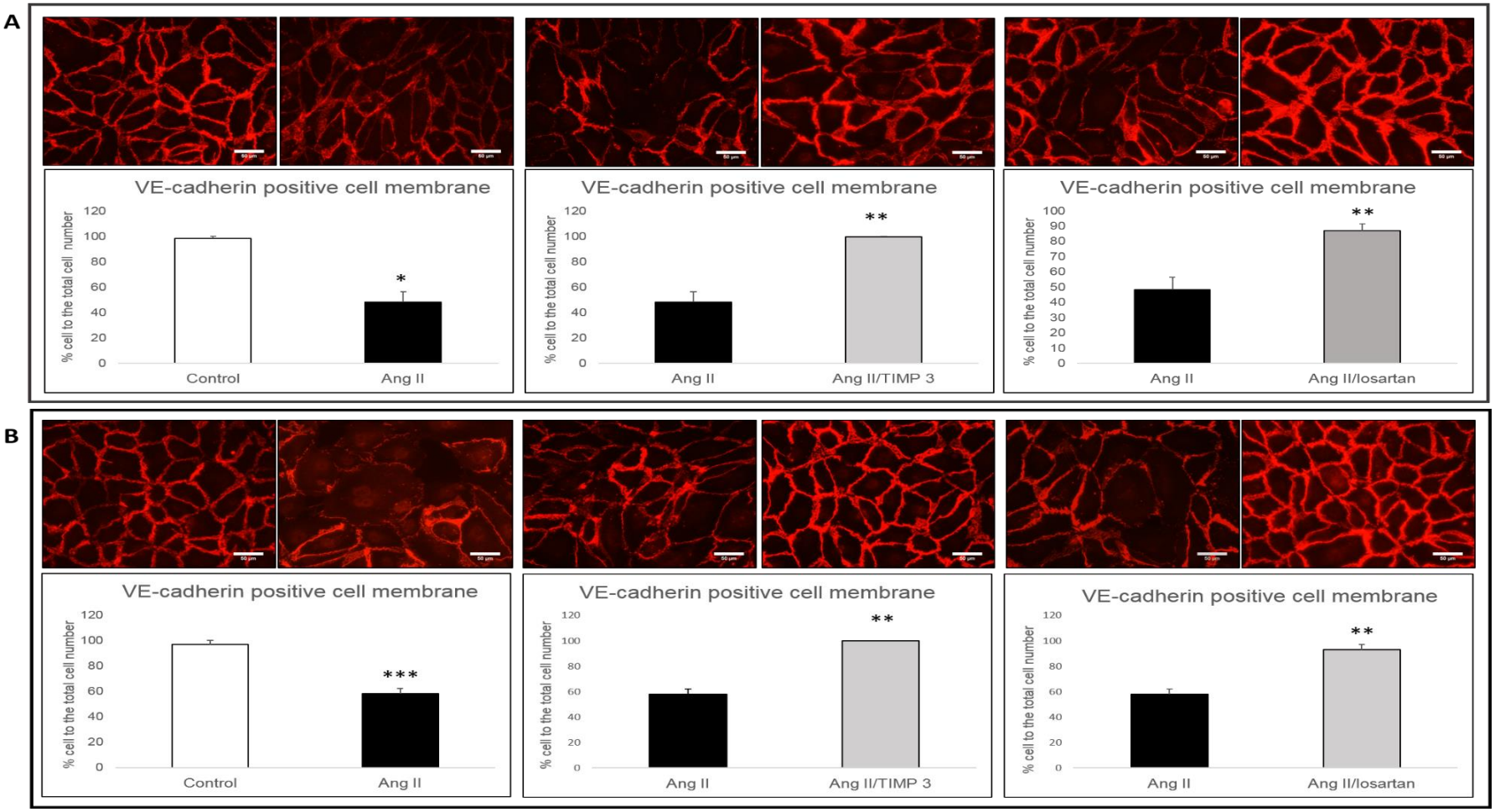

Figure 5.8: Effect of laminar flow and prolonged Ang II stimulation on HUVEC cell membrane VE-cadherin expression

*Representative images and quantification of HUVECs with VE-cadherin positive cell membranes, in x20 magnification fields of HUVECs untreated (control), Ang II treated (Ang II), or Ang II in combination with either TIMP-3 (5nM) or losartan (25µM) and subjected to either (A) static conditions or (B) laminar flow for 72 hours. Data is expressed as percentage of HUVECs with VE-cadherin positive membranes to the total cell number (mean±SEM; n=4). * denotes p<0.05, ** denotes p<0.01, *** denotes p<0.001, 2-tailed Student paired t test. Scale bars represent 50 µm.*

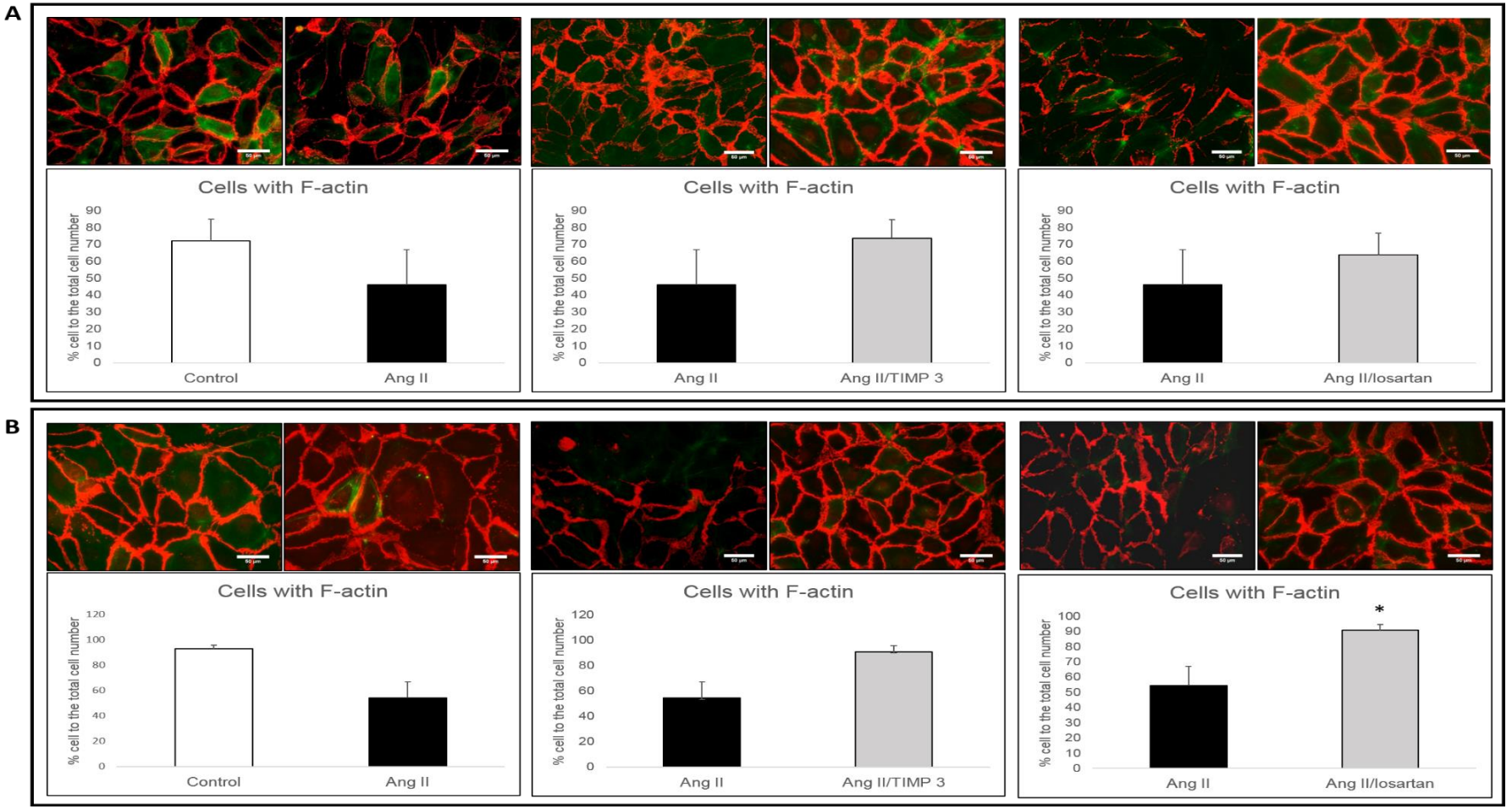

Figure 5.9: Effect of laminar flow and prolonged Ang II stimulation on HUVEC F-actin expression

*Representative images and quantification of HUVECs positive for F-actin, in x20 magnification fields of HUVECs untreated (control), Ang II treated (Ang II), or Ang II in combination with either TIMP-3 (5nM) or losartan (25μM) and subjected to either (A) static conditions or (B) laminar flow for 72 hours. Data is expressed as percentage of HUVECs immuno-positive for F-actin (green) in VE-cadherin co-labelled cells (red), relative to the total cell number (mean±SEM; n=4). * denotes p<0.05, 2-tailed Student paired t test. Scale bars represent 50 μm.*

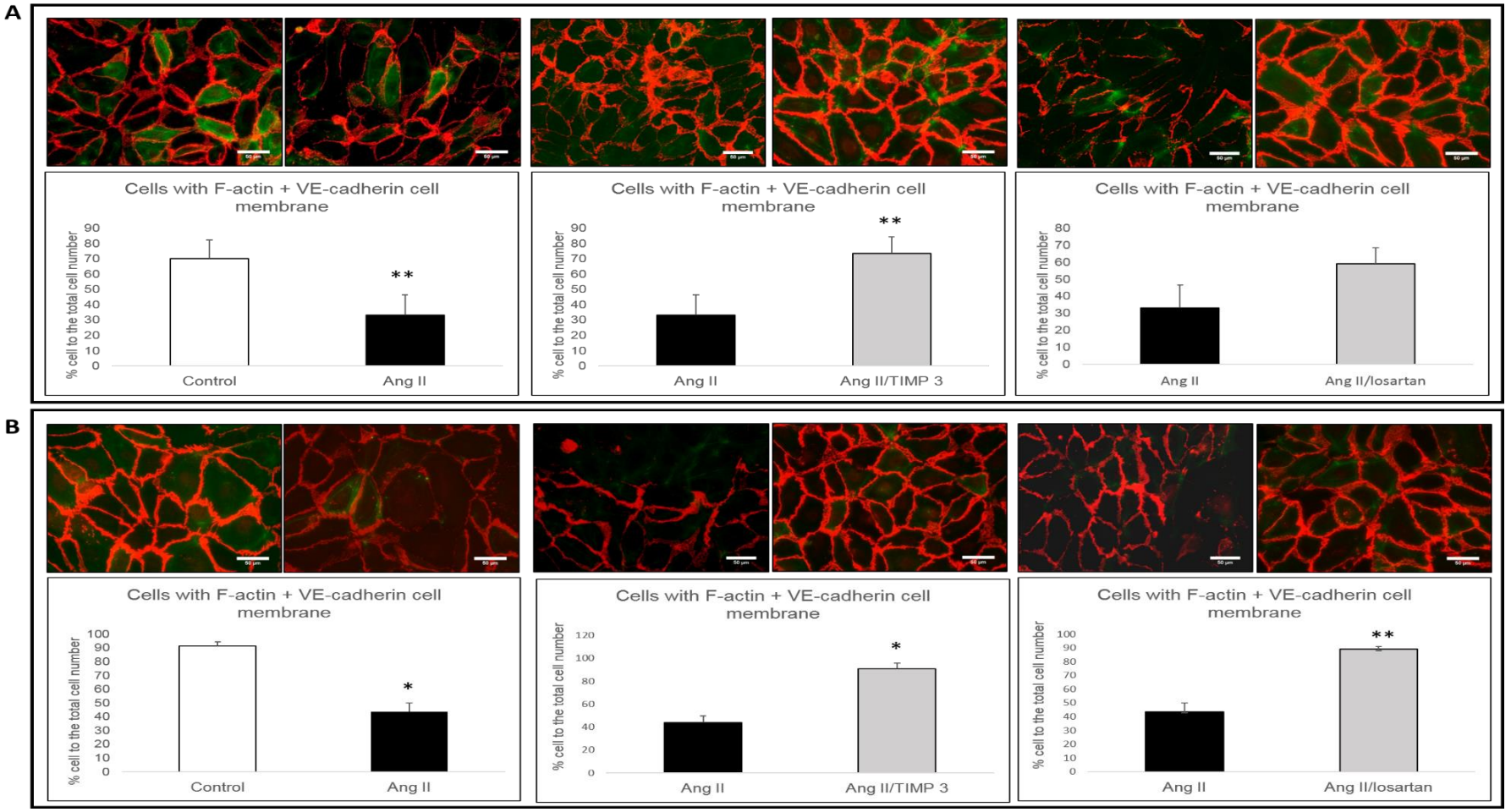

Figure 5.10: Effect of laminar flow and prolonged Ang II stimulation on HUVEC co-expression of F-actin and VE-cadherin

*Representative images and quantification of HUVECs positive for F-actin and VE-cadherin, in x20 magnification fields of HUVECs untreated (control), Ang II treated (Ang II), or Ang II in combination with either TIMP-3 (5nM) or losartan (25µM) and subjected to either (A) static conditions or (B) laminar flow for 72 hours. Data is expressed as percentage of HUVECs immuno-positive for both F-actin (green) and VE-cadherin (red), relative to the total cell number (mean±SEM; n=4). * denotes p<0.05, ** denotes p<0.01, 2-tailed Student paired t test. Scale bars represent 50 µm.*

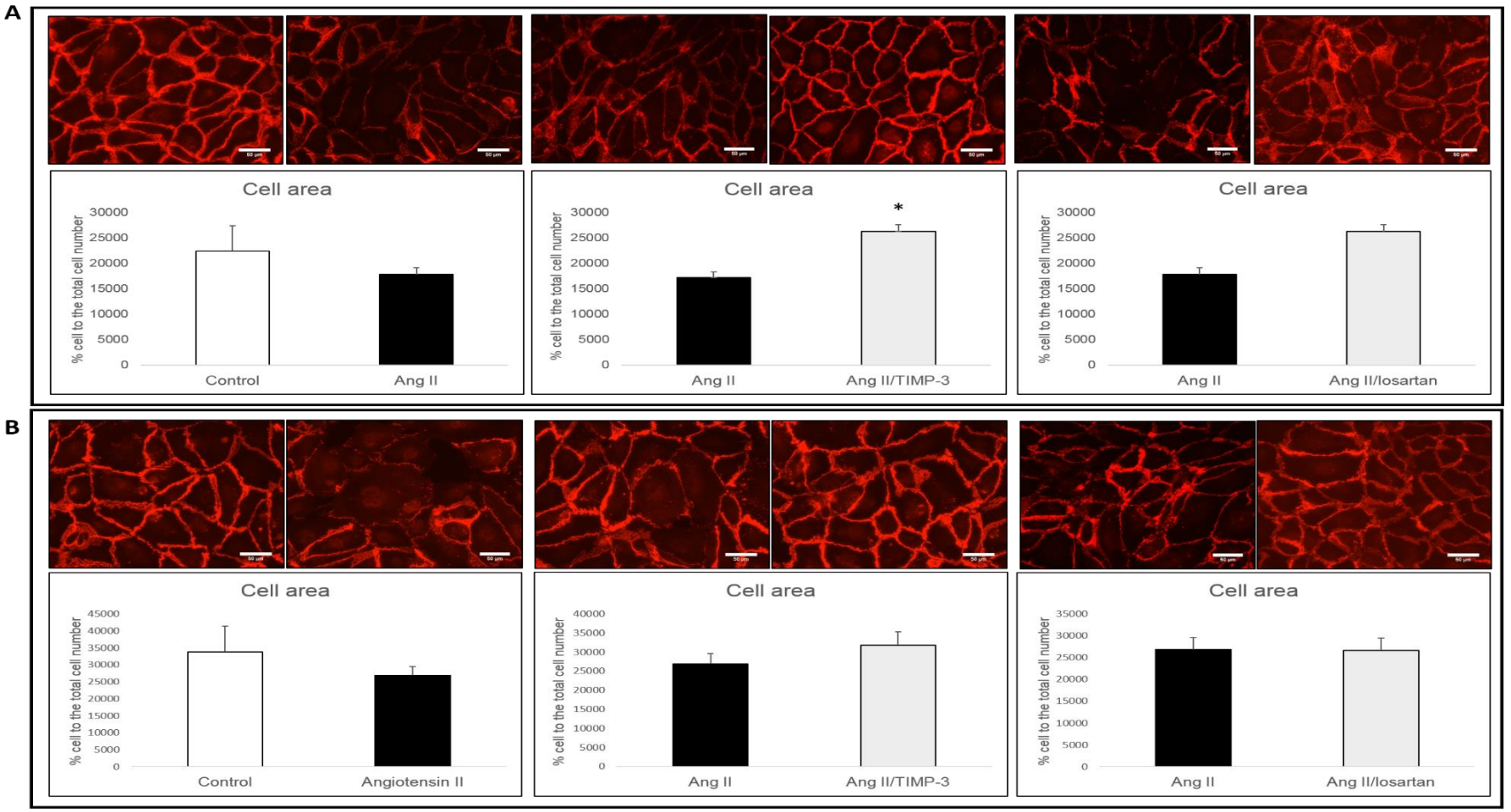

Figure 5.11 Effect of laminar flow and prolonged Ang II stimulation on HUVEC cell area

*Representative images and quantification of cell area. in VE-cadherin immuno-labelled x20 magnification fields of HUVECS untreated (control), Ang II treated (Ang II), or Ang II in combination with either TIMP-3 (5nM) or losartan (25μM) and subjected to either (A) static conditions or (B) laminar flow for 72 hours. Data is expressed as avergae cell area in μm^2 (mean±SEM; n=4). * denotes $p<0.05$, 2-tailed Student paired t test. Scale bars represent 50 μm.*

5.9.3.4 β-catenin

It has been previously demonstrated that when membrane-localised and intact VE-cadherin is present on endothelial cells, the cytoplasmic portion of VE-cadherin is bound to β-catenin and interacts with the cytoskeleton, preventing its nuclear translocation and subsequent signalling [316]. Considering Ang II stimulation induced loss of cell membrane-localised VE-cadherin in HUVECs, effects of prolonged Ang II adminstration alongside altered shear stress on β-catenin localisation were assessed. As illustrated in Figure 5.12, static and laminar flow-exposed HUVECs treated with Ang II for 72 hours displayed significantly increased intracellular expression of β-catenin compared to untreated control cells (static 46%; $P<0.01$; and laminar flow 56%; $P<0.05$; $n=4$; Figure 5.12 A and B, respectively). As expected, Ang II-induced intracellular accumulation of β-catenin, under both static and laminar flow conditions, was significantly suppressed by either recombinant TIMP-3 addition (static 37%; $P<0.01$; and laminar flow 98%; $P<0.01$; $n=4$; Figure 5.12 A and B, respectively) or losartan co-incubation (static 43%; $P<0.05$; and laminar flow 67%; $P<0.05$; $n=4$; Figure 5.12 A and B, respectively). It should be noted that uder laminar flow, TIMP-3 addition almost comletely abolished the Ang II intracellular accumulation β-catenin.

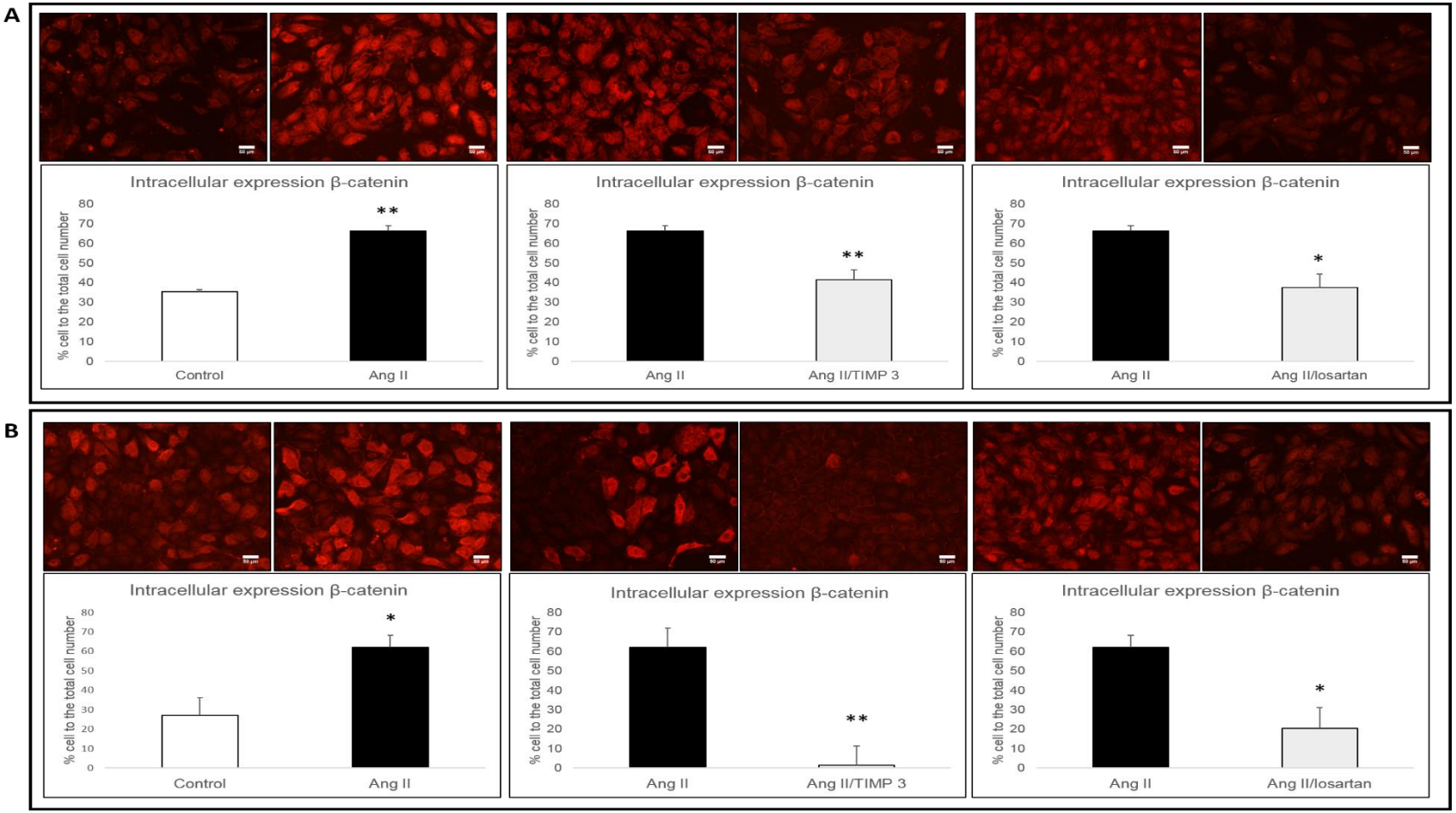

Figure 5.12: Effect of laminar flow and prolonged Ang II stimulation on HUVEC intracellular β-catenin accumulation

*Representative images and quantification of HUVEC intracellular expression of β-catenin, in x20 magnification fields of HUVECs untreated (control), Ang II treated (Ang II) or Ang II in combination with either TIMP-3 (5nM) or losartan (25μM) and subjected to either (A) static conditions or (B) laminar flow for 72 hours. Data is expressed as percentage of HUVECs with intracellular β-catenin (red) to the total cell number (mean±SEM; n=4). * denotes p<0.05, ** denotes p<0.01, 2-tailed Student paired t test. Scale bars represent 50 μm.*

5.10 Conclusion

In summary, the data presented within this chapter demonstrates that Ang II stimulation alongside hemodynamic changes alters endothelial cell VE-cadherin expression and localisation, which may result in activation of the β-catenin signalling pathway and is also associated with modulation of their morphology and function including an increased susceptibility to apoptosis alongside. Furthermore, Ang II-induced effects on HUVECs *in vitro* appear largely AT1R-dependent as they can be reversed with losartan. Moreover, Ang II-mediated proteolytic effects on VE-cadherin expression may underlie the observed effects on endothelial cell function, as exogenous TIMP-3 imparts restorative outcomes. Indeed, these findings are in part consistent with the previous *ex vivo data* and published findings, however more investigations are required to ascertain whether interventions such as TIMP-3 addition can exert protective effects on Ang II-induced aneurysm formation and the realtionship with effects on endothelial cell behaviour.

5.11 Discussion

Accumulating evidence suggests that ECs play an important role in aneurysm pathogenesis. Therefore, this chapter investigated the effect of Ang II alongside inhibitors of MMPs and Ang II signalling, TIMP-3 and losartan respectively, on EC behaviour in both *ex vivo* and *in vitro* models of EC shear stress. Specifically, the effect of Ang II on VE-cadherin expression was analysed within the novel *ex vivo* bio-reactor aneurysm model using human umbilical cord arteries described within this thesis. Additionally, the effect of Ang II on HUVECs was determined within an *in vitro* system using a rocker as a model of mechanotransduction. Within the isolated cells, effects on cell morphology, VE-cadherin expression and localisation of β-catenin were assessed. In order to ascertain if Ang II effects were a direct result of Ang II signalling and dysregulated MMP expression, potential protective effects of losartan and TIMP-3 were also interrogated. The use of both *ex vivo* and *in vitro* systems should provide useful to elucidate the underlying molecular mechanisms of Ang II on endothelial dysfunction with direct relevance to AAA formation. Moreover, findings replicative of those previously demonstrated in human aortic endothelial cells and aortic aneurysm tissues would support the use of the ex vivo model for future aneurysm studies.

5.11.1 Effects on EC behaviour wihin the *ex vivo* model of aneurysm

The effect of *ex vivo* pulsatile laminar flow for 24 hours on HUVEC behaviour was assesed in human umbilical cord artery, through immmunocytochemistry and subsequent confocal microscopy for VE-cadherin expression. Unfortunately, due to a lack of human umbilical cord towards the end of my PhD study, only 1N was studied so the findings are observational. Nonetheless, VE-cadherin labelling was clearly observed at cell junctions in untreated umbilical cord arteries whereas marked intracellular accumulation was evident within ECs of Ang II-infused arteries. In agreement with these findings, previous studies have shown that the expression of VE-cadherin is expressed at the periphery of ECs [317], and Miao *et al*. also showed that VE-cadherin immuno-staining was continuously distributed at the entire periphery of rat aortic ECs under either static conditions or under laminar flow for 24 hours [318]. Furthermore, Bodor *et al.* hypothesised that HUVECs in response to Ang II stimulation increased their permeability. Accordingly, treating HUVECs with Ang II for 48 hours and immuno-labelling cells for VE-cadherin revealed weaker peripheral staining for VE-cadherin which was associated with the fromation of surface openings and caveolae [306].

These preliminary *ex vivo* findings suggest hemodynamic changes in association with Ang II exposure alters the expression of VE-cadherin in ECs, which may in turn modulate their morphology and function. However, as only arteries from one donor were examined in the current study, further investigation is necessary to confirm these novel findings. Moreover, the change in cellular distribution of VE-cadherin with shear stress and Ang II-infusion justifies in vitro studies with HUVECs to further examine these changes and related effects on β-catenin expression.

5.11.2 Effects of Ang II and laminar flow on EC behaviour *in vitro*

In line with the *ex vivo* observations, subjection of HUVECs to Ang II within a simple *in vitro* flow model for 24 hours resulted in loss of membrane-localised VE-cadherin expression, which was comaparably reversed by treatment with either recombinant TIMP-3 (to block MMP activity) or losartan (a Ang II signalling inhibitor). These findings demonstrate the *in vitro* system is suitable for assesing modulation of EC function and behaviour as the VE-cadherin changes replicate those from within the *ex vivo* model, but also confirm the potential contribution of MMPs to the Ang II-dependent effects. The observed loss of membrane-localised VE-cadherin with Ang II stimulation was accompanied by intracellular accumulation of VE-cadherin alongside a decrease in cell area, an indicator of increased permeability. These effects were again suppressed by co-incubation with either recombinant TIMP-3 or losartan. Indeed, changes in VE-cadherin localisation in ECs during vascular injury have been previoulsy shown to increase permeability [304], which is associated with phosphorylation of VE-cadherin and its subsequent internalisation [305]. While Bodor e*t al.* demnstrated that Ang II increased the permeability of human umbilical cord veins, [306] which is also associated with heightened VE-cadherin internalisation [319].

In agreement with the above findings, Wu *et al.* demonstrated pulmonary microvascular ECs stimulated with Ang II exhibited reduced VE-cadherin expression compared to untreated cells [320]. Moreover, while membrane-localised VE-cadherin is phosphorylated under physiological conditions, Ang II adminstration dephosphorylated VE-cadherin at the Tyr685 (Y685) residue, which was associated with its reduced expression [320]. Subsequently, VE-cadherin dephosphorylation induced actin cytoskeletal rearrangement and endothelial dysfunction [320]. Additionally, Cholan *et al*. showed that six hours Ang II treatment of human microvascular ECs reduced VE-cadherin mRNA expression, although two hours treatment did not affect expression it altered VE-cadherin localisation through loss of membrane localisation [321].

Validating the modulation of cell membrane VE-cadherin expression is through Ang II signalling, co-adminstration of the AT1R blocker losartan restored cell membrane VE-cadherin expression to that of controls. Furthermore, Ang II-mediated MMP activity can be proposed as a mechanism regulating VE-cadherin cellular localisation, as TIMP-3 co-adminstration protected from cell mebrane VE-cadherin loss. Both of these observations are novel, as no publications could be identified examing the effect of these interventions on VE-cadherin expression in ECs. Although in support, losartan adminstration within a pig vein stenosis model was associated with increased VE-cadherin expression in ECs [322]. Furthermore, both inhibitors have been shown to be protective on AAA formation; losartan suppressed aneurysm formation in a mouse Marfan syndrome model [80], while TIMP-3 has been shown to exert anti-aneurysmal propoertiesin the Ang II-induced mouse model of AAA formation [186].

5.11.3 Effects of prolonged Ang II-infusion and laminar flow on EC behaviour *in vitro*

To align with the findings from the *ex vivo* model of aneurysm, the effect of 24 hours *in vitro* Ang II-adminstration in combination with laminar flow on VE-cadherin expression in HUVECs were also assessed after 72 hours stimulation, alongside proliferation and apoptosis. Interestingly, Ang II has been proposed to exert both growth promoting and anti-proliferative effects on ECs which appears to be dependent on their disparate expression of angiotensin AT1- and AT2-receptors, with and AT1R mediating growth and AT2R inducing anti-proliferative actions [323]. However, in the current study no effect of Ang II on HUVEC proliferation was observed under either static or laminar flow conditions, or accordingly with losartan administration. TIMP-3 did mildly reduce proliferation rates under both conditions to a comparable rate, implying that a protease-mediated pathway is involved in the high basal proliferation rate observed in HUVECs, which is Ang II and flow-independent.

HUVECs stimulated with Ang II under either static or flow conditions increased HUVEC susceptibility to apoptosis, which could be blocked by co-administration of recombinant TIMP-2 or losartan. These observations are in part supported by Dimmeler and colleagues who showed Ang II exerted a dose-dependent pro-apoptotic effect on HUVECs under static culture, which could be blunted through co-incubation with inhibitors of both AT1R and AT2R but not individually [302]. AT1R-dependent pro-apoptotic effects of Ang II on human coronary ECs have also been demonstrated, as survival was promoted through losartan co-administration [324]. As such, it can be proposed that Ang II induction of EC apoptosis is mediated in part through proteases (such as MMPs) as losartan and TIMP-3 respectively are protective. Indeed, there is published evidence demonstrating metalloproteinase activity can induce EC apoptosis, which is associated with loss of VE-cadherin and β-catenin at the cell periphery

[325]. Moreover, decreased F-actin fibres were reported in cells with reduced cell size alongside diffuse intra-cellular β-catenin accumulation and increased permeability [325]. In agreement, the data presented here demonstrates prolonged Ang II administration (similarly to the 24-hour incubation findings) stimulated loss of HUVEC membrane-localised VE-cadherin and its association with F-actin expression, alongside concomitant intra-cellular accumulation of both VE-cadherin and β-catenin. Moreover, losartan co-treatment blocked these effects suggesting that the actions of Ang II are predominantly through AT1R. Furthermore, supporting a deleterious effect of MMPs on EC VE-cadherin expression, localisation and subsequent function, addition of TIMP-3 also reversed the Ang II-induced actions. Collectively, these new findings alongside the published literature suggest MMP-mediated VE-cadherin regulation alters EC function potentially through modulating the Wnt/β-catenin signalling pathway. Indeed, Cong *et al.* demonstrated that membrane-tethered cadherin-β-catenin complexes require dissociation and subsequent nuclear translaocation of β-catenin to induce Wnt/β-catenin signalling [326]. In another study Cuevas *et al.* showed that Ang II can induce the β-catenin-dependent signalling in mouse duct cells alongside induction of β-catenin target genes [327]. Similar activation of the Wnt/β-catenin signalling pathway has been revelaed in rat cardiomyocytes and cardiac fibroblasts after Ang II infusion [328] [329]. It would therefore be pertinent to verify in future studies if indeed the Wnt/β-catenin signalling is activated in HUVECs with Ang II-stimulation through VE-cadherin-dependent effects.

Although in-depth analysis of the Ang II-mediated effects on EC function were beyond the scope of this thesis, the findings support the need for further studies, especially in order to elucidate the cross-talk between Ang II-dependent MMP regulation and Wnt/β-catenin signalling, particularly in the context of aneurysm development and progression. In addition, the possibility of other mechanisms mediated by Ang II should also be considered. Indeed, as a selective Ang II type 1 receptor (AT1R) inhibitor, losartan can also block numerous nodes of TGF-β signalling both directly and indirectly [80]. Losartan can inhibit TGF-β canonical signalling through ERK [80] and Smad2 and therefore suppresses expression of TGF-β responsive genes including numerous growth factors and ECM molecules such as collagens [80] [330]. As such, losartan can prevent aneurysm formation in the fibrillin-1–deficient mouse model of Marfan syndrome [80, 331] and is deployed in the clinic for aortic dilatation prevention in patients with Marfan Syndrome [330, 332]. It is also well characterised that TGF-β signalling can additionally regulate the expression of MMPs [333] and may add a supplementary mechanism why TIMP-3 administration and losartan addition had similar effects on VE-cadherin expression/localisation, β-catenin levels and cell morphology in ECs. This potential cross-talk between the Ang II and TGF-β pathways with regards to VE-cadherin modulation and MMP expression warrants further investigation.

Chapter 6

6 Validation of an *ex vivo* model of aneurysm through modulating either MMP or TGF-β activity

6.1 Introduction

6.1.1 Therapies for AAA

AAA is a life-threatening condition which is associated with a high mortality [38, 164]. A combination of genetic and predisposing factors contributes to the irreversible dilatation of the aorta [334]. Once the aorta is dilatated, it has a risk of rupture and this risk is increased as the diameter of the aorta increases [335]. Furthermore, there are no therapies to stabilise a dilatated aorta and prevent further dilatation, or ideally to reverse aortic dilatation and restore to its normal diameter [32]. In addition, the pathogenesis of AAA is not fully understood, therefore further studies are required to elucidate the molecular mechanisms underlying AAA formation and progression [217].

Accordingly, numerous experimental mouse models have been developed to aid interrogation and clarification of the mechanisms central to the pathogenesis of AAA [127], Within such models, recent findings have suggested that modulating the expression and activity of MMPs or the TGF-β signalling pathways may represent viable therapeutic targets to prevent aneurysm formation, progression and rupture [80, 160, 186]. Specifically, strategies including selective inhibition of MMP-12 activity, microRNA inhibitors to restore TIMP-3 expression, or monoclonal neutralising antibodies (NAb) which blunt TGF-β signalling, has shown beneficial effects through retardation of aneurysm formation in mice [80, 160, 186]. However, and as previously mentioned, the experimental mouse models used in AAA studies involved a high rate of spontaneous death, chiefly attributable to aortic dissection or rupture. The data presented within this thesis so far supports the human *ex vivo* aneurysm model as a viable alternative to mouse studies as underlying mechanisms including dysregulated proteolysis are shared. In order to validate the *ex vivo* aneurysm model, the effectiveness of the interventions successful within the mouse AAA models were tested within the *ex vivo* model to ascertain if similar beneficial effects were observed. Such validation would lend further support for the *ex vivo* model as a tool for research studies investigating aneurysm pathogenesis, alongside

testing of potential new therapeutics, resulting in a potential reduction of mouse numbers currently used in aneurysm research.

6.1.2 Effect of MMP or TGF-β modulation on e*x vivo* aneurysm formation and regression

The principle of the *ex vivo* aneurysm model is the same as described within Chapter 3, where arteries isolated from human umbilical cord are placed within a bio-reactor system. Human umbilical arteries are subjected to unidirectional flow at 6.5 dynes/cm^2 to induce concentric dilatation typical of AAA formation. The findings within Chapter 3 demonstrate that Ang II infusion within the bio-reactor system for 72 hours results in aneurysm formation, characterised by increased the total vessel area (dilatation), medial thinning, loss of elastin content, and reduced in medial cell number. Within this chapter, either recombinant TIMP-3 (to inhibit protease activity), a selective MMP-12 inhibitor (RXP470), or a TGF-β NAb have been co-administered to Ang II-infused umbilical cord arteries within the bio-reactor system for 72 hours in order to assess the potential of the above interventions to suppress aneurysm formation. Furthermore, to ascertain if the selected interventions can blunt the progression of existing aneurysms and potentially lead to their regression, aneurysms were allowed to develop through Ang II infusion within the *ex vivo* bio-reactor system for 72 hours, then either recombinant TIMP-3, RXP470, or the TGF-β NAb was co-administered alongside Ang II for a further 72 hours

TIMP-3

MMPs display marked proteolytic activity and are able to degrade all major ECM components found within blood vessels [47]. TIMPs are most potent endogenous inhibitors of MMPs, and consequently the balance between MMP and TIMP levels requires tight regulation during homeostasis and alterations in the balance underlies numerous pathologies, including most cardiovascular diseases. Four TIMPs have been identified in vertebrates (TIMP-1 to 4), which form tight complexes with MMPs, blocking their activity [47]. Several studies have focused specifically on the role of TIMP-3 in aneurysm formation [185, 186]. Two independent studies showed that genetic ablation of TIMP-3 in Apoe or Ldlr-deficient mice induced aberrant vascular remodelling and abdominal aortic aneurysm formation associated with increased proteolysis and ECM degradation [185, 186]. In addition, increased expression of miR-181b in human AAA tissues correlated with a reduction in TIMP-3 levels, and restoration of TIMP-3 in mice through delivery of a miR-181b specific inhibitor suppressed aortic aneurysm development and progression [186]. In addition, TIMP-3 mRNA expression is reduced in Apoe-deficient mice treated with Ang II for 4 weeks alongside cigarette smoke exposure, a known AAA risk factor [336]. In conclusion, the above findings provide support for a beneficial

effect of TIMP-3 on aneurysms, and similar favourable effects should be replicated in a prospective ex vivo model of aneurysm.

Inhibition of TGF-β signalling

TGF-β is a cytokine involved in several cellular functions such as proliferation, adhesion, migration and apoptosis; as well as being involved in ECM remodeling [337]. In brief and as shown in Figure 6.1, TGF-β interacts with the TGF-β type II receptor (TGFβRII). TGFβRII is auto-phosphorylated and phosphorylates the type I receptor (TGFβRI) on the cell surface and subsequently activates receptor-regulated Smads (R-Smads), including Smad2 and Smad3. Active R-Smads can then activate common-partner Smads (Co-Smads) such as Smad4, triggering translocation of the complex to the nucleus to regulate the transcription of specific target genes including certain MMPs [338, 339]. Several studies in mouse models have shown activation of the TGF-β signaling pathway during the progression of AAA compared to control mice [77, 80, 340]. *King et al.* used a neutralising antibody to block CXCL10-dependent TGF-β activity in the Ang II-infused Apoe-deficient mouse model, which resulted in reduced abdominal aortic dilatation [77]. Similarly, Habashi *et al.* showed increased in TGF-β signalling in a AAA-susceptible Marfan syndrome mouse model, and that systemic delivery of a TGF-β NAb reduced AAA severity [80]. Another study focused on human sections of aortic aneurysmal tissue compared to healthy tissue and revealed heightened TGF-β activity in aneurysmal tissue which was linked to decreased proliferation and increased apoptosis of VSMCs and associated dilatation observed in AAA samples [340]. However other studies have proposed a protective role of TGF-β in AAA development, particularly in the presence of marked inflammation [341]. This crucial discrepancy on the role of TGF-β requires further studies to better clarify its role in aneurysm formation and progression, particularly between non-inflamed and inflamed variations of the pathology. Nonetheless, effects of TGF-β neutralisation is a valid approach to test the validity of novel aneurysm models.

MMP-12 inhibition

MMP-12 is a member of the MMP family and formerly known as macrophage metalloelastase and suggested to play a prominent role in aneurysm formation and rupture. In healthy blood vessels MMP activity is largely regulated by TIMPs, however several studies have shown that in response to injury there is an imbalance between MMPs and TIMPs, favouring MMP activity and subsequent aneurysm formation [256]. Accordingly, investigators have aimed to identify which MMPs are increased within the aneurysmal aortic wall, and as such numerous studies have discerned MMP-12 expression to correlate with aneurysm formation and therefore represent a therapeutic target [179, 342, 343]. Using the peri-aortic $CaCl_2$ application mouse model, *Longo et al*. demonstrated reduced aortic dilatation in MMP12-deficient mice compared

to wild-type controls, suggesting MMP-12 contributes to aneurysm growth [179]. In humans, aortic wall MMP-12 activity was shown to be increased in aortic dissection patients compared to healthy controls. Similarly, serum concentration of MMP-12 followed the same pattern, being higher in aortic dissection patients [342]. While Annabi *et al.* also found the activity of MMP-12, together with MMP-1 and MMP-9, was increased in patients with AAA, compared to healthy individuals [343]. Finally, Di Gregoli *et al.* demonstrated that administration of the MMP-12 inhibitor RXP470 to AAA-susceptible reduced rates of aneurysm expansion and rupture [186]. Collectively, these findings support using MMP-12 inhibition as an effective strategy to retard aneurysm formation and therefore test potential new experimental models of aneurysm.

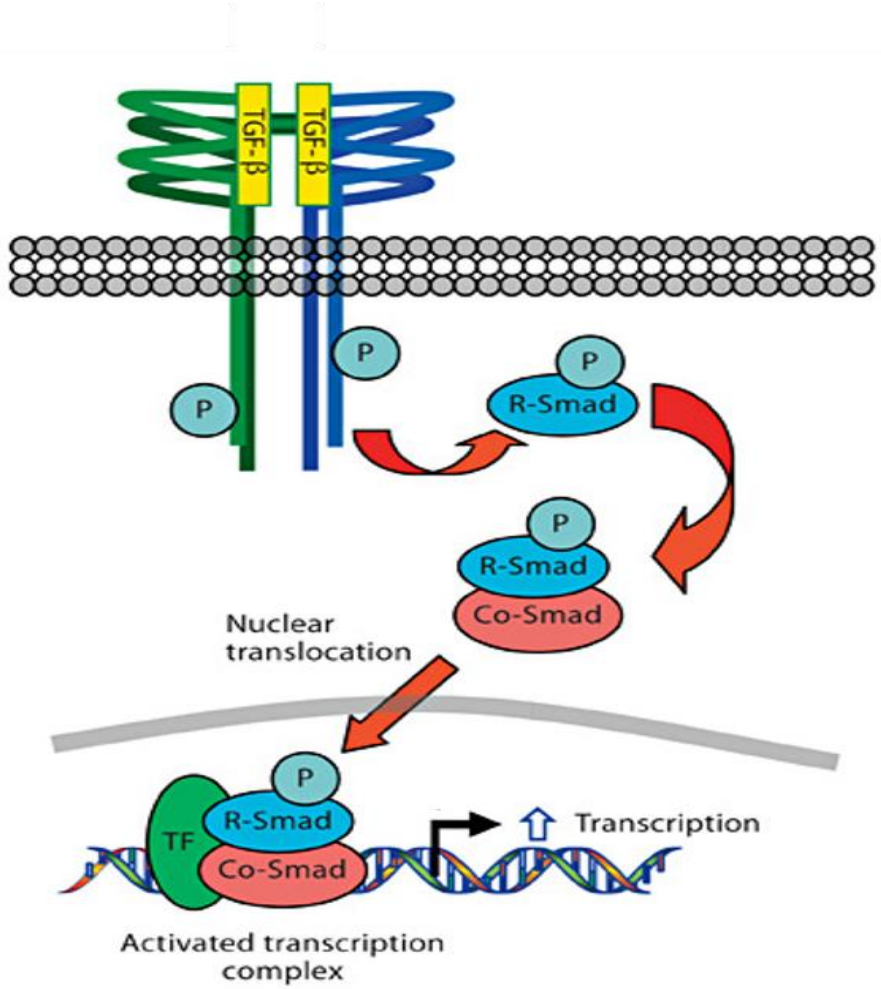

Figure 6.1: TGF-β classical signalling pathway

TGF-β binds a homodimer of the type II receptor (green) that then becomes auto-phosphorylated and subsequently phosphorylates the type I receptor (blue). This activates the smad pathway (a receptor (R)-Smad that binds and activates common (Co)-Smad), which then translocates into the nucleus and induces gene transcription. Figure modified from Jones et al. 2009 [337].

6.2 Aim of this chapter

The aim of this chapter was to characterise and validate an *ex vivo* aneurysm model by using strategies that have been previously shown to be effective in mouse models of aneurysm formation and rupture. Therefore, specific inhibitors of MMP activity and TGF-β signalling were introduced within the system. Additionally, the same interventions were added to the system after aneurysms had been allowed to develop within umbilical cord arteries (3 days treatment with Ang II), to assess the role of the interventions on established aneurysms in an attempt to stop progression, or even promote regression.

6.3 Results

6.3.1 Validation of an *ex vivo* model of aneurysm formation

6.3.1.1 Ex vivo model of aneurysm formation with TIMP-3/Ang II co-administration compared to Ang II alone

This study evaluated whether the addition of TIMP-3 within the bio-reactor system could retard Ang II-induced aneurysm formation, analogous to the *in vivo* mouse findings. Indeed, co-incubation of 5nM recombinant TIMP-3 (rTIMP-3) retarded Ang II-induced medial thinning in umbilical cord arteries, resulting in a significant increase in medial thickness compared to control vessels (97%, $p<0.01$; n=5; Figure 6.2). In addition, rTIMP-3 prevented Ang II-induced elastin loss, as elastin content was increased in Ang II-infused treated with rTIMP-3 compared to Ang II alone, (169%, $p<0.05$; n=5; Figure 6.3). Finally, TIMP-3 also retarded the vessel dilatation induced by Ang II, as evidenced by a significant decrease in total vessel area in rTIMP 3 treated Ang II-infused arteries compared to Ang II alone (42%, $p<0.05$; n=5; Figure 6.4).

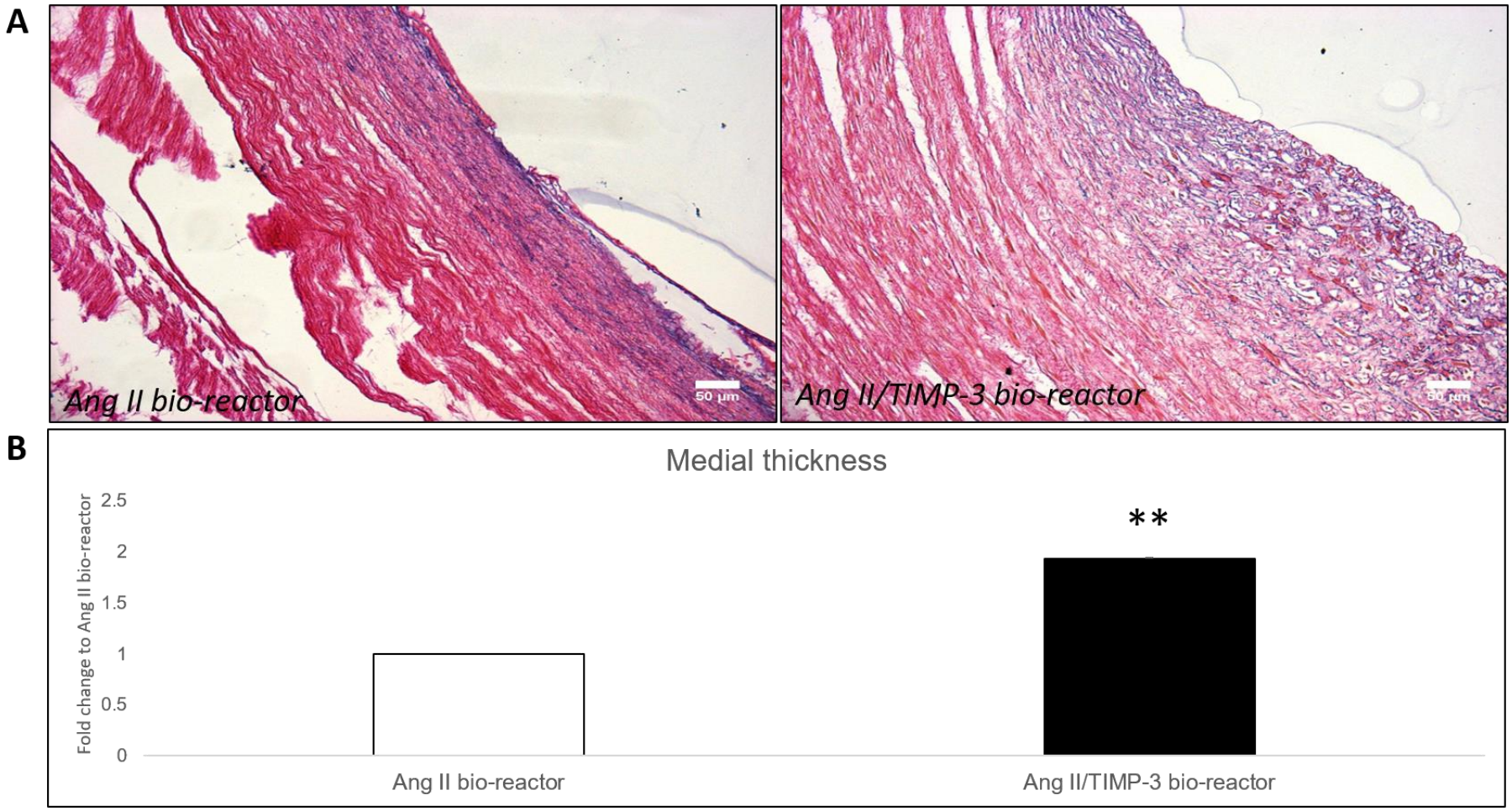

Figure 6.2: Co-administration of TIMP-3 reduced Ang II-induced medial thinning

*Representative images (A) and quantification (B) of medial thickness assessed in ten x20 magnification fields of EVG stained sections from human umbilical cord arteries after incubation within a bio-reactor for 72 hours with Ang II (Ang II bio-reactor) or with Ang II and 5nM rTIMP-3 (Ang II/TIMP-3 bio-reactor). Data is expressed as a fold change in medial thickness of the Ang II/TIMP-3 treated arteries compared to Ang II treated arteries (mean±SEM; n=5). ** denotes p<0.01 versus Ang II alone, 2-tailed Student paired t test. Scale bars represent 50 µm.*

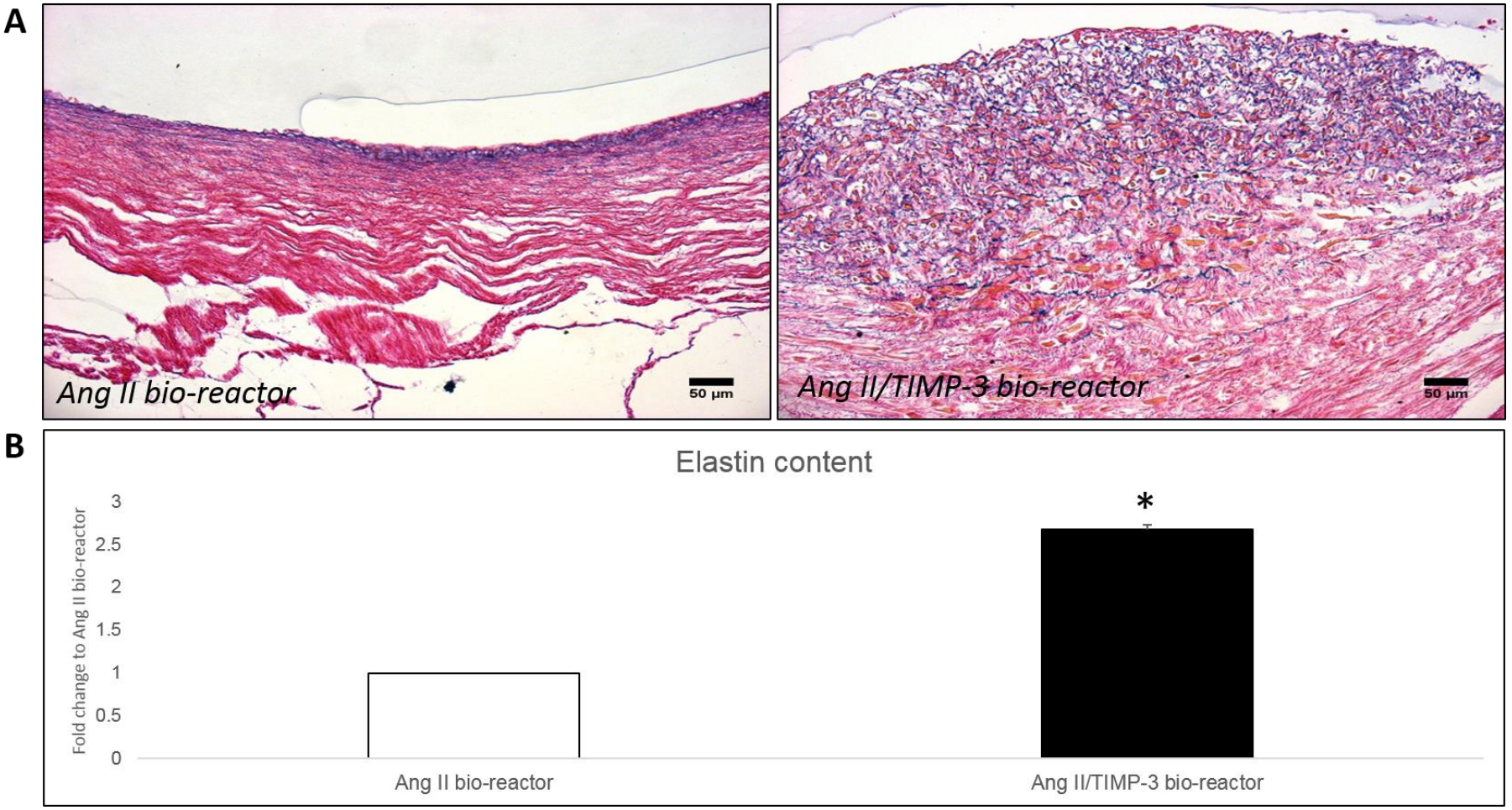

Figure 6.3: Co-administration of TIMP-3 prevented Ang II-induced loss of elastin content

*Representative images (A) and quantification (B) of elastin content assessed in ten x20 magnification fields of EVG stained sections from human umbilical cord arteries after incubation within a bio-reactor for 72 hours with Ang II (Ang II bio-reactor) and with Ang II or 5 nM rTIMP-3 (Ang II/TIMP-3 bio-reactor). Data is expressed as a fold change in elastin content of the Ang II/TIMP-3 treated arteries compared to Ang II treated arteries (mean±SEM; n=5). ** denotes p<0.01 versus Ang II alone, 2-tailed Student paired t test. Scale bars represent 50 µm.*

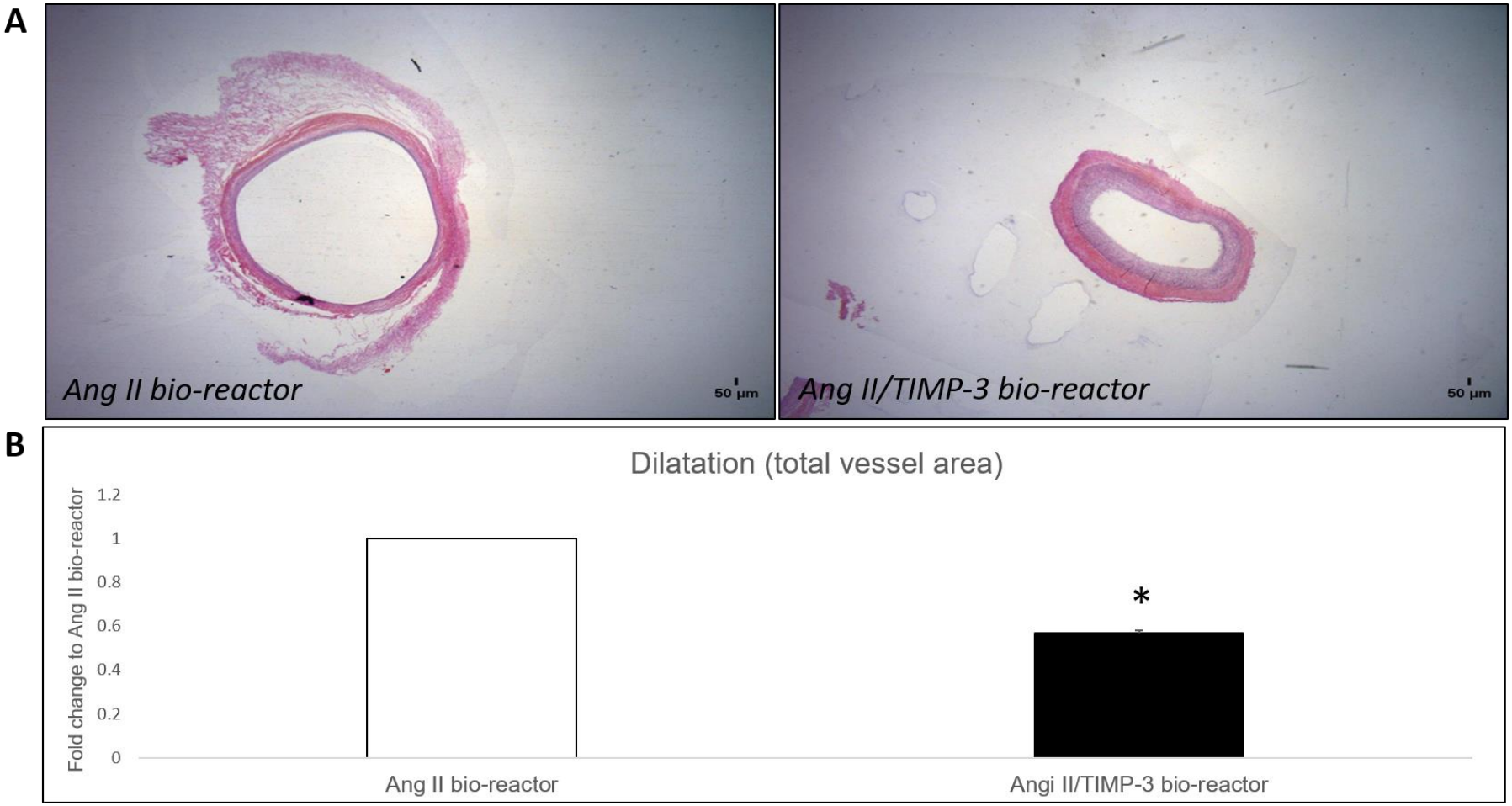

Figure 6.4: Co-administration of TIMP-3 suppressed Ang II-induced dilatation

*Representative images (A) and quantification (B) of dilatation (total vessel area) assessed in ten x1.25 magnification fields of EVG stained sections from human umbilical cord arteries after incubation within a bio-reactor for 72 hours with Ang II (Ang II bio-reactor) or with Ang II and 5nM rTIMP-3 (Ang II/TIMP-3 bio-reactor). Data is expressed as a fold change in total vessel area of the Ang II/TIMP-3 treated arteries compared to Ang II treated arteries (mean±SEM; n=5). * denotes p<0.05 versus Ang II alone, 2-tailed Student paired t test. Scale bars represent 50 µm.*

6.3.1.2 Ex vivo model of aneurysm formation with TGF-β NAb/Ang II co-administration compared to Ang II alone

The effect of inhibiting the TGF-β signaling pathway was next assessed in order to further validate the *ex vivo* model of aneurysm. As shown in Figure 6.5, human umbilical cord arteries subjected to co-incubation of Ang II (5μM) and a TGF-β neutralising antibody (TGF-β NAb) (0.25μg/ml) under a pulsatile laminar flow rate of 6.5 dynes/cm^2 for 72 hours, significantly retarded Ang II-induced medial thinning as evidenced by an increase in medial thickness compared to Ang II alone arteries (124%; $p<0.05$; n=5). Furthermore, umbilical cord artery elastin content was increased within Ang II/TGF-β NAb co-treated vessels compared to arteries exposed to Ang II alone (214%; $p<0.05$; n=5; Figure 6.6). Finally, Ang II/TGF-β NAb co-incubation blunted vessel dilatation, as observed through a decrease in total vessel area in comparison to Ang II-treated arteries (33%; $p<0.01$; n=5; Figure 6.7).

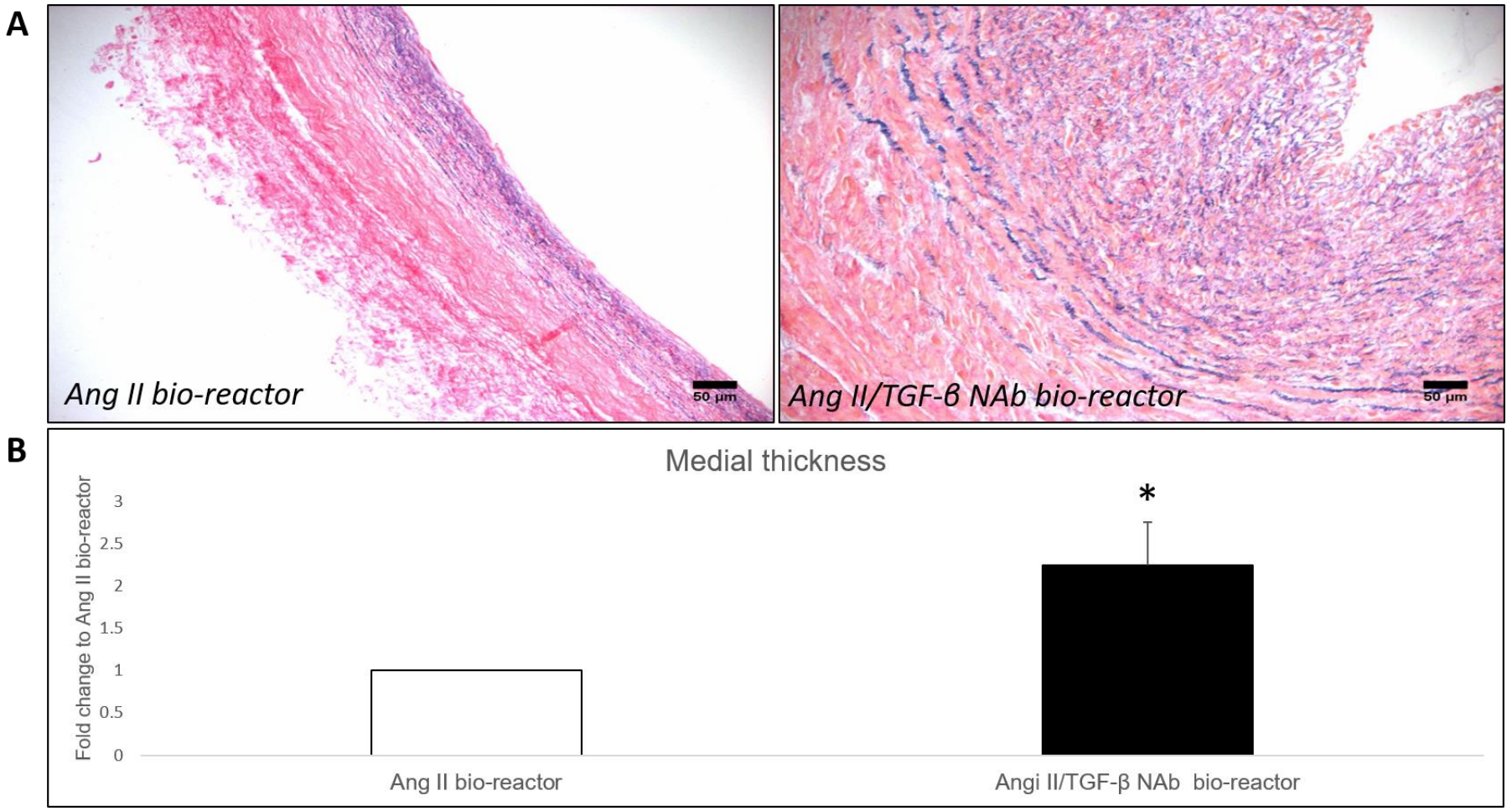

Figure 6.5: Co-administration of a TGF-β NAb reduced Ang II-induced medial thinning

*Representative images (A) and quantification (B) of medial thickness assessed in ten x20 magnification fields of EVG stained sections from human umbilical cord arteries after incubation within a bio-reactor for 72 hours with Ang II (Ang II bio-reactor) or with Ang II and 250ng/ml TGF-β neutralising antibody (Ang II/ TGF-β NAb bio-reactor). Data is expressed as a fold change in medial thickness of the Ang II/ TGF-β NAb treated arteries compared to Ang II treated arteries (mean±SEM; n=5). * denotes $p<0.05$ versus Ang II alone, 2-tailed Student paired t test. Scale bars represent 50 µm.*

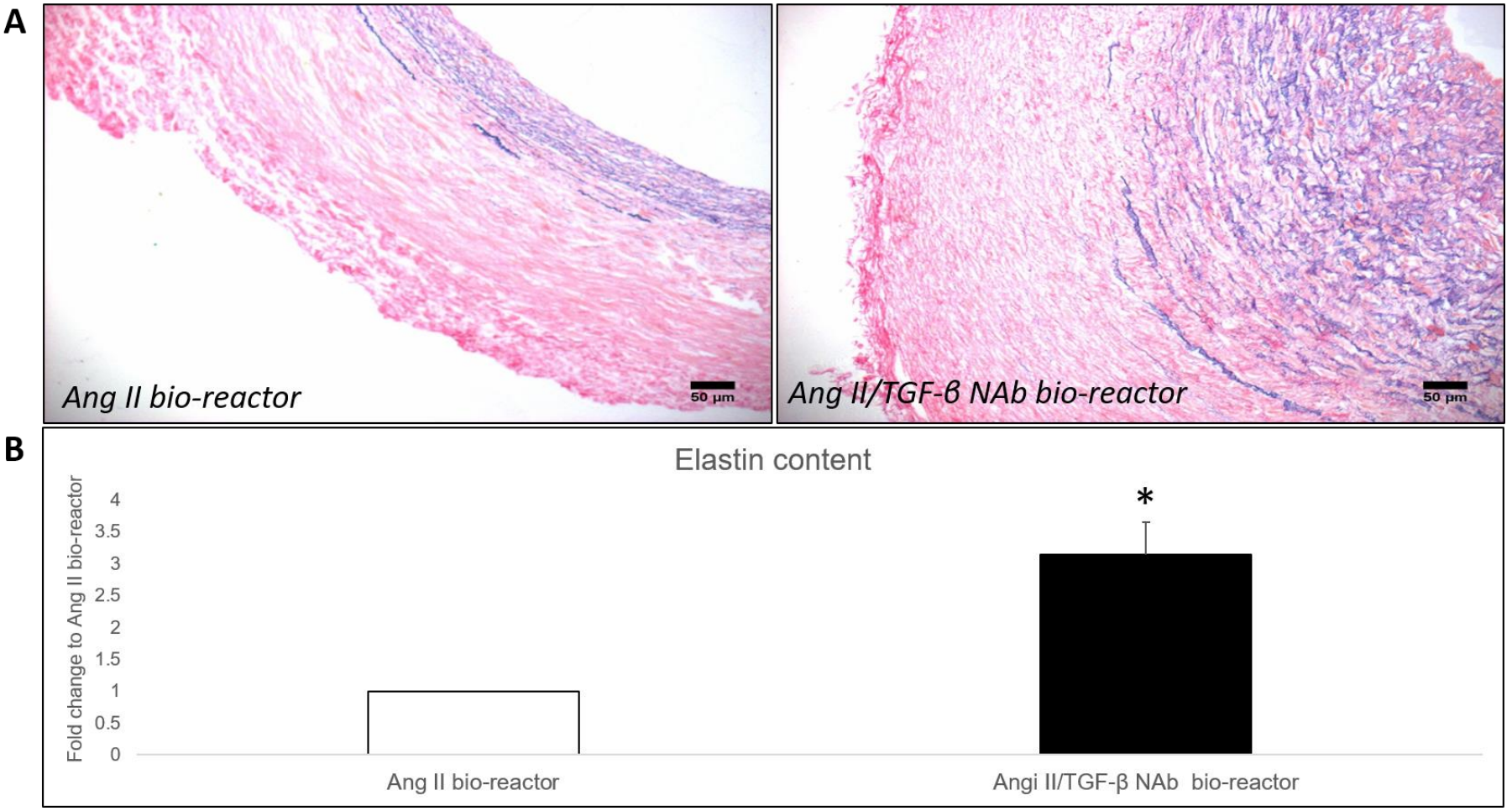

Figure 6.6: Co-administration of a TGF-β NAb prevented Ang II-induced loss of elastin content

*Representative images (A) and quantification (B) of elastin content assessed in ten x20 magnification fields of EVG stained sections from human umbilical cord arteries after incubation within a bio-reactor for 72 hours with Ang II (Ang II bio-reactor) or with Ang II and 250ng/ml TGF-β neutralising antibody (Ang II/ TGF-β NAb bio-reactor). Data is expressed as a fold change in elastin content of the Ang II/ TGF-β NAb treated arteries compared to Ang II treated arteries (mean±SEM; n=5). * denotes p<0.05 versus Ang II alone, 2-tailed Student paired t test. Scale bars represent 50 µm.*

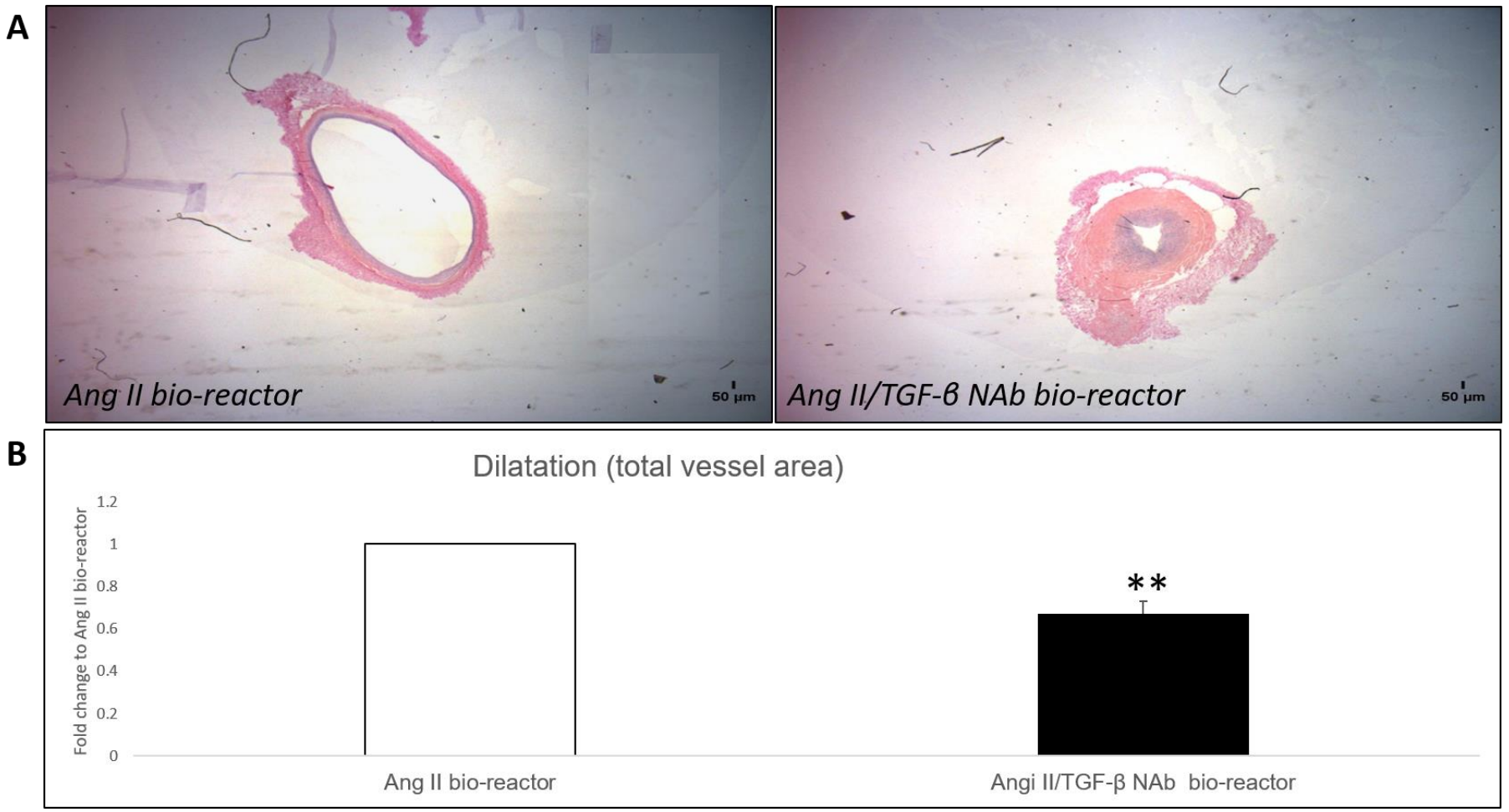

Figure 6.7: Co-administration of a TGF-β NAb suppressed Ang II-induced dilatation

*Representative images (A) and quantification (B) of dilatation (total vessel area) in ten x1.25 magnification fields of EVG stained sections from human umbilical cord arteries after incubation within a bio-reactor for 72 hours with Ang II (Ang II bio-reactor) or with Ang II and 250ng/ml TGF-β neutralising antibody (Ang II/ TGF-β NAb bio-reactor). Data is expressed as a fold change in total vessel area of the Ang II/ TGF-β NAb treated arteries compared to Ang II treated arteries (mean±SEM; n=5). ** denotes p<0.01 versus Ang II alone, 2-tailed Student paired t test. Scale bars represent 50 µm.*

6.3.1.3 Ex vivo model of aneurysm formation with MMP-12 inhibitor (RXP470) /Ang II co-administration compared to Ang II alone

The third intervention deployed to validate the *ex vivo* model of aneurysm, based on findings in mouse models of aneurysm formation, was administration of a selective MMP-12 inhibitor termed RXP470.Accordingly, human umbilical cord arteries were treated with a combination of Ang II (5µM) and RXP470 (10nM) under pulsatile laminar flow conditions with a flow rate of 6.5 dynes/cm^2 for 72 hours. As shown in Figure 6.8, RXP470 inhibited Ang II-induced medial thinning as evidenced by significantly increasing the medial thickness of umbilical cord arteries infused with Ang II, compared to Ang II alone (74%; $p<0.05$; n=5; Figure 6.8). Additionally, RXP470 administration reversed Ang II-induced elastin loss, as evidenced through increased elastin content within RXP470-treated vessels compared to Ang II alone (141%; $p<0.05$; n=5; Figure 6.9). Finally, MMP-12 inhibition by use of RXP470 retarded Ang II-induced arterial dilatation, as observed by a decrease in total vessel area of Ang II/RXP470 co-treated arteries compared to the Ang II treated vessels (33%; $p<0.001$; n=5; Figure 6.10).

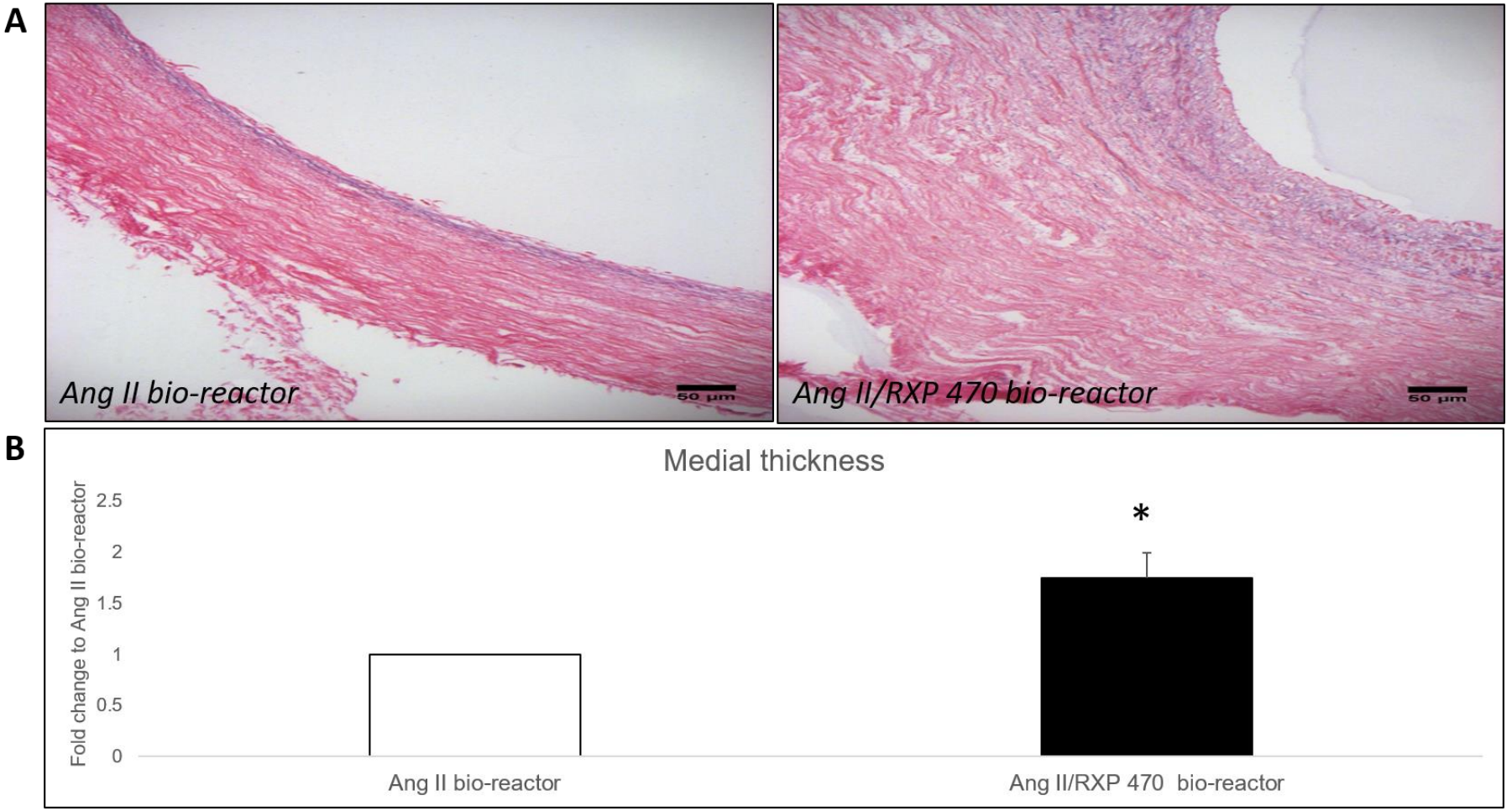

Figure 6.8: Co-administration of RXP470 reduced Ang II-induced medial thinning

*Representative images (A) and quantification (B) of medial thickness assessed in ten x20 magnification fields of EVG stained sections from human umbilical cord arteries after incubation within a bio-reactor for 72 hours with Ang II (Ang II bio-reactor) or with Ang II and 10nM RXP470 (Ang II/RXP470). Data is expressed as a fold change in medial thickness of the Ang II/ RXP470 treated arteries compared to Ang II treated arteries (mean±SEM; n=5). * denotes $p<0.05$ versus Ang II alone, 2-tailed Student paired t test. Scale bars represent 50 µm.*

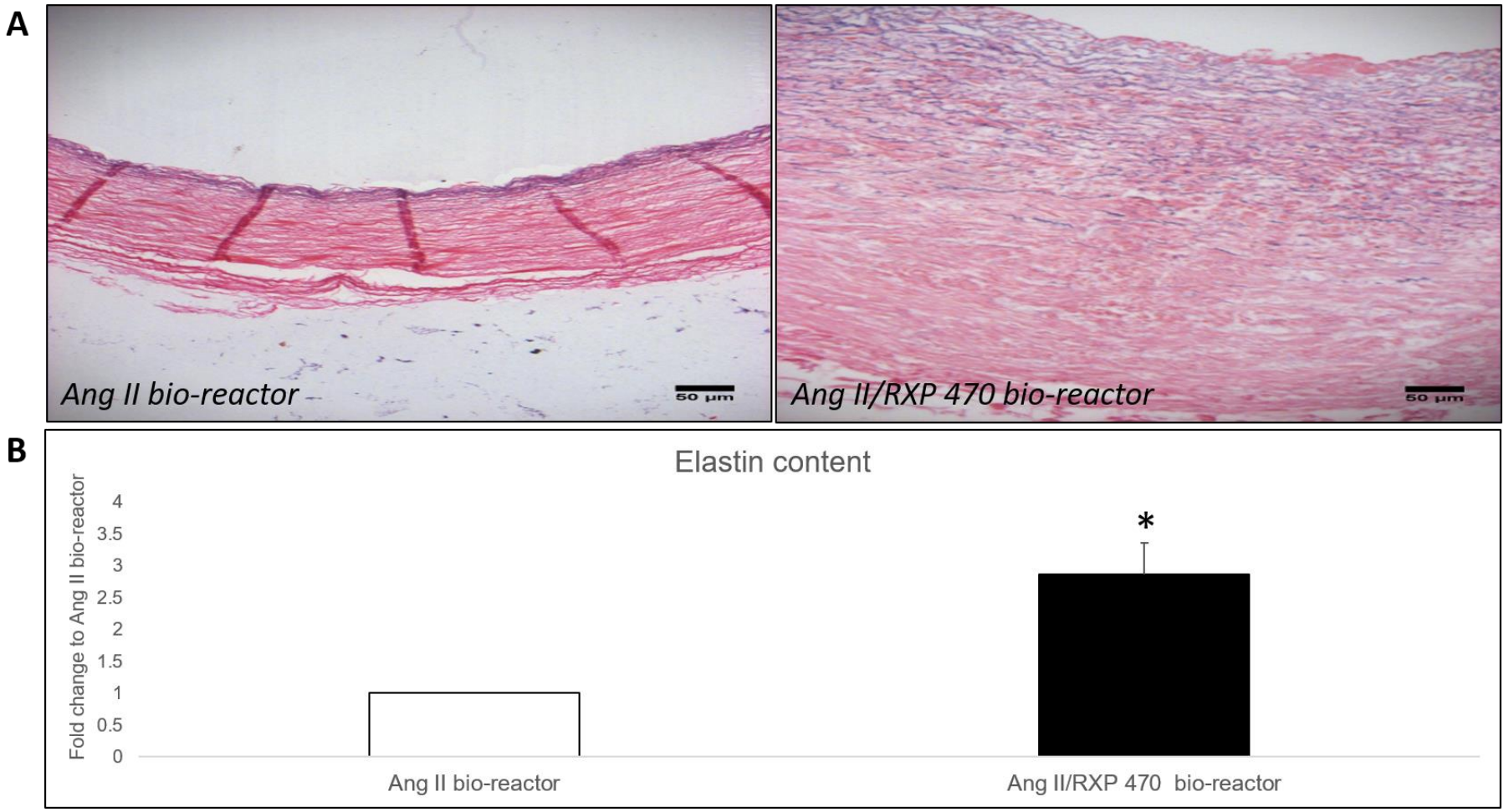

Figure 6.9: Co-administration of RXP470 prevented Ang II-induced loss of elastin content

Representative images (A) and quantification (B) of elastin content assessed in ten x20 magnification fields of EVG stained sections from human umbilical cord arteries after incubation within a bio-reactor for 72 hours with Ang II (Ang II bio-reactor) or with Ang II and 10nM RXP470(Ang II/RXP470). Data is expressed as a fold change in elastin content of the Ang II/ RXP470 treated arteries compared to Ang II treated arteries (mean±SEM; n=5).
** denotes p<0.05 versus Ang II alone, 2-tailed Student paired t test. Scale bars represent 50 µm.*

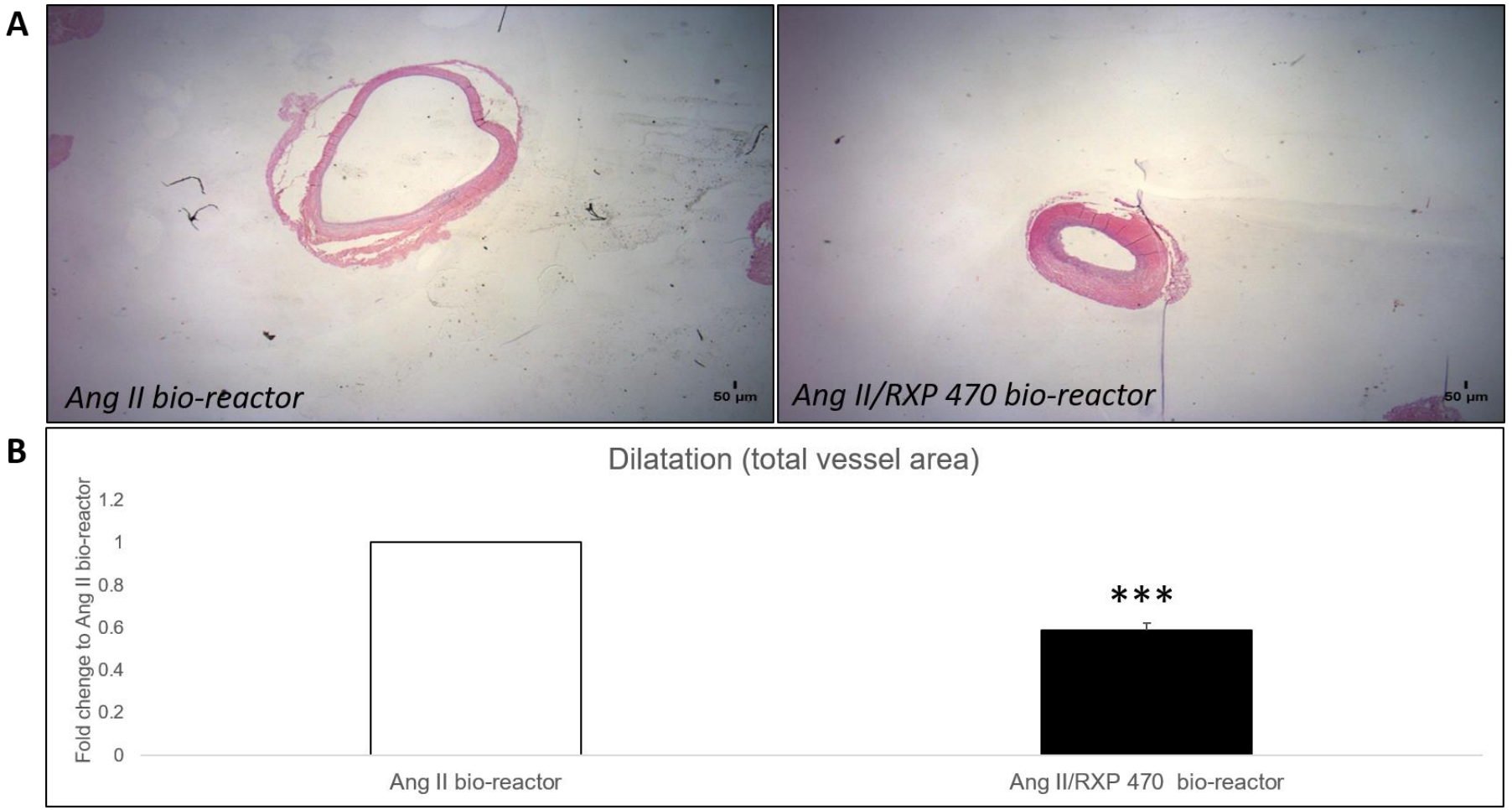

Figure 6.10: Co-administration of RXP470 suppressed Ang II-induced dilatation

*Representative images (A) and quantification (B) of dilatation (total vessel area) assessed in ten x1.25 magnification fields of EVG stained sections from human umbilical cord arteries after incubation within a bio-reactor for 72 hours with Ang II (Ang II bio-reactor) or with Ang II and 10nM RXP470 (Ang II/RXP470). Data is expressed as a fold change in total vessel area of the Ang II/ RXP470 treated arteries compared to Ang II treated arteries (mean±SEM; n=5). *** denotes p<0.001 versus Ang II alone, 2-tailed Student paired t test. Scale bars represent 50 µm.*

6.3.2 Therapeutic testing in an *ex vivo* model of established aneurysm formation

The three interventions assessed above (rTIMP-3, a TGF-β NAb, and the selective MMP-12 inhibitor RXP470) for their ability to retard aneurysm formation within the *ex vivo* model were additionally evaluated within the bio-reactor system on umbilical cord arteries with existing aneurysms (three days post Ang II-infusion), to determine if they could halt progression and even regress Ang II-induced aneurysm formation. In brief, human umbilical cord arteries were cut into five equal pieces and subjected to Ang II (5μM) under pulsatile laminar flow conditions with a flow rate of 6.5 dynes/cm^2 for 72 hours. After 72 hours media was changed and four pieces were treated respectively with: Ang II (5μM) only, Ang II + rTIMP-3 (5nM), Ang II + TGF-β NAb (250ng/ml), or Ang II + RXP470 (10nM). The fifth piece of artery was kept after 72 hours as a baseline control. All four arteries were then placed in a bio-reactor for an additional 72 hours before collection for the following parameters; total vessel area, medial thickness, elastin content and cell density.

As shown in Figure 6.11, the medial thickness within six day Ang II-infused umbilical cord arteries was not significantly altered with any of the three interventions assessed (rTIMP-3,TGF-β NAb, and RXP470), when compared to Ang II only (at three or six days; n=5; Figure 6.11). Although TGF-β NAb or RXP470 supplementation also failed to halt Ang II-induced elastin loss in six day-infused arteries, rTIMP-3 co-administration significantly increased cord artery elastin content, when compared to both three and six day Ang II-treated controls ($p<0.05$; n=5; Figure 6.12). With regards to dilatation, while rTIMP-3 and TGF-β NAb treatments were ineffective, MMP-12 inhibition with RXP470 administration surprisingly increased total vessel area when compared to Ang II alone arteries at both time points ($p<0.05$; n=5, Figure 6.13). Similar to elastin loss, medial cell density was increased in rTIMP-3 co-treated vessels compared to Ang II only at both three and six day incubation ($p<0.01$; n=5; Figure 6.14), whereas no change was observed with either TGF-β NAb or RXP470 treatment. Interestingly and as shown in Figure 6.11, Figure 6.12 and Figure 6.13, none of the four parameters assessed were significantly affected by prolonged Ang II infusion, as observed by comparing three day and six day Ang II treated arteries.

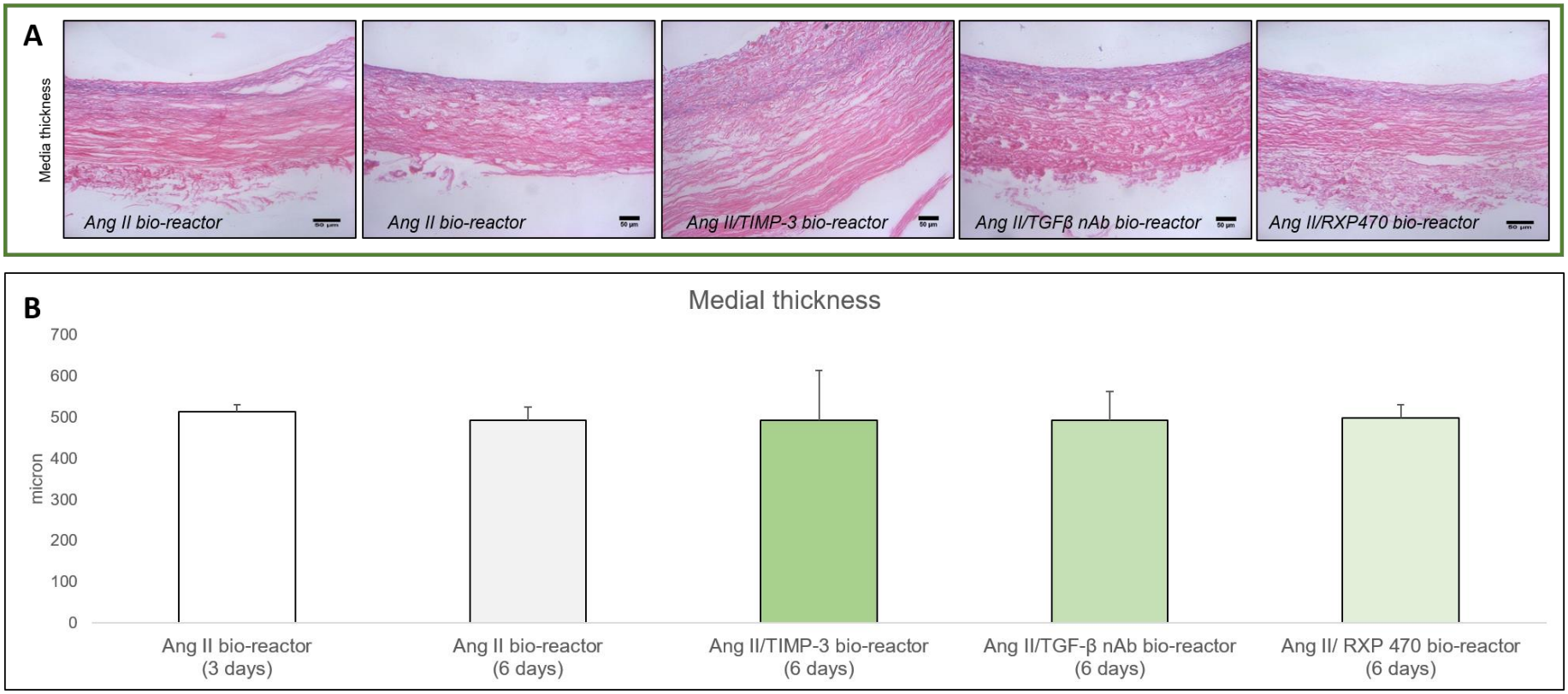

Figure 6.11: Effect of rTIMP-3, TGF-β NAb, or RXP470 co-administration on six-day Ang II-induced ex vivo aneurysm medial thickness

Representative images (A) and quantification (B) of medial thickness assessed in ten x 20 magnification fields of EVG stained sections from human umbilical cord arteries after incubation within a bio-reactor for 3 or 6 days with Ang II (Ang II bio-reactor 3 days and Ang II bio-reactor 6 days, respectively), or Ang II for first 3 days followed by Ang II plus either rTIMP-3 (Ang II/TIMP-3@5nM), TGF-β NAb (Ang II/TGF-β NAb@250ng/ml), or RXP470 (Ang II/RXP470@10nM) for a further 3 days. Data is expressed as average medial thickness. (mean±SEM; n=5). Scale bars represent 50 µm. p>0.05 versus Ang II alone at 3 days and 6 days, repeated measures ANOVA. Scale bars represent 50 µm.

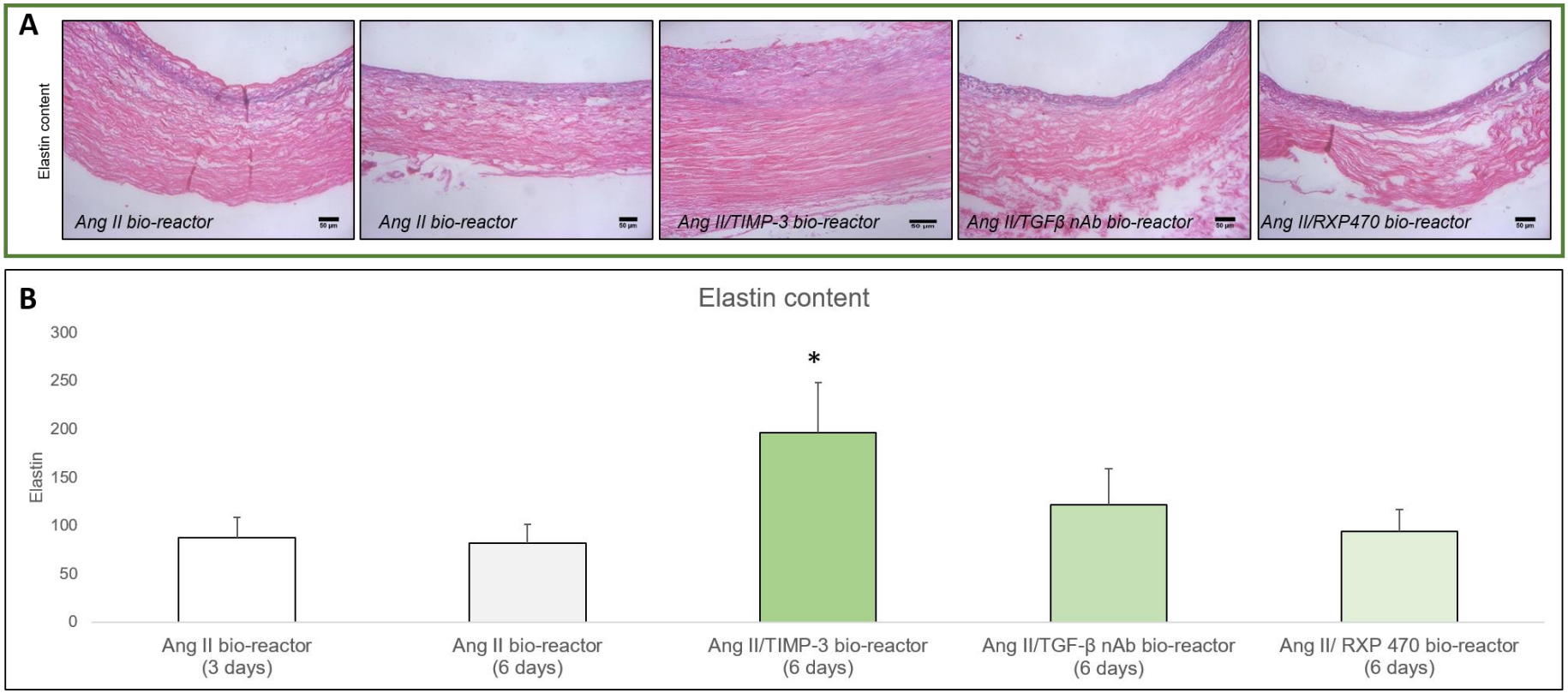

Figure 6.12: Effect of rTIMP-3, TGF-β NAb, or RXP470 co-administration on six-day Ang II-induced ex vivo aneurysm elastin content

*Representative images (A) and quantification (B) of elastin content assessed in ten x 20 magnification fields of EVG stained sections from human umbilical cord arteries after incubation within a bio-reactor for 3 or 6 days with Ang II (Ang II bio-reactor 3 days and Ang II bio-reactor 6 days, respectively), or Ang II for first 3 days followed by Ang II plus either rTIMP-3 (Ang II/TIMP-3@5nM), TGF-β NAb (Ang II/TGF-β NAb@250ng/ml), or RXP470 (Ang II/RXP470@10nM) for a further 3 days. Data is expressed as average elastin content. (mean±SEM; n=5). * denotes p<0.05 versus Ang II alone at 3 days and 6 days, repeated measures ANOVA. Scale bars represent 50 µm.*

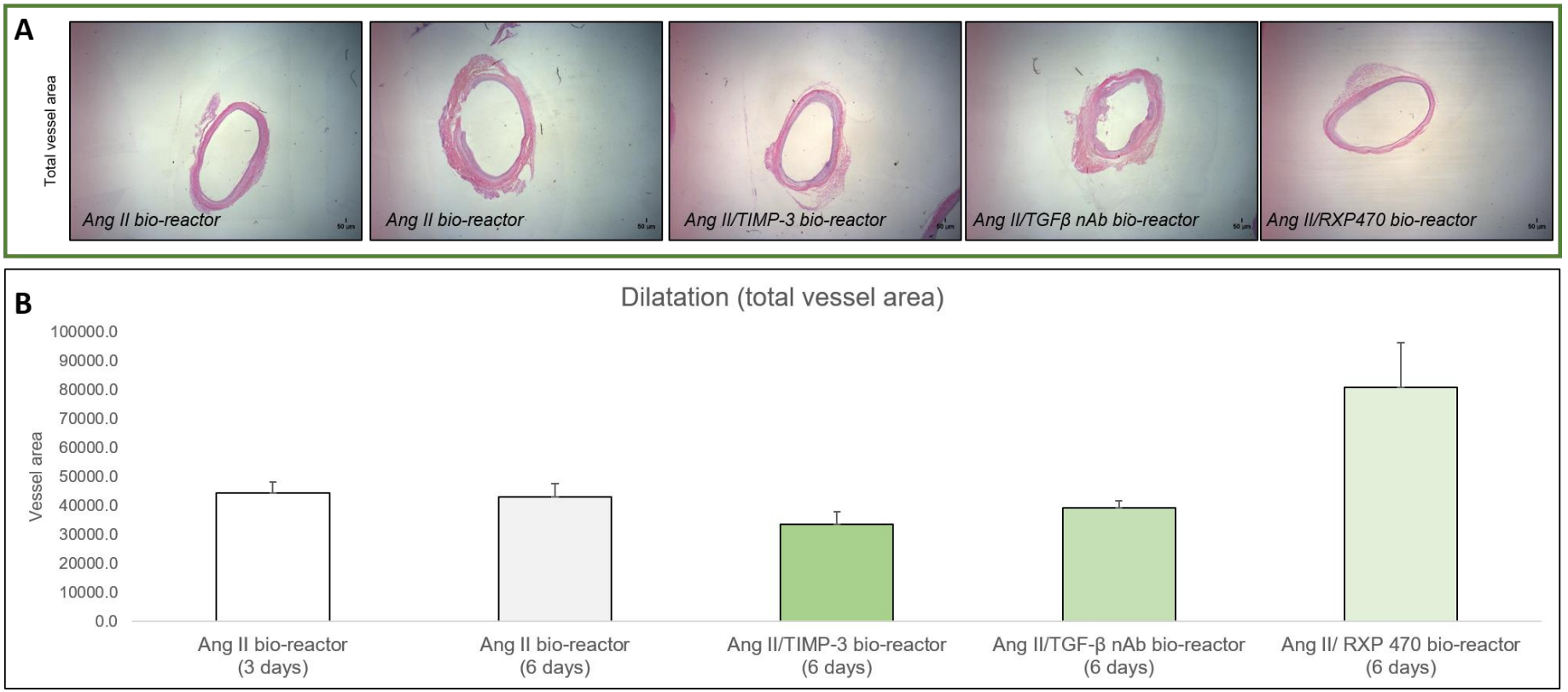

Figure 6.13: Effect of rTIMP-3, TGF-β NAb, or RXP470 co-administration on six-day Ang II-induced ex vivo aneurysm dilatation

*Representative images (A) and quantification (B) of total vessel area assessed in ten x 20 magnification fields of EVG stained sections from human umbilical cord arteries after incubation within a bio-reactor for 3 or 6 days with Ang II (Ang II bio-reactor 3 days and Ang II bio-reactor 6 days, respectively), or Ang II for first 3 days followed by Ang II plus either rTIMP-3 (Ang II/TIMP-3@5nM), TGF-β NAb (Ang II/TGF-β NAb@250ng/ml), or RXP470 (Ang II/RXP470@10nM) for a further 3 days. Data is expressed as average total vessel area. (mean±SEM; n=5). * denotes p<0.05 versus Ang II alone at 3 days and 6 days, repeated measures ANOVA. Scale bars represent 50 µm.*

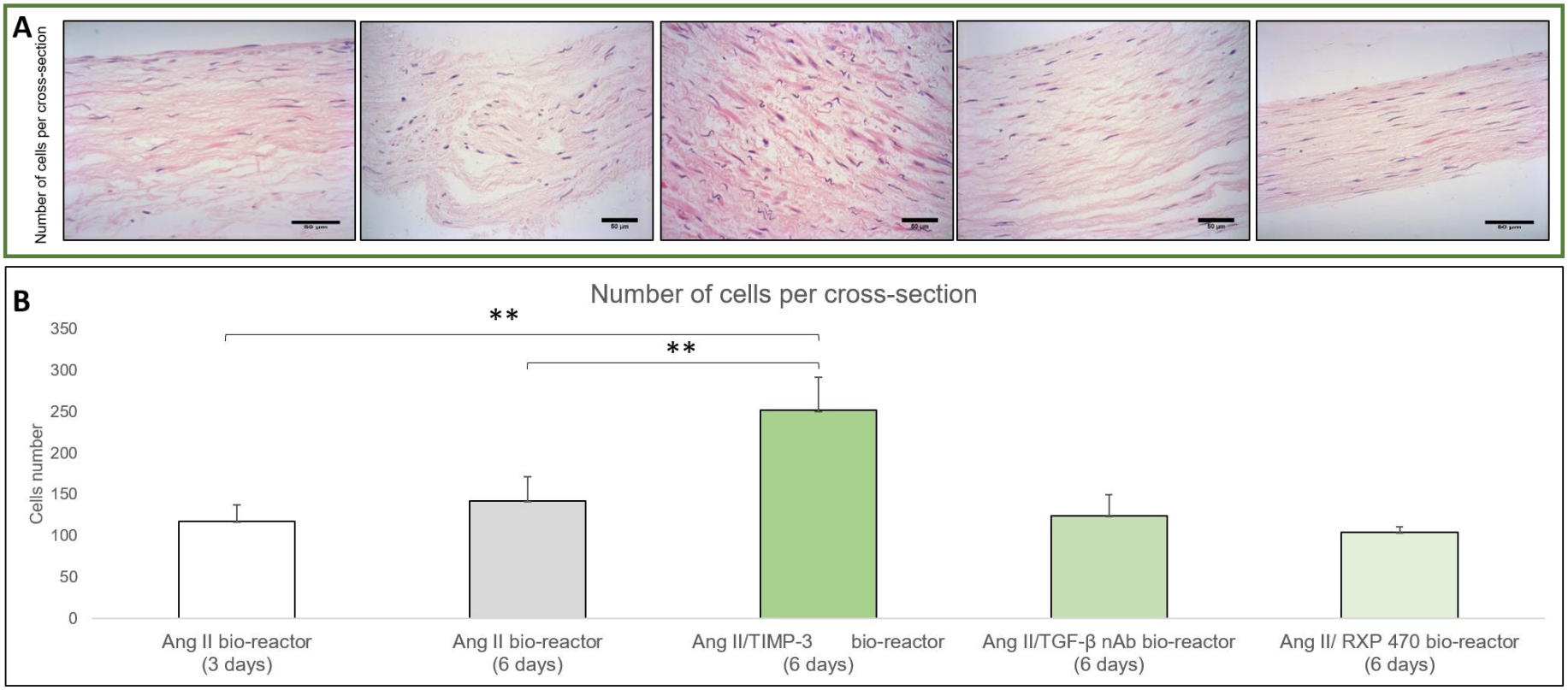

Figure 6.14: Effect of rTIMP-3, TGF-β NAb, or RXP470 co-administration on six-day Ang II-induced ex vivo aneurysm cell density

*Representative images (A) and quantification (B) of medial cell number (cell density) assessed in ten x 20 magnification fields of H&E stained sections from human umbilical cord arteries after incubation within a bio-reactor for 3 or 6 days with Ang II (Ang II bio-reactor 3 days and Ang II bio-reactor 6 days, respectively), or Ang II for first 3 days followed by Ang II plus either rTIMP-3 (Ang II/TIMP-3@5nM), TGF-β NAb (Ang II/TGF-β NAb@250ng/ml), or RXP470 (Ang II/RXP470@10nM) for a further 3 days. Data is expressed as average cell density. (mean±SEM; n=5). ** denotes p<0.01 versus Ang II alone at 3 days and 6 days, repeated measures ANOVA. Scale bars represent 50 µm.*

6.4 Conclusion

The first aim of this chapter was to characterise and validate the *ex vivo* aneurysm model through the use of interventions shown to be effective in mouse models of aneurysm formation. Firstly, co-incubation with TIMP-3 and Ang II for 72 hours within a bio-reactor significantly increased umbilical artery medial thickness, increased elastin content, and reduced the medial cell loss along with the reduction in vessel area. Similarly, inhibition of either TGF-β or MMP-12 exerted similar protective effects. The observed morphological and compositional changes induced by these three strategies within the *ex vivo* model are consistent with those observed in the mouse model, supporting use of the *ex vivo* model for future aneurysm formation studies. A further aim of this chapter was to investigate whether deployment of the above interventions could halt aneurysm progression and even regress aneurysms which had already developed, as is currently required in the clinical setting. In contrast to its beneficial effects on aneurysm formation, TGF-β neutralisation was ineffective on pre-existing aneurysms within the *ex vivo* model, although evidence in the literature supports divergent effects of TGF-β perturbation on aneurysms at different stages and phenotypes. Similarly, despite advantageous effects during aneurysm development, MMP-12 inhibition also failed to apply beneficial effects on pre-existing aneurysms, and unexpectedly increased vessel dilatation. However, unpublished findings in mice from our laboratory have shown similar contrasting effects on aneurysms which is influenced by vascular bed and level of inflammation. Finally, despite no change in medial thickness or dilatation of human umbilical cord arteries with TIMP-3 addition, both the loss of elastin content and diminished cell density were reversed by TIMP-3 in established aneurysm, mirroring such beneficial effects during aneurysm formation. Endorsing these findings, stabilisation of pre-existing aneurysms in mice with TIMP-3 over-expression (through miR-181b inhibition) was largely due to increased elastin content and associated with lowered frequencies of apoptosis [186]. As such, for future therapeutic studies to stabilise existing aneurysms (or even prevent development), strategies to restore or over-express TIMP-3 hold most promise. Moreover, the effects of the selected interventions in the *ex vivo* aneurysm model are largely in agreement with those reported within animal models, validating the use of the model for aneurysm studies, before moving into animal systems or replacing them completely.

6.5 Discussion

Mouse models of aneurysm formation have been widely used to elucidate the molecular pathways underlying aneurysm formation and rupture [127]. Furthermore, many additional experiments have been performed in mice assessing interventions for their potential to block aneurysm progression and ideally be as therapeutics for existing aneurysms in an effort to stabilise and even regress the disease [80, 160, 186]. While potentially furthering our knowledge on aneurysm formation and progression and identifying novel therapeutic avenues, such experiments use a large number of mice, many of which will suffer sudden death, and therefore raise issues around ethical use of animals in scientific research. Indeed, routinely an experiment testing a novel molecule for therapeutic intervention, will require three groups of mice in order to assess at least three different concentrations to determine the best dose to be used in subsequent large animal experiments or clinical trials in humans. Consequently, this equates to roughly 50 mice merely for testing one inhibitor. The studies within this Chapter were undertaken to determine if the novel *ex vivo* Ang II-infusion aneurysm model could be validated and support its use in future aneurysm studies. Additionally, inhibitors were utilised to assess potential modulation of aneurysm progression and even regression of aneurysms which had already developed. The main hypothesis of this Chapter was therefore that interventions shown to be effective at suppressing aneurysm formation within mouse models of aneurysm would also be successful within the *ex vivo* Ang II-infused human umbilical cord artery model. The interventions should create the same morphological and cellular changes in an *ex vivo* aneurysm model in order to characterise and validate its potential. The identification of a novel human *ex vivo* model to study aneurysm formation and rupture could reduce and subsequently replace the number of mice used for aneurysm studies, addressing two of the key principles of the 3Rs.

6.5.1 TIMP-3

It has been proposed that AAA are associated with the activation of multiple signalling pathways, that correlate in irreversible ECM remodelling. However, the precise mechanisms and their potential overlap leading to such irreversible changes remain poorly characterised, although it is established that degradation of collagen and elastin contributes to the alterations within the structure of the vessel wall [16]. Furthermore, the increased expression and activity or numerous proteases, especially members of the MMP family, are thought to act as major contributors to elastin and collagen degradation. Such irreparable damage within the vessel wall is considered a key underlying process driving aneurysm progression [106]. Accordingly, strategies to dampen MMP activity within the aneurysm wall have been pursued as a potential

therapeutic option to reduce aneurysm development, progression and rupture [80, 160, 186]. Animal studies deploying broad-spectrum MMP inhibitors including hydroxamate-based compounds or tetracycline derivatives such as tetracycline, have proven effective at reducing elastin degradation and loss alongside limiting dilatation within mouse and rat AAA models [176, 189, 190, 344-347]. Additionally, genetic modulation of distinct TIMPs has similarly established the capacity of these endogenous inhibitors to suppress elastin degradation and associated aneurysm development [183-186, 348].

Specifically, several studies have focused on the role of TIMP-3 in AAA formation. Basu *et al.* demonstrated reduced collagen and elastin content within aortic aneurysms of TIMP-3 deficient mice infused with Ang II for two weeks, when compared to wild-type control animals [185]. In addition, TIMP-3-deficient mice exhibited greater aortic dilatation (50%) compared to wild type mice (20%), alongside increased disruption of their medial elastin fibres [185]. Di Gregoli *et al.* reported similar effects of TIMP-3 deletion within the Ang II infused (four weeks) Apoe-deficient AAA model [186]. Moreover, elevation of TIMP-3 levels through delivery of a miR-181b inhibitor (as miR-181b targets and down-regulates TIMP-3 expression) suppressed the occurrence of aortic aneurysm formation alongside r which was associated with increased aortic elastin content, findings additionally replicated in Ldlr-deficient mice [186] . Importantly, miR-181b inhibition and associated elevation of TIMP-3 expression attenuated the progression of pre-existing aortic aneurysms in parallel with increased elastin content and reduced dilatation [186].

In line with the above findings within animal models of aneurysm, TIMP-3 supplementation within the *ex vivo* aneurysm model exerted similar beneficial effects, as observed through preservation of arterial elastin content alongside reduced medial thinning and associated dilatation. These results support the *ex vivo* aneurysm model as a viable replacement for animal models which also use Ang II-infusion as an aneurysm inducer. However, these findings and most published studies have assessed effects of various interventions on the formation of aneurysms, whereas reports examining effects on established aneurysms are scant. Due to the asymptomatic nature of aneurysm pathogenesis and the high-risk of rupture in most serendipitously identified aneurysms, assessment of interventions to stabilise and potentially reverse existing aneurysms are required. It is therefore pertinent to determine whether the favourable effects of TIMP-3 supplementation on aneurysm formation reported in this Chapter persists in pre-existing aneurysms within the *ex vivo* aneurysm model. Although the beneficial suppression of Ang II-induced arterial dilatation and associated medial thinning during aneurysm formation afforded by TIMP-3 supplementation were lost with TIMP-3 addition to pre-existing aneurysms, preservation of elastin content persisted. Furthermore, the

decrease in medial cell density fostered by Ang II stimulation was attenuated by TIMP-3 treatment of existing aneurysmal umbilical cord arteries.

While the favourable effects of TIMP-3 on restoring elastin content within Ang II-infused cord arteries can be attributed to inhibition of MMP activity (although not directly demonstrated within this thesis), the modulation of medial cell number requires further clarification. However, it is plausible that the loss of VSMCs within Ang II-treated arteries is also a result of increased elastin degradation, as increased elastinolysis in mouse aneurysms is associated with VSMC apoptosis [221], while MMP-12 activity (and therefore elastin degradation) is also associated with vascular apoptosis [160]. As such, TIMP-3 mediated repression of MMP activity and associated elastin degradation may directly promote VSMC survival, and therefore account for the diminished loss of medial cells within the *ex vivo* model. However, rat VSMC apoptosis can be induced through non-physiological adenoviral over-expression of TIMP-3 [349]. Although studies deploying recombinant TIMP-3 have demonstrated its ability to promote survival of neurons and mesenchymal stem cells [350], while local application of recombinant TIMP-3 in a pig myocardial infarction model had no reported deleterious effects on cell viability [351]. Taking the above findings into consideration alongside the data presented in Chapters 3 and 4 demonstrating Ang II induces VSMC loss *in vitro* and *ex vivo* and rTIMP-3 supplementation prevents Ang II-induced cell loss ex vivo after three or six days, a pro-survival effect of TIMP-3 is more likely within the *ex vivo* model. The *in vitro* findings in Chapter 4 argue against an effect on VSMC proliferation, although Zhai *et al.* showed that TIMP-3 can retard VSMC proliferation, alongside blunting the expression/activity of MMP-2 and MMP-9 [313]. However, such a mechanism would be contrary to the findings presented here, as Ang II-induced cell density is not reduced by TIMP-3 addition, it is increased.

6.5.2 Inhibition of TGF-β signalling

Based on the available data from animal studies, it was hypothesised that inhibition of TGF-β signalling within the *ex vivo* aneurysm model would reduce aneurysm formation. Indeed, introduction of a TGF-β neutralising antibody had comparable protective effects on Ang II-treated arteries as recombinant TIMP-3 administration. Although inhibition of TGF-β signalling prevented the development of aneurysms within the *ex vivo* model, it was ineffective when administered to Ang II-infused arteries with pre-existing aneurysms. Although there are limited studies assessing the effects of TGF-β perturbation on established aneurysms, a recent study provides support for the disparate findings within this Chapter. Chen *et al.* demonstrated that administration of a TGF-β NAb to mice alongside Ang II-infusion after 28 days affected aneurysm aortic aneurysm formation but was ineffective in mice previously infused with Ang

II to permit development of established aneurysms [352]. As such, modulation of TGF-β signalling harbours the potential to modulate aneurysm development but not beneficially affect pre-existing aneurysm, therefore limiting its therapeutic potential.

Indeed, the role of TGF-β in aortic aneurysms and dissections has remained controversial within the literature as a result of conflicting reports showing beneficial effects of TGF-β in AAA formation while others propose a detrimental role for TGF-β signalling [341]. Wang *et al.* supported a vascular protective role for TGF-β, as delivery of a TGF-β neutralising antibody to Ang II-infused mice resulted in increased aortic dissection rates [79]. Interestingly, blunting the activity of TGF-β was associated with increased MMP-12 activity and inflammation, leading the authors to propose TGF-β suppresses inflammation during aneurysm formation, resulting in reduced macrophage accumulation and associated MMP-12 expression and activity, a potent elastase [79]. Conversely, other studies have shown a detrimental role of TGF-β in aneurysm formation. King *et al.* demonstrated mice deficient for the chemokine Cxcl10 were predisposed to Ang II-induced aortic aneurysm formation, which could be diminished by systemic delivery of a TGF-β NAb [77]. Additionally, Habashi *et al.* showed that mice carrying a fibrillin-1 mutation to replicate Marfan syndrome developed marked ascending aortic aneurysms with profound elastin degradation and SMAD2 phosphorylation, indicative of TGF-β activity, which were all reversed through administration of a TGF-β Nab [80].

As mentioned in 6.1.2 the classical TGF-β signalling pathway involves the activation of the Smad complex which can increase transcription of MMPs and therefore potentially contribute to ECM degradation [337]. However, other studies have suggested that inhibition of TGF-β signaling increased MMP-12 expression and activity and implied heightened vessel wall TGF-β expression and activation functions to reduce AAA expansion [353, 354]. The results presented within this Chapter support a detrimental role of the TGF-β signalling pathway in aneurysm development, further corroborating the applicability of the ex vivo model for aneurysm studies. However, it should be noted that there are no inflammatory cells within the *ex vivo* system, and the published findings discussed above infer inhibition of TGF-β signalling may adversely affect aneurysms where an inflammatory component plays a major role. Indeed, this discrepancy may explain why TGF-β inhibition is beneficial on aneurysms within the ascending aorta and models which mimic genetic mutations such as Marfan's syndrome, but ineffective or even detrimental in inflammatory aneurysms, such as those with super-imposed atherosclerosis. This potential limitation should be considered with regards to the *ex vivo* aneurysm model, especially if TGF-β signalling is under consideration.

6.5.3 MMP-12 inhibitor

As mentioned previously, many studies have demonstrated increased expression of MMPs in human and experimental mouse aneurysm tissues, supporting a central role for dysregulated MMP expression and activity in the formation, progression, and rupture of aneurysms [164]. In particular, numerous studies have implied a central role for MMP-12 in the pathogenesis of aortic aneurysms [160, 179]. Consequently, administration of a selective MMP-12 inhibitor (RXP470) was assessed for its ability to attenuate aneurysm formation and progression within the *ex vivo* aneurysmal model, and hence provide further validation of its suitability. In line with a protective effect of TIMP-3 administration (which could potentially blunt MMP-12 activity), and TGF-β NAb addition (which can result in repressed MMP-12 expression), co-incubation of RXP470 suppressed all the pro-aneurysmal effects of Ang II on human umbilical cord arteries within the *ex vivo* bio-reactor system. However, RXP470 was less potent than TIMP-3 in affecting the progression of pre-existing aneurysms, with elastin content, medial cell density, and medial thickness all unchanged by RXP470 co-administration. Surprisingly, arterial dilatation was significantly increased in RXP470-treated arteries with existing arteries, an opposing effect to that observed in RXP470 during aneurysm formation. This divergence implies MMP-12 inhibition is protective during aneurysm formation but deleterious to established aneurysms. In support of these paradoxical findings, recent findings from my supervisor's lab (published in abstract form only) [186] has demonstrated that MMP-12 inhibition (with RXP470) protects from abdominal aortic aneurysm formation in mice but promotes ascending aortic dissections, and effect also observed in Mmp12-deficient mice. Obviously, these discrepant findings warrant further investigation, especially if MMP-12 inhibition is to be pursued as a therapeutic option for stabilising -pre-existing aneurysms.

RXP470 is a phosphinic peptide and considered a highly selective inhibitor of MMP-12, with a previous demonstrating its athero-protective effect in Apoe-deficient mice, which was associated with reduced medial elastin fragmentation [160]. Curci *et al.* showed a higher expression of MMP-12 in samples of atherosclerotic and AAA tissues when compared to normal aorta [172], In the $CaCl_2$ mouse model of aortic aneurysm formation, Longo *et al.* demonstrated that MMP-12 deficient mice display reduced elastin fragmentation and dilation, in comparison to wild-type animals [179]. However, mice with systemic MMP-12 deficiency were not protected from elastase-induced abdominal aortic aneurysmal dilatation [178], but this may be due to elastase-infusion mimicking the effects of MMP-12 (itself a potent elastase), and it is therefore not surprising MMP-12 deficiency was ineffective. Indeed, elastase-infusion results in marked elastin fibre degradation, which is suppressed by MMP-12 deficiency in both the Ang II and $CaCl_2$ mouse models of aortic aneurysm. As its original name suggests (macrophage metalloelastase), MMP-12 is preferentially expressed by macrophages and

plays a central role in monocyte/macrophage accumulation at sites of injury and during multiple inflammatory diseases, which would support RXP470 exerting efficacious effects where inflammation is dominant, such as in atherosclerotic aneurysms. However, recent studies have shown that vascular smooth muscle cells under certain conditions also express abundant MMP-12. Wu and colleagues revealed that human aortic medial and intimal VSMCs express MMP-12 at the mRNA and protein levels [355]. Moreover, stimulation with PDGF-BB (an inducer of VSMC phenotypic modulation and subsequent growth), increased MMP-12 expression and secretion [355]. Indeed, *in vitro* studies showed aortic VSMCs isolated from MMP-12-deficient mice displayed reduced proliferation rates, which could be reversed through addition of recombinant active-MMP-12 [254]. Furthermore, acute vascular injury has also been shown to induce arterial VSCM MMP-12 expression which was associated with phenotypic modulation, alongside the development of arterial stiffening and concomitant loss of elasticity [356]. In relation, increased arterial stiffness is associated with a heightened risk of arterial dissection in patients with cardiovascular disease [357].

Therefore, while substantial data support a pathogenic role for MMP-12 in AAA, divergent effects can be observed depending on the location of the aneurysm (for example ascending vs. abdominal aorta) or the extent of inflammation. Nonetheless, the findings from both the aneurysm formation and progression studies within this Chapter support the relevance of the human *ex vivo* model. Indeed, utilisation of a novel (importantly) human model of aneurysm formation and progression, should aid future studies aimed at elucidating the underlying mechanisms of both stages of aneurysms alongside aortic dissections, especially if the model can be modified to include the incorporation of inflammatory and circulating lipoproteins.

Chapter 7

General discussion and future work

7 General discussion

7.1 Development and characterisation of a human *ex vivo* model of aneurysm

Presently, the number of *in vivo* mouse experiments is increasing and are regularly published in high impact factor journals. Additionally, the use of large animal models for aneurysm studies, such as pigs and sheep, are becoming more common [131, 181]. In line with the remit of the NC3Rs whose aim is to implement the refinement, reduction, and replacement of animals in research, the main aim of this thesis was to develop, characterise and validate a reproducible *ex vivo* human model of aneurysm formation which could potentially reduce the number of experimental mice used to study aneurysms. A suitable *ex vivo* aneurysm model utilising human tissue would be additionally advantageous as it would be applicable for the testing of new therapeutics and therefore further reduce the number of mice needed for *in vivo* validative dose-response studies for example.

Previous studies have also attempted to develop *ex vivo* models for aneurysm research purposes, however in contradiction with the NC3Rs ethos, such approaches have been restricted to use of porcine carotid arteries or porcine abdominal aortae, rather than human [199, 200]. As such, the development of a human *ex vivo* model of aneurysm formation using easily accessible and appropriate human blood vessels would support its translational potential research applicability, alongside addressing aspects of the 3Rs.

Within this thesis, a basic bio-reactor set-up is described which involved the use of arteries isolated from human umbilical cord, and subsequent exposure to unidirectional laminar flow at 6.5 dynes/cm^2 (the set-up is summarised in Figure 7.1). An advantage of the umbilical cord artery was its length, allowing five equal lengths from one artery to be isolated for parallel experiments and therefore permitting paired statistical analysis. Assessing the effect of agents shown to be pro-aneurysmal in mice within the bio-reactor set-up, demonstrated that pre-treatment of human umbilical cord arteries with $CaCl_2$ for 15 minutes and subsequent placement within the bio-reactor set up resulted in reduced elastin content, medial thickness

and cell density, whereas vessel dilatation was unaffected. Therefore, while some of the morphological, compositional, and cellular changes associated with aneurysm formation were altered, the lack of effect on dilatation implies the $CaCl_2$ application approach is not appropriate for aneurysm induction within the bio-reactor set-up. Contrary to these findings, $CaCl_2$ peri-arterial application was associated with aneurysmal changes in carotid arteries of rabbits, including an increase in vessel diameter [358]. Similarly, peri-aortic application of $CaCl_2$ induced aortic dilatation in multiple mouse studies [133]. The discrepancy between the published literature and the findings within this thesis may be due to the concentration of $CaCl_2$ used, differences in the monitoring period after $CaCl_2$ application, or species variances. These rodent *in vivo* studies use $CaCl_2$ concentrations ranging between 0.1 and 0.68 M, with 0.25 M the most commonly used [133]. Such a concentration is not physiological and would be toxic within the human body, and the bio-reactor set-up is a closed system and therefore a $CaCl_2$ concentration of 0.25M is particularly high and may primarily induce cell apoptosis rather than act on cell contraction and induce dilatation. The bio-reactor set-up was only run for 72 hours and this may not be enough to induce marked vessel dilation after peri-arterial $CaCl_2$ application. Indeed, a meta-analysis of studies utilising the rodent peri-aortic $CaCl_2$ application model showed that minimal increases are observed within the first week, and that pro-longed monitoring is required to enable detection of significant vessel dilatation [133]. As such, it would be worthwhile in the future to determine if maintaining arteries with prior exposure to $CaCl_2$ application for longer time periods within the bio-reactor set-up results in marked vessel dilatation, Nonetheless and in agreement with the published literature, a reduction in elastin content and VSMC loss appear pre-cursors to vessel dilatation during aneurysm formation.

With regards to the introduction of Ang II into the bio-reactor set-up, findings were consistent with the Ang II-infused mouse model of AAA, with both displaying elastin and collagen degeneration, loss of VSMCs, medial thinning and vessel dilatation [63, 130, 226], which are also observed in human AAA samples [216]. As such, utilising arteries isolated from human umbilical cord within the bio-reactor set-up alongside infusion of Ang II, reproducibly resulted in the formation of aneurysms, supporting this set-up as a novel *ex vivo* model of aneurysm formation.

In order to characterise the model, examination of changes in MMP/TIMP expression alongside effects on VSMC and EC function were undertaken and revealed alterations in line with those observed in the rodent models of aneurysm and the pathogenesis of human aortic aneurysms. Numerous studies have proposed a deleterious role for MMPs in the vascular extracellular matrix degradation which in part underlies AAA formation [164, 171, 179, 359]. While the expression of some MMPs were differentially expressed when exposing umbilical cord arteries to pulsatile laminar flow within the bio-reactor set-up (MMP-3, MMP-9 and MMP-

12) increased expression of MMP-10 and MMP-19 was associated with Ang II-induced aneurysm formation within the *ex vivo* model. Specifically, arterial MMP-3 expression was downregulated under laminar flow, while MMP-9 and MMP-12 were upregulated, two MMPs considered pro-aneurysmal. However, studies by others have shown that the expression of MMP-9 and MMP-12 can firstly decrease after 1-week treatment with aneurysm inducers and then increase after longer-term exposure to the same inducers [249]. This suggests a temporal regulation of MMP during aneurysm formation and therefore future studies assessing MMP expression patterns during prolonged incubation within the *ex vivo* aneurysm model would be informative.

The increased expression of MMP-10 and MMP-19 may be exclusive to the *ex vivo* model of aneurysm, and by inference the human umbilical cord arteries. However, there are several lines of evidence in support of these observations, including data to suggest a pro-aneurysmal role for aberrant MMP-10 expression. Elevated MMP-10 expression in mice has been associated with dilatation and rupture of blood vessels, in part through effects on endothelial cell adhesion [360]. Furthermore, analysis of SNPs for MMPs and TIMPs in AAA patients revealed a positive association in an MMP-10 polymorphism and AAA diameter increase [289]. With regards to MMP-19, an MMP/TIMP focussed array of human ascending aortic aneurysms identified MMP-19 as one of only two MMPs positively correlated with increased aortic dilatation [212]. Subsequent immunohistochemical analysis demonstrated that MMP-19 was expressed predominantly by endothelial cells in patients with non-dilated aortas, whereas dilated aortas displayed marked medial MMP-19 expression alongside that within endothelial cells [212]. Although beyond the scope of the present study, it would be interesting to pursue the roles of these two MMPs in aneurysm formation using the *ex vivo* model alongside validative studies in human cells and tissues.

As previously mentioned, the *ex vivo* aneurysmal model employing Ang II-infusion of human umbilical cord arteries can be considered as a potential system to study aneurysm formation and progression as it displays morphological and compositional changes pertinent to AAA formation in humans and mouse models. Further support and characterisation came from the findings that approaches shown to exert anti-aneurysmal effects in mouse models of aortic aneurysms (rTIMP-3 addition, TGF-β neutralisation, and MMP-12 inhibition) were also effective within the *ex vivo* aneurysm model. Indeed, striking similarities on vessel dilatation, medial thinning and elastin content were observed with the interventions, between the *ex vivo* model and the published mouse studies [80, 160, 186]. A such, corroboration of anti-aneurysmal treatments within the *ex vivo* model further support the translatability of the *ex vivo* Ang II-infusion aneurysm model as a viable alternative for *in vivo* mouse models.

Although not commonly undertaken within the Ang II-infusion mouse model of AAA, in order to assess the effectiveness of potential novel therapies to treat and stabilise aneurysms, a suitable model should harbour aneurysms. Accordingly, as rTIMP-3 addition, TGF-β neutralisation, and MMP-12 inhibition were all effective at blunting aneurysm formation within the *ex vivo* model, their ability to affect established aneurysms was assessed. While, TGF-β neutralisation or MMP-12 inhibition were largely ineffective, exogenous TIMP-3 prevented the VSMC loss and elastin degeneration observed in progressing aneurysms within the *ex vivo* model. Encouragingly, loss of TIMP-3 promotes aneurysms in the Ang II-induced mouse model while TIMP-3 restoration prevents aneurysm formation and importantly, the progression of existing aortic aneurysms [186].

Taken together, the consistent anti-aneurysmal effects afforded through TIMP-3 addition/over-expression within the ex vivo model and mouse studies, support the use of the *ex vivo* model for aneurysm research, especially with regards to the involvement of MMPs. Furthermore, alongside the observations in mouse models and human histopathological findings, over-expression or restoration of TIMP-3 expression is consistently identified as a potential therapeutic approach to inhibit aneurysm progression and rupture, and possibly hold the ability to regress existing aneurysms, although further research is obviously required before clinical trials could be commenced.

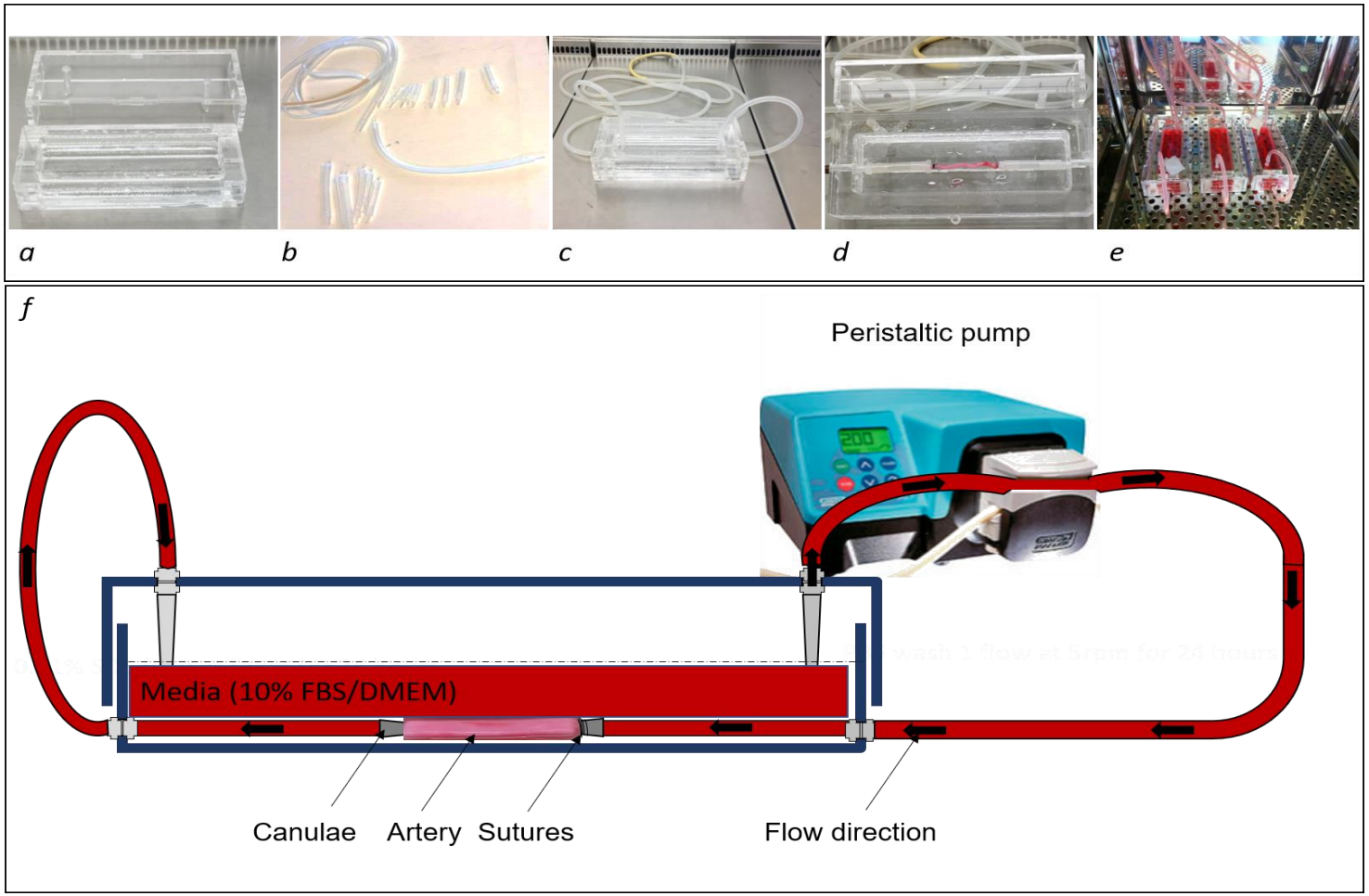

Figure 7.1: **Bio-reactor set-up of *ex vivo* aneurysm model testing**

(a) Bio-reactor chambers; (b) silicone tubes and cannulae; (c) over-view of the closed chamber with tubing; (d) an example artery inserted within the bio-reactor chamber; (e) a complete bio-reactor set-up analysing three paired arterial segments (within an incubator);(f) Schematic diagram detailing the bio-rector set-up including connection to a peristaltic pump in order to create unidirectional laminar flow at 6.5 dynes/cm^2.

7.1.1 *In vitro* studies on VSMC

As umbilical cord artery was deployed within the *ex vivo* model, it was important to determine if the cells within these arteries behave similarly to those from within the aorta in order to provide further validation of umbilical cord artery use in an aneurysm model. VSMCs are the primary cell type within the media of the arterial wall and regulate vessel contraction and relaxation, and therefore vessel diameter [51]. Evidence obtained from human pathological studies and well-established mouse models of aneurysm, have demonstrated a major role for MMPs in the pathogenesis of aortic aneurysms [127, 128]. Additionally, MMPs have been shown to drive the remodelling processes involved in coronary and carotid atherosclerosis, and restenosis subsequent to clinical interventions including coronary artery bypass grafting and stent deployment [236]. Investigation of the expression of MMPs and TIMPs in VSMCs isolated from human umbilical cord in response to Ang II or $CaCl_2$ revealed limited changes, alongside discrepancies in mRNA and protein expression particularly with $CaCl_2$ stimulation. Considering the reproducible aneurysm formation within the Ang II-infused *ex vivo* model, changes in VSMC MMP expression are of importance, and showed MMP-2, MMP-10, and MMP-12 to be up-regulated while MMP-3 levels were decreased, These findings in Ang II-stimulated umbilical cord artery VSMCs are largely in agreement with the observations in whole arteries from within the *ex vivo* model system, especially MMP-10. Unfortunately, MMP-19 expression was not assessed within the VSMCs, and MMP-2 levels were not determined within the *ex vivo* arterial samples, limiting conclusion on their roles within the aneurysm model. Interestingly, Ang II or $CaCl_2$ stimulation of VSMCs revealed a disparity between MMP-3 mRNA and protein expression, which might be due to a post-transcriptional mechanism involving microRNA-regulation of MMP-3. Indeed, previous unpublished findings from my supervisor's laboratory has identified a number of microRNA that regulate the expression of MMP-3 in human umbilical cord ECs which have been exposed to pro-inflammatory stimuli. Other studies have also proposed a contribution of microRNA regulation of MMPs. For instance, Liao *et al.* suggested the involvement of miR-320 in post-transcriptional regulation of MMPs-1, − 8, − 9, and − 12 in both heathy and aortic dissection patients [361]. Furthermore, two studies have suggested the involvement of two microRNA, miR-712 and miR-205, in the regulation of MMP activity and endothelial inflammation [362, 363]. It was suggested that silencing the activity of these microRNA in Ang II infused Apoe-deficient mice could prevent AAA development [363]. Therefore, further studies elucidating the mechanisms underlying Ang II or $CaCl_2$-dependent microRNA regulation of MMPs are warranted, particularly with regard to aortic aneurysm development. Unexpectedly, Ang II stimulation additionally increased the expression of TIMP-1 TIMP-2 and TIMP-3 (but not TIMP-4), whereas, $CaCl_2$ had no effect on TIMP levels. However, this may represent a positive feedback response in

order to negate heightened MMP activity, as previously also observed in human aneurysm tissues and mouse model where select MMPs are over-expressed [50].

While vessel wall damage due to injury or to pathological conditions can result in dysregulated proteolysis, it can also induce a switch of VSMC phenotype from contractile to synthetic, which has been associated with MMP activity [55]. VSMC phenotypic modulation is considered an early event during the development of aortic aneurysms and is associated with changes in the expression of distinct MMPs [38]. Accordingly, umbilical cord artery VSMCs stimulated with Ang II or $CaCl_2$ down-regulated their expression of contractile VSMC phenotype markers including αSM actin, SMMHC11, transgelin, and caldesmon, suggesting a shift from a contractile to a synthetic VSMC phenotype typical of AAA formation. Indeed, Fang *et al*. showed a phenotypic change in 24-hour Ang II-stimulated rat VSMCs, underlined by the decreased expression of αSM actin, calponin and transgelin compared to unstimulated cells [292]. Furthermore, they found further reduction in contractile-associated markers after 72 hours' Ang II treatment, suggesting a complete phenotypic change in VSMCs to a synthetic form requires pro-longed exposure to phenotypic modulators or perhaps some form of synergism [292]. Indeed, assessment of contractile VSMC markers in *ex vivo* arteries revealed that while some contractile VSMC phenotypic markers were down-regulated after subjection to flow within a bio-reactor, suppression of all four markers were only observed with additional infusion of Ang II, suggesting a shift towards a fully synthetic phenotype requires synergism between two complimentary pathways, such as cyclic stretch and Ang II signalling.

The surprising differences in responses between Ang II and $CaCl_2$-induced effects on VSMC MMP/TIMP expression alongside aneurysm formation within the *ex vivo* model, may be explained through their differing mechanisms of action. While Ang II signals through its cognate receptors, the actions of $CaCl_2$ are less well characterised. Indeed, although Ang II stimulation did not alter VSMC morphology, $CaCl_2$ markedly altered VSMC morphology and induced clump formation, changes characteristic of nodular calcification which has been previously linked to aneurysm formation [285]. Furthermore, a senescence *in vitro* assay clearly showed that the number of VSMCs undergoing senescence was increased subsequent to $CaCl_2$ stimulation, suggesting an involvement of a senescence-associated mechanism underlying the aneurysmal effects observed with $CaCl_2$. Indeed, accelerated VSMC senescence has been linked to the development and progression of aortic aneurysms, and may contribute to the medial VSMC depletion observed in the human disease and animal mouse models, and that within the *ex vivo* model, although not sufficient to induce vessel dilatation [364].

Taken together, VSMC phenotypic modulation alongside up-regulation of select MMPs, characteristics of aneurysm formation in the Ang II-infusion mouse model and human aortic aneurysms, are consistently observed within the Ang II-infusion *ex vivo* model developed during this PhD. Alongside the morphological and compositional changes, these additional findings further support the applicability of the *ex vivo* model of aneurysm for future studies. Specifically, studies aimed at elucidating mechanisms or therapeutics regulating VSMC phenotypic modulation and dysregulated proteolysis during aneurysm formation will be particularly suited to the *ex vivo* model.

7.1.2 *In vitro* studies on ECs

As with VSMCs, EC dysfunction has been linked to the development of numerous cardiovascular diseases, and in particular to the pathogenesis of aneurysms [301]. Examination of ECs within the Ang II-infusion *ex vivo* aneurysm model suggested changes to their morphology and function, as cell membrane-localised VE-cadherin expression was reduced with a concomitant accumulation of intra-cellular expression. Similarly, other studies have shown Ang II-stimulation of HUVECs increased their permeability which was associated with loss of peripheral VE-cadherin expression [306]. The observations within the *ex vivo* model were validated *in vitro* using a simple model of mechanotransduction to model laminar flow, as evidenced by Ang II-induced loss of membrane-associated VE-cadherin expression alongside intra-cellular accumulation. As expected, co-incubation with the AT1R antagonist losartan reversed these effects, while addition of recombinant TIMP-3 was also protective. In line with cytosolic VE-cadherin accumulation, Ang II stimulated HUVECs also displayed nuclear β-catenin translocation, a pre-requisite for canonical Wnt/β-catenin signalling. Moreover, the diminished cell-membrane VE-cadherin expression was associated with loss of F-actin levels, suggesting Ang II induced re-distribution of VE-cadherin In HUVECs is accompanied by reorganisation of the actin cytoskeleton. Again, the Ang II-dependent effects on β-catenin localisation and cell morphology were retarded by losartan or TIMP-3 addition, suggesting Ang II-mediated MMP-dependent proteolysis of VE-cadherin modulates all the subsequent effects observed, although direct demonstration of this mechanism is required to confirm this hypothesis.

Together these findings suggest that HUVECs stimulated with Ang II *in vitro* and *ex vivo* alters the expression of key structural proteins such as VE-cadherin, which may subsequently alter their function and subsequent effects on VSMCs. Direct demonstration that Ang II-induced changes in VE-cadherin localisation and associated β-catenin nuclear accumulation induced activation of the canonical Wnt/β-catenin signalling pathway was not validated but would be

necessary in order to take the novel observations further. Due to time constraints and limited tissue supplies, assessment of TIMP-3 addition on EC morphology and function within the *ex vivo* aneurysm model was not investigated but considering the protective effects *in vitro* alongside the anti-aneurysmal role of TIMP-3 addition within the *ex vivo* model, this would be pertinent to investigate further.

7.2 Limitations

A general limitation of the current study is the use of human umbilical cord arteries rather than the use of a human abdominal aorta. However, the structure and composition of the umbilical cord artery is similar to other arteries in that it consists of three concentric layers: intima, media, and adventitia. The only marked difference is that umbilical arteries (similar to pulmonary arteries) carry deoxygenated blood which travels back to the placenta to be re-oxygenated again by the mother [365]. The deoxygenated nature of the blood vessel (rather than oxygenated as is the case with the aorta) may affect the specific response to aneurysm inducers. However, the agreement in effects of Ang II on arterial changes in morphology, composition, and MMP expression between the *ex vivo* model and both human aneurysms and the current mouse models suggest a high degree of similarity. As such, human umbilical cord artery represents a good alternative to human aortic tissue and is more readily available for use in aneurysm research experiments.

Considering the majority of human abdominal aortic aneurysms display super-imposed atherosclerosis and marked inflammatory cell accumulation, an additional general limitation of the *ex vivo* model is the lack of inflammation. However, this is also a caveat with most mouse models of AAA and does not limit their use or publication in high impact journals, and the main intention of the *ex vivo* model is to replicate and ideally replace current animal models of aneurysm. Nonetheless, inflammation plays a central role in AAA formation and rupture in humans [70] and would ideally be incorporated into the *ex vivo* model. This issue could be partially solved by flowing blood through the umbilical cord arteries and focus on inflammatory pathway. Unfortunately, there was insufficient time alongside a lack of appropriate ethics for obtaining cord-blood samples to perform such experiments. Hopefully, these will be performed in the near future alongside alterations in the direction of flow in order to determine whether focal aneurysms can be induced.

More specific to the experiments in this thesis, several technical issues were encountered during the development of the model when attempting to ensure its reproducibility. Firstly, the

development of the novel model required many experimental tests before full optimisation of the bio-reactor set-up. This optimisation process was further hampered by the limited availability of human umbilical cord. Human umbilical cords are an invaluable resource that are shared between several research groups within our Department. Additionally, the ethics also limits the number of samples which are permitted to be retrieved and used in research, which has been beyond my control to manage. However, these hurdles have been overcome and the Ang II-induced *ex vivo* aneurysm model has been standardised and reproducibility confirmed, permitting the assessment of agents known to induce aneurysm formation in well-characterised mouse models. Moreover, *in vitro* experiments on ECs were performed during the last months of my PhD, therefore time and financial restrictions affected the number of experiments that could be performed, while the *en face* preparation and associated immunocytochemistry/confocal microscopy required extensive optimisation.

7.3 Future work

Due to time restrictions, the work suggested below could not be performed during this PhD, but would complement the findings presented.

7.3.1 Complete the studies on the *ex vivo* aneurysm model

The Ang II-infusion umbilical cord artery *ex vivo* aneurysm model generated within this thesis displays similar pathological characteristics of AAA formation and progression as the current mouse models, whereas $CaCl_2$ application filed to induce vessel dilatation. A third animal model of AAA formation is the elastase-perfusion model [45]. Elastase was not considered as an inducer for the *ex vivo* model as a key molecular effector pathway of aneurysm generation is dysregulated proteolysis, including increased MMP expression/activity, which the elastase model would circumvent as elastase is a member of the protease family. However, to replicate the three approaches used in mouse models of AAA formation, the elastase model could be investigated within the bio-rector set-up using umbilical cord artery. In brief, this would involve intraluminal introduction of elastase (50U bovine type I pancreatic elastase) into 5 cm lengths of umbilical cord artery for 30 minutes, before placement into the bio-reactor system for 72 hours.

7.3.2 Effect of long-term *ex vivo* aneurysm model experiments (7, 14 or 28 days within bio-reactor)

A salient clinical manifestation of aneurysm formation is vessel wall rupture/dissection. As such, long-term placement of human umbilical cord artery within the *ex vivo* bio-reactor

aneurysm model in the presence of Ang II should be assessed for its ability to induce rupture/dissection. As in the previous experiments, human umbilical cord would be inserted into the bio-reactor set-up at 6.5 dynes/cm^2 using media containing 5µM Ang II. These experiments will involve changing the media every four days and running them for 7, 14, or 28 days, to mimic the Ang II-induced AAA model. As in previous experiments, histological parameters would be assessed. Interestingly, during the course of this PhD, incidences of arterial dissection/rupture were observed within the *ex vivo* aneurysm model but were infrequent and not examined further.

7.3.3 Effect of laminar or directional flow to induce fusiform or saccular aneurysm

The human umbilical cord arteries were subjected to laminar flow at 6.5 dynes/cm^2 for 72 hours, with the inclusion of Ang II in order to create a diffuse concentric aneurysm which is typical of fusiform aneurysms. Fusiform aneurysms display a bulge on all sides of a blood vessel. However human umbilical cord arteries could also be exposed to directional flow to induce localised eccentric aneurysms which are typical of saccular aneurysms. A saccular aneurysm usually has a bulge on only one side of the blood vessel. To conduct such experiments, it would be necessary to bend the cannula in order to create an angled flow and induce focal dilation at one side of the artery wall.

7.3.4 Ang II administration on MMP expression in *ex vivo* bio-reactor cultured human umbilical cord arteries

The Western blotting data from umbilical cord arteries under laminar flow showed an up-regulation of MMP-10 and MMP-19 in response to Ang II treatment, as well as an increase in MMP-9 and MMP-12 in response to laminar flow, and downregulation of MMP-3. However, changes in MMP expression was only assessed at 72 hours. It would be interesting to perform longer-term experiments to see whether the pattern changes or remains constant. In addition, perturbation of MMP-10 or MMP-19 with the model alongside over-expression of MMP-3 would be worthwhile to determine whether the observed changes in their expression are causal or an association with aneurysm formation.

7.3.5 *In vitro* studies on VSMC

The QPCR data showed an up-regulation of MMP-2 and MMP-12 in response to Ang II treatment as well as an increase of MMP-3 and MMP-10 in response to $CaCl_2$. However, there were discrepancies at the protein level. TIMPs expression was mainly down-regulated with a $CaCl_2$ however TIMPs-1, -2, and -3 were up-regulated in response to Ang II treatment. To further assess the inconsistencies between the mRNA and protein levels of select MMPs,

microRNA expression could be investigated to which are predicted regulators of the MMPs of interest. Furthermore, as it is the proteolytic activity of MMPs which is the salient biologically relevant output, gel and in situ zymography should be performed in order to measure the proteolytic activity of significantly regulated MMPs, so as to validate if the protein expression findings translate to increased activity.

7.3.6 *In vitro* studies on ECs

The effects of Ang II on endothelial cell VE-cadherin expression have been investigated both *ex vivo* and *in vitro*. However due to the lack of adequate human umbilical cords, only one *ex vivo* assessment was performed, it is therefore considered an observational study. Certainly, the interesting effects observed in the one experiment require validation in at least five more arteries to determine whether the findings are reproducible and robust. Additionally, a simplistic and easy to use *in vitro* rocker has been deployed to model mechanotransduction, which has evident limitations. Therefore, it would be ideal to confirm the data obtained with his model in an additional well-characterised *in vitro* system, such as the Ibidi Flow System (https://ibidi.com/perfusion-system/112-ibidi-pump-system.html).

7.4 Final remarks

In conclusion, the main data presented in this thesis demonstrates that the novel *ex vivo* model of aneurysm employing Ang II infusion of human umbilical cord artery, induced morphological and compositional changes associated with human aneurysms and aneurysm formation in animal models, which are reversed by exogenous TIMP-3, perturbation of TGF-β signalling through use of a TGF-β NAb, or MMP-12 inhibition using the selective inhibitor RXP470 (as summarised in Figure 7.2). Additionally, *in vitro* studies on VSMCs and ECs showed phenotypic transition, MMP/TIMP regulation, along with haemodynamic changes in response to Ang II. Collectively, these findings support the use of this model for aneurysm studies, supplanting ethically challenging animal experiments. The main findings of the Ang II aneurysmal model are summarising in Table 7.1

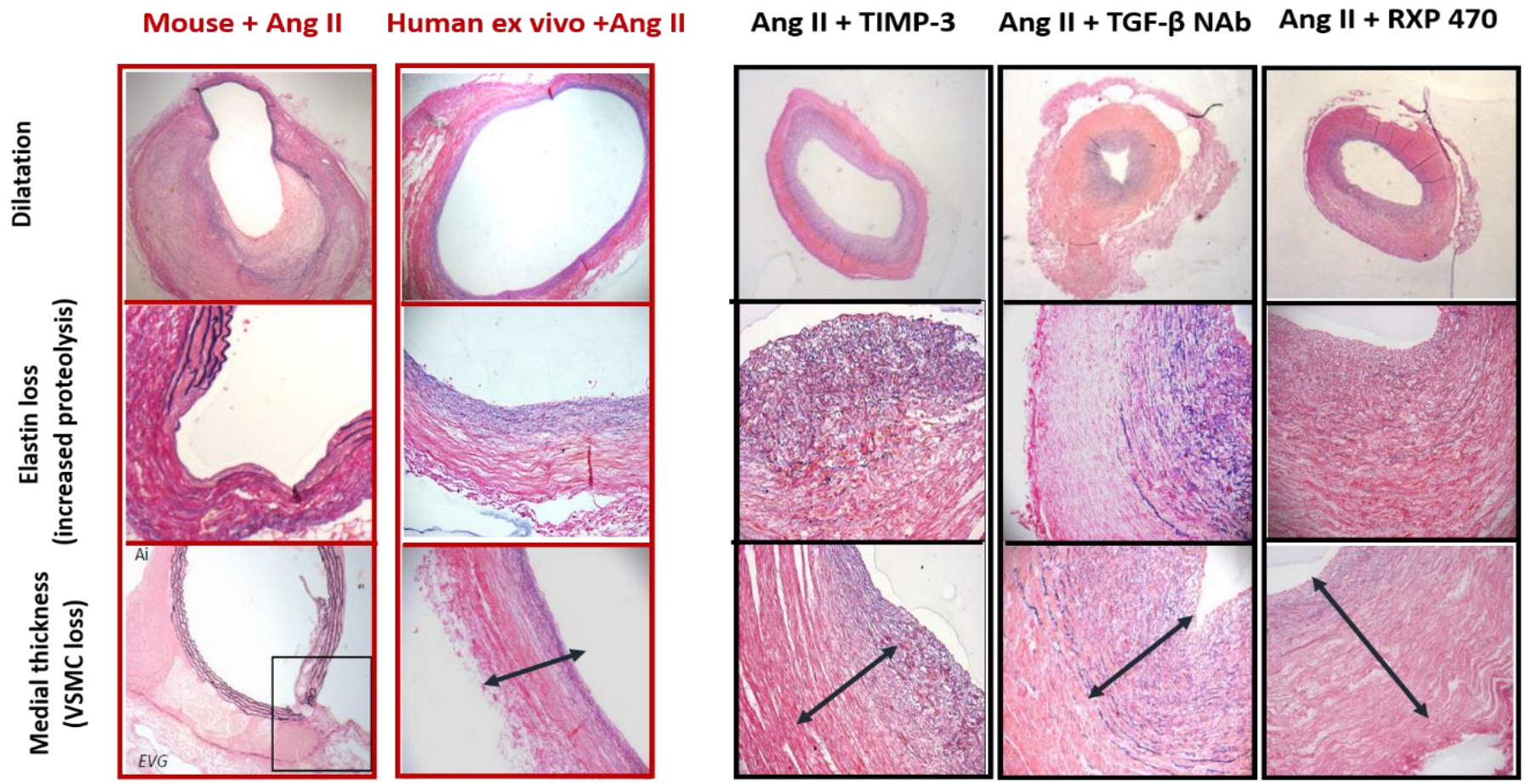

Figure 7.2: **Main findings from the *ex vivo* aneurysm model**

On the left side (in red boxes) dilatation, elastin loss and media thickness in the Ang II-induced mouse aneurysm model compared to the human ex vivo model. On the right side (in black boxes) the application of three interventions; recombinant TIMP-3, a TGF-β neutralising antibody (NAb) and a selective MMP-12 inhibitor (RXP 470) inhibited Ang II-induced dilatation, elastin degradation and medial thinning.

Table 71: The effect of the bio-reactor system without and with Ang II-infusion on human umbilical cord arteries

The vessel dilatation, medial thickness, elastin content, nuclei per cross-section, collagen content, MMP-3, MMP-9, MMP-10, MMP-12 and MMP-19 expression in baseline, untreated bio-reactor and Ang II bio-reactor umbilical cord arteries.

	BASELINE	UNTREATED BIO-REACTOR	ANG II BIO-REACTOR	EFFECT OF ANG II
Vessel dilatation	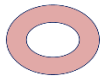	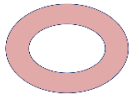	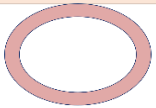	*-Increased vessel dilatation in response to untreated bio-reactor* *- Increased vessel dilatation in response to untreated bio-reactor*
Medial thickness	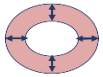	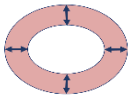	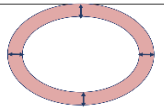	*-No change in medial thickness in response to untreated bio-reactor* *- Decreased in medial thickness in response to Ang II bio-reactor*
Elastin content	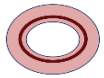	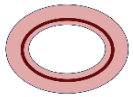	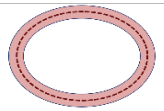	*-No change in elastin content in response to untreated bio-reactor* *- Decreased in elastin content in response to Ang II bio-reactor*
Number of cells per cross-section	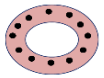	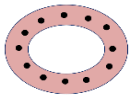	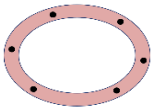	*-No change in number of cells per cross-section in response to untreated bio-reactor* *- Decreased in number of cells per cross-section in response to Ang II bio-reactor*
Collagen content	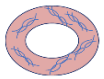	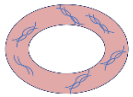	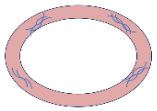	*-No change in collagen content in response to untreated bio-reactor* *- Decreased in collagen content in response to Ang II bio-reactor*
MMP-3	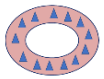	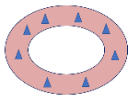	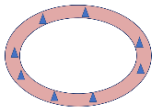	*-Decreased in MMP-3 expression in response to untreated bio-reactor* *- No further change in MMP-3 Increased vessel dilatation in response to untreated bio-reactor*
MMP-9 **MMP-12**	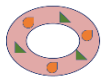	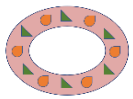	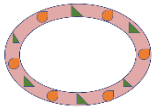	*-Increased in MMP-9 and MMP-12 expression in response to untreated bio-reactor* *- No further change in MMP-9 and MMP-12 in response to Ang II bio-reactor*
MMP-10 **MMP-19**	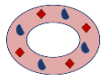	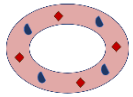	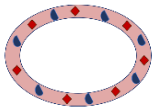	*-No change in MMP-10 and MMP-19 expression in response to untreated bio-reactor* *- Increased in MMP-10 and MMP-12 in response to Ang II bio-reactor*

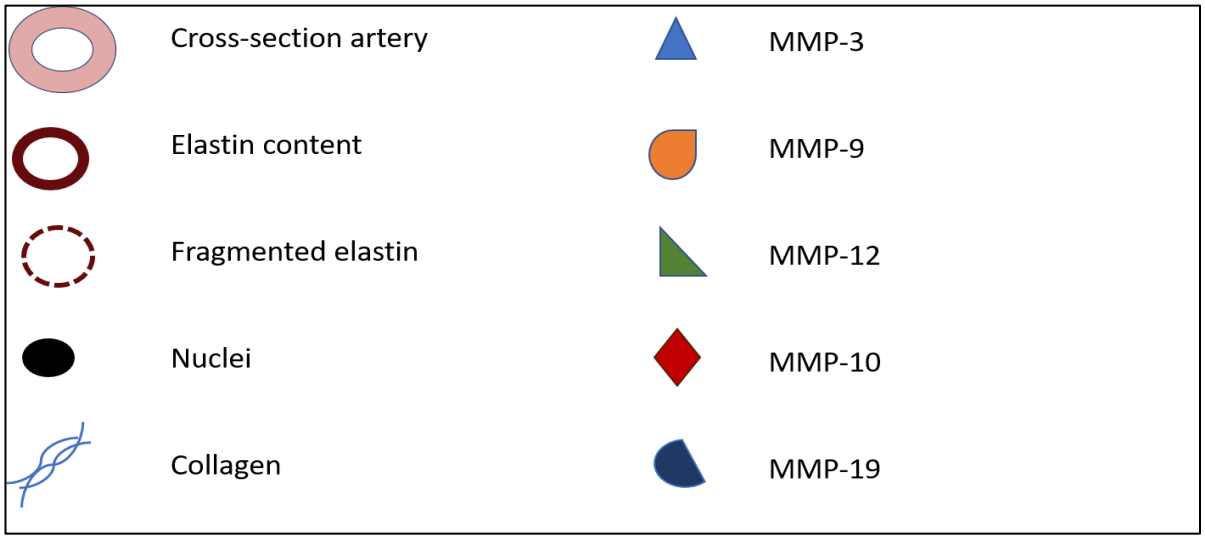
Cross-section artery
Elastin content
Fragmented elastin
Nuclei
Collagen
MMP-3
MMP-9
MMP-12
MMP-10
MMP-19

8 References

1. Howard, D.P.J., et al., *Age-specific incidence, risk factors and outcome of acute abdominal aortic aneurysms in a defined population.* The British Journal of Surgery, 2015. **102**(8): p. 907-915.
2. Li, Z.-Z. and Q.-Y. Dai, *Pathogenesis of abdominal aortic aneurysms: role of nicotine and nicotinic acetylcholine receptors.* Mediators of inflammation, 2012. **2012**: p. 103120-103120.
3. Michel, J.-B., et al., *Novel aspects of the pathogenesis of aneurysms of the abdominal aorta in humans.* Cardiovascular Research, 2011. **90**(1): p. 18-27.
4. Scott, R.A.P., *The Multicentre Aneurysm Screening Study (MASS) into the effect of abdominal aortic aneurysm screening on mortality in men: a randomised controlled trial.* The Lancet, 2002. **360**(9345): p. 1531-1539.
5. Tarbell, J.M., et al., *Fluid Mechanics, Arterial Disease, and Gene Expression.* Annual Review of Fluid Mechanics, 2014. **46**(1): p. 591-614.
6. Miyake, T. and R. Morishita, *Pharmacological treatment of abdominal aortic aneurysm.* Cardiovascular Research, 2009. **83**(3): p. 436-443.
7. Etminan, N. and G.J. Rinkel, *Unruptured intracranial aneurysms: development, rupture and preventive management.* Nature Reviews Neurology, 2016. **12**: p. 699.
8. Wagenseil, J.E. and R.P. Mecham, *Vascular extracellular matrix and arterial mechanics.* Physiological reviews, 2009. **89**(3): p. 957-989.
9. Witter, K., Z. Tonar, and H. Schöpper, *How many Layers has the Adventitia? – Structure of the Arterial Tunica Externa Revisited.* Journal of Veterinary Medicine, 2017. **46**(2): p. 110-120.
10. Urabe, G., et al., *Structural analysis of adventitial collagen to feature aging and aneurysm formation in human aorta.* Journal of Vascular Surgery, 2016. **63**(5): p. 1341-1350.
11. O'Gara Patrick, T., *Aortic Aneurysm.* Circulation, 2003. **107**(6): p. e43-e45.
12. Kuivaniemi, H., C.D. Platsoucas, and M.D. Tilson, 3rd, *Aortic aneurysms: an immune disease with a strong genetic component.* Circulation, 2008. **117**(2): p. 242-252.
13. Lederle, F.A., G.R. Johnson, and S.E. Wilson, *Abdominal aortic aneurysm in women.* Journal of Vascular Surgery, 2001. **34**(1): p. 122-126.
14. Kent, K.C., *Abdominal Aortic Aneurysms.* New England Journal of Medicine, 2014. **371**(22): p. 2101-2108.
15. Pan, J.-H., et al., *Macrophage migration inhibitory factor is associated with aneurysmal expansion.* Journal of Vascular Surgery, 2003. **37**(3): p. 628-635.
16. Aggarwal, S., et al., *Abdominal aortic aneurysm: A comprehensive review.* Experimental and Clinical Cardiology, 2011. **16**(1): p. 11-15.

17. Forsdahl Signe, H., et al., *Risk Factors for Abdominal Aortic Aneurysms.* Circulation, 2009. **119**(16): p. 2202-2208.

18. Sakalihasan, N., et al., *Family members of patients with abdominal aortic aneurysms are at increased risk for aneurysms: analysis of 618 probands and their families from the Liège AAA Family Study.* Annals of Vascular Surgery, 2014. **28**(4): p. 787-797.

19. Isselbacher Eric, M., *Thoracic and Abdominal Aortic Aneurysms.* Circulation, 2005. **111**(6): p. 816-828.

20. Akai, A., et al., *Family history of aortic aneurysm is an independent risk factor for more rapid growth of small abdominal aortic aneurysms in Japan.* Journal of Vascular Surgery, 2015. **61**(2): p. 287-290.

21. Geng, L., et al., *Elevation of ADAM10, ADAM17, MMP-2 and MMP-9 expression with media degeneration features CaCl2-induced thoracic aortic aneurysm in a rat model.* Experimental and Molecular Pathology, 2010. **89**(1): p. 72-81.

22. von Kodolitsch, Y. and P.N. Robinson, *Marfan syndrome: an update of genetics, medical and surgical management.* Heart (British Cardiac Society), 2007. **93**(6): p. 755-760.

23. Losenno, K.L., R.L. Goodman, and M.W.A. Chu, *Bicuspid aortic valve disease and ascending aortic aneurysms: gaps in knowledge.* Cardiology Research and Practice, 2012. **2012**: p. 145202-145202.

24. Töpel, I., N. Zorger, and M. Steinbauer, *Inflammatory diseases of the aorta: Part 1: Non-infectious aortitis.* Gefasschirurgie, 2016. **21**(Suppl 2): p. 80-86.

25. Fink, H.A., et al., *The accuracy of physical examination to detect abdominal aortic aneurysm.* Archives of Internal Medicine, 2000. **160**(6): p. 833-836.

26. Kontopodis, N., et al., *Advances in determining abdominal aortic aneurysm size and growth.* World journal of radiology, 2016. **8**(2): p. 148-158.

27. Kuzmik, G.A., A.X. Sang, and J.A. Elefteriades, *Natural history of thoracic aortic aneurysms.* Journal of Vascular Surgery, 2012. **56**(2): p. 565-571.

28. Kim Joon, B., et al., *Risk of Rupture or Dissection in Descending Thoracic Aortic Aneurysm.* Circulation, 2015. **132**(17): p. 1620-1629.

29. Booher, A.M. and K.A. Eagle, *Diagnosis and management issues in thoracic aortic aneurysm.* American Heart Journal, 2011. **162**(1): p. 38-46.e1.

30. Lindsay, M.E. and H.C. Dietz, *Lessons on the pathogenesis of aneurysm from heritable conditions.* Nature, 2011. **473**: p. 308.

31. Norman, P.E. and J.T. Powell, *Site Specificity of Aneurysmal Disease.* Circulation, 2010. **121**(4): p. 560-568.

32. Danyi, P., J. Elefteriades, and I. S Jovin, *Medical Therapy of Thoracic Aortic Aneurysms Are We There Yet?* Circulation, 2011. **124**: p. 1469-76.

33. Vorkapic, E., et al., *Imatinib treatment attenuates growth and inflammation of angiotensin II induced abdominal aortic aneurysm.* Atherosclerosis, 2016. **249**: p. 101-109.

34. Yan, Y.-W., et al., *Zinc Prevents Abdominal Aortic Aneurysm Formation by Induction of A20-Mediated Suppression of NF-κB Pathway.* Plos One, 2016. **11**(2): p. e0148536.

35. Hirsch Alan, T., et al., *ACC/AHA 2005 Practice Guidelines for the Management of Patients With Peripheral Arterial Disease (Lower Extremity, Renal, Mesenteric, and Abdominal Aortic).* Circulation, 2006. **113**(11): p. e463-e654.

36. Beck, A.W., et al., *Predicting 1-year mortality after elective abdominal aortic aneurysm repair.* Journal of Vascular Surgery, 2009. **49**(4): p. 838-844.

37. Lee, H.-G., D.G. Clair, and K. Ouriel, *Ten-year Comparison of All-Cause Mortality after Endovascular or Open Repair of Abdominal Aortic Aneurysms: A Propensity Score Analysis.* World Journal of Surgery, 2013. **37**(3): p. 680-687.

38. Ailawadi, G., et al., *Smooth muscle phenotypic modulation is an early event in aortic aneurysms.* The Journal of Thoracic and Cardiovascular Surgery, 2009. **138**(6): p. 1392-1399.

39. Buijs, R.V.C., et al., *Calcification as a Risk Factor for Rupture of Abdominal Aortic Aneurysm.* European Journal of Vascular and Endovascular Surgery, 2013. **46**(5): p. 542-548.

40. Tsamis, A., J.T. Krawiec, and D.A. Vorp, *Elastin and collagen fibre microstructure of the human aorta in ageing and disease: a review.* Journal of The Royal Society Interface, 2013. **10**(83).

41. Shoulders, M.D. and R.T. Raines, *Collagen structure and stability.* Annual Review of Biochemistry, 2009. **78**: p. 929-958.

42. Hellenthal, F.A.M.V.I., et al., *Biomarkers of AAA progression. Part 1: extracellular matrix degeneration.* Nature Reviews Cardiology, 2009. **6**: p. 464.

43. Berillis, P., *The Role of Collagen in the Aorta's Structure.* The Open Circulation & Vascular Journal, 2013. **6**.

44. Wagenseil, J.E. and R.P. Mecham, *Elastin in large artery stiffness and hypertension.* Journal of Cardiovascular Translational Research, 2012. **5**(3): p. 264-273.

45. Anidjar, S., et al., *Elastase-induced experimental aneurysms in rats.* Circulation, 1990. **82**(3): p. 973-981.

46. Carmo, M., et al., *Alteration of Elastin, Collagen and their Cross-links in Abdominal Aortic Aneurysms.* European Journal of Vascular and Endovascular Surgery, 2002. **23**(6): p. 543-549.

47. Nagase, H., R. Visse, and G. Murphy, *Structure and function of matrix metalloproteinases and TIMPs.* Cardiovascular Research, 2006. **69**(3): p. 562-573.

48. Johnson, J., *Emerging regulators of vascular smoothmuscle cell function in the development and progression of atherosclerosis.* Cardiovascular Research, 2014. **103**.

49. Lu, H. and M. Aikawa, *Many Faces of Matrix Metalloproteinases in Aortic Aneurysms.* Arteriosclerosis, Thrombosis, and Vascular Biology, 2015. **35**(4): p. 752-754.

50. Johnson, J., *Matrix metalloproteinases and their inhibitors in cardiovascular pathologies: current knowledge and clinical potential.* Metalloproteinases In Medicine, 2014. **1**: p. 21-36.

51. Lacolley, P., et al., *The vascular smooth muscle cell in arterial pathology: a cell that can take on multiple roles.* Cardiovascular Research, 2012. **95**(2): p. 194-204.

52. Beamish, J.A., et al., *Molecular regulation of contractile smooth muscle cell phenotype: implications for vascular tissue engineering.* Tissue engineering. Part B, Reviews, 2010. **16**(5): p. 467-491.

53. Patel, R., et al., *Synthetic smooth muscle cell phenotype is associated with increased nicotinamide adenine dinucleotide phosphate oxidase activity: Effect on collagen secretion.* Journal of Vascular Surgery, 2006. **43**(2): p. 364-371.

54. Metz, R.P., J.L. Patterson, and E. Wilson, *Vascular Smooth Muscle Cells: Isolation, Culture, and Characterization*, in *Cardiovascular Development: Methods and Protocols*, X. Peng and M. Antonyak, Editors. 2012, Humana Press: Totowa, NJ. p. 169-176.

55. Louis, S.F. and P. Zahradka, *Vascular smooth muscle cell motility: From migration to invasion.* Experimental and Clinical Cardiology, 2010. **15**(4): p. e75-e85.

56. Newby, A.C., *Matrix metalloproteinases regulate migration, proliferation, and death of vascular smooth muscle cells by degrading matrix and non-matrix substrates.* Cardiovascular Research, 2006. **69**(3): p. 614-624.

57. George, S.J. and A. Dwivedi, *MMPs, Cadherins, and Cell Proliferation.* Trends in Cardiovascular Medicine, 2004. **14**(3): p. 100-105.

58. López-Candales, A., et al., *Decreased vascular smooth muscle cell density in medial degeneration of human abdominal aortic aneurysms.* The American journal of Pathology, 1997. **150**(3): p. 993-1007.

59. Williams, H., et al., *MMP-7 mediates cleavage of N-cadherin and promotes smooth muscle cell apoptosis.* Cardiovascular Research, 2010. **87**(1): p. 137-146.

60. Baker, A.H., D.R. Edwards, and G. Murphy, *Metalloproteinase inhibitors: biological actions and therapeutic opportunities.* Journal of Cell Science, 2002. **115**(19): p. 3719.

61. Sun, J., et al., *Endothelium as a Potential Target for Treatment of Abdominal Aortic Aneurysm %J Oxidative Medicine and Cellular Longevity.* Oxidative Medicine and Cellular Longevity, 2018. **2018**: p. 12.

62. Cines, D.B., et al., *Endothelial Cells in Physiology and in the Pathophysiology of Vascular Disorders.* Blood, 1998. **91**(10): p. 3527.

63. Rateri, D.L., et al., *Depletion of endothelial or smooth muscle cell-specific angiotensin II type 1a receptors does not influence aortic aneurysms or atherosclerosis in LDL receptor deficient mice.* Plos One, 2012. **7**(12): p. e51483-e51483.

64. Zhou, J., et al., *Regulation of vascular smooth muscle cell turnover by endothelial cell-secreted microRNA-126: role of shear stress.* Circulation Research, 2013. **113**(1): p. 40-51.

65. Ramella, M., et al., *Endothelial MMP-9 drives the inflammatory response in abdominal aortic aneurysm (AAA).* American journal of translational research, 2017. **9**: p. 5485-5495.

66. Dimitroulis, D., et al., *Telomerase expression on aortic wall endothelial cells is attenuated in Abdominal Aortic Aneurysms compared to healthy nonaneurysmal aortas.* Journal of Vascular Surgery, 2011. **54**: p. 1778-83.

67. Harris, E.S. and W.J. Nelson, *VE-cadherin: at the front, center, and sides of endothelial cell organization and function.* Current Opinion in Cell Biology, 2010. **22**(5): p. 651-658.

68. Wu, Z., et al., *Dephosphorylation of Y685-VE-Cadherin Involved in Pulmonary Microvascular Endothelial Barrier Injury Induced by Angiotensin II %J Mediators of Inflammation.* Mediators of Inflammation, 2016. **2016**: p. 10.

69. Davies, P.F., *Hemodynamic shear stress and the endothelium in cardiovascular pathophysiology.* Nature clinical practice. Cardiovascular medicine, 2009. **6**(1): p. 16-26.

70. Shimizu, K., N. Mitchell Richard, and P. Libby, *Inflammation and Cellular Immune Responses in Abdominal Aortic Aneurysms.* Arteriosclerosis, Thrombosis, and Vascular Biology, 2006. **26**(5): p. 987-994.

71. Li, H., et al., *Modulation of Immune-Inflammatory Responses in Abdominal Aortic Aneurysm: Emerging Molecular Targets %J Journal of Immunology Research.* Journal of Immunology Research, 2018. **2018**: p. 15.

72. Middleton, R.K., et al., *The pro-inflammatory and chemotactic cytokine microenvironment of the abdominal aortic aneurysm wall: A protein array study.* Journal of Vascular Surgery, 2007. **45**(3): p. 574-580.

73. A M V I Hellenthal, F., et al., *Biomarkers of abdominal aortic aneurysm progression. Part 2: inflammation.* Nature Reviews Cardiology, 2009. **6**: p. 543-52.

74. Xiong, W., et al., *Blocking TNF-alpha attenuates aneurysm formation in a murine model.* Journal of immunology (Baltimore, Md. : 1950), 2009. **183**(4): p. 2741-2746.

75. Nakao, T., et al., *Genetic Ablation of MicroRNA-33 Attenuates Inflammation and Abdominal Aortic Aneurysm Formation via Several Anti-Inflammatory Pathways.* Arteriosclerosis, Thrombosis, and Vascular Biology, 2017. **37**(11): p. 2161-2170.

76. Sprague, A.H. and R.A. Khalil, *Inflammatory cytokines in vascular dysfunction and vascular disease.* Biochemical Pharmacology, 2009. **78**(6): p. 539-552.

77. King, V.L., et al., *Interferon-gamma and the interferon-inducible chemokine CXCL10 protect against aneurysm formation and rupture.* Circulation, 2009. **119**(3): p. 426-435.

78. Shi, G.P., et al., *Cystatin C deficiency in human atherosclerosis and aortic aneurysms.* The Journal of Clinical Investigation, 1999. **104**(9): p. 1191-1197.

79. Wang, Y., et al., *TGF-beta activity protects against inflammatory aortic aneurysm progression and complications in angiotensin II-infused mice.* The Journal of clinical investigation, 2010. **120**(2): p. 422-432.

80. Habashi, J.P., et al., *Losartan, an AT1 antagonist, prevents aortic aneurysm in a mouse model of Marfan syndrome.* Science (New York, N.Y.), 2006. **312**(5770): p. 117-121.

81. Matt, P., et al., *Circulating transforming growth factor-beta in Marfan syndrome.* Circulation, 2009. **120**(6): p. 526-532.

82. Baas, A.F., et al., *Association of the TGF-beta receptor genes with abdominal aortic aneurysm.* European journal of Human Genetics 2010. **18**(2): p. 240-244.

83. Kiechl, S., et al., *Osteoprotegerin Is a Risk Factor for Progressive Atherosclerosis and Cardiovascular Disease.* Circulation, 2004. **109**(18): p. 2175-2180.

84. Jono, S., et al., *Serum osteoprotegerin levels and long-term prognosis in subjects with stable coronary artery disease.* Journal of Thrombosis and Haemostasis, 2010. **8**(6): p. 1170-1175.

85. Koole, D., et al., *Osteoprotegerin Is Associated With Aneurysm Diameter and Proteolysis in Abdominal Aortic Aneurysm Disease.* Arteriosclerosis, Thrombosis, and Vascular Biology, 2012. **32**(6): p. 1497-1504.

86. Filis, K., et al., *Osteopontin and Osteoprotegerin as Potential Biomarkers in Abdominal Aortic Aneurysm before and after Treatment.* International scholarly research notices, 2014. **2014**: p. 461239-461239.

87. Harrison, S., et al., *Interleukin-6 receptor pathways in abdominal aortic aneurysm.* Eur Heart J, 2012. **34**.

88. Vainas, T., et al., *Serum C-Reactive Protein Level Is Associated With Abdominal Aortic Aneurysm Size and May Be Produced by Aneurysmal Tissue.* Circulation, 2003. **107**(8): p. 1103-1105.

89. Badger, S.A., et al., *C-reactive protein (CRP) elevation in patients with abdominal aortic aneurysm is independent of the most important CRP genetic polymorphism.* Journal of Vascular Surgery, 2009. **49**(1): p. 178-184.

90. Cao, H., et al., *Homocysteine Level and Risk of Abdominal Aortic Aneurysm: A Meta-Analysis.* Plos One, 2014. **9**(1): p. e85831.

91. Polat, M., et al., *Plasma homocysteine level is elevated in patients on isotretinoin therapy for cystic acne: A prospective controlled study.* Journal of Dermatological Treatment, 2008. **19**(4): p. 229-232.

92. Karlsson, L., et al., *Detection of Viable Chlamydia pneumoniae inAbdominal Aortic Aneurysms.* European Journal of Vascular and Endovascular Surgery, 2000. **19**: p. 630-5.

93. Golledge, J., et al., *Association Between Osteopontin and Human Abdominal Aortic Aneurysm.* Arteriosclerosis, Thrombosis, and Vascular Biology, 2007. **27**(3): p. 655-660.

94. Jayalath, R.W., S.H. Mangan, and J. Golledge, *Aortic Calcification.* European Journal of Vascular and Endovascular Surgery, 2005. **30**(5): p. 476-488.

95. Chowdhury, M.M., et al., *Editor's Choice – Calcification of Thoracic and Abdominal Aneurysms is Associated with Mortality and Morbidity.* European Journal of Vascular and Endovascular Surgery, 2018. **55**(1): p. 101-108.

96. McCarty, M.F. and J.J. DiNicolantonio, *The Molecular Biology and Pathophysiology of Vascular Calcification.* Postgraduate Medicine, 2014. **126**(2): p. 54-64.

97. Ladich, E., et al., *Vascular diseases: aortitis, aortic aneurysms, and vascular calcification.* Cardiovascular Pathology, 2016. **25**(5): p. 432-441.

98. Kim, E.-D., et al., *Association of abdominal aortic calcification with lifestyle and risk factors of cardiovascular disease.* Korean journal of family medicine, 2013. **34**(3): p. 213-220.

99. Matsumoto, K.-I., et al., *Proteomic analysis of calcified abdominal and thoracic aortic aneurysms*. Vol. 30. 2012. 417-29.

100. Orriols, M., et al., *Down-regulation of Fibulin-5 is associated with aortic dilation: role of inflammation and epigenetics.* Cardiovascular Research, 2016. **110**(3): p. 431-442.

101. Thompson, M.M., et al., *Angiogenesis in abdominal aortic aneurysms.* European Journal of Vascular and Endovascular Surgery, 1996. **11**(4): p. 464-469.

102. Kubis, N. and B.I. Levy, *Vasculogenesis and angiogenesis: molecular and cellular controls. Part 1: growth factors.* Interventional neuroradiology : journal of peritherapeutic neuroradiology, surgical procedures and related neurosciences, 2003. **9**(3): p. 227-237.

103. Sano, M., et al., *Lymphangiogenesis and angiogenesis in abdominal aortic aneurysm.* Plos One, 2014. **9**(3): p. e89830-e89830.

104. Vijaynagar, B., et al., *Potential role for anti-angiogenic therapy in abdominal aortic aneurysms.* European Journal of Clinical Investigation, 2013. **43**(7): p. 758-765.

105. Sakuda, H., et al., *Media conditioned by smooth muscle cells cultured in a variety of hypoxic environments stimulates in vitro angiogenesis. A relationship*

to transforming growth factor-beta 1. The American journal of Pathology, 1992. **141**(6): p. 1507-1516.

106. Choke, E., et al., *Increased Angiogenesis at the Site of Abdominal Aortic Aneurysm Rupture.* Annals of the New York Academy of Sciences, 2006. **1085**(1): p. 315-319.

107. Escudero, P., et al., *Combined treatment with bexarotene and rosuvastatin reduces angiotensin-II-induced abdominal aortic aneurysm in apoE−/− mice and angiogenesis.* British Journal of Pharmacology, 2015. **172**(12): p. 2946-2960.

108. Kessler, K., et al., *Angiogenesis and remodelling in human thoracic aortic aneurysms.* Cardiovascular Research, 2014. **104**(1): p. 147-159.

109. Insull, W., *The Pathology of Atherosclerosis: Plaque Development and Plaque Responses to Medical Treatment.* The American Journal of Medicine, 2009. **122**(1, Supplement): p. S3-S14.

110. Finn Aloke, V., et al., *Concept of Vulnerable/Unstable Plaque.* Arteriosclerosis, Thrombosis, and Vascular Biology, 2010. **30**(7): p. 1282-1292.

111. Ilhan, F. and S.T. Kalkanli, *Atherosclerosis and the role of immune cells.* World journal of clinical cases, 2015. **3**(4): p. 345-352.

112. Libby, P., *Inflammation in atherosclerosis.* Nature, 2002. **420**: p. 868.

113. Golledge, J. and P.E. Norman, *Atherosclerosis and abdominal aortic aneurysm: cause, response, or common risk factors?* Arteriosclerosis, Thrombosis, and Vascular Biology, 2010. **30**(6): p. 1075-1077.

114. Auerbach, O. and L. Garfinkel, *Atherosclerosis and Aneurysm of Aorta in Relation to Smoking Habits and Age.* CHEST, 1980. **78**(6): p. 805-809.

115. Peshkova, I.O., G. Schaefer, and E.K. Koltsova, *Atherosclerosis and aortic aneurysm – is inflammation a common denominator?* The FEBS Journal, 2015. **283**(9): p. 1636-1652.

116. Lee, A.J., et al., *Smoking, atherosclerosis and risk of abdominal aortic aneurysm.* European Heart Journal, 1997. **18**(4): p. 671-676.

117. Reed, D., et al., *Are aortic aneurysms caused by atherosclerosis?* Circulation, 1992. **85**(1): p. 205-211.

118. Hebballi, R. and J. Swanevelder, *Diagnosis and management of aortic dissection.* Continuing Education in Anaesthesia Critical Care & Pain, 2009. **9**(1): p. 14-18.

119. Gawinecka, J., F. Schönrath, and A. von Eckardstein, *Acute aortic dissection: pathogenesis, risk factors and diagnosis.* Swiss Medical Weekly, 2017. **147**.

120. Tong, J., Y. Cheng, and G.A. Holzapfel, *Mechanical assessment of arterial dissection in health and disease: Advancements and challenges.* Journal of Biomechanics, 2016. **49**(12): p. 2366-2373.

121. Juang, D., C. Braverman Alan, and K. Eagle, *Aortic Dissection.* Circulation, 2008. **118**(14): p. e507-e510.

122. Criado, F.J., *Aortic dissection: a 250-year perspective.* Texas Heart Institute journal, 2011. **38**(6): p. 694-700.

123. Paul Tran, T. and A. Khoynezhad, *Current management of type B aortic dissection.* Vascular health and risk management, 2009. **5**: p. 53-63.

124. K Lempel, J., et al., *Aortic Arch Dissection: A Controversy of Classification.* Radiology, 2014. **271**: p. 131457.

125. Feng, J., et al., *Aortic dissection is associated with reduced polycystin-1 expression, an abnormality that leads to increased ERK phosphorylation in vascular smooth muscle cells.* European journal of Histochemistry 2016. **60**(4): p. 2711-2711.

126. Vianello, E., et al., *Acute phase of aortic dissection: A pilot study on CD40L, MPO, and MMP-1, -2, 9 and TIMP-1 circulating levels in elderly patients.* Immunity & Ageing, 2016. **13**.

127. Daugherty, A. and A. Cassis Lisa, *Mouse Models of Abdominal Aortic Aneurysms.* Arteriosclerosis, Thrombosis, and Vascular Biology, 2004. **24**(3): p. 429-434.

128. Trollope, A., et al., *Animal models of abdominal aortic aneurysm and their role in furthering management of human disease.* Cardiovascular Pathology, 2011. **20**(2): p. 114-123.

129. Tsui, J.C., *Experimental models of abdominal aortic aneurysms.* The Open Cardiovascular Medicine Journal, 2010. **4**: p. 221-230.

130. Daugherty, A., M.W. Manning, and L.A. Cassis, *Angiotensin II promotes atherosclerotic lesions and aneurysms in apolipoprotein E–deficient mice.* The Journal of Clinical Investigation, 2000. **105**(11): p. 1605-1612.

131. Sénémaud, J., et al., *Translational Relevance and Recent Advances of Animal Models of Abdominal Aortic Aneurysm.* Arteriosclerosis, Thrombosis, and Vascular Biology, 2017. **37**(3): p. 401-410.

132. Phillips, E.H., et al., *Morphological and Biomechanical Differences in the Elastase and AngII apoE(-/-) Rodent Models of Abdominal Aortic Aneurysms.* BioMed Research International, 2015. **2015**: p. 413189-413189.

133. Wang, Y., S. Krishna, and J. Golledge, *The calcium chloride-induced rodent model of abdominal aortic aneurysm.* Atherosclerosis, 2013. **226**(1): p. 29-39.

134. Papke Christina, L., Y. Yamashiro, and H. Yanagisawa, *MMP17/MT4-MMP and Thoracic Aortic Aneurysms.* Circulation Research, 2015. **117**(2): p. 109-112.

135. Yu, C. and R.W. Jeremy, *Angiotensin, transforming growth factor β and aortic dilatation in Marfan syndrome: Of mice and humans.* IJC Heart & Vasculature, 2018. **18**: p. 71-80.

136. Nguyen Dinh Cat, A., et al., *Angiotensin II, NADPH oxidase, and redox signaling in the vasculature.* Antioxidants & Redox Signaling, 2013. **19**(10): p. 1110-1120.

137. Berk, B.C., J. Haendeler, and J. Sottile, *Angiotensin II, atherosclerosis, and aortic aneurysms.* The Journal of Clinical Investigation, 2000. **105**(11): p. 1525-1526.

138. Tong, L. and V. Tergaonkar, *Rho protein GTPases and their interactions with NFκB: crossroads of inflammation and matrix biology.* Bioscience Reports, 2014. **34**(3): p. e00115.

139. Nataatmadja, M., et al., *Angiotensin II Receptor Antagonism Reduces Transforming Growth Factor Beta and Smad Signaling in Thoracic Aortic Aneurysm.* The Ochsner Journal, 2013. **13**(1): p. 42-48.

140. Rodríguez-Vita, J., et al., *Angiotensin II Activates the Smad Pathway in Vascular Smooth Muscle Cells by a Transforming Growth Factor-β–Independent Mechanism.* Circulation, 2005. **111**(19): p. 2509-2517.

141. Brasier, A., B. Ju, and R. Tilton, *Multifaceted Role of Angiotensin II in Vascular Inflammation and Aortic Aneurysmal Disease*, in *Etiology, Pathogenesis and Pathophysiology of Aortic Aneurysms and Aneurysm Rupture*. 2011.

142. Hamblin, M., et al., *Vascular smooth muscle cell peroxisome proliferator-activated receptor-γ deletion promotes abdominal aortic aneurysms.* Journal of Vascular Surgery, 2010. **52**(4): p. 984-993.

143. Watanabe, K., et al., *Group X secretory PLA(2) in neutrophils plays a pathogenic role in abdominal aortic aneurysms in mice.* American Journal of Physiology-Heart and Circulatory Physiology, 2012. **302**: p. H95-104.

144. Chen, Q., et al., *Matrix Metalloproteinases: Inflammatory Regulators of Cell Behaviors in Vascular Formation and Remodeling %J Mediators of Inflammation.* Mediators of Inflammation, 2013. **2013**: p. 14.

145. Parastatidis, I., et al., *Overexpression of Catalase in Vascular Smooth Muscle Cells Prevents the Formation of Abdominal Aortic Aneurysms.* Arteriosclerosis, Thrombosis, and Vascular Biology, 2013. **33**.

146. Gong, Y., et al., *Inflammatory macrophage migration requires MMP-9 activation by plasminogen in mice.* The Journal of clinical investigation, 2008. **118**(9): p. 3012-3024.

147. Visse, R. and H. Nagase, *Matrix Metalloproteinases and Tissue Inhibitors of Metalloproteinases.* Circulation Research, 2003. **92**(8): p. 827-839.

148. Lu, P., et al., *Extracellular matrix degradation and remodeling in development and disease.* Cold Spring Harbor perspectives in biology, 2011. **3**(12): p. 10.1101/cshperspect.a005058 a005058.

149. Sternlicht, M.D. and Z. Werb, *How matrix metalloproteinases regulate cell behavior.* Annual Review of Cell and Developmental Biology, 2001. **17**: p. 463-516.

150. Morrison, C., et al., *Matrix metalloproteinase proteomics: Substrates, targets, and therapy.* Current Opinion in Cell Biology, 2009. **21**: p. 645-53.

151. Jackson, B.C., D.W. Nebert, and V. Vasiliou, *Update of human and mouse matrix metalloproteinase families.* Human Genomics, 2010. **4**(3): p. 194.

152. Murphy, G., et al., *Matrix metalloproteinases in arthritic disease.* Arthritis Research & Therapy, 2002. **4**(3): p. S39.

153. Somerville, R., S. A Oblander, and S. S Apte, *Matrix metalloproteinases: Old dogs with new tricks.* Genome biology, 2003. **4**: p. 216.

154. Arpino, V., M. Brock, and S.E. Gill, *The role of TIMPs in regulation of extracellular matrix proteolysis.* Matrix Biology, 2015. **44-46**: p. 247-254.

155. Brew, K. and H. Nagase, *The tissue inhibitors of metalloproteinases (TIMPs): An ancient family with structural and functional diversity.* Biochimica et biophysica acta, 2010. **1803**: p. 55-71.

156. Fanjul-Fernández, M., et al., *Matrix metalloproteinases: Evolution, gene regulation and functional analysis in mouse models.* Biochimica et Biophysica Acta (BBA) - Molecular Cell Research, 2010. **1803**(1): p. 3-19.

157. Benjamin, M.M. and R.A. Khalil, *Matrix metalloproteinase inhibitors as investigative tools in the pathogenesis and management of vascular disease.* Experientia supplementum (2012), 2012. **103**: p. 209-279.

158. Tallant, C., A. Marrero, and F.X. Gomis-Rüth, *Matrix metalloproteinases: Fold and function of their catalytic domains.* Biochimica et Biophysica Acta (BBA) - Molecular Cell Research, 2010. **1803**(1): p. 20-28.

159. Manicone, A.M. and J.K. McGuire, *Matrix metalloproteinases as modulators of inflammation.* Seminars in Cell & Developmental Biology, 2008. **19**(1): p. 34-41.

160. Johnson, J.L., et al., *A selective matrix metalloproteinase-12 inhibitor retards atherosclerotic plaque development in apolipoprotein E-knockout mice.* Arteriosclerosis, Thrombosis, and Vascular Biology, 2011. **31**(3): p. 528-535.

161. Di Gregoli, K., et al., *MicroRNA-24 Regulates Macrophage Behavior and Retards Atherosclerosis.* Arteriosclerosis, Thrombosis, and Vascular Biology, 2014. **34**(9): p. 1990-2000.

162. Johnson Jason, L., et al., *Suppression of Atherosclerotic Plaque Progression and Instability by Tissue Inhibitor of Metalloproteinase-2.* Circulation, 2006. **113**(20): p. 2435-2444.

163. Nissinen, L. and V.-M. Kähäri, *Matrix metalloproteinases in inflammation.* Biochimica et Biophysica Acta (BBA) - General Subjects, 2014. **1840**(8): p. 2571-2580.

164. Aziz, F. and H. Kuivaniemi, *Role of matrix metalloproteinase inhibitors in preventing abdominal aortic aneurysm.* Annals of Vascular Surgery, 2007. **21**(3): p. 392-401.

165. Lindholt, J.S., et al., *The Plasma Level of Matrix Metalloproteinase 9 may Predict the Natural History of Small Abdominal Aortic Aneurysms. A Preliminary Study.* European Journal of Vascular and Endovascular Surgery, 2000. **20**(3): p. 281-285.

166. Davis, V., et al., *Matrix Metalloproteinase-2 Production and Its Binding to the Matrix Are Increased in Abdominal Aortic Aneurysms.* Arteriosclerosis, Thrombosis, and Vascular Biology, 1998. **18**(10): p. 1625-1633.

167. Elmore, J.R., et al., *Expression of Matrix Metalloproteinases and TIMPs in Human Abdominal Aortic Aneurysms.* Annals of Vascular Surgery, 1998. **12**(3): p. 221-228.

168. Wilson, W.R.W., et al., *Matrix metalloproteinase 8 (neutrophil collagenase) in the pathogenesis of abdominal aortic aneurysm.* BJS, 2005. **92**(7): p. 828-833.

169. Martín-Alonso, M., et al., *Deficiency of MMP17/MT4-MMP Proteolytic Activity Predisposes to Aortic Aneurysm in Mice.* Circulation Research, 2015. **117**(2): p. e13-e26.

170. Nollendorfs, A., et al., *The expression and localization of membrane type-1 matrix metalloproteinase in human abdominal aortic aneurysms.* Journal of Vascular Surgery, 2001. **34**(2): p. 316-322.

171. Newman, K.M., et al., *Identification of matrix metalloproteinases 3 (stromelysin-1) and 9 (gelatinase B) in abdominal aortic aneurysm.* Arteriosclerosis and Thrombosis: A Journal of Vascular Biology, 1994. **14**(8): p. 1315-1320.

172. Curci, J.A., et al., *Expression and localization of macrophage elastase (matrix metalloproteinase-12) in abdominal aortic aneurysms.* The Journal of Clinical Investigation, 1998. **102**(11): p. 1900-1910.

173. Kugo, H., et al., *The effects of nicotine administration on the pathophysiology of rat aortic wall.* Biotechnic & Histochemistry, 2017. **92**(2): p. 141-148.

174. Defawe, O., et al., *TIMP-2 and PAI-1 mRNA levels are lower in aneurysmal as compared to athero-occlusive abdominal aortas.* Cardiovascular Research, 2003. **60**: p. 205-13.

175. Lipp, C., et al., *Expression of a Disintegrin and Metalloprotease in Human Abdominal Aortic Aneurysms.* Journal of Vascular Research, 2012. **49**(3): p. 198-206.

176. Airhart, N., et al., *Smooth muscle cells from abdominal aortic aneurysms are unique and can independently and synergistically degrade insoluble elastin.* Journal of Vascular Surgery, 2014. **60**(4): p. 1033-1042.e5.

177. Ikonomidis, J.S., et al., *Plasma biomarkers for distinguishing etiologic subtypes of thoracic aortic aneurysm disease.* The Journal of Thoracic and Cardiovascular Surgery, 2013. **145**(5): p. 1326-1333.

178. Pyo, R., et al., *Targeted gene disruption of matrix metalloproteinase-9 (gelatinase B) suppresses development of experimental abdominal aortic aneurysms.* The Journal of Clinical Investigation, 2000. **105**(11): p. 1641-1649.

179. Longo, G.M., et al., *Matrix metalloproteinases 2 and 9 work in concert to produce aortic aneurysms.* The Journal of Clinical Investigation, 2002. **110**(5): p. 625-632.

180. Mao, N., et al., *Phenotypic switching of vascular smooth muscle cells in animal model of rat thoracic aortic aneurysm.* Interactive CardioVascular and Thoracic Surgery, 2015. **21**(1): p. 62-70.

181. Lu, H., et al., *Novel Mechanisms of Abdominal Aortic Aneurysms.* Current Atherosclerosis Reports, 2012. **14**(5): p. 402-412.

182. Silence, J., D. Collen, and H.R. Lijnen, *Reduced Atherosclerotic Plaque but Enhanced Aneurysm Formation in Mice With Inactivation of the Tissue Inhibitor of Metalloproteinase-1 (TIMP-1) Gene.* Circulation Research, 2002. **90**(8): p. 897-903.

183. Allaire, E., et al., *Local overexpression of TIMP-1 prevents aortic aneurysm degeneration and rupture in a rat model.* The Journal of Clinical Investigation, 1998. **102**(7): p. 1413-1420.

184. Di Gregoli, K., et al., *Differential effects of tissue inhibitor of metalloproteinase (TIMP)-1 and TIMP-2 on atherosclerosis and monocyte/macrophage invasion.* Cardiovascular Research, 2016. **109**(2): p. 318-330.

185. Basu, R., et al., *Loss of Timp3 gene leads to abdominal aortic aneurysm formation in response to angiotensin II.* The Journal of Biological Chemistry, 2012. **287**(53): p. 44083-44096.

186. Di Gregoli, K., et al., *MicroRNA-181b Controls Atherosclerosis and Aneurysms Through Regulation of TIMP-3 and Elastin.* Circulation Research, 2017. **120**(1): p. 49-65.

187. Liu, J., et al., *Mechanism of inhibition of matrix metalloproteinase-2 expression by doxycycline in human aortic smooth muscle cells.* Journal of Vascular Surgery, 2003. **38**(6): p. 1376-1383.

188. Manning Michael, W., A. Cassis Lisa, and A. Daugherty, *Differential Effects of Doxycycline, a Broad-Spectrum Matrix Metalloproteinase Inhibitor, on Angiotensin II–Induced Atherosclerosis and Abdominal Aortic Aneurysms.* Arteriosclerosis, Thrombosis, and Vascular Biology, 2003. **23**(3): p. 483-488.

189. Moore, G., et al., *Suppression of experimental abdominal aortic aneurysms by systemic treatment with a hydroxamate-based matrix metalloproteinase inhibitor (RS 132908).* Journal of Vascular Surgery, 1999. **29**(3): p. 522-532.

190. A. Bigatel, D., et al., *The matrix metalloproteinase inhibitor BB-94 limits expansion of experimental abdominal aortic aneurysms.* Journal of Vascular Research, 1999. **29**: p. 130-8; discussion 138.

191. Mosorin, M., et al., *Use of doxycycline to decrease the growth rate of abdominal aortic aneurysms: A randomized, double-blind, placebo-controlled pilot study.* Journal of Vascular Surgery, 2001. **34**(4): p. 606-610.

192. Lindeman Jan, H.N., et al., *Clinical Trial of Doxycycline for Matrix Metalloproteinase-9 Inhibition in Patients With an Abdominal Aneurysm.* Circulation, 2009. **119**(16): p. 2209-2216.

193. E Hackmann, A., et al., *A Randomized, Placebo-Controlled Trial of Doxycycline after Endoluminal Aneurysm Repair.* Journal of Vascular Surgery, 2008. **48**: p. 519-26; discussion 526.

194. Ding, R., et al., *Matrix Metalloproteinases in the Aneurysm Wall of Patients Treated with Low-Dose Doxycycline.* Vascular, 2005. **13**(5): p. 290-297.

195. Baxter, B., et al., *Prolonged administration of doxycycline in patients with small asymptomatic abdominal aortic aneurysms: Report of a prospective (Phase II) multicenter study.* Journal of Vascular Research, 2002. **36**: p. 1-12.

196. Lysgaard Poulsen, J., J. Stubbe, and J.S. Lindholt, *Animal Models Used to Explore Abdominal Aortic Aneurysms: A Systematic Review.* European Journal of Vascular and Endovascular Surgery, 2016. **52**(4): p. 487-499.

197. Moxon, J.V., et al., *Diagnosis and monitoring of abdominal aortic aneurysm: current status and future prospects.* Current problems in cardiology, 2010. **35**(10): p. 512-548.

198. Saraff, K., et al., *Aortic Dissection Precedes Formation of Aneurysms and Atherosclerosis in Angiotensin II-Infused, Apolipoprotein E-Deficient Mice.* Arteriosclerosis, Thrombosis, and Vascular Biology, 2003. **23**(9): p. 1621-1626.

199. Riches, K., et al., *Exploring smooth muscle phenotype and function in a bioreactor model of abdominal aortic aneurysm.* Journal of Translational Medicine, 2013. **11**: p. 208.

200. Wang, J., et al., *Ex vivo blood vessel bioreactor for analysis of the biodegradation of magnesium stent models with and without vessel wall integration.* Acta Biomaterialia

2016. **50**.

201. Anwar, M., et al., *The Effect of Pressure-Induced Mechanical Stretch on Vascular Wall Differential Gene Expression.* Journal of Vascular Research, 2012. **49**: p. 463-78.

202. Müller-Marschhausen, K., J. Waschke, and D. Drenckhahn, *Physiological hydrostatic pressure protects endothelial monolayer integrity.* American Journal of Physiology-Cell Physiology, 2008. **294**(1): p. C324-C332.

203. Lu, D. and S. Kassab Ghassan, *Role of shear stress and stretch in vascular mechanobiology.* Journal of The Royal Society Interface, 2011. **8**(63): p. 1379-1385.

204. Califano, J.P. and C.A. Reinhart-King, *Exogenous and endogenous force regulation of endothelial cell behavior.* Journal of Biomechanics, 2010. **43**(1): p. 79-86.

205. dela Paz, N.G. and P.A. D'Amore, *Arterial versus venous endothelial cells.* Cell and Tissue Research, 2009. **335**(1): p. 5-16.

206. Taylor, C.A., et al., *In Vivo Quantification of Blood Flow and Wall Shear Stress in the Human Abdominal Aorta During Lower Limb Exercise.* Annals of Biomedical Engineering, 2002. **30**(3): p. 402-408.

207. Les, A.S., et al., *Quantification of Hemodynamics in Abdominal Aortic Aneurysms During Rest and Exercise Using Magnetic Resonance Imaging and Computational Fluid Dynamics.* Annals of Biomedical Engineering, 2010. **38**(4): p. 1288-1313.

208. Luchtefeld, M., et al., *Angiotensin II induces MMP-2 in a p47phox-dependent manner.* Biochemical and Biophysical Research Communications, 2005. **328**(1): p. 183-188.

209. Touyz, R.M., *Intracellular mechanisms involved in vascular remodelling of resistance arteries in hypertension: role of angiotensin II.* Experimental Physiology, 2005. **90**(4): p. 449-455.

210. Cao, J., et al., *Rapamycin inhibits CaCl2-induced thoracic aortic aneurysm formation in rats through mTOR-mediated suppression of proinflammatory mediators.* Molecular Medicine Reports, 2017. **16**.

211. Cassis, L.A., et al., *ANG II infusion promotes abdominal aortic aneurysms independent of increased blood pressure in hypercholesterolemic mice.* American Journal of Physiology-Heart and Circulatory Physiology, 2009. **296**(5): p. H1660-H1665.

212. Jackson, V., et al., *Matrix metalloproteinase 14 and 19 expression is associated with thoracic aortic aneurysms.* The Journal of Thoracic and Cardiovascular Surgery, 2012. **144**(2): p. 459-466.

213. Didangelos, A., et al., *Extracellular matrix composition and remodeling in human abdominal aortic aneurysms: a proteomics approach.* Molecular & cellular proteomics : MCP, 2011. **10**(8): p. M111.008128-M111.008128.

214. Thompson, R.W., P.J. Geraghty, and J.K. Lee, *Abdominal Aortic Aneurysms: Basic Mechanisms and Clinical Implications.* Current Problems in Surgery, 2002. **39**(2): p. 110-230.

215. Martufi, G. and T.C. Gasser, *Turnover of fibrillar collagen in soft biological tissue with application to the expansion of abdominal aortic aneurysms.* Journal of The Royal Society Interface, 2012. **9**(77): p. 3366-3377.

216. Abdul-Hussien, H., et al., *Collagen Degradation in the Abdominal Aneurysm: A Conspiracy of Matrix Metalloproteinase and Cysteine Collagenases.* The American Journal of Pathology, 2007. **170**(3): p. 809-817.

217. Kuivaniemi, H., et al., *Understanding the pathogenesis of abdominal aortic aneurysms.* Expert Review of Cardiovascular Therapy, 2015. **13**(9): p. 975-987.

218. Yamanouchi, D., et al., *Accelerated aneurysmal dilation associated with apoptosis and inflammation in a newly developed calcium phosphate rodent abdominal aortic aneurysm model.* Journal of vascular surgery, 2012. **56**(2): p. 455-461.

219. Daugherty, A. and L. Cassis, *Angiotensin II and abdominal aortic aneurysms.* Current hypertension reports, 2005. **6**: p. 442-6.

220. Satta, J., et al., *Increased turnover of collagen in abdominal aortic aneurysms, demonstrated by measuring the concentration of the aminoterminal propeptide of type III procollagen in peripheral and aortal blood samples.* Journal of Vascular Surgery, 1995. **22**(2): p. 155-160.

221. Basalyga Dina, M., et al., *Elastin Degradation and Calcification in an Abdominal Aorta Injury Model.* Circulation, 2004. **110**(22): p. 3480-3487.

222. Freestone, T., et al., *Inflammation and Matrix Metalloproteinases in the Enlarging Abdominal Aortic Aneurysm.* Arteriosclerosis, Thrombosis, and Vascular Biology, 1995. **15**(8): p. 1145-1151.

223. Tsuruda, T., et al., *Adventitial Mast Cells Contribute to Pathogenesis in the Progression of Abdominal Aortic Aneurysm.* Circulation Research, 2008. **102**(11): p. 1368-1377.

224. Kondratskyi, A., et al., *Ion channels in the regulation of apoptosis.* Biochimica et Biophysica Acta (BBA) - Biomembranes, 2015. **1848**(10, Part B): p. 2532-2546.

225. Pinton, P., et al., *Calcium and apoptosis: ER-mitochondria Ca2+ transfer in the control of apoptosis.* Oncogene, 2008. **27**(50): p. 6407-6418.

226. Cao, R.Y., et al., *The Murine Angiotensin II-Induced Abdominal Aortic Aneurysm Model: Rupture Risk and Inflammatory Progression Patterns.* Frontiers in Pharmacology, 2010. **1**: p. 9-9.

227. Landmesser, U., et al., *Angiotensin II Induces Endothelial Xanthine Oxidase Activation.* Arteriosclerosis, Thrombosis, and Vascular Biology, 2007. **27**(4): p. 943-948.

228. Acharya, G., et al., *Hemodynamic aspects of normal human feto-placental (umbilical) circulation.* Acta Obstetricia et Gynecologica Scandinavica, 2016. **95**(6): p. 672-682.

229. Li, Y., et al., *ANG II induces apoptosis of human vascular smooth muscle via extrinsic pathway involving inhibition of Akt phosphorylation and increased FasL expression.* American Journal of Physiology-Heart and Circulatory Physiology, 2006. **290**(5): p. H2116-H2123.

230. Nagata, S., *Apoptosis by Death Factor.* Cell, 1997. **88**(3): p. 355-365.

231. Rowe, V.L., et al., *Vascular smooth muscle cell apoptosis in aneurysmal, occlusive, and normal human aortas.* Journal of Vascular Surgery, 2000. **31**(3): p. 567-576.

232. Diep Quy, N., J.-S. Li, and L. Schiffrin Ernesto, *In Vivo Study of AT1 and AT2 Angiotensin Receptors in Apoptosis in Rat Blood Vessels.* Hypertension, 1999. **34**(4): p. 617-624.

233. López-Candales, A., et al., *Decreased vascular smooth muscle cell density in medial degeneration of human abdominal aortic aneurysms.* The American journal of Pathology, 1997. **150**: p. 993-1007.

234. Rudijanto, A., *The role of vascular smooth muscle cells on the pathogenesis of atherosclerosis.* Acta medica Indonesiana, 2007. **39**: p. 86-93.

235. Gill, S.E. and W.C. Parks, *Metalloproteinases and their inhibitors: regulators of wound healing.* The international journal of biochemistry & cell biology, 2008. **40**(6-7): p. 1334-1347.

236. Bonnans, C., J. Chou, and Z. Werb, *Remodelling the extracellular matrix in development and disease.* Nature reviews. Molecular Cell Biology, 2014. **15**(12): p. 786-801.

237. Tengiz, I., et al., *Elevated levels of matrix metalloprotein-3 in patients with coronary aneurysm: A case control study.* Current controlled trials in cardiovascular medicine, 2004. **5**: p. 10.

238. Johnson Jason, L., et al., *Matrix Metalloproteinase (MMP)-3 Activates MMP-9 Mediated Vascular Smooth Muscle Cell Migration and Neointima Formation in Mice.* Arteriosclerosis, Thrombosis, and Vascular Biology, 2011. **31**(9): p. e35-e44.

239. Ye, S., et al., *Progression of coronary atherosclerosis is associated with a common genetic variant of the human stromelysin-1 promoter which results in reduced gene expression.* The Journal of Biological Chemistry, 1996. **271**: p. 13055-13060.

240. Orbe, J., et al., *Different expression of MMPs/TIMP-1 in human atherosclerotic lesions. Relation to plaque features and vascular bed.* Atherosclerosis, 2003. **170**(2): p. 269-276.

241. Mercapide, J., et al., *Stromelysin-1/matrix metalloproteinase-3 (MMP-3) expression accounts for invasive properties of human astrocytoma cell lines.* International Journal of Cancer, 2003. **106**(5): p. 676-682.

242. Sangiorgi, G., et al., *Plasma Levels of Metalloproteinases-3 and -9 as Markers of Successful Abdominal Aortic Aneurysm Exclusion After Endovascular Graft Treatment.* Circulation, 2001. **104**(suppl_1): p. I-288-I-295.

243. Wilson, W.R.W., et al., *HMG-CoA Reductase Inhibitors (Statins) Decrease MMP-3 and MMP-9 Concentrations in Abdominal Aortic Aneurysms.* European Journal of Vascular and Endovascular Surgery, 2005. **30**(3): p. 259-262.

244. Galis Zorina, S. and J. Khatri Jaikirshan, *Matrix Metalloproteinases in Vascular Remodeling and Atherogenesis.* Circulation Research, 2002. **90**(3): p. 251-262.

245. Magid, R., T. Murphy, and Z. S Galis, *Expression of Matrix Metalloproteinase-9 in Endothelial Cells Is Differentially Regulated by Shear Stress ROLE OF c-Myc.* The Journal of Biological Chemistry, 2003. **278**: p. 32994-9.

246. Caley, M.P., V.L.C. Martins, and E.A. O'Toole, *Metalloproteinases and Wound Healing.* Advances in wound care, 2015. **4**: p. 225-234.

247. Montero, I., et al., *C-Reactive Protein Induces Matrix Metalloproteinase-1 and -10 in Human Endothelial Cells.* Journal of the American College of Cardiology, 2006. **47**: p. 1369-78.

248. Krampert, M., et al., *Activities of the matrix metalloproteinase stromelysin-2 (MMP-10) in matrix degradation and keratinocyte organization in wounded skin.* Molecular biology of the cell, 2004. **15**(12): p. 5242-5254.

249. Barbour, J.R., et al., *Temporal disparity in the induction of matrix metalloproteinases and tissue inhibitors of metalloproteinases after thoracic aortic aneurysm formation.* The Journal of Thoracic and Cardiovascular Surgery, 2006. **132**(4): p. 788-795.

250. Shipley, J.M., et al., *Metalloelastase is required for macrophage-mediated proteolysis and matrix invasion in mice.* Proceedings of the National Academy of Sciences of the United States of America, 1996. **93**(9): p. 3942.

251. Johnson, J.L., et al., *Divergent effects of matrix metalloproteinases 3, 7, 9, and 12 on atherosclerotic plaque stability in mouse brachiocephalic arteries.* Proceedings of the National Academy of Sciences of the United States of America, 2005. **102**(43): p. 15575.

252. Halpert, I., et al., *Matrilysin is expressed by lipid-laden macrophages at sites of potential rupture in atherosclerotic lesions and localizes to areas of versican deposition, a proteoglycan substrate for the enzyme.* Proceedings of the National Academy of Sciences of the United States of America, 1996. **93**(18): p. 9748-9753.

253. P W Scholtes, V., et al., *Carotid Atherosclerotic Plaque Matrix Metalloproteinase-12–Positive Macrophage Subpopulation Predicts Adverse Outcome After Endarterectomy.* Journal of the American Heart Association, 2012. **1**: p. e001040.

254. Dwivedi, A., S.C. Slater, and S.J. George, *MMP-9 and -12 cause N-cadherin shedding and thereby β-catenin signalling and vascular smooth muscle cell proliferation.* Cardiovascular Research, 2008. **81**(1): p. 178-186.

255. Stracke, J.O., et al., *Matrix metalloproteinases 19 and 20 cleave aggrecan and cartilage oligomeric matrix protein (COMP).* FEBS Letters, 2000. **478**(1-2): p. 52-56.

256. Theruvath, T.P., J.A. Jones, and J.S. Ikonomidis, *Matrix metalloproteinases and descending aortic aneurysms: parity, disparity, and switch.* Journal of Cardiac Surgery, 2012. **27**(1): p. 81-90.

257. Steucke, K.E., et al., *Vascular smooth muscle cell functional contractility depends on extracellular mechanical properties.* Journal of Biomechanics, 2015. **48**(12): p. 3044-3051.

258. Renard, M., et al., *Novel MYH11 and ACTA2 mutations reveal a role for enhanced TGFβ signaling in FTAAD.* International journal of cardiology, 2013. **165**(2): p. 314-321.

259. M Milewicz, D., et al., *Genetic Basis of Thoracic Aortic Aneurysms and Dissections: Focus on Smooth Muscle Cell Contractile Dysfunction.* Annual Review of Genomics and Human Genetics, 2008. **9**: p. 283-302.

260. Cairrão, E., et al., *Isolation and culture of human umbilical artery smooth muscle cells expressing functional calcium channels.* In Vitro Cellular & Developmental Biology - Animal, 2009. **45**(3): p. 175-184.

261. Kadner, A., et al., *Human umbilical cord cells for cardiovascular tissue engineering: a comparative study.* European Journal of Cardio-Thoracic Surgery, 2004. **25**(4): p. 635-641.

262. A Atlas, S., *The Renin-Angiotensin Aldosterone System: Pathophysiological Role and Pharmacologic Inhibition.* Journal of Managed Care Pharmacy 2007. **13**: p. 9-20.

263. Lemarié, C.A. and E.L. Schiffrin, *The angiotensin II type 2 receptor in cardiovascular disease.* Journal of the Renin-Angiotensin-Aldosterone System, 2009. **11**(1): p. 19-31.

264. Daugherty, A., M.W. Manning, and L.A. Cassis, *Antagonism of AT2 receptors augments angiotensin II-induced abdominal aortic aneurysms and atherosclerosis.* British Journal of Pharmacology, 2001. **134**(4): p. 865-870.

265. Li, X.C. and R.E. Widdop, *AT2 receptor-mediated vasodilatation is unmasked by AT1 receptor blockade in conscious SHR.* British Journal of Pharmacology, 2004. **142**(5): p. 821-830.

266. Tsutsumi, Y., et al., *Angiotensin II type 2 receptor overexpression activates the vascular kinin system and causes vasodilation.* The Journal of Clinical Investigation, 1999. **104**: p. 925-35.

267. Wynne, B.M., C.-W. Chiao, and R.C. Webb, *Vascular Smooth Muscle Cell Signaling Mechanisms for Contraction to Angiotensin II and Endothelin-1.* Journal of the American Society of Hypertension, 2009. **3**(2): p. 84-95.

268. Mehta, P.K. and K.K. Griendling, *Angiotensin II cell signaling: physiological and pathological effects in the cardiovascular system.* American Journal of Physiology-Cell Physiology, 2007. **292**(1): p. C82-C97.

269. Kawai, T., et al., *AT1 receptor signaling pathways in the cardiovascular system.* Pharmacological Research, 2017. **125**: p. 4-13.

270. Nouet, S. and C. Nahmias, *Signal Transduction from the Angiotensin II AT2 Receptor.* Trends in Endocrinology & Metabolism, 2000. **11**(1): p. 1-6.

271. Kothapalli, C.R., C.E. Gacchina, and A. Ramamurthi, *Utility of hyaluronan oligomers and transforming growth factor-beta1 factors for elastic matrix regeneration by aneurysmal rat aortic smooth muscle cells.* Tissue engineering. Part A, 2009. **15**(11): p. 3247-3260.

272. Yoshimura, K., et al., *Regression of abdominal aortic aneurysm by inhibition of c-Jun N-terminal kinase.* Nature medicine, 2006. **11**: p. 1330-8.

273. Wang, C., et al., *Angiotensin II increases matrix metalloproteinase 2 expression in human aortic smooth muscle cells via AT1R and ERK1/2.* Experimental Biology and Medicine 2015. **240**(12): p. 1564-1571.

274. Batra, J., et al., *Matrix metalloproteinase-10 (MMP-10) interaction with tissue inhibitors of metalloproteinases TIMP-1 and TIMP-2: binding studies and crystal structure.* The Journal of Biological Chemistry, 2012. **287**(19): p. 15935-15946.

275. Ikonomidis, J.S., et al., *Expression of matrix metalloproteinases and endogenous inhibitors within ascending aortic aneurysms of patients with bicuspid or tricuspid aortic valves.* The Journal of Thoracic and Cardiovascular Surgery, 2007. **133**(4): p. 1028-1036.

276. Castoldi, G., et al., *ANG II increases TIMP-1 expression in rat aortic smooth muscle cells in vivo.* American Journal of Physiology-Heart and Circulatory Physiology, 2003. **284**(2): p. H635-H643.

277. Rensen, S.S.M., P.A.F.M. Doevendans, and G.J.J.M. van Eys, *Regulation and characteristics of vascular smooth muscle cell phenotypic diversity.* Netherlands heart journal : monthly journal of the Netherlands Society of Cardiology and the Netherlands Heart Foundation, 2007. **15**(3): p. 100-108.

278. Branchetti, E., et al., *Oxidative stress modulates vascular smooth muscle cell phenotype via CTGF in thoracic aortic aneurysm.* Cardiovascular Research, 2013. **100**(2): p. 316-324.

279. Johnson, J.L., *Elucidating the contributory role of microRNA to cardiovascular diseases (a review).* Vascular pharmacology, 2019. **114**: p. 31-48.

280. Zhang, Z., et al., *Upregulation of TRPM7 Channels by Angiotensin II Triggers Phenotypic Switching of Vascular Smooth Muscle Cells of Ascending Aorta.* Circulation Research, 2012. **111**: p. 1137-46.

281. Bacakova, L., et al., *The Role of Vascular Smooth Muscle Cells in the Physiology and Pathophysiology of Blood Vessels*, in *Muscle Cell and Tissue* 2018.

282. Toro, L., A. Gonzalez-Robles, and E. Stefani, *Electrical properties and morphology of single vascular smooth muscle cells in culture.* American Journal of Physiology-Cell Physiology, 1986. **251**(5): p. C763-C773.

283. Kuma, S., et al., *ANGIOTENSIN II-INDUCED GROWTH OF VASCULAR SMOOTH MUSCLE CELLS IS ASSOCIATED WITH MODULATION OF CELL SURFACE AREA AND PLATELET-DERIVED GROWTH FACTOR RECEPTOR EXPRESSION.* Clinical and Experimental Pharmacology and Physiology, 2007. **34**(3): p. 153-160.

284. Boström, K., et al., *Bone morphogenetic protein expression in human atherosclerotic lesions.* The Journal of Clinical Investigation, 1993. **91**(4): p. 1800-1809.

285. Wada, T., et al., *Calcification of Vascular Smooth Muscle Cell Cultures.* Circulation Research, 1999. **84**(2): p. 166-178.

286. Guo, R.-w., et al., *Angiotensin II induces matrix metalloproteinase-9 expression via a nuclear factor-kappaB-dependent pathway in vascular smooth muscle cells.* Regulatory Peptides, 2008. **147**(1): p. 37-44.

287. Newby, A.C., et al., *Vulnerable atherosclerotic plaque metalloproteinases and foam cell phenotypes.* Thrombosis and haemostasis, 2009. **101**(6): p. 1006-1011.

288. Shen, M., et al., *Divergent Roles of Matrix Metalloproteinase 2 in Pathogenesis of Thoracic Aortic Aneurysm.* Arteriosclerosis, Thrombosis, and Vascular Biology, 2015. **35**(4): p. 888-898.

289. Ogata, Y., J.J. Enghild, and H. Nagase, *Matrix metalloproteinase 3 (stromelysin) activates the precursor for the human matrix metalloproteinase 9.* The Journal of Biological Chemistry, 1992. **267**(6): p. 3581-3584.

290. Huang, W.-C., et al., *Classical macrophage activation up-regulates several matrix metalloproteinases through mitogen activated protein kinases and nuclear factor-κB.* Plos One, 2012. **7**(8): p. e42507-e42507.

291. Jones, J.A., et al., *Alterations in membrane type-1 matrix metalloproteinase abundance after the induction of thoracic aortic aneurysm in a murine model.* American journal of physiology. Heart and circulatory physiology, 2010. **299**(1): p. H114-H124.

292. Li, F. and K.U. Malik, *Angiotensin II-induced Akt activation is mediated by metabolites of arachidonic acid generated by CaMKII-stimulated Ca2+-dependent phospholipase A2.* American Journal of Physiology-Heart and Circulatory Physiology, 2005. **288**(5): p. H2306-H2316.

293. Durham, A.L., et al., *Role of smooth muscle cells in vascular calcification: implications in atherosclerosis and arterial stiffness.* Cardiovascular Research, 2018. **114**(4): p. 590-600.

294. Castellano-Muñoz, M. and A.J. Ricci, *Role of intracellular calcium stores in hair-cell ribbon synapse.* Frontiers in Cellular Neuroscience, 2014. **8**: p. 162-162.

295. Mazurek, R., et al., *Vascular Cells in Blood Vessel Wall Development and Disease.* Advances in pharmacology (San Diego, Calif.), 2017. **78**: p. 323-350.

296. Bennett, H.S., J.H. Luft, and J.C. Hampton, *Morphological classifications of vertebrate blood capillaries.* American Journal of Physiology-Legacy Content, 1959. **196**(2): p. 381-390.

297. Rodrigues, S.F. and D.N. Granger, *Blood cells and endothelial barrier function.* Tissue barriers, 2015. **3**(1-2): p. e978720-e978720.

298. Mai, J., et al., *An evolving new paradigm: endothelial cells--conditional innate immune cells.* Journal of hematology & oncology, 2013. **6**: p. 61-61.

299. Vestweber, D., *VE-Cadherin.* Arteriosclerosis, Thrombosis, and Vascular Biology, 2008. **28**(2): p. 223-232.

300. Franck, G., J. Dai, and A. Fifre, *Reestablishment of the Endothelial Lining by Endothelial Cell Therapy Stabilizes Experimental Abdominal Aortic Aneurysms.* Journal of Vascular Surgery, 2013. **58**: p. 1140-1141.

301. Widmer, R.J. and A. Lerman, *Endothelial dysfunction and cardiovascular disease.* Global cardiology science & practice, 2014. **2014**(3): p. 291-308.

302. Dimmeler, S., et al., *Angiotensin II Induces Apoptosis of Human Endothelial Cells.* Circulation Research, 1997. **81**(6): p. 970-976.

303. Rajagopalan, S., et al., *Angiotensin II-mediated hypertension in the rat increases vascular superoxide production via membrane NADH/NADPH oxidase activation. Contribution to alterations of vasomotor tone.* The Journal of clinical investigation, 1996. **97**(8): p. 1916-1923.

304. Dejana, E., F. Orsenigo, and M.G. Lampugnani, *The role of adherens junctions and VE-cadherin in the control of vascular permeability.* Journal of Cell Science, 2008. **121**(13): p. 2115.

305. Gavard, J., *Endothelial permeability and VE-cadherin: a wacky comradeship.* Cell adhesion & migration, 2014. **8**(2): p. 158-164.

306. Bodor, C., et al., *Angiotensin II increases the permeability and PV-1 expression of endothelial cells.* American Journal of Physiology-Cell Physiology, 2011. **302**(1): p. C267-C276.

307. Bazzoni, G. and E. Dejana, *Endothelial Cell-to-Cell Junctions: Molecular Organization and Role in Vascular Homeostasis.* Physiological Reviews, 2004. **84**(3): p. 869-901.

308. Clevers, H. and R. Nusse, *Wnt/β-Catenin Signaling and Disease.* Cell, 2012. **149**(6): p. 1192-1205.

309. Vorp, D.A., *Biomechanics of abdominal aortic aneurysm.* Journal of biomechanics, 2007. **40**(9): p. 1887-1902.

310. Balaguru, U.M., et al., *Disturbed flow mediated modulation of shear forces on endothelial plane: A proposed model for studying endothelium around atherosclerotic plaques.* Scientific Reports, 2016. **6**: p. 27304.

311. Tucker, R.P., et al., *See-saw rocking: an in vitro model for mechanotransduction research.* Journal of The Royal Society Interface, 2014. **11**(97): p. 20140330.

312. Dardik, A., et al., *Differential effects of orbital and laminar shear stress on endothelial cells.* Journal of Vascular Surgery, 2005. **41**(5): p. 869-880.

313. Zhai, H., et al., *TIMP3 suppresses the proliferation and migration of SMCs from the aortic neck of atherosclerotic AAA in rabbits, via decreased MMP2 and MMP9 activity, and reduced TNFα expression.* Molecular medicine reports, 2018. **18**(2): p. 2061-2067.

314. Xu, F., et al., *Cardiovascular effects of losartan and its relevant clinical application.* Current medicinal chemistry, 2009. **16**(29): p. 3841-3857.

315. Nelson, C.M., et al., *Vascular endothelial-cadherin regulates cytoskeletal tension, cell spreading, and focal adhesions by stimulating RhoA.* Molecular biology of the cell, 2004. **15**(6): p. 2943-2953.

316. Schnittler, H.-J., B. Püschel, and D. Drenckhahn, *Role of cadherins and plakoglobin in interendothelial adhesion under resting conditions and shear stress.* American Journal of Physiology-Heart and Circulatory Physiology, 1997. **273**(5): p. H2396-H2405.

317. de Bruin, R.G., et al. *The RNA-binding protein quaking maintains endothelial barrier function and affects VE-cadherin and β-catenin protein expression*. Scientific reports, 2016. **6**, 21643 DOI: 10.1038/srep21643.

318. Miao, H., et al., *Effects of Flow Patterns on the Localization and Expression of VE-Cadherin at Vascular Endothelial Cell Junctions: In vivo and in vitro Investigations*. Vol. 42. 2005. 77-89.

319. Giannotta, M., M. Trani, and E. Dejana, *VE-Cadherin and Endothelial Adherens Junctions: Active Guardians of Vascular Integrity.* Developmental Cell, 2013. **26**(5): p. 441-454.

320. Wu, Z., et al., *VE-cadherin involved in the pulmonary microvascular endothelial cell barrier injury induced by angiotensin II through modulating the cellular apoptosis and skeletal rearrangement.* American journal of translational research, 2016. **8**(10): p. 4310-4319.

321. Manuneedhi Cholan, P., et al., *TRAIL protects against endothelial dysfunction in vivo and inhibits angiotensin-II-induced oxidative stress in vascular endothelial cells in vitro.* Free Radical Biology and Medicine, 2018. **126**: p. 341-349.

322. Zhu, J., et al., *Losartan ameliorates "upstream" pulmonary vein vasculopathy in a piglet model of pulmonary vein stenosis.* The Journal of Thoracic and Cardiovascular Surgery, 2014. **148**(6): p. 2550-2558.

323. Stoll, M., et al., *The angiotensin AT2-receptor mediates inhibition of cell proliferation in coronary endothelial cells.* The Journal of clinical investigation, 1995. **95**(2): p. 651-657.

324. Li, D., et al., *Proapoptotic effects of ANG II in human coronary artery endothelial cells: role of AT1receptor and PKC activation.* American Journal of Physiology-Heart and Circulatory Physiology, 1999. **276**(3): p. H786-H792.

325. Wu, W.-B. and T.-F. Huang, *Activation of MMP-2, cleavage of matrix proteins, and adherens junctions during a snake venom metalloproteinase-induced endothelial cell apoptosis.* Experimental Cell Research, 2003. **288**(1): p. 143-157.

326. Cong, F., et al., *Requirement for a nuclear function of beta-catenin in Wnt signaling.* Molecular and cellular biology, 2003. **23**(23): p. 8462-8470.

327. Cuevas, C.A., et al., *Angiotensin II increases fibronectin and collagen I through the β-catenin-dependent signaling in mouse collecting duct cells.* American journal of physiology. Renal physiology, 2015. **308**(4): p. F358-F365.

328. Deb, A., *Cell-cell interaction in the heart via Wnt/β-catenin pathway after cardiac injury.* Cardiovascular research, 2014. **102**(2): p. 214-223.

329. Zhao, Y., et al., *An essential role for Wnt/β-catenin signaling in mediating hypertensive heart disease.* Scientific Reports, 2018. **8**(1): p. 8996.

330. Brooke, B.S., et al., *Angiotensin II blockade and aortic-root dilation in Marfan's syndrome.* The New England journal of medicine, 2008. **358**(26): p. 2787-2795.

331. Xiong, W., et al., *MMP-2 regulates Erk1/2 phosphorylation and aortic dilatation in Marfan syndrome.* Circulation research, 2012. **110**(12): p. e92-e101.

332. Möberg, K., et al., *The Ghent Marfan Trial — A randomized, double-blind placebo controlled trial with losartan in Marfan patients treated with β-blockers.* International Journal of Cardiology, 2012. **157**(3): p. 354-358.

333. Wang, Y., et al., *Transforming growth factor-β and abdominal aortic aneurysms.* Cardiovascular Pathology, 2013. **22**(2): p. 126-132.

334. Hinterseher, I., G. Tromp, and H. Kuivaniemi, *Genes and abdominal aortic aneurysm.* Annals of vascular surgery, 2011. **25**(3): p. 388-412.

335. M Brown, P., D. T Zelt, and B. Sobolev, *The risk of rupture in untreated aneurysms: The impact of size, gender, and expansion rate.* Journal of Vascular Surgery, 2003. **37**: p. 280-4.

336. Stolle, K., et al., *Cigarette smoke enhances abdominal aortic aneurysm formation in angiotensin II-treated apolipoprotein E-deficient mice.* Toxicology Letters, 2010. **199**(3): p. 403-409.

337. Jones, J.A., F.G. Spinale, and J.S. Ikonomidis, *Transforming growth factor-beta signaling in thoracic aortic aneurysm development: a paradox in pathogenesis.* Journal of vascular research, 2009. **46**(2): p. 119-137.

338. Schmierer, B. and C.S. Hill, *TGFβ–SMAD signal transduction: molecular specificity and functional flexibility.* Nature Reviews Molecular Cell Biology, 2007. **8**: p. 970.

339. Benke, K., et al., *The role of transforming growth factor-beta in Marfan syndrome.* Cardiology Journal, 2013. **20**: p. 227-234.

340. Fukui, D., et al., *Overexpression of transforming growth factor β1 in smooth muscle cells of human abdominal aortic aneurysm.* European Journal of Vascular and Endovascular Surgery, 2003. **25**(6): p. 540-545.

341. Mallat, Z., H. Ait-Oufella, and A. Tedgui, *The Pathogenic Transforming Growth Factor-β Overdrive Hypothesis in Aortic Aneurysms and Dissections.* Circulation Research, 2017. **120**: p. 1718-1720.

342. Song, Y., et al., *Expression of matrix metalloproteinase-12 in aortic dissection.* BMC Cardiovascular Disorders, 2013. **13**(1): p. 34.

343. Annabi, B., et al., *Differential regulation of matrix metalloproteinase activities in abdominal aortic aneurysms.* Journal of Vascular Surgery, 2002. **35**(3): p. 539-546.

344. Prescott, M.F., et al., *Effect of Matrix Metalloproteinase Inhibition on Progression of Atherosclerosis and Aneurysm in LDL Receptor-Deficient Mice Overexpressing MMP-3, MMP-12, and MMP-13 and on Restenosis in Rats after Balloon Injury.* Annals of the New York Academy of Sciences, 1999. **878**(1): p. 179-190.

345. Boyle, J.R., et al., *Doxycycline inhibits elastin degradation and reduces metalloproteinase activity in a model of aneurysmal disease.* Journal of Vascular Surgery, 1998. **27**(2): p. 354-361.

346. Petrinec, D., et al., *Doxycycline inhibition of aneurysmal degeneration in an elastase-induced rat model of abdominal aortic aneurysm: Preservation of aortic elastin associated with suppressed production of 92 kD gelatinase.* Journal of Vascular Surgery, 1996. **23**(2): p. 336-346.

347. Curci, J.A., et al., *Pharmacologic suppression of experimental abdominal aortic aneurysms: A comparison of doxycycline and four chemically modified tetracyclines.* Journal of Vascular Surgery, 1998. **28**(6): p. 1082-1093.

348. Eskandari, M.K., et al., *Enhanced abdominal aortic aneurysm in TIMP-1-deficient mice1.* Journal of Surgical Research, 2005. **123**(2): p. 289-293.

349. Baker, A.H., et al., *Divergent effects of tissue inhibitor of metalloproteinase-1, -2, or -3 overexpression on rat vascular smooth muscle cell invasion, proliferation, and death in vitro. TIMP-3 promotes apoptosis.* The Journal of clinical investigation, 1998. **101**(6): p. 1478-1487.

350. Gibb, S.L., et al., *TIMP3 Attenuates the Loss of Neural Stem Cells, Mature Neurons and Neurocognitive Dysfunction in Traumatic Brain Injury.* STEM CELLS, 2015. **33**(12): p. 3530-3544.

351. Eckhouse, S.R., et al., *Local Hydrogel Release of Recombinant TIMP-3 Attenuates Adverse Left Ventricular Remodeling After Experimental Myocardial Infarction.* Science Translational Medicine, 2014. **6**(223): p. 223ra21.

352. Chen, X., et al., *TGF-β Neutralization Enhances AngII-Induced Aortic Rupture and Aneurysm in Both Thoracic and Abdominal Regions.* Plos One, 2016. **11**: p. e0153811.

353. Angelov Stoyan, N., et al., *TGF-β (Transforming Growth Factor-β) Signaling Protects the Thoracic and Abdominal Aorta From Angiotensin II-Induced Pathology by Distinct Mechanisms.* Arteriosclerosis, Thrombosis, and Vascular Biology, 2017. **37**(11): p. 2102-2113.

354. Dai, J., et al., *Overexpression of Transforming Growth Factor-β1 Stabilizes Already-Formed Aortic Aneurysms.* Circulation, 2005. **112**(7): p. 1008-1015.

355. Wu, L., et al., *Matrix metalloproteinase-12 gene expression in human vascular smooth muscle cells.* Genes to Cells, 2003. **8**(3): p. 225-234.

356. Liu, S.-L., et al., *Matrix metalloproteinase-12 is an essential mediator of acute and chronic arterial stiffening.* Scientific Reports, 2015. **5**: p. 17189.

357. Calvet, D., et al., *Increased Stiffness of the Carotid Wall Material in Patients With Spontaneous Cervical Artery Dissection.* Stroke, 2004. **35**(9): p. 2078-2082.

358. Gertz, S.D., A. Kurgan, and D. Eisenberg, *Aneurysm of the rabbit common carotid artery induced by periarterial application of calcium chloride in vivo.* The Journal of clinical investigation, 1988. **81**(3): p. 649-656.

359. Rodriguez, J.A., et al. *Metalloproteinases and atherothrombosis: MMP-10 mediates vascular remodeling promoted by inflammatory stimuli*. Frontiers in Bioscience : a journal and virtual library, 2008. **13**, 2916-2921 DOI: 10.2741/2896.

360. Chang, S., et al., *Histone Deacetylase 7 Maintains Vascular Integrity by Repressing Matrix Metalloproteinase 10.* Cell, 2006. **126**(2): p. 321-334.

361. Liao, M., et al., *A microRNA profile comparison between thoracic aortic dissection and normal thoracic aorta indicates the potential role of microRNAs in contributing to thoracic aortic dissection pathogenesis.* Journal of Vascular Surgery, 2011. **53**(5): p. 1341-1349.e3.

362. Son, D.J., et al., *The atypical mechanosensitive microRNA-712 derived from pre-ribosomal RNA induces endothelial inflammation and atherosclerosis.* Nature communications, 2013. **4**: p. 3000-3000.

363. Kim, C., et al., *Abstract 106: Prevention of Abdominal Aortic Aneurysm by Anti-MiRNA-712 or Anti-miR-205 in Angiotensin II--Infused Mice.* Arteriosclerosis, Thrombosis, and Vascular Biology, 2014. **34**(suppl_1): p. A106-A106.

364. Liao, S., et al., *Accelerated Replicative Senescence of Medial Smooth Muscle Cells Derived from Abdominal Aortic Aneurysms Compared to the Adjacent Inferior Mesenteric Artery.* Journal of Surgical Research, 2000. **92**(1): p. 85-95.

365. McGrath, J.C., et al., *Contraction of human umbilical artery, but not vein, by oxygen.* The Journal of Physiology, 1986. **380**(1): p. 513-519.